

Electronic Thesis and Dissertation Repository

12-14-2013 12:00 AM

Effects of Excitation Pressure on Variegation and Global Gene Expression in *Arabidopsis thaliana*

Rainer Bode, *The University of Western Ontario*

Supervisor: Norman Hüner, *The University of Western Ontario*

A thesis submitted in partial fulfillment of the requirements for the Doctor of Philosophy degree in Biology

© Rainer Bode 2013

Follow this and additional works at: <https://ir.lib.uwo.ca/etd>



Part of the [Biology Commons](#), [Genomics Commons](#), and the [Plant Biology Commons](#)

Recommended Citation

Bode, Rainer, "Effects of Excitation Pressure on Variegation and Global Gene Expression in *Arabidopsis thaliana*" (2013). *Electronic Thesis and Dissertation Repository*. 994.
<https://ir.lib.uwo.ca/etd/994>

This Dissertation/Thesis is brought to you for free and open access by Scholarship@Western. It has been accepted for inclusion in Electronic Thesis and Dissertation Repository by an authorized administrator of Scholarship@Western. For more information, please contact wlsadmin@uwo.ca.

**EFFECTS OF EXCITATION PRESSURE ON VARIEGATION AND
GLOBAL GENE EXPRESSION IN *ARABIDOPSIS THALIANA***

(Spine title: EXCITATION PRESSURE, VARIEGATION AND GENE
EXPRESSION)

(Thesis format: Integrated-Article)

by

Rainer Bode

Graduate Program in
Biology

A thesis submitted in partial fulfillment
of the requirements for the degree of

Doctor of Philosophy

The School of Graduate and Postdoctoral Studies
The University of Western Ontario
London, Ontario, Canada

THE UNIVERSITY OF WESTERN ONTARIO
SCHOOL OF GRADUATE AND POSTDOCTORAL STUDIES

CERTIFICATE OF EXAMINATION

Supervisor

Dr. Norman Hüner

Examiners

Dr. Danielle Way

Dr. Denis Maxwell

Dr. Chris Brandl

Dr. Elizabeth Weretilnyk

The thesis by

Rainer Bode

entitled:

**The Effects of Excitation Pressure on Variegation and Global Gene
Expression in *Arabidopsis thaliana***

is accepted in partial fulfilment of the
requirements for the degree of

Doctor of Philosophy

Date _____

Chair of the Thesis Examination Board

ABSTRACT

I assessed the effects of photosystem II excitation pressure on chloroplast biogenesis and leaf sectoring in the *Arabidopsis thaliana* variegated mutants *im*, *spotty*, *var1*, *var2*, *chs5* and *atd2*. The plants were grown under varying degrees of excitation pressure induced by growth at increasing irradiance at different temperatures and the extent of variegation was quantified throughout the plant's development. I found that the degree of variegation was positively correlated with excitation pressure, regardless of whether high light or low temperature was used to induce increased excitation pressure in all the mutants tested. This was irrespective of whether the mutation causing the variegated phenotype in the first place affected photosynthetic electron transport or not. Additional experiments examining chloroplast development in wild-type and *im* were performed, utilizing etiolated seedlings greening at high and low excitation pressure and they revealed a role for IM acting as an electron safety valve in photosynthetic electron transport, alleviating excitation pressure during the first 3-12 h of greening, ensuring an orderly chloroplast development. Further I analysed the effects of excitation pressure short-term stress and long-term acclimation on global gene expression in wild-type *A. thaliana*, in order to assess whether retrograde signalling resulting from excitation pressure causes mainly changes in photosynthesis associated transcripts, or if the plant's response to thylakoid redox imbalance extends beyond the chloroplast. To modulate the redox state of the photosynthetic electron transport chain I used high light, low temperature and two specific inhibitors of electron transport. In order to acclimate plants to high excitation pressure they were grown at either low temperature or high irradiance. Gene expression was monitored using whole genome microarrays and it could be shown that while the stress response resulted in a drastic change in gene expression associated with photosynthesis and a large number of other metabolic pathways, the acclimation strategy to excitation pressure rather involved genes associated with gene expression and development. Even though the stress and the acclimation response function in fundamentally different ways, they temporally overlap, as ca. 30 % of all genes regulated by acclimation were already differentially expressed one hour into the stress response.

KEYWORDS:

Photosynthesis

Excitation Pressure

Chloroplast Biogenesis

Variation

Immutans

PTOX

Retrograde Regulation

Redox Signaling

CO-AUTHORSHIP STATEMENT

A version of Chapter 2 has been previously published as:

Rosso, D.; Bode, R.; Li, W.; Król, M.; Saccon, D., Wang, S.; Schillaci, L.A.; Rodermeil, S.R.; Maxwell, D.P.; Hüner, N.P.A. (2009). Photosynthetic Redox Imbalance Governs Leaf Sectoring in the *Arabidopsis thaliana* Variegation Mutants *immutans*, *spotty*, *var1*, and *var2*.

The Plant Cell, Vol. 21: 3473–3492

www.plantcell.org

Copyright American Society of Plant Biologists.

Contribution of co-authors:

- Rosso D: developed imaging technique; experimental design: figure 2, figure 3B+C, figure 6, figure S1; leaf excision experiment: figure 4A-H; photoacclimation to excitation pressure : figure 5A+B, figure S2; correlation between excitation pressure and variegation: figure 7; chloroplast development: figure 9; development of PSII photochemistry: figure 10
- Bode R: developed imaging technique, imaging and quantification of wt, *im*, *spotty*, *var1* and *var2*: figure 8, figure S3, figure S4; effects of HL pulse on greening: figure 11, figure S6; PS II and PS I reaction center protein quantification: figure S5; created collage for cover image of Plant Cell vol 21(11)
- Li W: gene expression (qRT-PCR): figure 9D+E, figure 12
- Król M: technical assistance with protein quantification: figure 9C, figure S5
- Saccon D: helped with development of imaging technique (4th year student): figure 3B+C
- Wang S: determination of plant growth by counting leaf initials (NSERC, USRA): figure 3A
- Schillaci LA: helped with protein quantification: figure 9C
- Rodermeil SR: critical comments on the manuscript; provided seeds for *im* and *spotty*
- Maxwell DP: critical comments on the manuscript; provided excitation pressure model: figure 1; critical reading of the final manuscript
- Hüner NPA: principal investigator; critical comments on the final manuscript

ACKNOWLEDGEMENTS

At first, I would like to express my gratitude towards my supervisor Dr. Norman Hüner for being an exceptionally excellent mentor, as he provided me with his extensive expertise in plant sciences and long time experience in academia. During my years as his student I benefitted from his availability and his patience for regular and lengthy discussions about my research and while he motivated me and gave me professional direction he managed to encourage me to develop into an independent researcher at the same time. I also benefitted from his extensive funds as well as his vast network of international collaborators, but foremost I am grateful that I had the chance to pursue my PhD under a supervisor whom I can respect that much on a personal level.

Next, I would like to thank my Advisory Committee, Dr. Denis Maxwell and Dr. Vojislava Grbic for providing extensive criticism, advice and discussion on my work over the years.

Then, it is David Scaduto who deserves a lot of thanks from me, because he went way beyond the call of duty while helping me growing plants and quantifying variegation.

I am also thankful to all of the members of the Hüner Lab and the Environmental Stress Biology Group, who not only created a nurturing working environment, but also provided interesting insights about their own research and thus, widening my knowledge about stress in plants and algae.

On a more personal note, I am grateful for being born into a world where the Ramones have happened and I consider myself lucky that I have been inspired by their true greatness from an early age on.

My girlfriend Bibiana Alcala-Valencia certainly deserves special thanks from me, as she supported and believed in me and was there for me when I needed her to be.

Last but not least I would like to thank my dear parents, who always provided me with the support I needed. Without them, this would have never been possible.

TABLE OF CONTENTS

CERTIFICATE OF EXAMINATION	ii
Abstract.....	iii
Keywords:.....	iv
Co-Authorship Statement.....	v
Acknowledgements.....	vi
Table of Contents.....	vii
List of Tables.....	xii
List of Figures.....	xiii
List of Appendices.....	xv
List of Abbreviations.....	xvii
CHAPTER 1	1
1 General Introduction:.....	1
1.1 Light Energy Capture and Transfer.....	3
1.1.1 Linear Electron Transport.....	5
1.1.2 Cyclic Electron Transport Around PS II.....	6
1.1.3 Cyclic Electron Transport Around PS I.....	6
1.1.4 Chlororespiration.....	7
1.2 Energy Balance and Excitation Pressure.....	8
1.3 Photoprotective Mechanisms Against Excitation Pressure.....	10
1.3.1 Short-Term Response to Excitation Pressure.....	10
1.3.2 Long-Term Response to Excitation Pressure.....	11
1.4 Retrograde Signaling.....	14
1.5 Variegation Mutants.....	16
1.5.1 Chloroplast Biogenesis.....	18

1.5.2	PTOX/IMMUTANS	19
1.5.3	Other Variegated Mutants.....	20
1.6	THESIS OBJECTIVES:	22
1.7	References.....	24
CHAPTER 2	30
2	Photosynthetic Redox Imbalance Governs Leaf Sectoring in the <i>Arabidopsis thaliana</i> Variegation Mutants <i>immutans</i>, <i>spotty</i>, <i>var1</i>, and <i>var2</i>	30
2.1	Introduction.....	32
2.2	Methods.....	40
2.2.1	Growth Conditions.....	40
2.2.2	Determination of Growth Rate.....	40
2.2.3	Quantification of Variegation	41
2.2.4	Chlorophyll Analyses.....	42
2.2.5	Room Temperature Chlorophyll a Fluorescence	42
2.2.6	SDS-PAGE and Immunoblots	43
2.2.7	RNA Isolation, cDNA Synthesis, and Real-Time qRT-PCR	44
2.2.8	Accession Numbers	44
2.3	Results.....	45
2.3.1	Plant Growth	45
2.3.2	Effects of Irradiance and Temperature on the Extent of Leaf Variegation.....	50
2.3.3	Effects of Irradiance and Temperature on Excitation Pressure and Photoacclimation.....	53
2.3.4	Interaction of Photoperiod, Temperature, and Irradiance on Excitation Pressure and Leaf Variegation	58
2.3.5	Differential Changes in PS II Photochemistry During Greening of Cotyledons	66
2.3.6	Effects of a Short Pulse of High Light on Greening in Cotyledons.....	69
2.3.7	Effects of Greening on IM and AOX1a Expression	72

2.4 Discussion.....	75
2.5 References.....	82
2.6 Supplemental Figures and Tables.....	90
CHAPTER 3.....	96
3 Arabidopsis Mutants <i>atd2</i> and <i>chs5</i> Display Leaf Variegation in Response to Excitation Pressure Despite a Lack of Involvement in Photosynthetic Electron Transport.....	96
3.1 Introduction.....	96
3.2 Material and Methods.....	100
3.2.1 Plant Growth.....	100
3.2.2 Determination of Growth Rate.....	100
3.2.3 Quantification of Variegation.....	100
3.3 Results:.....	102
3.3.1 Plant Growth Kinetics:.....	102
3.3.2 Effects of Growth Irradiance and Temperature on Variegation.....	112
3.3.3 Patterns of Leaf Variegation in Different Arabidopsis Mutants:.....	117
3.4 Discussion:.....	119
3.5 References:.....	122
CHAPTER 4.....	125
4 Short Term Effects of Changes in Excitation Pressure on Global Gene Expression in <i>Arabidopsis thaliana</i>.....	125
4.1 Introduction:.....	125
4.2 Material and Methods:.....	128
4.2.1 Plant Growth.....	128
4.2.2 Chlorophyll a Fluorescence.....	128
4.2.3 P700 Measurements.....	129
4.2.4 RNA Extraction.....	129

4.2.5	RNA Quality Assessment, Probe Preparation and GeneChip Hybridization	130
4.2.6	Quantitative Real-Time RT-PCR:.....	130
4.2.7	Functional Analysis of Differentially Regulated Genes:	131
4.3	Results:.....	132
4.3.1	Chlorophyll a Fluorescence (Excitation pressure and P700).....	132
4.3.2	Determination of Differential Gene Expression	135
4.3.3	High-Light and Low-Temperature Shift Experiments.....	135
4.3.4	The Effects of Chemical Inhibitors on Gene Expression.....	138
4.3.5	Contribution of PQH ₂ and PS II to Gene Expression	140
4.3.6	Comparison of HEP, PQH ₂ and PS II as Redox Sensors of Gene Expression.....	140
4.3.7	Functional Analysis (MapMan):.....	141
4.3.8	Real-time RT-PCR:.....	148
4.4	Discussion:.....	149
4.5	References:.....	153
4.6	Supplemental Figures.....	156
4.7	Supplemental Tables.....	163
CHAPTER 5	186
5	Effects of Long Term Acclimation to Excitation Pressure on Global Gene Expression in <i>Arabidopsis thaliana</i>	186
5.1	Introduction.....	186
5.2	Material and Methods:	190
5.2.1	Plant Growth.....	190
5.2.2	Chlorophyll a Fluorescence	190
5.2.3	RNA Extraction	190
5.2.4	RNA Quality Assessment, Probe Preparation and GeneChip Hybridization	191

5.2.5	Quantitative Real-time RT-PCR:.....	192
5.2.6	Functional Analysis of Differentially Regulated Genes:.....	192
5.3	Results:.....	193
5.3.1	Acclimation to HEP	194
5.3.2	Differential Gene Expression in Plants Acclimated to Various Growth Regimes.....	197
5.3.3	Real-Time RT-PCR	201
5.3.4	Functional Characterisation of Gene Expression:.....	201
5.4	Discussion:.....	210
5.5	References:.....	214
5.6	Supplemental Figures.....	218
6	CONCLUSIONS:.....	221
6.1	SUMMARY	228
6.2	Future Research	229
6.3	References:.....	230
7	VITA	232

LIST OF TABLES

Table 3.1: Logarithmic Growth Rate Constants	103
Table 5.1 Transcription Factors Changed by Acclimation to HEP.	206
Table 5.2 Transcription Factors Changed by Both Short Term and Long Term Exposure to HEP	209

LIST OF FIGURES

Figure 1.1: Model of the Photosynthetic Electron Transport Chain.....	4
Figure 1.2: A Variegation Mutant.....	17
Figure 2.1 Photosynthetic Redox and Leaf Variegation.....	31
Figure 2.2 The Redox State of the PQ Pool Is a Sensor of Environmental Change.....	35
Figure 2.3 The Experimental Design to Assess the Effects of Light and Temperature on the Development of Variegation in the <i>im</i> Mutant of <i>Arabidopsis</i>	46
Figure 2.4 Analysis of Leaf Initiation and Variegation During Seedling Development	49
Figure 2.5 Leaf Phenotype and Quantified Variegation of Excised Leaves.....	52
Figure 2.6 The Effects of Irradiance and Temperature on Excitation Pressure and Photoacclimation in <i>im</i>	55
Figure 2.7 The Effects of Excitation Pressure and Continuous Light on Leaf Variegation ...	57
Figure 2.8 Correlation Between Variegation of <i>im</i> Seedlings and Excitation Pressure Experienced Under Various Growth Conditions	59
Figure 2.9 Variegation Mutant Phenotypes	60
Figure 2.10 The Effects of Irradiance on Chloroplast Development.....	63
Figure 2.11 The Development of Photosystem II Photochemistry in WT and <i>im</i>	67
Figure 2.12 The Effects of a HL Pulse on Greening in WT and <i>im</i> Cotyledons	70
Figure 2.13 The Effect of Greening on the Relative Expression Levels of IM and AOX1a..	74
Figure 3.1 Representative Images of Variegated <i>Arabidopsis</i> Mutants	105-106
Figure 3.2 <i>Arabidopsis</i> Mutant Growth Curves.....	109-111
Figure 3.3 Quantification of Variegation in <i>im</i> , <i>spotty</i> , <i>var1</i> , <i>var2</i> , <i>atd2</i> and <i>chs5</i>	114-115

Figure 3.4 Development in Phenotype of the <i>Arabidopsis chs5</i> Mutant	118
Figure 4.1 Quantification of Excitation Pressure in <i>Arabidopsis</i> Leaves after Different Stress Treatments.....	133
Figure 4.2 Intersystem Electron Transport in Response to Inhibitor Treatment	134
Figure 4.3 Number of Genes Regulated by HL and LT	137
Figure 4.4 Comparison of Differentially Expressed Genes in Different Groups	139
Figure 4.5 MapMan Display of Major Metabolic Pathways	143-144
Figure 4.6 Display of Cellular Responses.....	146
Figure 5.1 Representative Photographs of <i>Arabidopsis</i> Acclimated to Various Light and Temperature Regimes	193
Figure 5.2 The Effects of Growth Irradiance and Temperature on Excitation Pressure and Photoacclimation.....	195
Figure 5.3 Determination of Differential Gene Expression.....	196
Figure 5.4 Comparison of Differentially Expressed Genes Between Different Groups.....	199
Figure 5.5 Common Gene Expression in HEP Stress and Acclimation	200
Figure 5.6 MapMan Display of Gene Expression Data.....	203
Figure 6.1 . A Model of Chloroplast Redox Sensing and its Effects on Both a Cellular and an Organismal Scale	227

LIST OF APPENDICES

Supplemental Figure S 2.1 Growth Kinetics of WT and <i>im</i> Seedlings	90
Supplemental Figure S 2.2 Acclimation of <i>im</i> to HEP at Low Temperature	91
Supplemental Figure S 2.3 Extent of Variegation of the <i>var1</i> , <i>var2</i> and <i>im</i> (<i>spotty</i>) Mutants of <i>Arabidopsis</i>	92
Supplemental Figure S 2.4 Variegation Mutant Phenotypes at Low Temperature	93
Supplemental Figure S 2.5 The Biogenesis of Photosystem II and Photosystem I Reaction Centers	94
Supplemental Figure S 2.6 The Effects of a HL Pulse on Greening in WT and <i>im</i> Cotyledons	95
Supplemental Figure S 4.1 Quantification of Excitation Pressure in Plants after Various Stress Treatments	156
Supplemental Figure S 4.2 Number of Genes Regulated by Inhibitors.....	157
Supplemental Figure S 4.3 MapMan Display of Major Metabolic Pathways	158
Supplemental Figure S 4.4 MapMan Display of Major Metabolic Pathways at Various Cut-Off Levels	159-160
Supplemental Figure S 4.5 Comparison of qRT-PCR and Microarray Expression Data.....	162
Supplemental Figure S 5.1 Comparison of qRT-PCR and Microarray Expression Data.....	218
Supplemental Figure S 5.2 MapMan Display of Gene Expression Data.....	220
Supplemental Table S 4.1 Real-time assay IDs.....	163
Supplemental Table S 4.2 Expression Data of a Subset of Genes Regulated by HEP and Involved in Major Metabolic Pathways.....	164

Supplemental Table S 4.3 Expression Data of a Subset of Genes Regulated by PQH ₂ and Involved in Major Metabolic Pathways.....	175
Supplemental Table S 4.4 Expression Data of a Subset of Genes Regulated by PS II and Involved in Major Metabolic Pathways.....	183

LIST OF ABBREVIATIONS

A ₀	Chl <i>a</i> electron acceptor in PS II
A ₁	phylloquinone electron acceptor in PS I
<i>act2</i>	mRNA transcript for actin-2
ADP	adenosine diphosphate
ANOVA	analysis of variance
AOX	alternative oxidase
APX	aspartate peroxidase
<i>atd2</i>	<i>Arabidopsis thaliana amidophosphoribosyl-transferase2 deficient</i> , a variegated mutant
ATP	adenosine triphosphate
ATPase	adenosine triphosphate-synthase
CAT	catalase
Chl	Chlorophyll
<i>chs5</i>	<i>Arabidopsis thaliana chilling sensitive1</i> , a variegated mutant
CL	continuous light
CP43	core antenna protein of PS II
CP47	core antenna protein of PS II
Cyt	Cytochrome
Cyt b ₆ f	Cytochrome b ₆ f complex
D1/D2	reaction center proteins of PS II
DBMIB	2,5-dibromo-3-methyl-6-isopropylbenzoquinone
DCMU	3-(3',4'-dichlorophenyl)-1,1-dimethylurea
E _k	irradiance at which maximum photosynthetic yield matches photosynthetic capacity
EP	excitation pressure
F _A /F _B /F _X	iron-sulphur clusters; electron acceptors in PS I
Fd	ferredoxin
FNR	ferredoxin/NADP ⁺ reductase
FtsH	membrane bound ATP-dependant metalloprotease
F _V /F _M	maximum photochemical efficiency of PS II
HEP	high excitation pressure
HL	high light
<i>im</i>	<i>Arabidopsis thaliana immutans</i> , a variegated mutant plant
IM	IMMUTANS protein
LHC	light harvesting complex
Lhca	light harvesting complex of PS I
Lhcb	light harvesting complex of PS II
LT	low temperature

NADP ⁺	nicotineamide adenine dinucleotide phosphate (oxidized form)
NADPH	nicotineamide adenine dinucleotide phosphate (reduced form)
NPQ	non-photochemical quenching
OEC	oxygen evolving complex
P ₆₈₀	reaction center chlorophyll dimer of PS II (reduced form)
P ₆₈₀ ⁺	reaction center chlorophyll dimer of PS II (oxidized form)
P ₆₈₀ ⁺	reaction center chlorophyll dimer of PS I (oxidized form)
P ₇₀₀	reaction center chlorophyll dimer of PS I (reduced form)
PAGE	polyacrylamide gel electrophoresis
PC	plastocyanin
PCR	polymerase chain reaction
PET	photosynthetic electron transport
PETC	photosynthetic electron transport chain
pheo	pheophytin
pmf	proton motive force
POR	NADPH: protochlorophyllide oxidoreductase
PPFD	photosynthetic photon flux density
PQ	plastoquinone
PQH ₂	plastoquinol
PS I	photosystem I
PS II	photosystem II
PTOX	plastid terminal oxidase
Q _A	primary quinone electron acceptor of PS II (oxidized form)
Q _A ⁻	primary quinone electron acceptor of PS II (reduced form)
Q _B	secondary quinone electron acceptor of PS II (oxidized form)
qP	relative redox state of Q _A
qRT-PCR	quantitative real-time PCR
RbcL	large subunit of Rubisco
RbcS	small subunit of Rubisco
Rubisco	Ribulose-1,5-bisphosphate carboxylase/oxygenase
SOD	superoxide dismutase
TOC-TIC	translocon of the outer/inner chloroplast membrane
<i>var1</i>	<i>Arabidopsis thaliana variegated1</i> , a variegated mutant
<i>var2</i>	<i>Arabidopsis thaliana variegated2</i> , a variegated mutant
WT	wild-type
σ _{PSII}	effective absorption cross-section of PS II
τ ⁻¹	rate at which photosynthetically generated electrons are consumed

CHAPTER 1

1 GENERAL INTRODUCTION:

Photosynthesis is a process intrinsic to all photoautotrophic life on this planet, including cyanobacteria, algae, and land plants, and converts energy harvested from sunlight into chemical energy that is used to fuel biochemical processes, such as carbon, nitrogen and sulfur assimilation. In addition, photosynthesis produces molecular oxygen by oxidizing water molecules to protons and O₂ and utilizing the electrons to generate NADPH and ATP. As a result of photosynthesis about 10¹¹ metric tons of carbon are fixed annually which translates into 130 terawatts of energy that are produced every year (Whitmarsh & Govindjee, 1999) and since it first appeared 3,500 million years ago it has enriched 21 % of our planet's atmosphere with O₂ (Buick, 2008). Thus, photosynthesis is an essential process, since the vast majority of all life on earth is heterotrophic or aerobic.

While cyanobacteria lack organized cellular compartments for photosynthesis, it is localized to organelles called chloroplasts in algae and plants. Chloroplasts are bordered by two membranes, the inner- and the outer membrane, surrounding a compartment called stroma, the location for the carbon fixing processes of photosynthesis. Within the stroma there is the thylakoid membrane, which possesses a high degree of complexity, with stacked regions (grana-lamellae) and non-stacked regions (stroma-lamellae), while the space this membrane encloses is called lumen. The thylakoids are the site of light absorption and transformation into chemical energy as they are the matrix for the proteins of the photosynthetic electron transport chain (PETC) which is composed of a series of multi-protein heterocomplexes, pigments and a small number of non-protein electron carrier molecules (Figure 1.1). The major complexes of the PETC display an uneven lateral distribution along the thylakoid membrane and while photosystem II (PS II) is located in the grana lamellae, photosystem I (PS I) and the ATP-synthase complex (ATPase) can be found in the stroma lamellae. Other components like

plastoquinone (PQ) and the cytochrome b_6f complex (Cyt b_6f) are distributed ubiquitously over the thylakoid membrane.

1.1 *Light Energy Capture and Transfer*

During photosynthesis light energy is absorbed by pigments located in the light harvesting antennae of the photosystems and funneled into the reaction centers. When the energy has reached the reaction centers ca. 3 – 6 % is stored via photochemistry, but the remainder of it is lost as fluorescence and heat. The energy transfer between the pigments occurs via Förster resonance energy transfer, a phenomenon occurring when the two chromophores are in very close proximity to each other (1–10 nm), utilizing nonradiative dipole–dipole coupling allowing the energy to be transported a relatively long distance in a very short time (Förster 1965; Blankenship 2002). The initial absorption of light energy in the light harvesting complexes (LHCs) of PS II and the subsequent transfer to P₆₈₀ is possibly the fastest biological process existing in nature as it happens on a femto- to picosecond timescale (Hüner et al, 2003). Once the energy has reached the primary electron donors of their respective photosystem reaction center (PS II: P₆₈₀ and PS I: P₇₀₀) charge separation occurs and electrons are transferred to their respective primary acceptors (Andreásson and Vänngård, 1988).

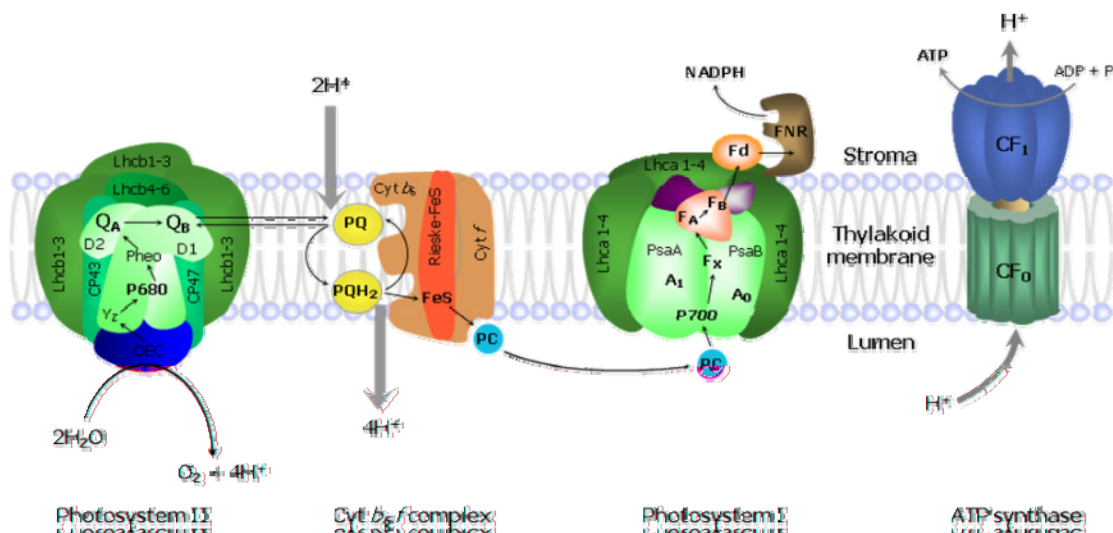


Figure 1.1: Model of the Photosynthetic Electron Transport Chain

The linear electron transport of the Z-scheme is depicted with solid black arrows, starting with the splitting of water at the oxygen evolving complex (OEC) going all the way to the reduction of NADPH performed by the Ferredoxin-NADP⁺-reductase (FNR). The translocation of protons across thylakoid by PQ/Cyt b₆f and the ATP synthase is indicated by gray arrows. PS II: On the luminal side the oxygen evolving complex is attached to the reaction center consisting of the D1 and D2 proteins binding the special Chl a dimer P₆₈₀, pheophytin and the quinones Q_A and Q_B. Surrounding the reaction center are the core antennae CP43 and CP47 and attached to them is the minor outer antennae polypeptide Lhcb4-6. The outer most antennae consist of a trimer of Lhcb1-3. The Cyt b₆f complex receives electrons from PQH₂ at the Cyt b₆ domain attached to the Rieske FeS protein. Ultimately Cyt f is oxidized by PC which then freely diffuses through the lumen until itself is oxidized by PS I. The reaction center of PS I consists of the polypeptides PsaA and PsaB which bind the special pair Chl a P₇₀₀, the electron acceptors A₀ and A₁ and the iron/sulphur cluster F_X. Attached to the reaction center is the PsaC polypeptide holding two additional iron sulphur clusters (F_A and F_B) and the outer antennae composed of a Lhca1-4 trimer. Ultimately PS I reduces the water soluble protein Fd which is then utilized by the FNR to catalyze the reduction of NADP⁺ to NADPH. The ATP synthase is composed of the CF₀ domain functioning as a trans-membrane proton channel and the stromal CF₁ domain catalyzing the phosphorylation of ATP. This figure is courtesy of D.P. Maxwell.

1.1.1 *Linear Electron Transport*

The Z-scheme of photosynthesis was proposed by Hill and Bendall in 1960 and is used to explain the basic mechanisms of electron transport from PS II to PS I (Figure 1.1). Once light energy is transferred from the antennae to P_{680} in PS II it enters an excited state (P_{680}^*) and charge separation occurs creating a radical pair $P_{680}^+Pheo^-$ within a timeframe of nanoseconds to microseconds. This radical pair then transfers the electron to the quinone acceptor Q_A , which is bound to the D2 polypeptide forming a new radical pair $P_{680}^+Q_A^-$ which subsequently transfers the electron to Q_B another PQ molecule that is reversibly bound to the D1 protein at the Q_B binding site creating the semiquinone Q_B^- . In order to fully reduce Q_B^- it requires an additional electron and hence the closed reaction center must be re-opened with an electron donated from OEC. The $[4Mn^{2+}]$ cluster withdraws electrons from water, splitting it into H^+ and O_2 and donates these electrons to a specific tyrosine residue on the D1 protein (Tyr_{161} or Y_Z) which transfers them to P_{680}^+ , thus re-opening the PS II reaction centers again. Once Q_B^- has been fully reduced, it acquires two protons from the stroma and dissociates from PS II, diffusing through the thylakoid membrane as plastoquinol (PQH_2).

Once PQH_2 has reached Cyt b_6f it binds to the quinol oxidizing site (Q_O) on the luminal side of Cyt b_6 and transfers one electron to the Rieske-FeS center. The transport of the electron from PS II to Cyt b_6f happens within milliseconds and is the slowest and hence rate limiting step of linear electron transport (Haehnel, 1984). During a process called Q-cycling the second electron is transferred to Cyt b_6 and a total of 4 protons is released into the lumen, contributing to the trans-thylakoid proton gradient (Cape et al, 2006). The two electrons are subsequently transferred from the Rieske-FeS center to Cyt f and from there they leave the complex and the membrane via PC, a blue copper protein that diffuses through the lumen to PS I.

PC is now negatively charged and binds to a positively charged PsaF subunit on the luminal side of PS I where it transfers its electron to a closed reaction center (P_{700}^+), re-opening it in the process. Once charge separation has occurred in the reaction center of

PS I, fueled by funneled excitation energy from LHC I to P_{700} , the reaction center is closed (P_{700}^+) again. Subsequently a series of electron acceptors is reduced, such as A_0 , A_1 , F_X , F_A and F_B until the electron finally reaches Fd on the stromal side of PS I. The stromal enzyme FNR utilizes two electrons it has accepted from Fd to reduce one molecule of NADPH (Blankenship, 2002).

1.1.2 *Cyclic Electron Transport Around PS II*

Apart from linear electron transport as described in the Z-scheme of photosynthesis above, there are alternative pathways of electron transport within the thylakoid membrane.

In order to prevent photo-inhibition promoted by oxidative damage in PS II during conditions that prevent closed reaction centers to re-open in a timely manner, there is the option of re-cycling electrons around PS II. When the electron replenishment from the OEC to the reaction center is impaired, the accumulation of P_{680}^+ can be prevented by the donation of an electron from Cyt b_{559} . Subsequently Cyt b_{559} is reduced by PQH_2 , thus creating a cyclic flow of electrons around PS II (reviewed by Shinopoulos & Brudvig, 2012).

1.1.3 *Cyclic Electron Transport Around PS I*

When PS II suffers from photo-inhibition and/or there is a shortage of $NADP^+$ substrate for NADPH biosynthesis, PS I has the option to perform another type of cyclic electron transport, thus maintaining the trans-thylakoidal proton gradient and consequently ATP synthesis. Arnon and co-workers discovered, as early as 1967 and 1975 that Fd is capable of donating electrons to Cyt b_6f instead of FNR, when the electron supply from PS II is insufficient. Thus, the necessary proton motive force (μmf) for photophosphorylation is maintained and hence the activity of the Calvin-Benson cycle can be sustained. The way Fd transports the electrons to the Q_0 site of Cyt b_6 is not fully understood and the contribution of cyclic electron transport to steady state photosynthesis remains ambiguous (Schöttler et al, 2011).

1.1.4 *Chlororespiration*

Another alternative electron transport pathway is the chlororespiratory pathway, which was first proposed by Bennoun in 1982, long before its components were identified. He anticipated a respiratory pathway in the thylakoids involving a dehydrogenase utilizing stromal NAD(P)H to reduce the PQ-pool in the dark while at the same time transporting protons into the lumen, in order to fuel ATP synthesis in the dark. The other element of this pathway involves a plastid terminal oxidase (PTOX) analogous to the alternative oxidase (AOX) of the mitochondrial electron transport chain, which is able to oxidize PQH₂ and donate the electrons and protons to molecular oxygen, creating water (McDonald et al, 2011).

1.2 *Energy Balance and Excitation Pressure*

A major challenge photosynthetic organisms are facing consists in the discrepancy of rate constants and temperature sensitivities between different types of processes within the PETC. The extremely fast (10^{-15} - 10^{-12} s) and temperature insensitive biophysical process of light energy trapping is combined with the much slower (10^{-3} s) and very temperature sensitive biochemical electron transport along the thylakoid membrane and metabolic processes (e.g. C-, N-, S-assimilation) which ultimately utilizes the harvested energy (Hüner & Grodzinski, 2011). In order to overcome the disparity of approximately 10 orders of magnitude between these rate constants, plants have evolved mechanisms to dissipate excess energy. Energy which is not processed via photochemistry can be quenched by the process of non-photochemical quenching (NPQ). NPQ can take place in the antennae complexes by the photoprotective carotenoids of the xanthophyll cycle (Demmig-Adam et al, 1999; Horton et al, 2008), or in the reaction center by charge recombination (Krause & Weis 1991; Hüner et al, 2006). Both mechanisms protect the PS II reaction center from over-excitation in an environment where light and temperature fluctuate permanently. The balance between absorbing light energy and either processing it photochemically or dissipating it via NPQ is called photostasis and can be summarized by the equation: $\sigma_{PSII} \cdot E_k = \tau^{-1}$ (Falkowski and Chen, 2003; Hüner *et al.* 2003). σ_{PSII} constitutes the absorption cross section of PS II, while E_k is the level of irradiance at which maximum photosynthetic quantum yield balances the maximum photosynthetic capacity and τ^{-1} is the metabolic sink capacity of the plant, namely the rate at which metabolism (e.g. C-, N- and S-assimilation) is able to utilize photosynthetically generated electrons. Of course light energy is also absorbed at PS I, yet its photochemical turnover rate is much higher than PS II and is not considered to be limiting. Hence PS I is not considered in the equation describing photostasis (Ke, 2001). The product of $\sigma_{PSII} \cdot E_k$ is temperature insensitive in a biologically viable range and represents the flux of light energy transferred within the antennae to the reaction center of PS II. The metabolic rate τ^{-1} on the other hand depends on biochemically

driven metabolic pathways highly sensitive to temperature, nutrient limitation or salt stress (Maxwell et al, 1995; Cruz et al., 2003; Huang et al., 2005). Hence, if the level of irradiance increases significantly or if low temperature, or any other factors decrease the rate of metabolism it creates an imbalance in the equation: $\sigma_{\text{PSII}} \cdot E_k > \tau^{-1}$. This imbalance constitutes a physiological stress condition that has been named PS II excitation pressure (EP) (Hüner et al, 1998; Ensminger et al, 2006; Wilson et al, 2006; Pfannschmidt & Yang, 2012).

Since the oxidation of reduced PQH₂ constitutes the rate limiting step in intersystem PET, high EP (HEP) results first in a strong reduction of the PQ pool and subsequently, due to the lack of oxidized PQ able to accept electrons from PS II, in the disproportionate closure of PS II reaction centers (P₆₈₀⁺ Pheo Q_A⁻). The proportion of closed reaction centers can be quantified in vivo using Chl *a* fluorescence measuring photochemical quenching in PS II (Dietz et al, 1985; Schreiber et al, 1994; Maxwell et al, 1995; Baker, 2008). The pigments in PS II continue to absorb and transfer light energy, regardless of whether the reaction centers are closed or not. Excited Chl molecules in the reaction centers can enter the triplet state and react with molecular oxygen, relaxing the Chl but also resulting in the formation of singlet oxygen (¹O₂), a highly reactive oxygen species (ROS) detrimental to pigments, lipids, proteins, RNA and DNA (op den Camp et al, 2003; Apel & Hirt, 2004). This photo-oxidation of mainly PS II components results in chronic photoinhibition, due to irreversible damage to PS II. Both plants and algae have developed an array of protection and acclimation mechanisms, in order to prevent this from happening.

1.3 *Photoprotective Mechanisms Against Excitation Pressure*

To move from a state of HEP ($\sigma_{\text{PSII}} \cdot E_k > \tau^{-1}$) towards the desired photostasis ($\sigma_{\text{PSII}} \cdot E_k = \tau^{-1}$) photoautotrophs can either increase the sink capacities (τ^{-1}) or decrease the absorption cross section of PS II (σ_{PSII}). Since this imbalance can either be caused by high light or by low temperature and other processes decreasing the metabolic rate, all of these factors induce the same photoprotective response mechanism (Hüner et al, 1998; Hüner et al, 2003; Ensminger et al, 2006; Wilson et al, 2006), which can be separated into short-term stress responses, or long-term acclimation strategies.

1.3.1 *Short-Term Response to Excitation Pressure*

1.3.1.1 *Nonphotochemical Quenching*

The first line of defense and hence a short-term stress measure, against HEP consists of the xanthophyll cycle. During this process NPQ is performed by a group of carotenoids called xanthophylls, located in the antennae of PS II. When the trans-thylakoid ΔpH -gradient increases, an enzyme called violaxanthin de-epoxidase removes the two epoxide groups from the xanthophyll pigment called violaxanthin. As a carotenoid, violaxanthin is a light harvesting pigment and its transformation is catalyzed in two subsequent steps. The first de-epoxidation step results in antheraxanthin, and the second and final step in zeaxanthin. The function of this pigment is to accept excitation energy from excited $^1\text{Chl}^*$ and subsequently dissipating the energy as heat. Thus, the light energy never reaches the reaction center. Once the trans-thylakoidal ΔpH -gradient decreases again, another enzyme, zeaxanthin epoxidase restores the epoxide groups in zeaxanthin in two steps, creating first antheraxanthin and then violaxanthin (Demmig-Adams et al, 1999; Wilson et al, 2003)

Apart from the NPQ mechanism employing the xanthophylls cycle in the antenna complexes, there is another form of energy dissipation as heat and it is located in the PS II reaction centers. Once the reaction centers are closed and the primary quinone acceptors (Q_A^- and Q_B^-) are reduced, an alteration in their redox potential, induced by

HEP can cause them to recombine their negative charges with the positively charged donors from the oxygen evolving complex (S-states). The resulting charge recombination results in dissipation of excitation energy as heat and can be detected using thermoluminescence (Hüner et al, 2006; Ivanov et al, 2006; Pockock et al. 2007).

1.3.1.2 *State Transition*

Instead of altering LHC gene expression some organisms have been observed to display a different approach, as they undergo a process called state transition, a short term stress response to HEP. In the first state it was shown that the over-excitation of PS II compared to PS I results in a strongly reduced PQ pool which subsequently activates a Ser-Thr protein kinase, called Stt7. Once activated, this kinase phosphorylates the outer light harvesting complexes for PS II, which are then laterally displaced in the thylakoid membrane and connected to PSI. In this second state σ_{PSII} is decreased and at the same time the rate at which PS I can process electrons generated at PS II is increased. This process is reversible: once the PQ pool is oxidized, a phosphatase dephosphorylates LHC II so it detaches from PS I and rejoins PS II (Allen et al, 1981; Rochaix, 2004; Kargul and Barber, 2008)

1.3.2 *Long-Term Response to Excitation Pressure*

1.3.2.1 *Modulation of Photosystem Stoichiometry*

One aspect of HEP is that the metabolism cannot process the electrons generated at PS II fast enough, resulting in an accumulation of PQH₂. Thus a long term HEP acclimation strategy decreasing σ_{PSII} is to decrease the total amount of PS II while at the same time increasing the total amount of PS I. Pfannschmidt et al. (1999) showed that alterations in the redox state of PQ lead to changes in the transcript levels of *psbA*, the gene which codes for the D1 reaction center protein of PS II and *psaA* / *psaB* which are the transcripts for the reaction center proteins of PS I.

1.3.2.2 *Modulation of Sink Capacity*

While the previously mentioned strategies to cope with HEP focused on the decrease of σ_{PSII} , many cold tolerant overwintering plant species achieve photostasis by the increase of their metabolic rate (τ^{-1}). Winter rye and winter wheat have been shown as a long term acclimation strategy, to up-regulate enzymes involved in carbon metabolism (i.e. *rbcl*, *cFBPase*) resulting, amongst other metabolites, in an increased sucrose accumulation, which has a double function in being a carbon deposit and a cryoprotectant at the same time. Additionally these plants displayed an increased rate of respiration and show increased accumulation of biomass, due to an increased growth rate, all strategies to increase τ^{-1} (Gray et al., 1997; Savitch et al, 2002; Dahal et al, 2012).

1.3.2.3 *ROS Scavenging*

Ultimately, during conditions of extreme irradiance or extreme cold, or when both factors are combined, non-acclimated plants will suffer HEP to the degree that ROS will be produced. The main ROS in the chloroplast are singlet oxygen ($^1\text{O}_2$), superoxide anion radical ($\text{O}_2\cdot^-$) and H_2O_2 and apart from being important signaling molecules at moderate concentrations, they have detrimental effects on the entire photosynthetic machinery at elevated concentrations. In order to detoxify these ROS, plants have developed a large variety of different ROS-scavenging molecules, be it enzymes such as superoxide dismutase (SOD), catalase (CAT) and ascorbate peroxidase (APX), or other molecular species, such as glutathione, β -carotene, tocopherol, or ascorbate. This array of ROS-scavengers attenuates the photo-oxidative damage promoted by HEP (op den Camp et al, 2003; Gill & Tuteja, 2010). While these antioxidants are present at all times, they can be counted as a short-term stress mechanism, yet plants acclimate to HEP upon long term exposure, via the up-regulation of antioxidant gene expression.

1.3.2.4 *Acclimation to HEP via Modulation of LHC*

Another effective mechanism to reduce the absorption cross section of PS II (σ_{PSII}) is the modulation of size and composition of PS II as a long term acclimation strategy. In 1995 Escoubas et al. and Maxwell et al. found an inverse relationship between size of LHC II and growth irradiance in the unicellular algae, *Dunaliella tertiolecta* and *Chlorella vulgaris*. They could show that not only are the Lhcb proteins less abundant, but their transcript levels also decreased along with a decrease in total Chl content and a dramatic increase in Chl *a/b* ratios, not only in response to high light, but also in response to growth at low temperature. Additionally it was shown that the use of a specific PET inhibitor preferentially reducing PQ caused the same effect as high light and low temperature, while the addition of an inhibitor oxidizing PQ had the opposite effect. It was concluded that neither high light nor low temperature *per se* caused the remodeling of LHC II, but it was excitation pressure sensed through the reduction state of PQ, regulating nuclear gene expression via retrograde regulation.

1.4 *Retrograde Signaling*

All these mechanisms to prevent or alleviate HEP or its detrimental effects on the thylakoids rely at least to some degree on the regulation of both nuclear and chloroplast gene expression in phototrophic eukaryotes. The chloroplast holds its own genome, but only a small fraction (< 5 %) out of the roughly 3000 chloroplast proteins are encoded in this plastid genome, while the rest is located in the nucleus (Koussevitzky et al. 2007). Sometimes the same enzyme complex, as for example the Calvin-Benson cycle enzyme Ribulose-1,5-bisphosphate carboxylase/oxygenase (Rubisco), has one nuclear encoded small subunit and a chloroplast encoded large subunit. This spatial disparity of gene expression necessitates a tight orchestration, administered by a process called retrograde signaling during which nuclear gene expression is regulated by signals emitted from the chloroplast. Various elements of the PETC (i.e. PS II, PQ, PS I and the proton motive force of the pH gradient along the thylakoid membrane) have been identified as sensors for stress in the chloroplast, along with ROS, intermediates of Chl biosynthesis and various photosynthetic metabolites (reviewed by Fernández & Strand, 2008). Many of these sensors trigger distinct reactions, as is the case in PS II and PS I which were shown to induce distinct transcription profiles from each other (Bräutigam et al, 2009). This notion was supported with the discovery of distinct ROS signaling pathways which in some cases appeared to be not only distinct but even antagonizing each other, depending on the individual ROS (i.e. singlet oxygen and H₂O₂) species and where they are generated. ¹O₂ developed under HEP at the reaction centers of PS II has been hypothesized to be recognized as a signal and forwarded to the cytosol by two isoforms of the plastid protein EXECUTER (Lee et al, 2007), while little is known about the perception of PS I generated O₂^{•-} except that it presumably needs to be dismutated to H₂O₂ in order to achieve the stability necessary for a signaling molecule (Laloi et al, 2007). Other signaling pathways appear to integrate a variety of distinct plastid signals. In *Arabidopsis* the kinase STN7 receives signals from both PQH₂ and Fd at the reducing site of PS I and appears to modulate nuclear gene expression in response to both

(Pesaresi et al. 2010). Another well studied sensor is Mg-Protoporphyrin IX, an intermediate of Chl biosynthesis and it has been shown that its accumulation is responsible for regulation of plastid and nuclear encoded photosynthetic genes utilizing the chloroplast polypeptide GUN1 to propagate the signal. Once the signal has reached the nucleus it activates the AP2 type transcription factor ABI4 which then regulates transcription of chloroplast targeted genes (e.g. *lhcb*) (Koussevitzky et al. 2007). In spite of extensive research in this field not one of the signaling pathways is fully understood today. In particular the means of transport of the signals from the plastid to the nucleus remains equivocal.

1.5 *Variegation Mutants*

The definition of variegated plants has been formulated as “any plant that develops patches of different colors in its vegetative parts” (Kirk & Tilney-Bassett, 1978). The predominant colors are green, white and yellow/orange and for the most part the non-green patches are caused by an impairment in chloroplast biogenesis, leading to a lack of photosynthetic pigments, such as Chl and in some cases carotenoids (Figure 1.2). Variegation can be either induced exogenously, by partial shading of the plant, pathogen attack or a variety of nutrient deficiencies, or it can be endogenous in form of a mutation. Mutations leading to a variegated phenotype can have their origin in either the nuclear genome, in the mitochondria or the chloroplasts (Yu et al, 2007). Some variegated mutants have distinct genotypes in green sectors and white sectors, which may arise from the insertion of a transposable element into a gene, which is subsequently excised, reconstituting the wild-type gene, in some tissue, but not in others. Many variegated plants, nevertheless, show the same genotype in both sectors. In either case the mutation impairs the completion of chloroplast development.

It is also noteworthy to state, that the sectoring these plants display can have a multitude of patterns. Some grass-like plants display alternating stripes of green and white sectors, while other plants are green at the base of the leaf and white at the margins, or vice versa. Again other plants display a reticulate form of variegation, with mostly pale leaves but normally green leaf veins, or vice versa. Many mutants display an entirely chaotic type of variegation, where differentially colored sectors do not seem to follow any particular scheme. Some mutants display a gradual transition from one sector to another while some show very strict boundaries between the sectors.

While most of the time the variegated phenotype is a disadvantage for the plant, because it goes along with decreased photosynthesis capacity, some plants display variegation to attract specific pollinator species.



Figure 1.2: A Variegation Mutant

The image displays the *immutans* variegation mutant of *Arabidopsis thaliana*. The plant displays a chaotic pattern of white and green sectors.

1.5.1 *Chloroplast Biogenesis*

The development of a chloroplast occurs, depending on the availability of light in the meristem during its early stages, from either etioplasts, or proplastids. Proplastids are small (0.5 – 1 μm in diameter) undifferentiated organelles devoid of pigments and form the precursors to all other forms of plastids (i.e. etioplasts, chloroplasts, chromoplasts, amyloplasts and gerontoplasts). In the absence of light, proplastids develop into etioplasts, which are roughly 5 – 10 times the size of their progenitors. Etioplasts possess a paracrystalline membrane structure called the prolamellar body (PLB), containing galacto-lipids, NADPH, basal levels of carotenoids, the Chl precursor protochlorophyllide bound to the enzyme protochlorophyllide oxidoreductase (POR) and the antioxidant enzyme superoxide dismutase (SOD). Radiating from the PLB there are membrane structures called pro-thylakoids, which already contain the CF_1 domain of the ATP synthase and several electron transport carriers (i.e. Cyt b_{559} , Cyt f , PC and Rieske FeS proteins) (Solymosi & Schoefs, 2010).

Upon exposure to light, both etioplasts and proplastids, fully develop into chloroplasts in a process called de-etiolation or greening. The light induces POR enzyme activity which results in the conversion of protochlorophyllide into chlorophyllide a , which is subsequently converted into Chl a and b . The POR enzyme disappears and sequentially the photosystems appear, first PS I followed by PS II and finally the LHCs. It takes ca 12 to 24 h for the PLB to disappear and develop into the thylakoid membrane with a fully functional PETC (Pogson & Albrecht, 2011).

Since the majority of all chloroplast proteins are encoded in the nucleus, the posttranslational import of these proteins into the plastid is indispensable for plastid biogenesis. While the orchestration of nuclear and plastid gene expression is performed by retrograde regulation, the nuclear proteins are targeted to the organelle and imported via a trans-membrane shuttling system, spanning both the outer and inner

membrane of the chloroplast, called the translocon of the outer/inner chloroplast membrane (TOC-TIC complex) (Pogson & Albrecht, 2011).

1.5.2 *PTOX/IMMUTANS*

The *immutans* (*im*) variegation mutant is one of the oldest *Arabidopsis* mutants and it was created and partially characterized by Rédei (1963) and Röbbelen (1968). Leaves are separated into green and white sectors (Figure 1.2) with the green sectors having normal chloroplasts and the white sectors are heteroplastidic, meaning while a few normal chloroplasts can be found in these cells, the majority of them lack any pigments. While the impaired plastids do not contain carotenoids, they accumulate the colorless carotenoid precursor phytoene and they lack organized lamellae structures, rendering them not functional (Wetzel et al, 1994). All cells of *im* carry a nuclear mutation in a small (40.5 kDa) thylakoid protein which is distantly related (26 % amino acid identity) to the mitochondrial alternative oxidase (AOX) and involved in carotenoid biosynthesis. In mitochondria, AOXs function as terminal oxidases by oxidizing the ubiquinone pool and donating the electrons directly to molecular oxygen. Interestingly, apart from their partial sequence identity, they share a specificity for the inhibitors salicylhydroxamid acid (SHAM) and propyl gallate (GA) (Vanleberghe & McIntosh, 1997). When the IM protein was expressed heterologously in *E. coli*, biochemical analyses showed a specific oxidase activity of IM for PQ while using molecular oxygen as a terminal electron acceptor (Josse et, 2003).

This functional homology to AOX in the mitochondria led to the hypothesis that IM could be a stress induced safety valve for excess electrons in intersystem electron transport, helping to re-open closed PS II reaction centers, by oxidizing PQH₂ and it was proposed that IM is indeed the elusive PTOX from the chlororespiratory pathway (Peltier and Cournac, 2002). This role as a safety-valve is disputed though, since Ort and Baker (2002) showed that chlororespiration only contributes 0.3 % towards the total intersystem electron flux capacity and Rosso et al. (2006) demonstrated that in fully developed and photosynthetically competent leaves IM cannot compete for electrons

with PS I. A very recent study (Fu et al, 2012) showed that AOX can substitute for IM, as it was demonstrated, when AOX is targeted to the chloroplast instead of the mitochondria, it can rescue the variegated phenotype in *im*.

Wu and co-workers (1999) proposed a model integrating the light sensitivity of the variegation patterns in the IM deficient *Arabidopsis* mutant (*im*), with its role in carotenoid synthesis and intersystem electron transport: The desaturation of phytoene to ζ -carotene is an essential step in carotenoid biosynthesis and performed by the enzyme phytoene desaturase (PDS) which transfers the electrons onto PQ. During high illumination regimes there is a lack of oxidized PQ available to accept these electrons, if there is no additional PQ oxidase (i.e. IM/PTOX) present. With no photo-protective carotenoids present, the PETC is photo-oxidized and white sectors are formed.

1.5.3 ***Other Variegated Mutants***

Despite their widespread occurrence in nature, very few variegation mutants have been described at a molecular level. Apart from *im*, probably the best described *Arabidopsis* mutant is *variegated-2* (*var2*). Just like *im* it has all-green cotyledons and displays a chaotic pattern of variegation but the variegated sectors are not perfectly white, since they still contain carotenoids and thus display a yellowish orange color next to the green sectors. The mutant plant lacks a gene product called FtsH2, a subunit of an ATP dependent metalloprotease hexamer heterocomplex (FtsH) which is anchored in the thylakoid membrane. FtsH consists of 4 different types of subunits (i.e. FtsH1; FtsH2; FtsH5 and FtsH8) with FtsH1 and FtsH5 being functionally interchangeable, as well as FtsH2 and FtsH8. The knockout of FtsH5 results in another variegated mutant named *variegated-1* (*var1*) which is phenotypically hard to distinguish from *var2*, while the knockout of FtsH1 and FtsH8 do not result in any obvious phenotype (Sakamoto et al, 2003). The FtsH complex is a crucial component in the repair cycle of the PS II reaction center, since it removes and degrades photo-oxidized D1 from the thylakoid membrane. The occurrence for both green and yellow sectors in *var1* and *var2* has been explained by Zhang et al (2010) with a threshold model, in which the amount of FtsH complex in

each proplastid determines whether it develops normally into a chloroplast, or if this development is halted, resulting in the lack of an organized thylakoid system and Chl.

Two other interesting variegated mutants of *Arabidopsis thaliana* are *amidophosphoribosyl-transferase2 deficient (atd2)* and *chilling sensitive5 (chs5)*, created by van der Graaff et al. (1997) and Schneider et al (1994), respectively. We know that amidophosphoribosyl-transferase2 is the leaf isoform of the enzyme catalyzing the first committed step of de-novo purine synthesis, thus the plant leaves have to rely on another isoform of the enzyme (amidophosphoribosyl-transferase1) active mostly in roots and flowers and it is presumably importing purine from there. Yet the level of purine in the leaves is apparently not always sufficient and chloroplast development can be halted at early stages resulting in a vesiculated chloroplast lacking organized lamellae and Chl (van der Graaff, 2004). All we know about *chs5*, is that it develops chlorotic sectors when exposed to lower temperatures (Schneider et al, 1994).

1.6 **THESIS OBJECTIVES:**

The aim of this thesis is to answer the following questions:

- 1. Does IM, the proposed terminal oxidase of the chlororespiratory pathway regulate the redox state of the PQ pool during early stages of chloroplast biogenesis to assure a proper assembly of the photosynthetic apparatus in *im*?**

In order to address this question, etiolated *im* seedlings were exposed to different levels of irradiance during the greening process and chloroplast development was monitored over time by measuring EP, photochemical efficiency, pigment content, mRNA and protein levels of several components of etioplasts, thylakoids and the Calvin-Benson cycle. If IM helps to oxidize PQH₂ during chloroplast development, EP should be lower in wild-type plants during the greening process.

- 2. Does excitation pressure control variegation in the *Arabidopsis thaliana* variegated mutants *im*, *spotty*, *var1*, *var2*, *atd2* and *chs5*?**

To assess whether light or temperature *per se* regulate the extent of variegation, the mutants were grown at various degrees of EP induced by increasing light (50, 150 and 450 $\mu\text{mol photons m}^{-2} \text{s}^{-1}$) and decreasing temperature (25 and 12 °C) regimes and the extent of variegation was quantified over the time of the plant's vegetative development. We know in some of these mutants the extent of variegation is increased when they are grown at higher light intensities. If growth at a lower temperature increases the extent of the variegated sectors irrespective of the level of irradiance the plant is exposed to, the sectoring is presumed to be controlled by HEP, instead.

3. What are the effects of short-term excitation pressure stress on global gene expression in *Arabidopsis* and how does the PQ pool and PS II contribute to retrograde signaling?

Previous research has shown that HEP regulates nuclear gene expression to promote chloroplast remodeling (Maxwell et al. 1995, Wilson et al 2003) yet Ndong and co-workers (2001) found evidence that HEP has an effect on gene expression without any obvious connection to photosynthesis or even the chloroplast (i.e. *wali*). To assess the extent of HEP-stress induced gene expression *Arabidopsis* wild type plants are grown under conditions of low EP and then shifted to either High Light or Low Temperature and gene expression is monitored via whole genome microarray analysis. To elucidate the roles of PQH₂ and PS II in retrograde signaling, specific inhibitors were applied which selectively oxidize or reduce the PQ-pool and the resulting change in gene expression is monitored, as described above.

4. What are the effects of long term acclimation to conditions of high excitation pressure on global gene expression in *Arabidopsis*?

The previously described photoprotective mechanisms against HEP are separated into a short-term stress response and long-term acclimation strategies (Section 1.3). I want to examine whether this temporal distinction extends to the level of global gene expression. For this purpose *Arabidopsis* wild-type plants were grown under and acclimated to varying degrees of EP modulated by growth at different levels of irradiance (50 and 450 $\mu\text{mol photons m}^{-2}\text{s}^{-1}$) and temperatures (25 and 12 °C). Gene expression was again monitored via whole genome microarray analysis and the results were compared to the short-term stress response.

1.7 References

- Allen, J.F., Bennett, J., Steinback, K.E., and Arntzen, C.J. (1981) Chloroplast protein phosphorylation couples plastoquinone redox state to distribution of excitation energy between photosystems. *Nature* 291: 25–29.
- Andréasson, L.E., Vänngård, T. (1988) Electron transport in photosystem I and II. *Annu Rev Plant Physiol Plant Mol Biol* 39: 379-411.
- Apel, K. and Hirt, H. (2004). Reactive oxygen species: metabolism, oxidative stress, and signal transduction. *Ann Rev Plant Biol* 55, 373-399.
- Arnon, D.I., Tsujimoto, H. I., McSwain, B.D. (1967) Ferredoxin and photosynthetic phosphorylation. *Nature* 214: 562-566.
- Arnon, D.I., Chain, R.K. (1975) Regulation of ferredoxin-catalyzed photosynthetic phosphorylation. *Proc Natl Acad Sci USA* 72: 4961-4965.
- Baker, N.R. (2008). Chlorophyll fluorescence: A probe of photosynthesis in vivo. *Ann Rev Plant Biol* 59, 89-113.
- Bennoun, P. (1982) Evidence for a respiratory chain in the chloroplast. *Proc Natl Acad Sci USA* 79 4352–4356.
- Blankenship, R.E. (2002) The basic principles of photosynthetic energy storage. In *Molecular Mechanisms of Photosynthesis*. Blackwell Science Ltd, London, pp: 1-10.
- Bräutigam, K., Dietzel, L., Kleine, T., Ströher, E., Wormuth, D., Dietz, K.J., Radke, D., Wirtz, M., Hell, R., Dörmann, P., Nunes-Nesi, A., Schauer, N., Fernie, A.R., Oliver, S.N., Geigenberger, P., Leister, D., and Pfannschmidt, T. (2009). Dynamic plastid redox signals integrate gene expression and metabolism to induce distinct metabolic states in photosynthetic acclimation in *Arabidopsis*. *Plant Cell* 21: 2715–2732.
- Britt, R.D. (1996) Oxygen evolution. In Ort, D.R., Yocum, C.F., eds, *Oxygenic Photosynthesis: The Light Reactions Vol.4* Kluwer Academic Publishers, Dordrecht, Netherlands, pp: 113-136.
- Buick, R. (2008). When did oxygenic photosynthesis evolve?. *Philos. Trans. R. Soc. Lond., B, Biol. Sci.* 363 (1504): 2731–43.
- Cape, J.L., Bowman, M.K., Kramer, D.M. (2006) Understanding the cytochrome bc complexes by what they don't do. The Q-cycle at 30. *Trends Plant Sci.* 11(1): 46-55.
- Cruz, J.L., Mosquim, P.R., Pelacani, C.R., Araújo, W.L., and DaMatta, F.M. (2003). Photosynthesis impairment in cassava leaves in response to nitrogen deficiency. *Plant Soil* 257: 417–423.

- Dahal, K., Kane, K., Gadapati, W., Webb, E., Savitch, L.V., Singh, J., Sharma, P., Sarhan, F., Longstaffe, F.J., Grodzinski, B., and Hüner, N.P.A. (2012). The effects of phenotypic plasticity on photosynthetic performance in winter rye, winter wheat and *Brassica napus*. *Phys. Plant.* 144: 169–188.
- Demmig-Adams, B., Adams III, W.W., Ebbert, V. and Logan, B.A. (1999). "Ecophysiology of the xanthophyll cycle", in *Advances in Photosynthesis . The Photochemistry of Carotenoids*, eds. H.A. Frank, A.J. Young, G. Britton and R.J. Cogdell (Kluwer Academic Publishers, Dordrecht) vol. 8, 245-269.
- Dietz, K.-J., Schreiber, U. and Heber, U. (1985). The relationship between the redox state of Q_A and photosynthesis in leaves at various carbon-dioxide, oxygen and light regimes. *Planta* 166, 219-226.
- Ensminger, I., Busch, F. and Hüner, N.P.A. (2006). Photostasis and cold acclimation: sensing low temperature through photosynthesis. *Physiol. Plant.* 126, 28-44.
- Escoubas, J.-M., Lomas, M., LaRoche, J. and Falkowski, P.G. (1995) Light intensity regulates cab gene transcription via the redox state of the plastoquinone pool in the green alga, *Dunaliella tertiolecta*. *Proc. Natl. Acad. Sci. U.S.A.* 92: 10237-10241.
- Falkowski, P.G., and Chen, Y.-B. (2003). Photoacclimation of light harvesting systems in eukaryotic algae. In *Advances in Photosynthesis and Respiration: Light-Harvesting Antennas in Photosynthesis*, Vol. 13, B.R. Green and W.W. Parsons, eds (Dordrecht, The Netherlands: Kluwer Academic Publishers), pp. 423–447.
- Fernández, A.P., and Strand, Å . (2008). Retrograde signalling and plant stress: Plastid signals initiate cellular stress responses. *Curr. Opin. Plant Biol.* 11: 509–513.
- Förster, T. (1965). "Delocalized Excitation and Excitation Transfer". In Sinanoglu, Oktay. *Modern Quantum Chemistry. Istanbul Lectures. Part III: Action of Light and Organic Crystals.* 3. New York and London: Academic Press. pp. 93–137.
- Fu, A.; Liu, H.; Yu, F.; Kambakam, S.; Luan, S.; Rodermel, S.R. (2012). Alternative oxidases (AOX1a and AOX2) can functionally substitute for plastid terminal oxidase in *Arabidopsis* chloroplasts. *Plant Cell* 24(4):1579-95
- Gill, S.S., and Tuteja, N (2010). Reactive oxygen species and antioxidant machinery in abiotic stress tolerance in crop plants. *Plant Physiol Biochem* 48(12):909-30
- Gray, G.R., Chauvin, L.-P., Sarhan, F., and Hüner, N.P.A. (1997) Cold acclimation and freezing tolerance. A complex interaction of light and temperature. *Plant Physiol.* 114: 467–474.
- Haehnel, W. (1984). Photosynthetic electron transport in higher plants. *Annu Rev Plant Physiol* 35: 659-693.
- Hill, R., Bendall, F. (1960) Function of the two cytochrome components in chloroplasts: A working hypothesis. *Nature* 186: 136-137.

- Horton, P., Johnson, M.P., Perez-Bueno, M.L., Kiss, A.Z. and Ruban, A.V. (2008). Photosynthetic acclimation: does the dynamic structure and macro-organisation of photosystem II in higher plant grana membranes regulate light harvesting states? *FEBS J.* 275, 1069-1079.
- Huang, C., He, W., Guo, J., Chang, X., Su, P., and Zhang, L. (2005). Increased sensitivity to salt stress in an ascorbate-deficient *Arabidopsis* mutant. *J. Exp. Bot.* 56: 3041–3049.
- Hüner, N.P.A., Öquist, G. and Sarhan, F. (1998) Energy balance and acclimation to light and cold. *Trends Plant Sci.* 3, 224-230.
- Hüner, N. P. A., Öquist, G. and Melis, A. (2003). "Photostasis in plants, green algae and cyanobacteria: the role of light harvesting antenna complexes", in *Advances in Photosynthesis and Respiration. Light Harvesting Antennas in Photosynthesis* eds. B.R. Green and W.W. (Kluwer Academic Publishers, Dordrecht) vol. 13, 401-421.
- Hüner, N.P.A., Ivanov, A.G., Sane, P.V., Pockock, T., Krol, M., Balseris, A., Rosso, D., Savitch, L.V., Hurry, V.M. and Öquist, G. (2006). "Photoprotection of Photosystem II: reaction centre quenching versus antenna quenching", in *Advances in Photosynthesis and Respiration . Photoprotection, Gene Regulation and Environment*, eds. B. Demmig-Adams, W.W. Adams III and A.K. Mattoo (Springer, Dordrecht) vol. 21: 55-173.
- Hüner, N.P.A. and Grodzinski, B. (2011). "Photosynthesis and photoautotrophy" in *Comprehensive Biotechnology*, ed. M. Moo-Young (Elsevier) vol. 1, 315-322
- Ivanov, A.G., Sane P.V., Krol, M., Gray G.R., Balseris, A., Savitch L.V., Öquist, G., Hüner, N.P.A. (2006) Acclimation to temperature and irradiance modulates PSII charge recombination. *FEBS Lett* 580(11): 2797-802.
- Josse, E.M., Alcaraz, J.P., Labouré, A.M., and Kuntz, M. (2003) In vitro characterization of a plastid terminal oxidase (IM). *Eur. J. Biochem.* 270: 3787–3794.
- Kargul, J., and Barber, J. (2008) Photosynthetic acclimation: Structural reorganisation of light harvesting antenna – role of redox dependent phosphorylation of major and minor chlorophyll *a/b* binding proteins. *FEBS Lett.* 275: 1056–1068.
- Ke, B. (2001). "Photosystem I - Introduction", in *Advances in Photosynthesis. Photobiochemistry and Photobiophysics* (Kluwer Academic Publishers, Dordrecht) vol. 10, 419-430.
- Kirk J.T.O. & Tilney-Bassett R.A.E. (1978) *The Plastids*, 2nd edn. Elsevier/North-Holland, Amsterdam, the Netherlands
- Koussevitzky, S., Nott, A., Mockler, T.C., Hong, F., Sachetto-Martins, G., Surpin, M., Lim, J., Mittler, R., and Chory, J. 2007. Signals from Chloroplasts Converge to Regulate Nuclear Gene Expression. *Science.* 316: 715-719.

- Krause, G.H. and Weis, E. (1991) Chlorophyll fluorescence and photosynthesis: the basics. *Ann. Rev. Plant Physiol. Plant Mol. Biol.* 42: 313-349.
- Laloi, C., Stachowiak, M., Pers-Kamczyc, E., Warzych, E., Murgia, I., Apel, K.: Cross-talk between singlet oxygen- and hydrogen peroxide-dependent signaling of stress responses in *Arabidopsis thaliana*. *Proc Natl Acad Sci U S A* 2007, 104:672-677.
- Lee, K.P., Kim, C., Landgraf, F., Apel, K. (2007) EXECUTER1- and EXECUTER2-dependent transfer of stress-related signals from the plastid to the nucleus of *Arabidopsis thaliana*. *Proc Natl Acad Sci U S A* 2007, 104:10270-10275.
- Martínez-Zapater JM. (1993). Genetic analysis of variegated mutants in *Arabidopsis*. *Journal of Heredity* 84, 138–140.
- Maxwell, D.P., Falk, S., and Hüner, N.P.A. (1995). Photosystem II excitation pressure and development of resistance to photoinhibition. Light-harvesting complex II abundance and zeaxanthin content in *Chlorella vulgaris*. *Plant Physiol.* 107: 687–694.
- McDonald, A.E., Ivanov, A.G., Bode, R., Maxwell D.P., Rodermel, S.R., Hüner, N.P.A. (2011) Flexibility in photosynthetic electron transport: The physiological role of plastoquinol terminal oxidase (PTOX). *Biochim Biophys Acta* 1807: 954-967.
- Ndong, C., Danyluk, J., Hüner, N.P.A., Sarhan, F. (2001) Survey of gene expression in winter rye during changes in growth temperature, irradiance or excitation pressure. *Plant Mol Biol* 45: 691-703.
- op den Camp, R., Przybyla, D., Ochsenein, C., Laloi, C., Kim, C., Danon, A., Wagner, D., Hideg, E., Göbel, C., Feussner, I., Nater, M., and Apel, K. (2003). Rapid induction of distinct stress responses after the release of singlet oxygen in *Arabidopsis*. *Plant Cell* 15: 2320–2332.
- Ort, D.R., Baker, N.R. (2002) A photoprotective role for O₂ as an alternative electron sink in photosynthesis? *Curr Opin Plant Biol* 5: 193-198.
- Peltier, G., and Cournac, L. (2002). Chlororespiration. *Annu. Rev. Plant Biol.* 53: 523–550.
- Pesaresi, P., Hertle, A., Pribil, M., Schneider, A., Kleine, T., Leister, D. (2010) Optimizing photosynthesis under fluctuating light – The role of Arabidopsis STN7 kinase. *Plant Signal Behav.* 5(1): 21-5
- Pfannschmidt, T., Nilsson, A., and Allen, J.F. (1999). Photosynthetic control of chloroplast gene expression. *Nature* 397: 625–628.
- Pfannschmidt, T., Yang, C. (2012) The hidden function of photosynthesis: a sensing system for environmental conditions that regulates plant acclimation responses. *Protoplasma* 249: 125–136
- Pocock, T., Sane, P.V., Falk, S., Hüner, N.P.A. (2007) Excitation pressure regulates the activation energy for recombination events in the photosystem II reaction centres of *Chlamydomonas reinhardtii*. *Biochem Cell Biol.* 85(6): 721-9.

- Pogson, B.J., Albrecht, V. (2011) Genetic dissection of chloroplast biogenesis and development: an overview. *Plant Physiol.* 155(4): 1545-51.
- Rédei, G.P. (1963). Somatic instability caused by a cysteine-sensitive gene in *Arabidopsis*. *Science* 139: 767–769.
- Rochaix, J.-D. (2004) Genetics of the biogenesis and dynamics of the photosynthetic machinery in eukaryotes. *Plant Cell* 16: 1650–1660.
- Röbelen, G. (1968) Genbedingte Rotlicht-Empfindlichkeit der Chloroplastendifferenzierung bei *Arabidopsis*. *Planta* 80, 237–254.
- Rosso, D., Ivanov, A.G., Fu, A., Geisler-Lee, J., Hendrickson, L., Geisler, M., Stewart, G., Król, M., Hurry, V., Rodermel, S.R., Maxwell, D.P., and Hüner, N.P.A. (2006) IMMUTANS does not act as a stress-induced safety valve in the protection of the photosynthetic apparatus of *Arabidopsis* during steady-state photosynthesis. *Plant Physiol.* 142: 1–12.
- Rosso, D. (2007) Redox regulation of variegation in the *immutans* mutant of *Arabidopsis thaliana*. PhD thesis. University of Western Ontario. Department of Biology.
- Sakamoto, W., Zaltsman, A., Adam, Z., and Takahashi, Y. (2003). Coordinated regulation and complex formation of yellow variegated1 and yellow variegated2, chloroplastic FtsH metalloproteases involved in the repair cycle of photosystem II in *Arabidopsis* thylakoid membranes. *Plant Cell* 15: 2843–2855.
- Savitch, L.V., Leonardos, E.D., Grodzinski, B., Hüner, N.P.A, Öquist, G. (2002) Two different strategies for light utilization in photosynthesis in relation to growth and cold acclimation. *Plant Cell Environ* 25: 761-771
- Schöttler, M.A., Albus, C.A., Bock, R. (2011) Photosystem I: Its biogenesis and function in higher plants. *J Plant Physiol.* 168(12): 1452-61
- Schneider, J.C.; Hugly, S.; Somerville, CR (1994). Chilling sensitive mutants of *Arabidopsis*. *Weeds World* 1: 2-6.
- Schreiber, U., Bilger, W. and Neubauer, C. (1994) "Chlorophyll fluorescence as a noninvasive indicator for rapid assessment of in vivo photosynthesis," in *Ecophysiology of Photosynthesis*, eds. E.D. Schulze and M.M. Caldwell (Springer-Verlag, Berlin), 49-70
- Shinopoulos, K.E., Brudvig, G.W. (2012) Cytochrome b₅₅₉ and cyclic electron transfer within photosystem II. *Biochim Biophys Acta.* 1817(1): 66-75.
- Solymsi, K., Schoefs, B. (2010) Etioplast and etio-chloroplast formation under natural conditions: the dark side of chlorophyll biosynthesis in angiosperms. *Photosynth Res.* 105(2): 143-166.
- van der Graaff, E.; Lamers, G.; Den Dulk-Ras, A.; Hooykaas, P.J.J. (1997). Developmental mutants of *Arabidopsis thaliana* obtained after gene tagging with an activator T-DNA construct. 8TH INTERNATIONAL CONFERENCE ON *ARABIDOPSIS* RESEARCH

- van der Graaff, E.; Hooykaas, P.; Lein, W.; Lerchl, J.; Kunze, G.; Sonnewald, U.; Boldt, R. 2004. Molecular analysis of "de novo" purine biosynthesis in solanaceous species and in *Arabidopsis thaliana*. *Front Biosci.* 1;9:1803-16.
- Vanlerberghe, G.C., McIntosh, L. (1997). ALTERNATIVE OXIDASE: From Gene to Function. *Annu Rev Plant Physiol Plant Mol Biol.* 48: 703-734.
- Wetzel, C.M., Jiang, C.Z., Meehan, L.J., Voytas, D.F., and Rodermel, S.R. (1994). Nuclear-organelle interactions: The *immutans* variegation mutant of *Arabidopsis* is plastid autonomous and impaired in carotenoid biosynthesis. *Plant J.* 6: 161–175.
- Whitmarsh, J., Govindjee (1999) The photosynthetic process. In Singhal, G.S., Renger, G., Sopory, S.K., Irrgang, K.D., Govindjee. *Concepts in photobiology: photosynthesis and photomorphogenesis.* Boston: Kluwer Academic Publishers. pp. 11–51.
- Wilson, K.E., Ivanov, A.G., Öquist, G., Grodzinski, B., Sarhan, F., Hüner, N.P.A. (2006) Energy balance, organellar redox status and acclimation to environmental stress. *Can. J. Bot.* 84, 1355-1370.
- Wilson, K.E., Krol, M. and Hüner, N.P.A. (2003) Temperature-induced greening of *Chlorella vulgaris*. The role of the cellular energy balance and zeaxanthin dependent nonphotochemical quenching. *Planta* 217, 616 - 627.
- Wu, D., Wright, D.A., Wetzel, C.M., Voytas, D.F., and Rodermel, S.R. (1999). The IMMUTANS variegation locus of *Arabidopsis* defines a mitochondrial alternative oxidase homolog that functions during early chloroplast biogenesis. *Plant Cell* 11: 43–55.
- Yu, F., Fu, A., Aluru, M., Park, S., Xu, Y., Liu, H., Liu, X., Foudree, A., Nambogga, M., and Rodermel, S.R. (2007). Variegation mutants and mechanisms of chloroplast biogenesis. *Plant Cell Environ.* 30: 350–365.
- Zhang, D.; Kato, Y; Zhang, L; Fujimoto, M; Tsutsumi, N; Sodmergen; Sakamoto, W. (2010) The FtsH Protease Heterocomplex in *Arabidopsis*: Dispensability of Type-B Protease Activity for Proper Chloroplast Development. *Plant Cell* 22: 3710–3725.

Chapter 2

2 PHOTOSYNTHETIC REDOX IMBALANCE GOVERNS LEAF SECTORING IN THE *ARABIDOPSIS THALIANA* VARIEGATION MUTANTS *IMMUTANS*, *SPOTTY*, *VAR1*, AND *VAR2*



Figure 2.1 Photosynthetic Redox and Leaf Variegation

November 2009 Plant Cell cover image, vol 21(11):

Variegated leaves display patterns of non-green (white or yellow) sectors, which lack chlorophyll, against the normally green background (plants on the left). *Arabidopsis im* mutants exhibit variegation due to a lesion in photosynthetic electron transport in the chloroplast. Rosso, Bode et al. (2009) developed a non-destructive technique using false imaging (two plants on the right column) to investigate the role of photosynthetic redox balance in establishing patterns of leaf variegation in *im* mutants. Variegation in mutant seedlings develops through interactions between irradiance and temperature, which create imbalances in the photosynthetic energy budget, resulting in the destruction of green chloroplasts in colorless sectors. Mutations involving components of the photosynthetic electron transport chain predispose chloroplasts to photo-oxidation under high excitation pressure.

2.1 *Introduction*

Plants sense light through an array of photoreceptors, including phytochromes (Rockwell et al., 2006; Bae and Choi, 2008), cryptochromes (Li and Yang, 2007), and the more recently discovered phototropins (Christie, 2007) that are critical for plant growth and development. However, in addition to the requirement for photoreceptors sensitive to spectral quality, the oxidation-reduction (redox) state of photosynthetic electron transport (PET) has been shown to act a sensor of cellular energy status (Hüner et al., 1998; Giraud et al., 2008; Murchie et al., 2009). Imbalances in the redox state of PET may occur whenever the absorption and transformation of light by the extremely fast, temperature-insensitive photochemical reactions of photosynthesis either exceed the capacity to use the photosynthetic electrons for reductive C, N, and S metabolism and/or exceed the capacity of the photosynthetic apparatus to dissipate excess energy non-photochemically as heat (Hüner et al., 1998; Pfannschmidt, 2003; Ensminger et al., 2006; Wilson et al., 2006; Murchie et al., 2009).

The redox state of PET has been shown to influence a diversity of phenomena from altering the excitation distribution between photosystems through state transitions controlled by STN7, a chloroplast thylakoid protein kinase in *Arabidopsis thaliana* (Rochaix, 2004; Kargul and Barber, 2008), to changes in organellar gene expression (Pfannschmidt et al., 1999; Pfannschmidt, 2003) and nuclear gene expression through retrograde regulation (Pfannschmidt, 2003; Fernández and Strand, 2008; Woodson and Chory, 2008; Pesaresi et al., 2009; Pfannschmidt et al., 2009), to changes in plant growth habit and morphology (Gray et al., 1997). Furthermore, tobacco (*Nicotiana tabacum*) plants deficient in ferredoxin-NADP(H) reductase exhibit a yellow-green phenotype due to the overreduction of the intersystem PET chain. The extent of this phenotype is directly dependent upon the irradiance to which the plants are exposed (Palatnik et al., 2003). Consequently, it has been suggested that the chloroplast has a dual role. Not only does it function as the primary energy transducer in all photoautotrophs, it also

functions as a sensor of environmental change (Hüner et al., 1998; Pfannschmidt, 2003; Wilson et al., 2006; Bräutigam et al., 2009; Murchie et al., 2009).

Early research with green algae indicated that a key sensor was the redox-state of plastoquinone (PQ), a mobile electron carrier that shuttles electrons from photosystem II (PS II) to the cytochrome b_6/f complex (Escoubas et al., 1995; Maxwell et al., 1995b; Wilson et al., 2003). This was based on experiments where the characteristic, yellow-green, high light phenotype brought about by acclimation to high irradiance could be mimicked by chemically modulating the redox status of the intersystem PQ pool with the electron transport inhibitor 2,5-dibromo-3-methyl-6-isopropylbenzoquinone (DBMIB) in *Dunaliella tertiolecta* (Escoubas et al., 1995) and *Chlorella vulgaris* (Wilson et al., 2003). Since DBMIB inhibits the oxidation of plastoquinol (PQH₂) by the cytochrome b_6/f complex, PS II keeps the PQ pool reduced in the light. This induces the high light phenotype, which is characterized by low chlorophyll content per cell, high chlorophyll a/b ratio (>10), accumulation of the carotenoid binding protein, but suppression of both Lhcb2 accumulation and *Lhcb2* expression, the nuclear gene that encodes the major PS II light-harvesting antenna polypeptide (Hüner et al., 1998).

While low temperature does not affect the rate of light absorption, it severely restricts the rate of downstream, enzyme catalyzed reactions. This restricts the capacity to use NADPH and ATP, the products of the PET, thus causing an over-reduction of the PQ pool due to negative feedback. As a consequence, the yellow, low-temperature phenotype is indistinguishable from the phenotype observed in the presence of DBMIB (Maxwell et al., 1995a; Wilson et al., 2003). By contrast, since DCMU prevents the exit of electrons from PS II into the PQ pool, photosystem I (PS I) is able to keep the PQ pool oxidized in the light. Under these conditions, cells exhibit a normal green phenotype that is associated with high chlorophyll content per cell, low chlorophyll a/b ratio (3.0 to 3.5), high levels of *Lhcb2* expression, and Lhcb2 accumulation (Escoubas et al., 1995; Wilson et al., 2003). This phenotype is mimicked by growth at either low irradiance or high temperature in *C. vulgaris* (Maxwell et al., 1995a; Wilson et al., 2003). More recent

research in *Arabidopsis* suggests that redox factors on the acceptor side of PS I may be important (Dietz, 2008). These and additional signals, including the precursor of chlorophyll synthesis, magnesium protoporphyrin (Strand et al., 2003), and reactive oxygen species (ROS) generated by the PET (Meskauskiene et al., 2001; op den Camp et al., 2003), may constitute a complex network of signals involved in the retrograde pathway of communication from the chloroplast to the nucleus (Koussevitzky et al., 2007; Fernández and Strand, 2008; Woodson and Chory, 2008). However, the putative role of Mg-protoporphyrin in retrograde signaling remains equivocal (Mochizuki et al., 2008; Moulin et al., 2008). Genetic analyses in *Arabidopsis* has identified STN7 (Bellafiore et al., 2005; Bonardi et al., 2005) as a chloroplast protein kinase involved in redox signaling essential for state transitions and photosynthetic acclimation (Pesaresi et al., 2009). However, the exact nature of the mechanisms by which the redox state of the chloroplast is signaled to the nucleus resulting in altered gene expression remains largely unknown.

Changes to the redox state of the PET chain are reflected in alterations to the excitation pressure of PS II. Excitation pressure can be formally defined as the relative measure of reduction state of Q_A , ($[Q_A^-]/[Q_A] + [Q_A^-]$) (Dietz et al., 1985; Hüner et al., 1998), the first stable electron acceptor of PS II. Excitation pressure can be measured noninvasively in intact tissues using chlorophyll *a* fluorometry (Krause and Weis, 1991) to measure the parameter 1-qP (Dietz et al., 1985; Maxwell et al., 1994; Adams et al., 1995).

Photoautotrophs are in photostasis when the photochemistry induced by the absorption of light is balanced either by use of photosynthetically generated electrons through metabolism and growth or through the capacity to dissipate excess energy as heat through nonphotochemical quenching (Figure 2.2) (Hüner et al., 2003). Under such conditions, excitation pressure is low, the PQ pool is in the oxidized state, and the organism exhibits a normal, green, low excitation pressure phenotype.

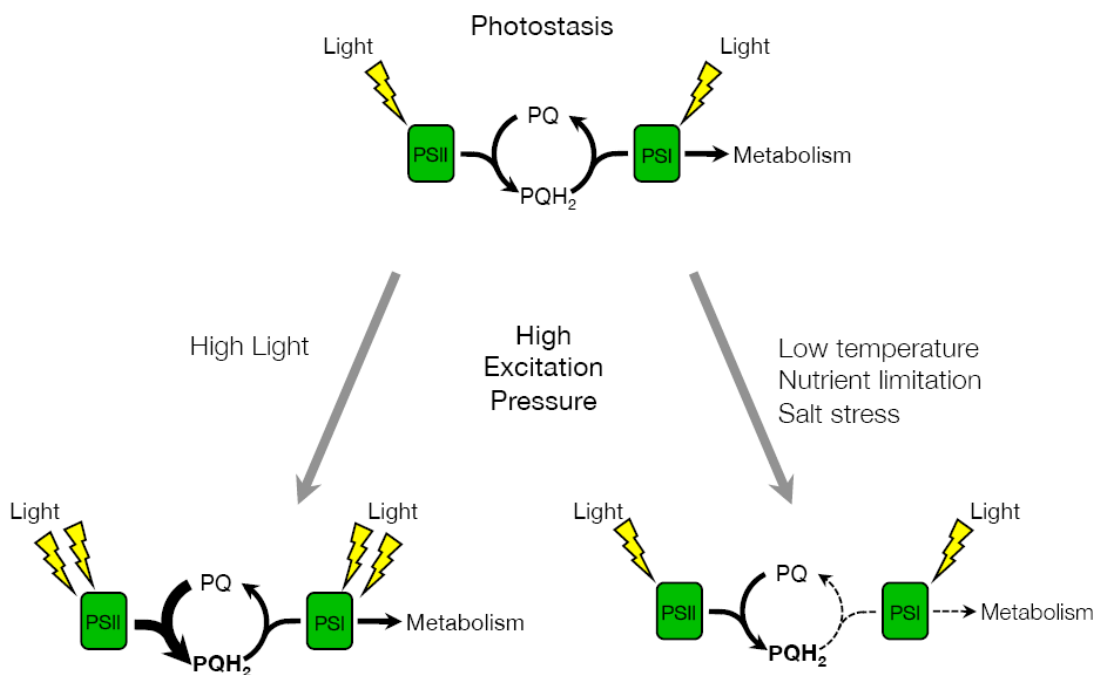


Figure 2.2 The Redox State of the PQ Pool Is a Sensor of Environmental Change

During steady state photosynthesis, the diffusion-dependent oxidation of PQH₂ is considered the rate-limiting step of PET. At photostasis (top), the rate of reduction of the PQ pool by electrons from PS II is balanced by its oxidation by PSI and the demands of downstream metabolism. Exposure of plants to high light (bottom left) results in PQH₂ accumulation, which is reflected by increased excitation pressure on PS II. High excitation pressure conditions can be also mimicked by other environmental conditions (bottom right) that limit the rate of the oxidation of the PQ pool by inhibiting downstream metabolism that consumes the electrons generated by PET.

However, myriad environmental stresses, including high irradiance (Escoubas et al., 1995), low temperature (Maxwell et al., 1995a, 1995b; Wilson and Hüner, 2000; Wilson et al., 2003), nitrogen deficiency (Cruz et al., 2003), and salt stress (Huang et al., 2005) increase excitation pressure due to energy imbalances between photochemistry and cellular energy use (Figure 2.2). In the single-cell green algae, *C. vulgaris*, *Dunaliella salina*, and *D. tertiolecta* (Escoubas et al., 1995; Maxwell et al., 1995a, 1995b) as well as the cyanobacterium *Plectonema boryanum* (Miskiewicz et al., 2000, 2002), this typically results in a high excitation pressure phenotype characterized by a decrease in chlorophyll per cell, a decreased abundance of pigments associated with the light-harvesting antenna, and a decreased photosynthetic efficiency typically associated with photoacclimation. These algae and *P. boryanum* adjust the structure and composition of light-harvesting complex II and phycobilisomes, respectively, reflecting their acclimation response to high excitation pressure.

The variegated phenotype is characterized by distinct green and white sectorized leaves (Rodermel, 2001, 2002; Miura et al., 2007). The green sectors contain normal chloroplasts, whereas the white sectors contain plastids devoid of chlorophyll and/or carotenoids (Rodermel, 2002; Miura et al., 2007). Variegated plants include the *immutans* (*im*) mutant of *Arabidopsis*, which was isolated and preliminarily characterized nearly 50 years ago (Rédei, 1963, 1975; Röbbelen, 1968). *im* is the result of a recessive mutation of the nuclear gene *IM* (Carol et al., 1999; Wu et al., 1999). Recent in vitro and in vivo evidence indicate that *IM* may be the elusive plastid terminal oxidase (PTOX), an ancillary component of the PET chain that is involved in the chlororespiratory pathway (Cournac et al., 2000; Josse et al., 2000, 2003; Joët et al., 2002; Peltier and Cournac, 2002; Fu et al., 2005; Shahbazi et al., 2007). It was first proposed by Bennoun (1982) that, during chlororespiration, reducing equivalents from the stroma are oxidized by an NAD(P)H dehydrogenase that in turn reduces the PQ pool. The function of *IM* in this chlororespiratory pathway would be to mediate the oxidation of plastoquinol (PQH₂) and the concomitant reduction of O₂ to water.

Chloroplasts and mitochondria represent the major redox compartments of plant cells that can communicate through the complex network of C- and N-metabolic pathways. Consequently, plant cellular energy metabolism involves the integration of light-dependent, photosynthetic redox reactions with the light-independent respiratory redox reactions of mitochondria (Noctor et al., 2007). The mitochondrial alternative oxidase (AOX) is upregulated under stress conditions and oxidizes the ubiquinone pool of the mitochondrial electron transport chain and lowers the potential for ROS production (Maxwell et al., 1999; McDonald, 2008). IM exhibits 37% sequence identity to AOX (Wu et al., 1999). Consequently, it was suggested that IM, like AOX, acts as an electron transport safety valve (Niyogi, 2000). Under stress conditions when the PET chain becomes overly reduced, IM may act as an alternative electron sink that, by consuming excess photosynthetically generated electrons, would minimize the formation of ROS (Niyogi, 2000). PTOX has been reported to reduce oxygen and was suggested to play an important photoprotective role in the high alpine plant species *Ranunculus glacialis* acclimated to low temperature (Streb et al., 2005). Furthermore, Stepien and Johnson (2009) reported that PTOX acts as an alternative electron sink in the salt-stressed halophyte *Thellungiella*. These effects were accompanied by a significant increase in the relative abundance of PTOX in *R. glacialis* (Streb et al., 2005) and *Thellungiella* but not in *Arabidopsis* (Stepien and Johnson, 2009). These data support the role of IM/PTOX as an alternative electron sink in alleviating overreduction of the PQ pool under unfavorable environmental conditions where PS I is limited on the acceptor side.

However, recent research comparing the function of IM in a knockout mutant as well as in overexpressing lines of *Arabidopsis* has shown that modulation of *IM* expression and polypeptide accumulation does not alter the flux of intersystem electrons reaching PS I during steady state photosynthesis nor does the presence or absence of IM affect sensitivity to photoinhibition in *Arabidopsis* (Rosso et al., 2006). Moreover, through meta-analyses of published *Arabidopsis* microarray data, Rosso et al. (2006) reported that IM expression was insensitive to a range of abiotic stresses. Taken together, these

results do not support the model of IM as a safety valve to regulate the redox state of the PQ pool during stress and acclimation in fully developed *Arabidopsis* leaves. By contrast, the meta-analysis revealed that IM did appear to be strongly regulated by development in *Arabidopsis* (Rosso et al., 2006). This is consistent with the observations of Aluru et al. (2001, 2009) who suggested that IM is required to protect against the potential for photo-oxidation during the development of chloroplasts, amyloplasts, and etioplasts.

Wu et al. (1999) proposed that the presence of white sectors in *im* plants occurs because IM plays a critical role in carotenoid biosynthesis due to its ability to oxidize the PQ pool. Briefly, a key enzyme in carotenoid synthesis is phytoene desaturase, which catalyzes the oxidation of phytoene to z-carotene, and this requires electron donation to PQ. The subsequent processing of z-carotene leads to the biosynthesis of the complete complement of carotenoids, including β -carotene, lutein, and zeaxanthin, which are required to protect the photosynthetic apparatus from photo-oxidation. By acting as a plastoquinol oxidase, IM helps to facilitate phytoene desaturase function. If the PQ pool remains reduced due to the lack of IM, carotenoid biosynthesis is blocked at the phytoene desaturase step, phytoene accumulates, and photobleaching results from an increase in chloroplastic ROS (Wetzel et al., 1994; Wu et al., 1999). Consistent with the notion that white sectoring is triggered by photo-oxidation (Aluru et al., 2009) is the fact that the variegated phenotype can be suppressed in *im* plants when grown under low-light conditions (Rédei, 1963; Wetzel et al., 1994; Aluru and Rodermel, 2004; Rosso et al., 2006).

We recently discovered that the suppression of the variegated phenotype by low light has a clear temporal component: if seedlings are germinated at 25 °C under a low irradiance of 5 $\mu\text{mol photons m}^{-2} \text{s}^{-1}$ for 7 d and subsequently shifted to growth at 50 $\mu\text{mol photons m}^{-2} \text{s}^{-1}$ for 35 d, *im* plants can be exposed to any growth irradiance and will still exhibit an all green phenotype indistinguishable from the wild type (Rosso et al., 2006). This refinement of the low light suppression of variegation suggests that

developmental stage has a critical role to play in whether or not the variegated phenotype will develop. In a recent detailed study, Miura et al. (2007) provided strong evidence that leaf variegation in the *var2* mutant of *Arabidopsis* is the result of an imbalance between the biosynthesis and degradation of the D1 protein, the Q_B binding, reaction center polypeptide of PS II, which transfers electrons to the PQ pool. However, these results still do not explain the variable pattern of sectoring typically observed during the development of a variegated leaf. Since *var2*, like *im*, is the result of a nuclear mutation, theoretically all cells should exhibit defective chloroplasts. Since this is not the case, Miura et al. (2007) conclude that further research is required to elucidate the physiological basis of the observed variegation patterns.

The objective of this study was to ascertain whether there is a physiological explanation for the green-white sectoring observed in variegated mutants of *Arabidopsis*. We hypothesized that the excitation pressure experienced early during leaf development governs the extent of variegation in the *im* mutant of *Arabidopsis*. Thus, changes in temperature should mimic the effects of irradiance on the extent of variegation observed. The development of a non-destructive imaging technique to quantify the kinetics of leaf variegation allowed us to test this hypothesis by examining the interactive effects of growth irradiance, growth temperature, and photoperiod on the extent of variegation during leaf expansion and chloroplast biogenesis.

2.2 *Methods*

2.2.1 *Growth Conditions*

Seeds of *Arabidopsis thaliana* (ecotype Columbia) wild type and the variegated mutants *im* (CS3157; AT4G22260), *var1* (CS271; AT5G42270), and *var2* (CS271; AT2G30950) were obtained from the ABRC (Columbus, OH), and *spotty* was generated as described previously (Wetzel et al., 1994). All seeds were germinated and grown under controlled environment conditions at 25 °C with a photosynthetic photon flux density of 5 $\mu\text{mol photons m}^{-2} \text{s}^{-1}$ for 1 week. Plants were thinned to one plant per pot and grown at either 25 or 12 °C with increasing irradiance of either 50, 150, or 450 $\mu\text{mol photons m}^{-2} \text{s}^{-1}$. All plants were grown with an 8/16-h day/night cycle to prevent the induction of flowering.

For the experiments that monitored the greening of cotyledons, wild-type and *im* seeds were sterilized with 20 % (v/v) bleach and 0.05 % (v/v) Tween 20 and placed on Petri plates containing 0.5x Murashige and Skoog basal salt mixture, pH 5.7, with 0.8 % (w/v) agar (McCourt and Keith, 1998), with 25 seeds per plate. The plates were placed in the dark at 4 °C for 3 d to ensure maximum, synchronized germination. Seeds were then removed from the cold treatment to 25 °C but remained in darkness for an additional 5 d. After this dark period, seeds were placed under CL at either 50 or 150 $\mu\text{mol photons m}^{-2} \text{s}^{-1}$ for a period of 24 h at 25 °C.

2.2.2 *Determination of Growth Rate*

Growth of both wild-type and *im* plants was measured by two methods. In the first method, leaf initials were observed under a dissecting microscope (LeicaWild M3B) and measured daily. Positive identification of leaf initials was standardized by counting only those leaf initials that were ≥ 1 mm. Second, growth of *Arabidopsis* was also measured by measuring leaf area as a function of time. Leaf area was measured using a dissecting microscope (LeicaWild M3B) at 4x, 10x, and 40x magnification attached to a CCD camera. Digital photos were taken, and leaf area was analyzed using imaging analysis software (Northern Eclipse Image Analysis Software 7.0; Empix Imaging). Leaf area was

measured by tracing and measuring the area of each leaf per plant. The image analysis software was calibrated with an object of known size for each magnification, and the number of pixels was divided by the appropriate conversion factor. Exponential growth rates of *Arabidopsis* leaf expansion were calculated by linear regression analysis on log-transformed data of leaf area (mm²) versus time. One-way analysis of variance (ANOVA) was performed to determine statistical significance between genotypes ($P \leq 0.05$) followed by a Bonferroni test to test for differences between group means at a 95 % confidence interval (Microcal Origin Lab 7.5; Origin Lab).

2.2.3 Quantification of Variegation

The extent of leaf variegation in *im* seedlings was estimated non-destructively from images captured by a CCD camera (Retiga 1300 monochrome 10 bit; Qimaging) attached to a dissecting microscope (Leica Wild M3B) at 4, 10, and 340 magnification as required. The camera was oriented directly over the center of the plant and the magnification selected on the dissecting microscope ensured that an image of the entire plant was captured for each measurement. Digital photos were analyzed using imaging analysis software (Northern Eclipse Image Analysis Software 7.0; Empix Imaging). The image analysis software was calibrated with an object of known size for each magnification, and the number of pixels was divided by the appropriate conversion factor. Images were then converted to grayscale, thereby creating a binary partitioning of the image intensities. An intensity value was determined, called the threshold value in order to separate green versus white sectors (Pham et al., 2000; Sezgin and Sankur, 2004). Threshold analysis was performed on each image captured to ensure that all green sectors could be clearly resolved from all white sectors irrespective of magnification. Total leaf area was measured by tracing and then calculating the area of each leaf per plant. Subsequently, the total area of white sectors per leaf was calculated and then divided by the total area of the leaf to determine the percentage of white sectors for each leaf examined. Statistical significance was determined by a one-way ANOVA at a

95 % confidence interval, followed by a Bonferroni test to test for differences between group means (Microcal Origin Lab 7.5; Origin Lab).

Variation during greening of wild-type and *im* etiolated cotyledons was assessed first by visual scoring of all cotyledons on each agar plate as either all green, all white, or variegated. Subsequently, this visual scoring of phenotype was verified by quantifying the total chlorophyll per germinated seedling from the same agar plates.

2.2.4 Chlorophyll Analyses

Chlorophyll was extracted from wild-type and *im* cotyledons with buffered 80 % (v/v) aqueous acetone containing 2.5 mM sodium phosphate buffer, pH 7.8, and was measured by the method of Porra et al. (1989). The absorbance of the extracts was measured at 663.6 and 646.6 nm and corrected to 750 nm for light scattering in a Beckman DU-640 spectrophotometer (Beckman Coulter). Total chlorophyll was divided by the total number of seedlings. One-way ANOVA was performed to determine statistical significance between genotypes ($P < 0.05$) followed by a Bonferroni test to test for differences group means at a 95 % confidence interval (Microcal Origin 7.5; Origin Lab).

2.2.5 Room Temperature Chlorophyll a Fluorescence

Light response curves and steady state fluorescence measurements were made using an Imaging PAM Chlorophyll Fluorometer (Heinz Walz). Samples were dark adapted for 20 min prior to all measurements. All fluorescence measurements were made at room temperature. The fluorescence parameters were calculated according to Schreiber et al. (1994). The maximum photochemical efficiency of PS II was calculated as F_v/F_m . Immediately after dark adaptation at room temperature, dark adapted leaves and cotyledons were exposed to a short (800 ms) pulse of saturating blue light ($6000 \mu\text{mol photons m}^{-2} \text{s}^{-1}$; $\lambda = 470 \text{ nm}$) provided by the Imaging PAM photodiode (IMAG-L; Heinz Walz). Non-photochemical quenching was calculated as q_N , and photochemical quenching was calculated as q_P (Schreiber et al., 1994). The relative reduction state of

PS II was calculated as 1-qP, which has been termed excitation pressure (Dietz et al., 1985; Hüner et al., 1998, 2003). Statistical significance was determined by a one-way ANOVA at a 95 % confidence interval, followed by a Bonferroni test to test for differences between group means (Microcal Origin Lab 7.5; Origin Lab).

2.2.6 **SDS-PAGE and Immunoblots**

Whole plants from both wild-type and *im* genotypes were frozen in liquid nitrogen and ground to a fine powder. Total protein was extracted by the addition of 4 % (w/v) SDS and heated for 20 min at 60 °C in a water bath, with occasional mixing using a vortex. Total protein was measured using a BCA protein assay kit (Pierce) by measuring the change in absorbance at 562 nm using a Beckman DU-640 spectrophotometer (Beckman Coulter). Polypeptides were loaded on an equal protein basis of 20 mg protein and were separated on a 12 % (w/v) SDS-PAGE according to the method of Laemmli (1970). Immunoblotting was performed by electrophoretically transferring the proteins from SDS-PAGE gel to a nitrocellulose membrane (Bio-Rad Laboratories). Immunodetection was performed using horseradish peroxidase–conjugated secondary antibodies (Sigma-Aldrich) and enhanced chemiluminescence according to the manufacturer (ECL; Amersham-Pharmacia Biotech).

Wild-type and *im* seedlings germinated and grown to the cotyledon stage in the dark and subsequently exposed to CL of either 50 or 150 $\mu\text{mol photons m}^{-2} \text{s}^{-1}$ at 25 °C. Seedlings were harvested either in the dark (time 0) or at various times during the greening period up to 72 h, immediately frozen in liquid nitrogen, and ground to a fine powder. Samples were loaded on an equal protein basis (7 μg protein per lane) and were separated as described above. Proteins were detected using specific polyclonal antibodies raised against protochlorophyllide oxidoreductase (POR) (1:1000 dilution; Agri-Sera), the light-harvesting complex associated with PS II (Lhcb2; 1:1000 dilution; Agri-Sera), PsbA and PsaB (1:2000 and 1:5000 dilution; Agri-Sera), and the large subunit of ribulose-1,5-bisphosphate carboxylase/oxygenase isolated from *Secale cereale* cv Musketeer (1:1000 dilution).

2.2.7 RNA Isolation, cDNA Synthesis, and Real-Time qRT-PCR

Wild-type and *im* seedlings were germinated and grown to the cotyledon stage on agar plates in the dark and subsequently exposed to CL of either 50 or 150 $\mu\text{mol photons m}^{-2} \text{s}^{-1}$ at 25 °C as described above. Seedlings were harvested either in the dark (time 0) or at various times during the greening period for up to a 24 h. Total RNA was extracted from these seedlings with the RNeasy plant mini kit (Qiagen). Total RNA (1 μg) was reverse transcribed with the high-capacity cDNA reverse transcriptase kit (Applied Biosystems). Real-time qPCR was performed using an Applied Biosystems 7900HT fast real time thermal cycler (Applied Biosystems) with primers designed for *IM*, *AOX1a*, *PHYA*, *PORA*, and an endogenous actin control gene, *ACT2*. The primers were designed between exon-exon boundaries to prevent amplification of genomic DNA. The primer sequences used are summarized in Supplemental Table 1 online. Quantitative analysis of gene expression was generated by the Power SYBR Green master mix kit (Applied Biosystems). Amplification for each gene was analyzed in the logarithmic phase. Relative quantification by comparative threshold cycle (C_T) analysis of *IM*, *AOX1a*, *PHYA*, and *PORA* was performed against an internal standard (*ACT2*), and all samples were subtracted against a calibrator sample, wild type grown in the dark (0 h) at either 50 or 150 $\mu\text{mol photons m}^{-2} \text{s}^{-1}$ depending on treatment. One-way ANOVA was performed to determine statistical significance between genotypes ($P \leq 0.05$) followed by a Bonferroni test to test for differences between group means at a 95 % confidence interval (Microcal Origin 7.5; Origin Lab).

2.2.8 Accession Numbers

Sequence data from this article can be found in the GenBank/EMBL data libraries and have the following *Arabidopsis* Genome Initiative locus identifiers: *ACT2*, At3g18780.2; *AOX1a*, At3g22370.1; *IM*, At4g22260.1; *PHYA*, At1g09570.1; *PORA*, At5g54190.1. Mutant lines used: *im* (CS3157; AT4G22260), *spotty* (AT4G22260), *var1* (CS271; AT5G42270), and *var2* (CS271; AT2G30950).

2.3 Results

2.3.1 Plant Growth

Consistent with our previous report (Rosso et al., 2006), the cotyledons and the first true leaves of *im* plants germinated and grown at 25 °C at an irradiance of 5 $\mu\text{mol photons m}^{-2} \text{s}^{-1}$ (25/5) for 7 d under a short-day photoperiod (8/16 h day/night) exhibited an all green phenotype (Figure 2.3). To determine whether growth irradiance and growth temperature affected the phenotype of the *im* mutant, the *im* seedlings subsequently were shifted to growth at either 50, 150, or 450 $\mu\text{mol photons m}^{-2} \text{s}^{-1}$ at 25 °C (25/50, 25/150, and 25/450). *im* seedlings exhibited a variegated phenotype upon exposure to growth irradiance greater than 50 $\mu\text{mol photons m}^{-2} \text{s}^{-1}$ at 25 °C (Figure 2.3; Figure 2.4). In parallel, *im* seedlings were shifted to growth at low temperature (12 °C) and increasing irradiance (12/50, 12/150, or 12/450) (Figure 2.4).

Leaf development in *im* seedlings was measured microscopically and visually on a daily basis by assessing the number of leaves initiated that were ≥ 1 mm in length. The wild type and *im* exhibited minimal differences in the rate of leaf initiation (0.0306 ± 0.001 leaves/day) throughout growth and development at 25/50 (Figure 2.4 A). After an initial lag period of ~ 7 d after the shift to increased growth irradiance, the rate of leaf initiation increased in both the wild-type and the *im* seedlings (Figure 2.4 A). Although both genotypes exhibited similar initial rates of leaf initiation at 25/150 (0.04 ± 0.001 leaves/day) and 25/450 (0.07 ± 0.001 leaves/day), the rate of leaf initiation in *im* seedlings deviated significantly from the wild type after ~ 27 d (Figure 2.4 A). Thus, leaf development in *im* seedlings appeared more sensitive to growth irradiance relative to wild-type seedlings at 25 °C.

Leaf expansion was assessed by measuring leaf area in both the wild type and *im* grown at 25 °C at 50, 150, and 450 $\mu\text{mol photons m}^{-2} \text{s}^{-1}$ (see Supplemental Figure S2.1). Both wildtype ($0.13 \text{ mm}^2/\text{day}$) and *im* seedlings ($0.12 \text{ mm}^2/\text{day}$) grown at 25/50 exhibited minimal differences in their exponential growth rates based on leaf area measurements.

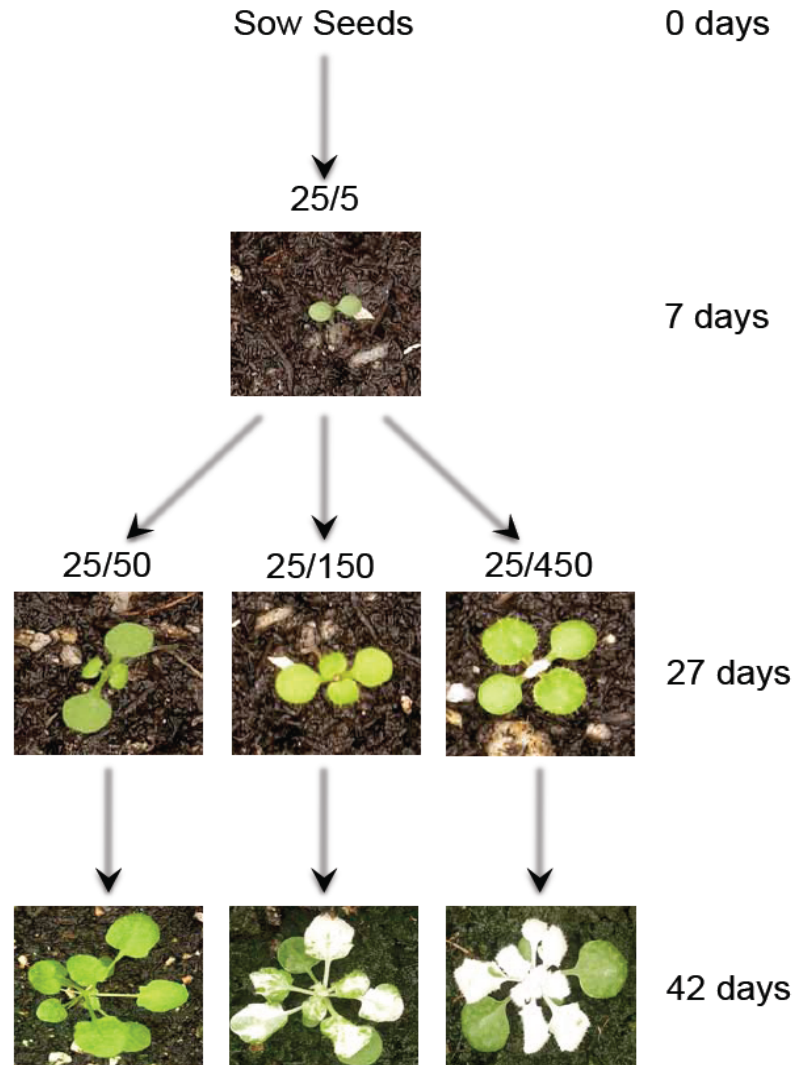


Figure 2.3 The Experimental Design to Assess the Effects of Light and Temperature on the Development of Variegation in the *im* Mutant of *Arabidopsis*

Seeds from both the wild type and *im* were germinated and allowed to grow at 25 °C under an irradiance of 5 $\mu\text{mol photons m}^{-2} \text{s}^{-1}$ (25/5) for 7 d. One group of these seedlings was shifted to either 50 (25/50), 150 (25/150), or 450 (25/450) $\mu\text{mol photons m}^{-2} \text{s}^{-1}$ for up to 42 d. In addition, a second group of the same seedlings was shifted to 12 °C at an irradiance of 50 (12/50), 150 (12/150), and 450 (12/450) $\mu\text{mol photons m}^{-2} \text{s}^{-1}$. All plants were grown with an 8/16-h day/night cycle. Photographs shown are only of *im* plants.

The exponential rate of leaf expansion appeared to be light saturated at 150 $\mu\text{mol photons m}^{-2} \text{s}^{-1}$ (0.20 mm^2/day) in *im* seedlings (see Supplemental Figure S2.1B), whereas the exponential rate of leaf expansion increased from 0.22 mm^2/day at 25/150 to 0.28 mm^2/day at 25/450 in wild-type seedlings (see Supplemental Figure S2.1A). The time required to reach the mid-log phase of growth at 25 °C increased from ~ 33 to 35 d at 50 $\mu\text{mol photons m}^{-2} \text{s}^{-1}$ to 15 to 17 days at 150 and 450 $\mu\text{mol photons m}^{-2} \text{s}^{-1}$ for both wild-type and *im* seedlings (see Supplemental Figure S2.1A). As expected, the time required to reach the mid-log phase of growth for both wild-type and *im* seedlings at 12°C increased approximately twofold at an irradiance of either 150 or 450 $\mu\text{mol photons m}^{-2} \text{s}^{-1}$ and; 1.2-fold at an irradiance of 50 $\mu\text{mol photons m}^{-2} \text{s}^{-1}$ compared with leaf expansion at 25 °C (see Supplemental Figure S2.1).

Figure 2.4. Analysis of Leaf Initiation and Variegation During Seedling Development.

(A) Kinetics of leaf initiation was assessed by counting, on a daily basis, the number of leaf initials that were greater than or equal to one mm in size for both WT (closed symbols) and *im* (open symbols) plants. Counting began exactly 7 days after seeding at $5 \mu\text{mol photons m}^{-2}\text{s}^{-1}$ at $25 \text{ }^{\circ}\text{C}$ to prevent the onset of white sectors in the cotyledons. Both genotypes were grown at $25 \text{ }^{\circ}\text{C}$ at an irradiance of either 50, 150, or $450 \mu\text{mol photons m}^{-2}\text{s}^{-1}$. All plants were grown under an 8/16 h day/night cycle.

(B, C) The kinetics of variegation in *im* seedlings. Variegation was estimated as the percentage of leaf area that was white in *im* plants using the non-destructive method described in “Materials and Methods”. Plants were grown at either $25 \text{ }^{\circ}\text{C}$ (B) or at $12 \text{ }^{\circ}\text{C}$ (C) at an irradiance of either 50, 150 or $450 \mu\text{mol photons m}^{-2}\text{s}^{-1}$. All plants were grown with an 8/16 h day/night cycle. Data represent the mean \pm SE from 10 plants per time point.

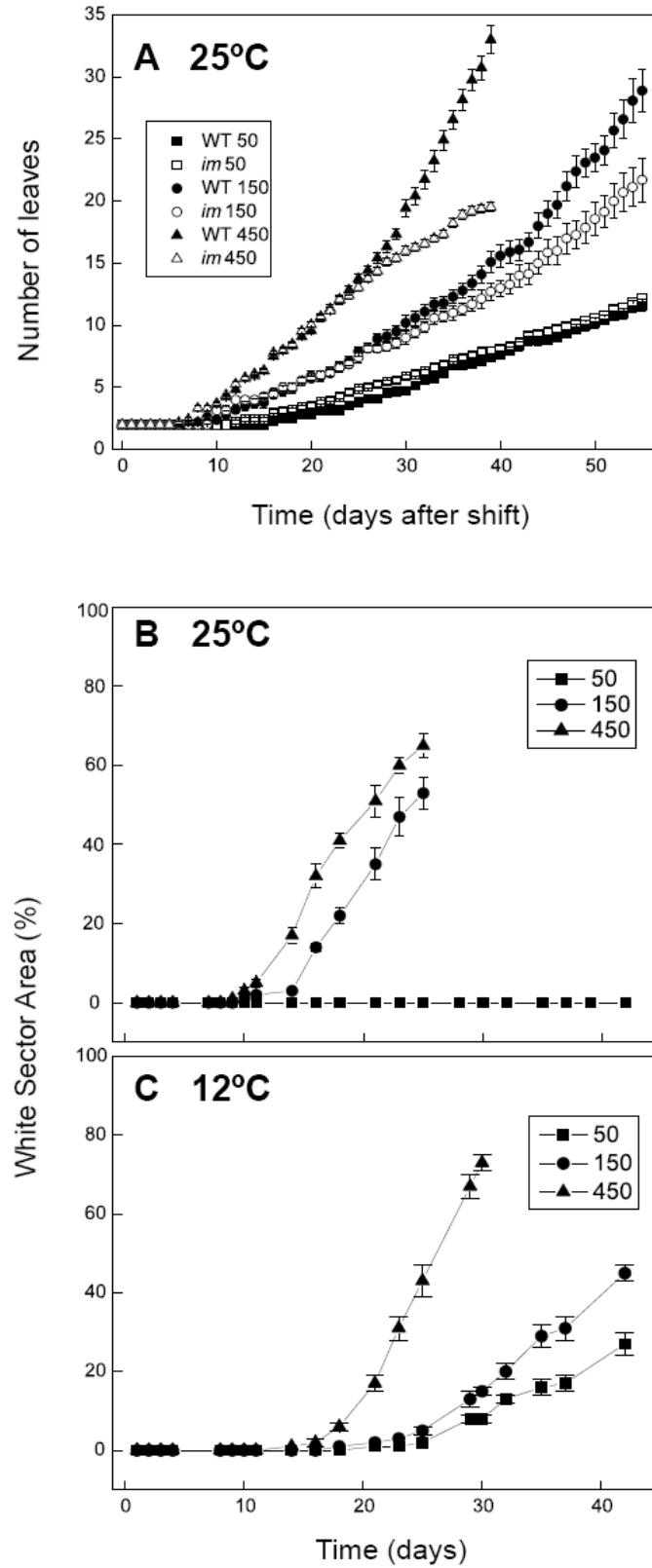


Figure 2.4 Analysis of Leaf Initiation and Variegation During Seedling Development

2.3.2 *Effects of Irradiance and Temperature on the Extent of Leaf Variegation*

The kinetics for the development of leaf variegation were quantified non-destructively in intact *im* seedlings initially germinated and grown at 25/5 and subsequently shifted to either 25/50, 25/150, or 25/450 by calculating the ratio of the area of white sectors to total leaf area per plant as a function of time. Leaves of *im* seedlings that developed at 25/50 produced no white sectors (Figure 2.4 B, closed squares) and thus exhibited an all green phenotype as previously reported by Rosso et al. (2006). However, after an initial lag of ~15 d, the percentage of leaf white sector areas increased to ~50 % at 25 d for seedlings grown at 25/150 (Figure 2.4 B, closed circles). Growth of *im* seedlings at 25/450 not only decreased the initial lag time for the development of white sectors to ~10 d but also increased the extent of variegation to ~65 % at 25 d after the shift from 25/5 (Figure 2.4 B, closed triangles).

If excitation pressure controls the variegated phenotype in *im* seedlings, then exposure to low temperature should enhance the development of leaf variegation. In contrast with growth of *im* seedlings at 25 °C, *im* seedlings exhibited a variegated phenotype at all irradiances tested during growth at 12 °C (Figure 2.4 C). *im* seedlings exhibited 25 % variegation when grown at 12 °C even at an irradiance of 50 $\mu\text{mol photons m}^{-2} \text{s}^{-1}$ for 42 d. Similar to that observed during growth at 25 °C, the lag time required to detect leaf variegation decreased with an increase in growth irradiance, and the extent of variegation increased as a function of growth irradiance as measured after 30 d (Figure 2.4 C). As expected, the lag time for the induction of the variegated phenotype increased ~1.5-fold during growth at either 12/150 or 12/450 (Figure 2.4 C) compared with growth at either 25/150 or 25/450 (Figure 2.4 B).

While using intact plants to measure the percentage of white sectors is an appropriate way to investigate the extent of variegation non-destructively, leaves of *Arabidopsis* exhibit overlap as the rosette develops. This would introduce a systematic error in our attempts to quantify the proportion of white versus green sectors in mature plants. To test the accuracy of our non-destructive method, we quantified the extent of

variegation using excised leaves, thus eliminating the potential error due to leaf overlap. Figure 2.5 illustrates the effects of growth irradiance at 25 °C (Figure 2.5 A to C) and 12 °C (Figures 2.5 D to F) on the extent of variegation in cotyledons (Figure 2.5, Cot.) and subsequent leaf pairs (1st to 4th) of the rosette. The trends for the effects of irradiance on the extent of variegation for excised leaves developed at either 25 °C (Figure 2.5 G) or 12 °C (Figure 2.5 H) were comparable to those estimated at the end of each experiment illustrated in Figures 2.4 B and C. However, we found that the non-destructive method systematically overestimated the proportion of white to green sectors by 5 to 10 % in mature plants compared with the destructive method. We noted with interest that cotyledons (Figures 2.5 A and 2.5 D, Cot.) and the first true leaves (Figures 2.5 A and 2.5 D, 1st) of *im* plants exhibited an all green phenotype irrespective of conditions during growth under an 8-h photoperiod (Figures 2.5 A to 2.5 F).

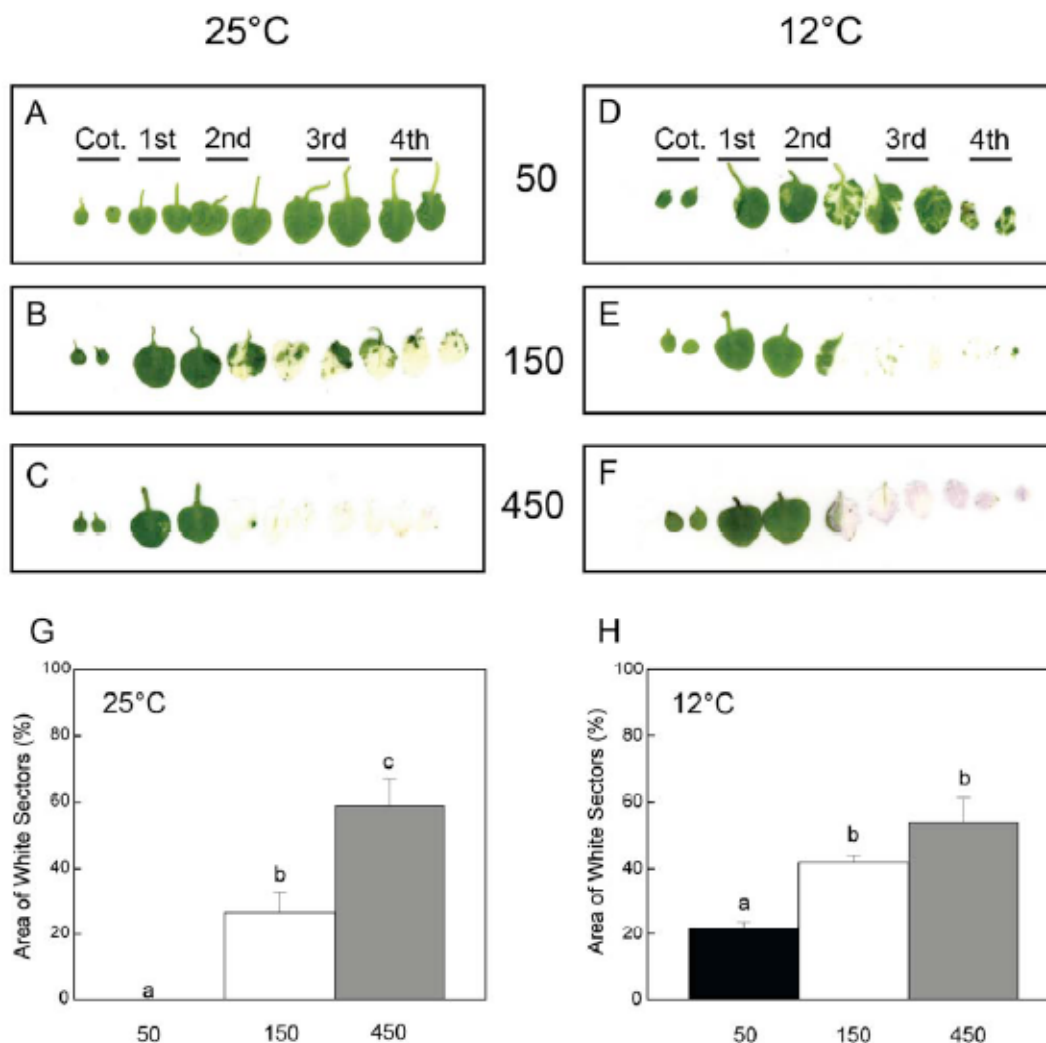


Figure 2.5 Leaf Phenotype and Quantified Variegation of Excised Leaves.

(A) to (C) Leaf scans performed on *im* plants that were grown at 25 °C and either 50, 150, or 450 $\mu\text{mol photons m}^{-2} \text{s}^{-1}$. The leaf scans are arranged in consecutive order of development, from the cotyledons (Cot.) to the 4th leaf pair. All plants were grown under an 8/16-h day/night cycle. (D) to (F) Leaf scans were performed as described above except *im* plants were grown at 12 °C and either 50, 150, or 450 $\mu\text{mol photons m}^{-2} \text{s}^{-1}$. (G) and (H) Quantification of variegation from the scans for *im* leaves developed at 25 °C (G) or 12 °C (H) and either 50, 150, or 450 $\mu\text{mol photons m}^{-2} \text{s}^{-1}$. Variegation was estimated as the percentage of white sectors as described in “Material and Methods”. Data represent the mean \pm SE calculated from two independent experiments with three to six different plants per treatment. Letters represent statistically significant differences between means at the 95 % confidence interval.

Our growth kinetic data indicated that low temperature increases the time required to reach mid-log phase of growth in wild-type and *im* plants. However, by comparing plants at the mid-log phase of growth, we were able to assess the interactive effects of growth irradiance and growth temperature on the extent of variegation in *im* seedlings at the same developmental stage. At mid log-phase during growth at 25 °C, the proportion of white sectors was 0, 8, and 25 % at 50, 150, and 450 $\mu\text{mol photons m}^{-2} \text{s}^{-1}$, respectively. By contrast, at mid-log phase during growth at 12 °C, the proportion of white sectors was 20, 40, and 60 % at 50, 150, and 450 $\mu\text{mol photons m}^{-2} \text{s}^{-1}$. Thus, when measured at the same developmental stage, *im* seedlings exhibited greater variegation at low temperature than at 25 °C irrespective of irradiance. Thus, it appears that the extent of variegation is the result of a complex interaction between growth irradiance and growth temperature.

2.3.3 ***Effects of Irradiance and Temperature on Excitation Pressure and Photoacclimation***

Excitation pressure, measured as $1 - qP$, is an estimate of the proportion of closed PS II reaction centers, which reflects the redox state of the PET chain. Consequently, excitation pressure should be sensitive to both irradiance and temperature (Dietz et al., 1985; Hüner et al., 1998, 2003; Wilson et al., 2006). Since IM is considered to be a plastid terminal oxidase capable of oxidizing the intersystem PQ pool (Joët et al., 2002; Josse et al., 2003, Aluru and Rodermel, 2004; Streb et al., 2005; Stepien and Johnson, 2009), we examined the effects of either changes in irradiance or temperature on excitation pressure in *im* seedlings. The data in Figure 2.6A illustrate the light response curves for excitation pressure in fully expanded leaves of *im* seedlings grown at 25/50, which results in an all green phenotype. At a measuring temperature of 25 °C (closed squares), excitation pressure in *im* seedlings exhibited the expected light saturation response to increasing measuring irradiance and resulted in an apparent quantum requirement, estimated from the initial slope of the light response curve, of 263 $\mu\text{mol photons m}^{-2} \text{s}^{-1}$ absorbed to close 50 % of the PS II reaction centers. However, lowering the measuring temperature from 25 to 5 °C (open squares) significantly increased

excitation pressure at any given irradiance, and as a result, the quantum requirement decreased to only 63 μmol photons absorbed to close 50 % of PS II reaction centers. The sensitivity of PS II reaction centers to closure increased fourfold by simply decreasing the measuring temperature from 25 to 5 °C (Figure 2.6A). Thus, excitation pressure in *im* seedlings responds to short-term light and temperature changes as expected (Maxwell et al., 1995a) and in a similar fashion to that observed for the wild type.

However, can *im* seedlings photoacclimate in response to increased growth irradiance? If so, then *im* seedlings should respond to increased growth irradiance by decreasing the efficiency of PS II reaction center closure. This can be detected as an increase in the quantum requirement for PS II closure measured as a decrease in the initial slope of the light response curve for excitation pressure. The data in Figure 2.6B illustrate that the initial slope of the light response curves for excitation pressure in green sectors decreased as the irradiance for growth and development of *im* seedlings increased from 50 to 450 $\mu\text{mol photons m}^{-2} \text{s}^{-1}$. As a consequence, the quantum requirement for PS II closure in green sectors increased with increasing growth irradiance from 298 to 439 to 610 $\mu\text{mol photons m}^{-2} \text{s}^{-1}$ absorbed to close 50 % of PS II reaction centers in *im* seedlings grown at 25/50, 25/150, and 25/450, respectively. Similar trends were observed for growth of *im* seedlings under increasing irradiance at 12 °C (see Supplemental Figure S2.2). Since *im* seedlings decreased their efficiency for PS II closure in response to either high growth irradiance or low growth temperature, we conclude that *im* seedlings photoacclimate to excitation pressure as reported previously for wheat (*Triticum aestivum*), rye (*Secale cereale*), the green algae *C. vulgaris* and *D. tertiolecta*, as well as the cyanobacterium *P. boryanum* (Hüner et al., 2003).

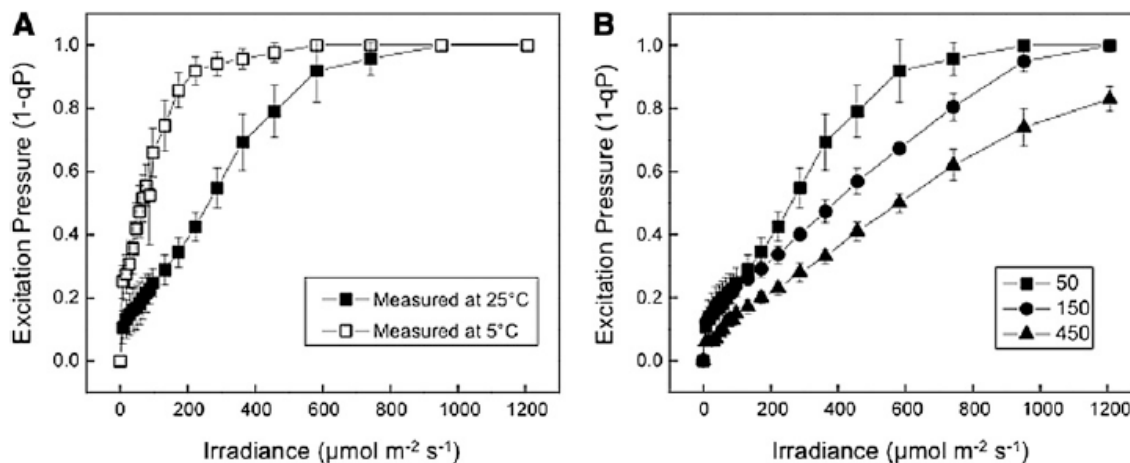
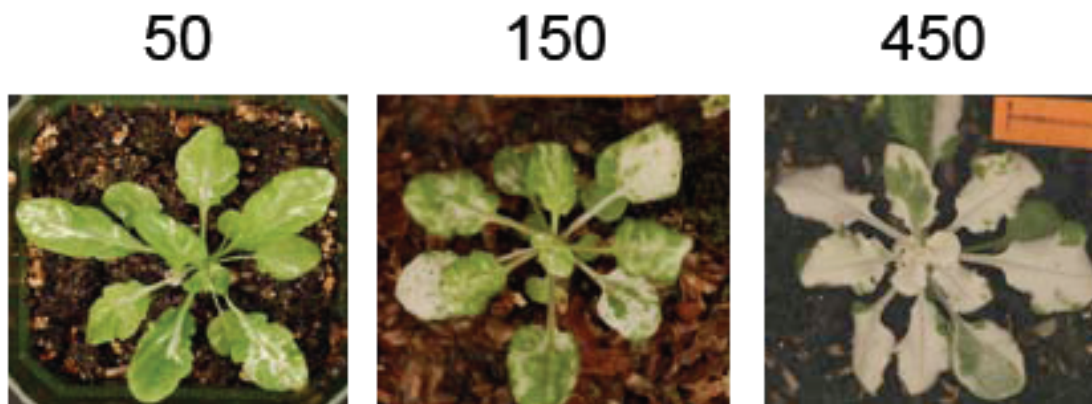


Figure 2.6 The Effects of Irradiance and Temperature on Excitation Pressure and Photoacclimation in *im*

(A) The effects of measuring temperature on excitation pressure (1-qP) light response curves for the *im* mutant of *A. thaliana*. *im* seedlings were grown to mid-log phase at 25 °C and 50 $\mu\text{mol photons m}^{-2}\text{s}^{-1}$. Excitation pressure was measured on attached leaves at either 25 °C (closed squares) or at 5 °C (open circles) with increasing irradiance from 0 – 1200 $\mu\text{mol photons m}^{-2}\text{s}^{-1}$. **(B)** The effects of growth irradiance on excitation pressure (1-qP) in attached leaves of *im* seedlings. Plants were grown to mid-log phase at either 25/50, 25/150 or 25/450 and measured at 25 °C with increasing irradiance from 0 – 1200 $\mu\text{mol photons m}^{-2}\text{s}^{-1}$. For both A and B, plants were grown with an 8/16 h day/night cycle and attached leaves were measured 4 h into the photoperiod. Data represent the mean \pm SE calculated from 2 independent experiments with 3-6 different plants per treatment.

Although excitation pressure may be calculated as either $1-q_P$ (Dietz et al., 1985; Schreiber et al., 1994; Hüner et al., 1998) or $1-q_L$ (Kramer et al., 2004; Baker, 2008), the use of the Heinz-Walz Imaging PAM (see Methods) precludes the ability to calculate q_L . However, our previous results (Rosso et al., 2006) indicate that although the absolute values of excitation pressure may vary depending upon whether it is calculated as $1-q_P$ or $1-q_L$, the trends do not.



**Figure 2.7 The Effects of Excitation Pressure and Continuous Light on Leaf
Variegation**

Representative photographs of *im* plants grown at 25 °C under continuous light of either 50, 150, or 450 $\mu\text{mol photons m}^{-2}\text{s}^{-1}$.

2.3.4 ***Interaction of Photoperiod, Temperature, and Irradiance on Excitation Pressure and Leaf Variegation***

Plant development is very sensitive to photoperiod (Bae and Choi, 2008). In our experimental design (Figures 2.3 and 2.4), all seedlings were grown under a short-day, 8-h photoperiod to prevent flowering and to ensure that they remained in the vegetative state over the course of our experiments. To assess the potential influence of photoperiod on the extent of variegation, we exposed *im* seedlings to continuous light (CL) under growth conditions of either 25/50, 25/150, or 25/450 (Figure 2.7). *im* seedlings grown under CL exhibited an increase in variegation at 25 °C as irradiance increased from 50 to 450 $\mu\text{mol photons m}^{-2} \text{s}^{-1}$ (Figure 2.7) similar to that observed for *im* seedlings grown under the short-day photoperiod (Figure 2.5). However, in contrast with growth under a short-day photoperiod and 50 $\mu\text{mol photons m}^{-2} \text{s}^{-1}$, which induced no variegation (Figures 2.4B and 2.5G), *im* seedlings grown under CL at the same irradiance exhibited 30% variegation (Figure 2.7), which is similar to that observed for *im* seedlings grown at 50 $\mu\text{mol photons m}^{-2} \text{s}^{-1}$ but at low temperature (12 °C) (Figures 2.4C and 2.5H).

The extent of variegation induced by CL also appeared to be a response to increased excitation pressure (Figure 2.7). At mid-log phase of vegetative growth, *im* seedlings grown under an 8-h photoperiod at 25/50 exhibited the lowest excitation pressure ($1-qP = 0.16 \pm 0.01$), at 25/150 exhibited moderate excitation pressure ($1-qP = 0.345 \pm 0.01$), whereas those grown at 25/450 exhibited the highest excitation pressure ($1-qP = 0.500 \pm 0.01$). Consequently, we observed a strong, positive correlation ($R^2 = 0.750$) between excitation pressure and the extent of variegation irrespective of whether excitation pressure was modulated by irradiance, low temperature, or by exposure to CL (Figure 2.8).

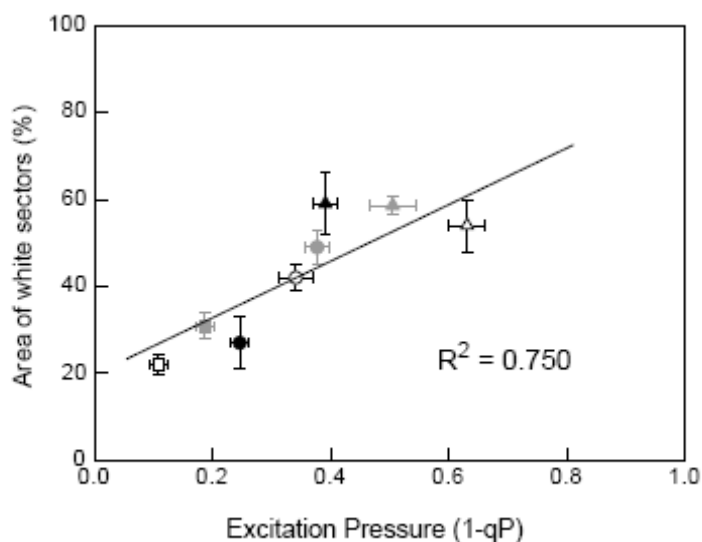


Figure 2.8 Correlation Between Variegation of *im* Seedlings and Excitation Pressure Experienced Under Various Growth Conditions

Variegation was measured as percent white sector area as described in Materials and Methods. All plants were germinated and grown for one week at $5 \mu\text{mol photons m}^{-2}\text{s}^{-1}$ at $25 \text{ }^\circ\text{C}$ under 8/16 h day night cycle and were then shifted to different temperature/irradiance conditions for the remainder of the experiment. Temperature/irradiance: closed circles, 25/150; closed triangles 25/450; open squares, 12/50; open circles, 12/150; open triangles, 12/450; closed squares, 25/50 CL; closed circles, 25/150 CL; closed triangles, 25/450 CL. Data represent the mean \pm SE with five to six different plants per treatment.

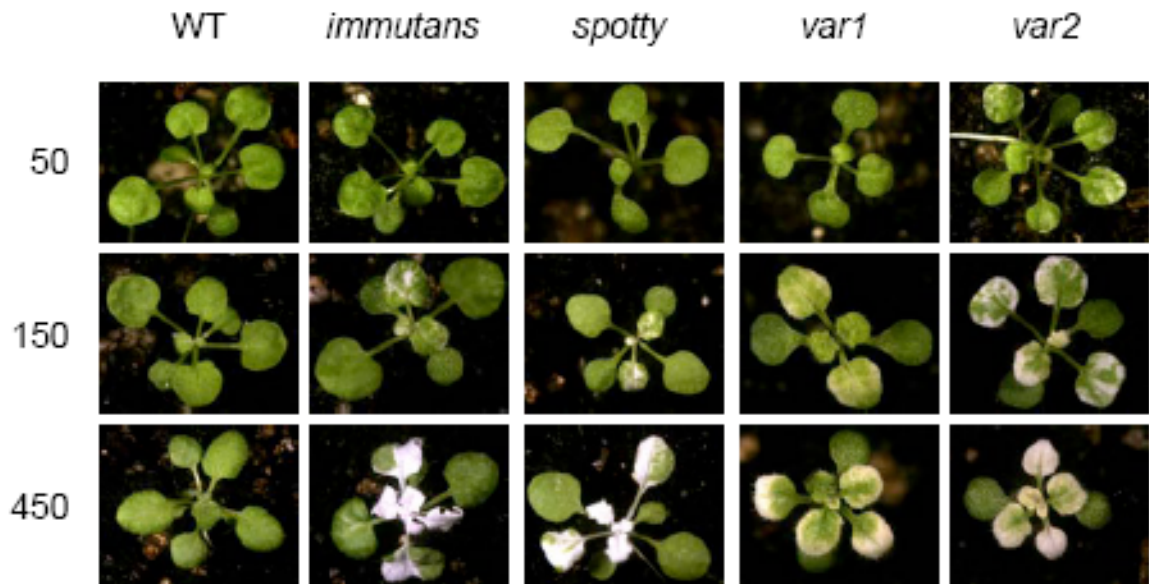


Figure 2.9 Variegation Mutant Phenotypes

Representative photographs of WT, *im*, *spotty*, *var1* and *var2* seedlings grown at 25 °C at an irradiance of either 50, 150, or 450 $\mu\text{mol photons m}^{-2}\text{s}^{-1}$.

In addition to *im*, several other mutants of *Arabidopsis*, such as *spotty*, *var1*, and *var2*, exhibit a variegated phenotype (Aluru et al., 2006; Miura et al., 2007). Consequently, we examined the effects of varying the growth irradiance regime at 25 °C for *spotty*, *var1*, and *var2* (Figure 2.9). The extent and pattern of variegation for *spotty* (Figure 2.9; see Supplemental Figure S2.3) was very similar to those observed for *im* (Figure 8). Although both *var1* and *var2* also exhibited an increase in the extent of variegation as a function of growth irradiance at 25 °C (Figure 2.9), the patterns of leaf sectoring and the pigmentation of the variegated sectors were distinct from those observed for either *im* or *spotty*. Furthermore, variegation in *var2* appeared to be more sensitive to growth irradiance than either *im*, *spotty*, or *var1* since significant variegation could be detected in the former even at the low growth irradiance of $50 \mu\text{mol m}^{-2} \text{s}^{-1}$ under an 8-h photoperiod (Figure 2.9; see Supplemental Figure S2.3). Irrespective of the irradiance, growth at 12 °C enhanced the extent of variegation in *spotty*, *var1*, and *var2* (see Supplemental Figure S2.4) as was observed for *im* (Figures 2.4 and 2.5; see Supplemental Figure S2.4). Since IM cannot compete with P700^+ of PS I for PS II generated electrons and hence decrease EP in fully expanded leaves of wild-type seedlings (Rosso et al., 2006), this prompted the question of why the absence of IM leads to variegation under high excitation pressure in *Arabidopsis*.

Figure 2.10. The Effects of Irradiance on Chloroplast Development. (A)

Representative photographs showing cotyledons of WT and *im* plants germinated at 25 °C and either 50 or 150 $\mu\text{mol photons m}^{-2}\text{s}^{-1}$.

(B) The effect of growth irradiance on the proportion of green seedlings in *im*. 625 seedlings (25 per agar plate) were germinated in the dark for a period of 5 days and subsequently exposed to continuous irradiance of either 50 or 150 $\mu\text{mol photons m}^{-2}\text{s}^{-1}$ for 24h at 25 °C. The number of green versus either variegated or white cotyledons was scored visually. Letters represent statistically significant differences between means at the 95 % confidence interval.

(C) Accumulation of chloroplast polypeptides in WT and *im* cotyledons as a function of time (h) during greening. Seeds were germinated in the dark for 5 days and subsequently exposed to continuous light of either 50 or 150 $\mu\text{mol photons m}^{-2}\text{s}^{-1}$ for up to 24 h at 25 °C. SDS-PAGE was carried out using equal amounts of protein per lane. Immunoblots were probed with polyclonal antibodies raised against POR, Lhcb2 and RbcL as described in Materials and Methods.

(D) Relative expression level of *PORA* mRNA during greening of dark grown WT and *im* cotyledons at either 50 or 150 $\mu\text{mol photons m}^{-2}\text{s}^{-1}$ using qRT-PCR. The relative expression levels of mRNA in 3 replicate samples were normalized to *Actin2* which served as the endogenous control and were standardized to a calibrator sample consisting of mRNA from dark grown WT seedlings (0 h) at both 50 and 150 $\mu\text{mol photons m}^{-2}\text{s}^{-1}$, at 25°C.

(E) Relative expression level of *PHYA* mRNA during greening of dark grown WT and *im* cotyledons at either 50 or 150 $\mu\text{mol photons m}^{-2}\text{s}^{-1}$ using qRT-PCR. All conditions are identical to those described in D.

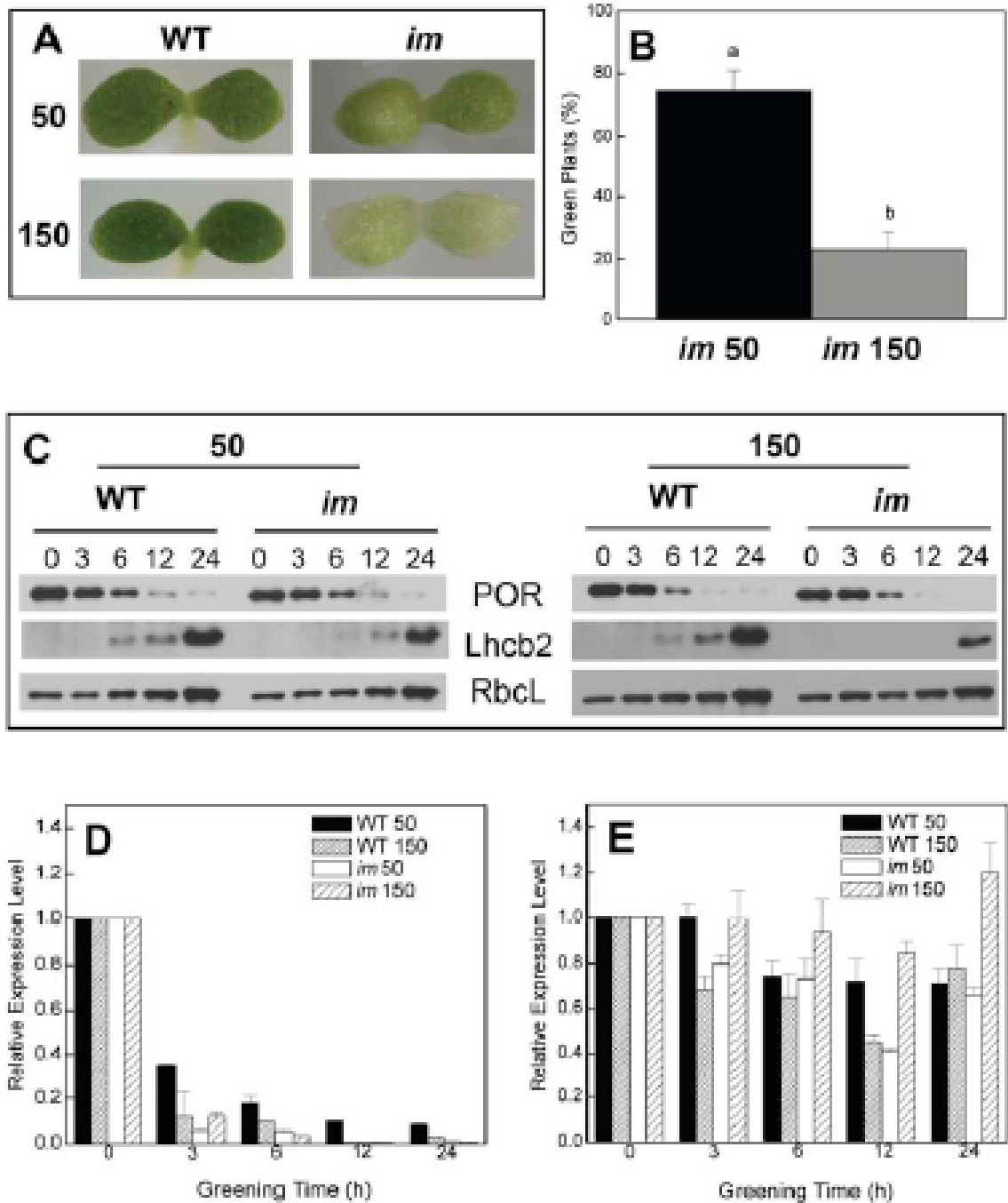


Figure 2.10 The Effects of Irradiance on Chloroplast Development

2.3.5 Greening of *im* Cotyledons

Since excitation pressure appeared to regulate the extent of variegation in *im* seedlings (Figure 2.8), we hypothesized that IM may be important in keeping the PQ pool oxidized early in chloroplast biogenesis during the assembly of the photosynthetic apparatus. To test this hypothesis, both wild-type and *im* knockout seedlings were germinated and grown in the dark prior to exposure to either low or high irradiance at 25 °C under CL conditions for 24 h. The greening of cotyledons was used to assess etioplast-to-chloroplast conversion in both the wild type and *im*. Although all wild-type cotyledons exhibited normal greening at either 50 or 150 $\mu\text{mol photons m}^{-2} \text{s}^{-1}$ (Figure 2.10A), 75 % of the *im* cotyledons that were subjected to greening at 50 $\mu\text{mol photons m}^{-2} \text{s}^{-1}$ exhibited an all green phenotype whereas 25 % were variegated (Figures 2.10A and 2.10B). By contrast, only 25 % of the *im* cotyledons that were subjected to greening at 150 $\mu\text{mol photons m}^{-2} \text{s}^{-1}$ exhibited an all green phenotype, whereas 75 % were variegated (Figures 2.10A and 2.10B). This visual scoring was confirmed by quantifying total chlorophyll per seedling after 24 h greening. Both wild-type (63 ± 11 ng chlorophyll/seedling) and *im* seedlings (64 ± 11 ng chlorophyll/seedling) exhibited similar chlorophyll levels when exposed to greening at 50 $\mu\text{mol photons m}^{-2} \text{s}^{-1}$. By contrast, the chlorophyll content of wildtype etiolated seedlings exposed to greening at 150 $\mu\text{mol photons m}^{-2} \text{s}^{-1}$ was 72 ± 6 ng chlorophyll/seedling, whereas greening of *im* etiolated seedlings at the same irradiance resulted in 56 % decrease in chlorophyll content (28 ± 5 ng chlorophyll/seedling). Furthermore, even after an extension of the greening time to 72 h at 150 $\mu\text{mol photons m}^{-2} \text{s}^{-1}$, 60 % of *im* seedlings exhibited an all white phenotype, 32 % were variegated, and 8 % exhibited an all green phenotype.

Protochlorophyllide oxidoreductase (POR) is the major polypeptide associated with the prolamellar bodies of etioplasts, and its disappearance represents an excellent marker for the conversion of etioplasts to chloroplasts (Biswal et al., 2003; Philippar et al., 2007; Sakamoto et al., 2008). Similarly, Lhcb2, a major polypeptide of PS II light-harvesting pigment protein complex, PsbA, the D1 reaction center polypeptide of PS II, and PsaA/B,

the reaction center polypeptide of PS I, were used as markers for the biogenesis of thylakoid membranes (Biswal et al., 2003; Minai et al., 2006). Ribulose-1,5-bisphosphate carboxylase/oxygenase was used as a marker for the development of Calvin cycle in the stroma of the chloroplast. The abundance of POR was comparable in wild-type and *im* etiolated cotyledons (Figure 2.10C, 0). Furthermore, POR abundance decreased similarly during greening under CL at either 50 or 150 $\mu\text{mol photons m}^{-2} \text{s}^{-1}$ such that minimal levels were detected after 24 h of greening in both wild-type and *im* cotyledons (Figure 2.10C). The kinetics for the disappearance of *PORA* mRNA (Figure 2.10D) was similar to that for the decrease in POR polypeptide levels during greening of both wild-type and *im* cotyledons irrespective of irradiance. In contrast with *PORA*, *PHYA* expression remained relatively constant throughout the greening process, and no trends in differential *PHYA* expression were observed during greening of wild-type and *im* cotyledons (Figure 2.10E).

As expected, Lhcb2 polypeptides were not detected in either wild-type or *im* etiolated cotyledons (Figure 2.10C, 0). The relative abundance of Lhcb2 increased similarly during greening of both genotypes when exposed to CL of 50 $\mu\text{mol photons m}^{-2} \text{s}^{-1}$. Lhcb2 was detected from 6 h after exposure to 50 $\mu\text{mol photons m}^{-2} \text{s}^{-1}$ and reached a maximum abundance after 24 h (Figure 2.10C). Although the kinetics of Lhcb2 accumulation during greening of wild-type cotyledons appeared to occur independently of irradiance, Lhcb2 accumulation during greening of *im* cotyledons appeared to be irradiance dependent. Lhcb2 was detected only after 24 h of greening of *im* cotyledons under CL at 150 $\mu\text{mol photons m}^{-2} \text{s}^{-1}$ and was present at reduced levels relative to greening of *im* cotyledons at 25/50 (Figure 2.10C). In the wild type, PsaB was detectable between 3 and 6 h followed by the detection of PsbA after 6 to 12 h of greening at 150 $\mu\text{mol photons m}^{-2} \text{s}^{-1}$, whereas their appearance was delayed during greening of *im* cotyledons relative to the wild type (see Supplemental Figure S2.5). RbcL was present in etiolated cotyledons, and its abundance increased similarly as a function of greening time in both wild-type and *im* seedlings irrespective of irradiance (Figure 2.10C).

2.3.5 *Differential Changes in PS II Photochemistry During Greening of Cotyledons*

The parameter F_v/F_m is a measure of the maximum photochemical efficiency of PS II and can be used as an indicator of the competence of PS II photochemistry and PET (Schreiber et al., 1994; Kramer et al., 2004; Baker, 2008). Upon exposure of etiolated wild-type (closed symbols) and *im* cotyledons (open symbols) to greening under CL at $50 \mu\text{mol photons m}^{-2} \text{s}^{-1}$, there was an initial lag of 3 h in F_v/F_m (Figure 2.11A). Maximum F_v/F_m was attained after 24 h in both the wild-type control ($F_v/F_m = 0.760 \pm 0.005$) and *im* cotyledons ($F_v/F_m = 0.658 \pm 0.023$). Thus, the final F_v/F_m of *im* cotyledons was only ~ 13 % lower than that of wild-type seedlings after 24 h of greening at low light (Figure 2.11A).

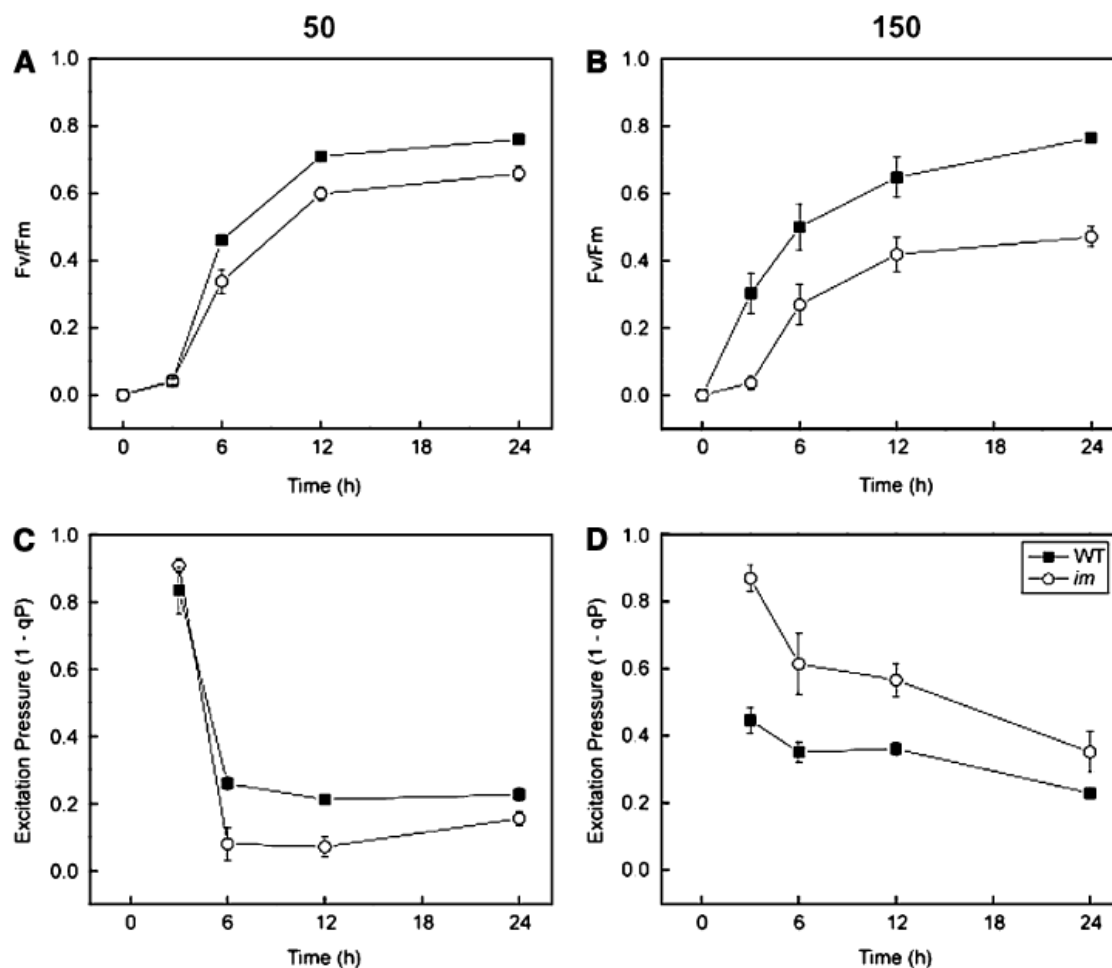


Figure 2.11 The Development of Photosystem II Photochemistry in WT and *im*

(A, B) Development of maximum PS II photochemical efficiency (F_v/F_m) during greening of etiolated WT and *im* cotyledons at 25 °C under an irradiance of either 50 (A) or 150 (B) $\mu\text{mol photons m}^{-2}\text{s}^{-1}$. Data represent mean \pm SE of 5-11 different seedlings per time point.

(C, D) The effect greening time on the excitation pressure ($1 - qP$) of etiolated WT and *im* cotyledons. For each time point, 250 seeds among 10 agar plates were germinated in the dark for 5 days and subsequently exposed to continuous light of either 50 or 150 $\mu\text{mol photons m}^{-2}\text{s}^{-1}$ for up to 24 h at 25°C. All seedlings were dark adapted for 20 min prior to measurement of F_v/F_m and $1 - qP$. Data represent the mean \pm SE from 5-11 different seedlings per time point.

When wild-type etiolated cotyledons were exposed to greening under CL at $150 \mu\text{mol photons m}^{-2} \text{s}^{-1}$, the F_v/F_m increased to 0.765 ± 0.01 after 24 h of exposure with no initial lag period (Figure 2.11B, closed symbols). By contrast, *im* etiolated cotyledons exposed to greening still exhibited an initial 3-h lag time after which F_v/F_m increased to a maximum of only 0.471 ± 0.03 after 24 h (Figure 10B, open symbols). Thus, after 24 h of greening at $150 \mu\text{mol photons m}^{-2} \text{s}^{-1}$, F_v/F_m of *im* cotyledons was 38 % lower than that of wild-type controls. The apparent inhibition of PS II photochemistry during greening at the higher irradiance in *im* cotyledons compared with the wild type (Figure 2.11B) is consistent with the inhibition of chlorophyll accumulation in *im* cotyledons (Figures 2.10A and 2.10B).

Concomitantly, excitation pressure (1-qP) was measured in both wild-type and *im* etiolated cotyledons exposed to greening under CL at $50 \mu\text{mol photons m}^{-2} \text{s}^{-1}$. After 3 h of exposure to CL, 80 to 90 % of the PS II reaction centers in wild-type (1-qP = 0.834 ± 0.07) and *im* cotyledons (1-qP = 0.908 ± 0.020) were still closed (Figure 2.11C). However, 1-qP decreased dramatically between 3 and 6 h of greening and remained relatively constant for the duration of the greening period such that after 24 h, wild-type cotyledons exhibited a 1-qP of 0.227 ± 0.020 and the mutant a 1-qP value of 0.160 ± 0.020 (Figure 2.11C). This indicates that PS II reaction centers opened rapidly in the first 6 h of greening at low irradiance for both wild-type and *im* cotyledons.

In contrast with greening at $50 \mu\text{mol photons m}^{-2} \text{s}^{-1}$, excitation pressure was significantly lower after 3 h of greening at $150 \mu\text{mol photons m}^{-2} \text{s}^{-1}$ in wild-type (1-qP = 0.446 ± 0.040) than *im* cotyledons (1-qP = 0.869 ± 0.040) (Figure 2.11D). This trend persisted throughout the 24-h greening process under CL at $150 \mu\text{mol photons m}^{-2} \text{s}^{-1}$, which indicates that a greater proportion of PS II reaction centers remained closed in *im* than wild-type cotyledons during greening under CL at $150 \mu\text{mol photons m}^{-2} \text{s}^{-1}$. Since *im* cotyledons cannot synthesize carotenoids involved in the xanthophyll cycle (Wetzels et al., 1994), non-photochemical quenching (qN) capacity did not change during the 24-h greening period, whereas wild-type cotyledons exhibited a 1.5-fold increase in qN

after 12 h of greening. Thus, the differential sensitivity of greening to irradiance in *im* compared with wild-type cotyledons was associated with the maintenance of a higher excitation pressure in *im* seedlings especially during the first 12 h of greening.

2.3.6 ***Effects of a Short Pulse of High Light on Greening in Cotyledons***

To test whether the apparent differential excitation pressure observed during the first 12 h of greening in the wild type versus *im* cotyledons (Figure 2.11D) affects chloroplast biogenesis, etiolated cotyledons of wild-type and *im* cotyledons were subjected to a single, 60-min pulse of high excitation pressure created by high light exposure (HL; 700 $\mu\text{mol photons m}^{-2} \text{s}^{-1}$) at various times during early chloroplast biogenesis and subsequently shifted back to a continuous low-light greening regime (LL; 15 $\mu\text{mol photons m}^{-2} \text{s}^{-1}$). If uninterrupted, this treatment should result in a comparable all green phenotype in the wild type as well as *im*. This HL irradiance was chosen because, based on the data presented in Figure 2.6B (closed squares), exposure to 700 $\mu\text{mol photons m}^{-2} \text{s}^{-1}$ would be sufficient to create maximum excitation pressure ($1-qP = 1.0$) in low-light-grown *im* seedlings. The data in Figure 2.12 (control) confirmed that the chlorophyll content of wild-type (Figure 2.12, black bar) and *im* cotyledons (Figure 2.12, white bar) subjected to greening for 24 h under the continuous LL were indeed comparable, indicating normal chloroplast biogenesis in both genotypes.

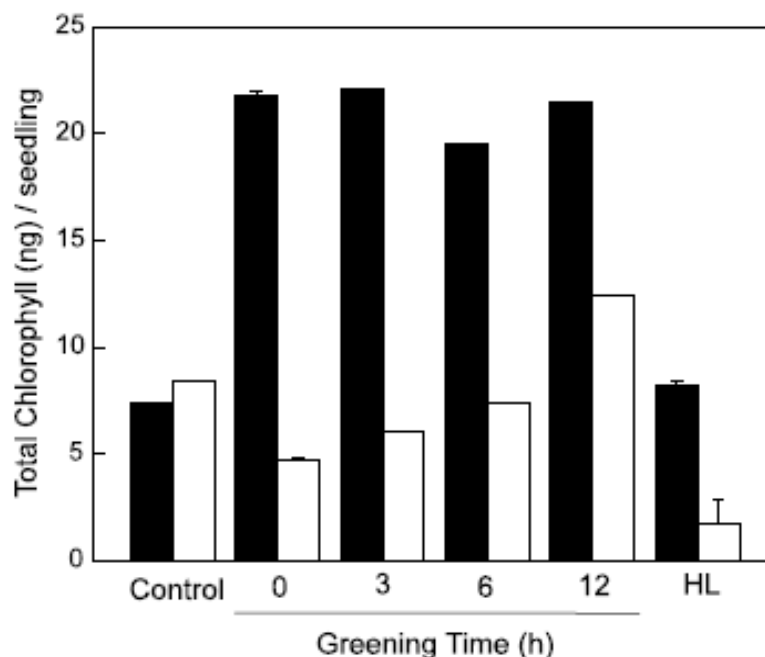


Figure 2.12 The Effects of a HL Pulse on Greening in WT and *im* Cotyledons

Seeds of WT and *im* were germinated on agar plates and grown in the dark as described for Figure 9. Etiolated cotyledons were then shifted to low light (LL, $15 \mu\text{mol photons m}^{-2}\text{s}^{-1}$) at 25°C to initiate greening. The extent of greening was quantified as total chlorophyll per seedling in WT (closed bars) and *im* (open bars). Control, etiolated cotyledons were exposed to greening under continuous LL for 24h. In addition, etiolated WT and *im* cotyledons were exposed to a 23h of greening at LL which was interrupted by a 60 min exposure to HL ($700 \mu\text{mol photons m}^{-2}\text{s}^{-1}$) either prior to exposure to greening at LL (0 greening time) or after 3h, 6h or 12h of greening under continuous LL. After the 60 min exposure to HL, cotyledons were transferred back to continuous LL to complete the 24h of greening. After 24h of greening, the total Chl accumulated per seedling was determined. The data represent the means \pm SD of 3 replicate Chl measurements within a single experiment. The number of seedlings used per treatment ranged between 80 and 150.

Exposure of wild-type etiolated cotyledons to a single, 60-min pulse of HL stimulated chlorophyll accumulation threefold to fourfold relative to controls during subsequent greening at LL regardless of time at which this pulse of HL was imposed within the first 12 h of greening. In contrast with the wild type, etiolated *im* cotyledons immediately exposed to 60 min of HL (Figure 2.12, 0 greening time, white bar) prior to subsequent greening for an additional 23 h at LL, exhibited a 50 % reduction in chlorophyll content relative to controls. Chlorophyll accumulation during greening of *im* cotyledons was also inhibited relative to controls when the HL pulse was imposed at either 3 or 6 h of greening at LL. However, the inhibition of chlorophyll accumulation in *im* cotyledons appeared to be less severe at either 3 or 6 h than at the 0 h greening time (Figure 2.12, white bars). Only after 12 h of greening at LL did the imposition of a 60 min pulse of HL stimulate chlorophyll accumulation by 60 % in *im* cotyledons. As expected, the trends for chlorophyll accumulation using either a 30- or 90-min pulse of HL were similar to that shown in Figure 2.12 except that the extent of the inhibition during greening of *im* cotyledons was lower using a 30-min pulse but greater with the 90-min pulse during the first 6 h of greening relative to the effects of the 60-min pulse of HL (see Supplemental Figure S2.6).

However, irrespective of the duration of the HL pulse, *im* cotyledons exhibited a 53 to 76 % stimulation in chlorophyll accumulation relative to controls when the HL pulse was imposed at 12 h of greening (see Supplemental Figure S2.6). By contrast, the HL pulse stimulated chlorophyll accumulation during the greening of wild-type cotyledons under LL irrespective of duration of the HL pulse (see Supplemental Figure S2.6). Although exposure of wild-type cotyledons to greening under continuous HL for 24 h resulted in chlorophyll levels comparable to those exposed to greening for 24 h at LL (Figure 2.12, HL, black bar), as expected, exposure of *im* cotyledons to the same continuous HL greening regime for 24 h inhibited chlorophyll accumulation by fourfold to fivefold (Figure 2.12, HL, white bar) such that these seedlings exhibited a white phenotype. Thus, chloroplast biogenesis in *im* seedlings appeared to be most sensitive to a brief HL exposure during the first 6 h of greening.

2.3.7 *Effects of Greening on IM and AOX1a Expression*

If IM plays an important role as a plastid terminal oxidase to keep the PQ pool oxidized during early biogenesis and assembly of the photochemical apparatus of *Arabidopsis*, we hypothesized that IM should be transiently expressed. Maximum expression should be induced rapidly during the onset of greening of wild-type *Arabidopsis* followed by a subsequent decrease in expression to constitutive levels after completion of the biogenesis and assembly of the photosynthetic apparatus. In addition, exposure to increased irradiance during greening should significantly enhance the transient expression levels of IM. The results for real-time quantitative RT-PCR (qRT-PCR) for IM expression in the wild type is illustrated in Figure 2.13A. In contrast with our hypothesis, the results show that the relative expression of IM increased gradually during greening of the wild type under CL at either 50 or 150 $\mu\text{mol photons m}^{-2} \text{s}^{-1}$. Furthermore, the relative expression levels of IM during greening of the wild type at 150 $\mu\text{mol photons m}^{-2} \text{s}^{-1}$ tended to be lower than that observed for greening at 50 $\mu\text{mol photons m}^{-2} \text{s}^{-1}$.

AOX expression has been shown to be an excellent marker for assessing redox energy imbalances in mitochondria (Vanlerberghe and McIntosh, 1997; Maxwell et al., 1999; Arnholdt-Schmitt et al., 2006; Noctor et al., 2007; McDonald, 2008). In contrast with IM, the relative expression of mitochondrial AOX1a did exhibit a transient stimulation of expression in the wild type but only when exposed to greening at 150 $\mu\text{mol photons m}^{-2} \text{s}^{-1}$ (Figure 2.13B). After 6 h of greening at 150 $\mu\text{mol photons m}^{-2} \text{s}^{-1}$, the relative AOX1a expression levels increased ~ 3.5 -fold and subsequently returned to control levels (Figure 2.13B, 0) after 24 h of greening. However, greening of wild-type etiolated cotyledons at 50 $\mu\text{mol photons m}^{-2} \text{s}^{-1}$ induced minimal changes in AOX1a expression compared with controls (Figure 2.13B, closed bars). Similar to the wild type, *im* etiolated cotyledons exposed to greening at 150 $\mu\text{mol photons m}^{-2} \text{s}^{-1}$ also exhibited a 3.5-fold stimulation in the relative expression of AOX1a after 6 h relative to controls (Figure 2.13B, 0). However, the relative level of AOX1a expression remained at approximately threefold even after 24 h in *im* cotyledons. Even exposure of *im* etiolated cotyledons to greening at 50 $\mu\text{mol photons m}^{-2} \text{s}^{-1}$ (Figure 2.13B, open bars) stimulated the relative

expression levels of AOX1a by twofold in *im* cotyledons, which remained relatively constant throughout the 24-h greening period. Thus, in contrast with the wild type, the stimulation of AOX1a expression in *im* cotyledons persisted throughout the greening period consistent with the proposed role of AOX1a in sensing mitochondrial redox imbalance (Giraud et al., 2008).

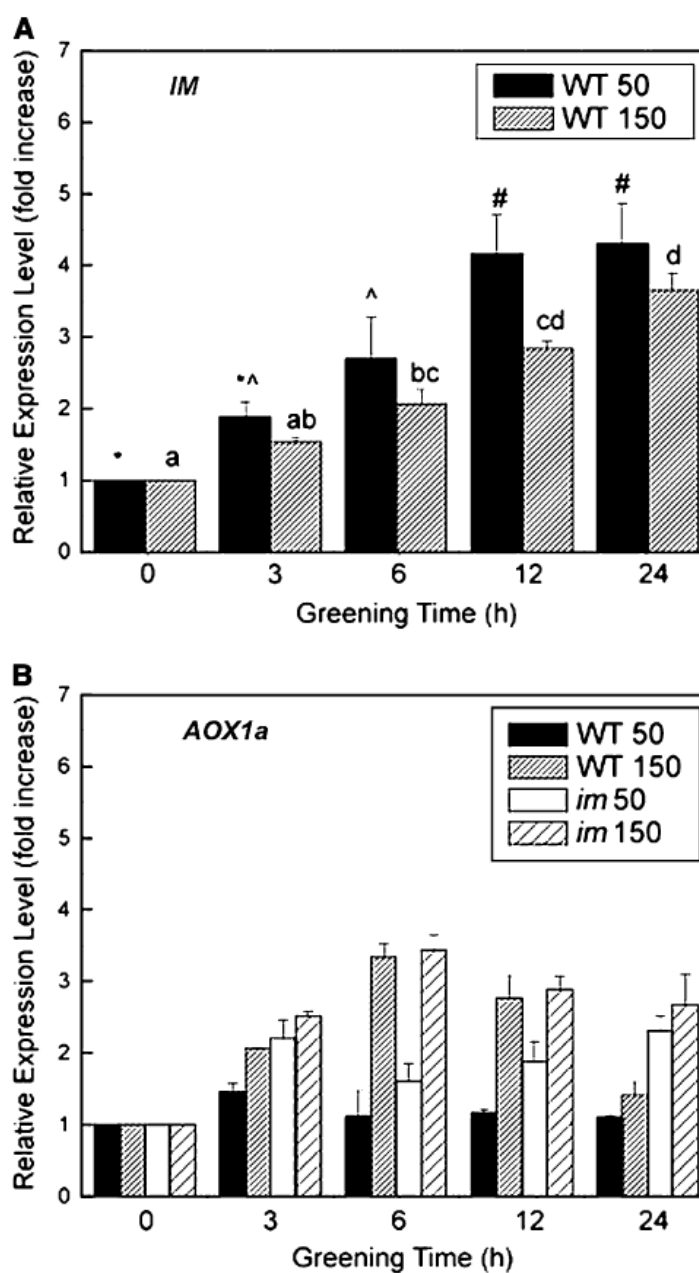


Figure 2.13 The Effect of Greening on the Relative Expression Levels of *IM* and *AOX1a*

Seeds of both WT and *im* were germinated in the dark for 5 days and subsequently exposed to continuous light of either 50 or 150 $\mu\text{mol photons m}^{-2}\text{s}^{-1}$ for up to 24h at 25 °C. Letters (a, b, c, d) and symbols (*, ^, #) above the bars indicate statistically significant differences. Relative expression levels of *IM* (A) and *AOX1a* (B) were quantified by qRT-PCR as described in “Material and Methods”. Data represent the means \pm SE of three replicate measurements.

2.4 Discussion

To elucidate the physiological basis for variegation in *im* seedlings, we established an in vivo, non-destructive assay to quantify the extent of variegation as a function of developmental time (Figures 2.4 and 2.5). We showed that both the rate of development of the variegated phenotype as well as the overall extent of variegation in *im* seedlings were strongly dependent upon growth irradiance with no variegation detected at a growth irradiance of $50 \mu\text{mol photons m}^{-2} \text{s}^{-1}$ at $25 \text{ }^\circ\text{C}$ and an 8-h photoperiod (Figures 2.4B and 2.5A). However, our results clearly indicate that the expression of the variegated phenotype cannot be explained as a simple irradiance effect since growth at the same low irradiance combined with low temperature ($12 \text{ }^\circ\text{C}$) (Figures 2.4C, 2.5D, and 2.5H) resulted in a significant increase in variegation of *im* seedlings.

As a consequence, the development of variegation in *im* seedlings appears to be a complex interaction of irradiance and temperature. We show that the extent of variegation in *im* seedlings is not caused by irradiance and temperature per se, but rather, is governed by excitation pressure which reflects the redox state of the PQ pool of the PET chain (Figure 2.2). This conclusion is supported by the results of Figure 2.8, which illustrate a strong, positive correlation between excitation pressure and the extent of variegation regardless of how the excitation pressure was generated. Light initially trapped and transformed through extremely fast, temperature-insensitive photochemistry (in the femtosecond [10^{-15} s] to nanosecond [10^{-9} s] time scale) represents the ultimate form of energy used through much slower, temperature-dependent biochemical processes (ms [10^{-3} s] to s to h time scales) to maintain cellular homeostasis, growth, and development in all photoautotrophs. Thus, imbalances between photochemistry and redox biochemistry result in modulation of the redox state of the PQ pool of PET (Figure 2.2) as well as the redox state of the ubiquinone pool of mitochondria (Figure 2.13B), indicating that information regarding energy imbalance is transferred between chloroplasts and mitochondria (Noctor et al., 2007; Aluru et al.,

2009). Furthermore, we conclude that variegation governed by the redox state of the PET chain is not restricted to *im*, but rather, also appears to govern variegation in *spotty*, *var1*, and *var2* (Figure 2.9; see Supplemental Figure S2.4). A common feature of all the mutants tested is that the mutations affect components of the PET chain. *im* and *spotty* are knockout mutants of IM/PTOX, a plastid terminal oxidase of the thylakoid membrane that uses PQH₂ as an electron donor. *var1* and *var2* are genes encoding FtsH5 and FtsH2, respectively, that appear to be involved in PS II photodamage and repair (Aluru et al., 2006; Miura et al., 2007).

Chloroplast biogenesis and the development of a functional photosynthetic apparatus is part of a complex photomorphogenic process in plants. Light has two important roles in this developmental process. First, light quality provides the necessary information for the initiation of photomorphogenesis and plant growth through an integrated network of photoreceptor mediated signal transduction pathways involving phytochromes (Rockwell et al., 2006; Bae and Choi, 2008), cryptochromes (Li and Yang, 2007; Ruckle et al., 2007), and phototropins (Christie, 2007), as well as a new non-photoreceptor signal transduction pathway involving the flavoprotein HAL (Sun et al., 2009). Our results indicate that irradiance and photoperiod influence the extent of variegation in *Arabidopsis*. Since photoreceptors respond to light and photoperiod, can the control of variegation through photoreceptors account for the variable extent of variegation reported here for *im*, *spotty*, *var1*, and *var2*?

In contrast with light and photoperiod, there is no evidence that photoreceptors respond to temperature. Since low temperature mimics the effects of irradiance on the extent of variegation, we conclude that the extent of variegation observed cannot be explained by the action of photoreceptors, such as phytochrome or cryptochrome. Furthermore, the induction of variegation under CL (Figures 2.7 and 2.12) can be explained on the basis that the absence of an 8-h photoperiod precludes the possibility for the dark relaxation of excitation pressure by respiratory metabolism in the absence of photosynthesis. Thus, excitation pressure is created by feedback inhibition of PET induced by the accumulation of photosynthetic end products under CL conditions.

The second role for light in plant photomorphogenesis is as the energy source for growth and development. The light trapped by the pigments of the photosystems is initially transformed through extremely fast, temperature-insensitive, photophysical, and photochemical processes. The biogenesis and assembly of PS I and PS II requires tight coordination between the de novo synthesis of chlorophyll and other pigments, lipids as well as chloroplast and nuclear-encoded proteins (Tobin and Silverthorne, 1985; Biswal et al., 2003; Eberhard et al., 2008; Sakamoto et al., 2008). Thus, this raises an important developmental question as to how a photoautotroph mitigates the potential damaging effects of photo-oxidation during the biogenesis and assembly of its photosystems prior to the establishment of a fully functional photosynthetic apparatus. Important photoprotective mechanisms during chloroplast biogenesis include transient stimulation of nonphotochemical dissipation of excess energy through the xanthophyll cycle (Murchie et al., 2009) as shown during early greening in barley (*Hordeum vulgare*; Król et al., 1999) as well as the induction of myriad plant oxidative stress genes including AOX (Aluru et al., 2009).

Since *im* seedlings are unable to biosynthesize photoprotective carotenoids involved in the xanthophyll cycle (Wetzel et al., 1994) and are thus impaired in their ability to modulate nonphotochemical quenching, we hypothesized that IM may play an important role in photoprotection from photo-oxidation during early chloroplast biogenesis and assembly of the photosynthetic apparatus prior to the establishment of full photosynthetic competence. The following data are consistent with this hypothesis. First, although greening at low irradiance indicated minimal differences in chloroplast biogenesis based on the disappearance of PORA and the appearance of Lhcb2 in the wild type and *im* (Figure 2.10C), the accumulation of Lhcb2, PsaB, and PsbA were delayed and the relative abundance of these thylakoid proteins was reduced in *im* cotyledons relative to the wild type during greening at $150 \mu\text{mol photons m}^{-2} \text{s}^{-1}$ (Figure 2.10C; see Supplemental Figure S2.5).

Furthermore, the observed kinetics for the disappearance of PORA and the appearance of PsaB, PsbA, and Lhcb2 during the greening of wild-type *Arabidopsis* cotyledons are

consistent with those published for chloroplast biogenesis in other photoautotrophs (Król et al., 1987; Biswal et al., 2003; Philippar et al., 2007; Sakamoto et al., 2008).

Second, although the development of maximum PS II photochemical efficiency (F_v/F_m) was stimulated by greening at $150 \mu\text{mol photons m}^{-2} \text{s}^{-1}$ in wild-type cotyledons (Figures 2.11B and 2.11A, closed symbols), greening at this higher irradiance impaired the development of PS II photochemistry in *im* cotyledons (Figures 2.11B and 2.11A, open symbols). These functional data are consistent with the biochemical data indicating a delayed appearance of both PS II and PS I reaction centers during greening of *im* compared with the wild-type (see Supplemental Figure S2.5).

Third, although the kinetics and the extent of the decrease in excitation pressure were comparable for *im* and wild-type cotyledons during greening at 25/50 (Figure 2.11C), excitation pressure after 3 h of greening at 25/150 was twofold higher in *im* (0.86) than wild-type cotyledons (0.45) (Figure 2.11D). However, this difference in excitation pressure between *im* and wild-type cotyledons gradually decreased as a function of greening time such that after 24 h, the difference in excitation pressure between *im* and wild-type cotyledons was only 30%. This indicates that *im* seedlings have a greater propensity to accumulate closed PS II reaction centers than wild-type seedlings especially during the early stages of greening.

Finally, the sensitivity of chloroplast biogenesis in *im* seedlings to a pulse of high excitation pressure was greatest between 0 and 6 h of greening (Figure 2.12; see Supplemental Figure S2.6). Only after 12 h of greening did the imposition of a pulse of high excitation pressure no longer inhibit chlorophyll accumulation relative to the control. In contrast with *im*, the imposition of the same pulse of high excitation pressure during greening of wild-type cotyledons stimulated chloroplast biogenesis regardless of the time during wild-type greening at which the pulse of high excitation pressure was imposed (Figure 2.12; see Supplemental Figure S2.6). Since the major difference in the complement of the redox components of the photosynthetic electron chain between wild-type and *im* seedlings is the absence of IM in the latter (Rosso et al., 2006), we conclude that IM has an important role in photoprotection from photo-oxidation by

lowering the excitation pressure during the initial early stages of chloroplast biogenesis in *Arabidopsis*. This photoprotective requirement for the presence of IM is developmentally dependent and becomes minimal in mature chloroplasts of *Arabidopsis* with a functional photosynthetic apparatus. However, we do not wish to imply that photoprotection through IM as a plastoquinol oxidase is the only mechanism induced during normal chloroplast biogenesis in *Arabidopsis*. The role of IM as a plastoquinol oxidase must be integrated over time with non-photochemical quenching (Król et al., 1999; Falkowski and Chen, 2003; Murchie et al., 2009), and the induction of antioxidant stress genes to prevent photo-oxidation during chloroplast biogenesis (Aluru et al., 2009).

We note with interest that, although the levels of expression of IM increase gradually as a function of greening time in wild-type cotyledons, there are minimal differences in expression levels during greening at either 25/50 or 25/150 (Figure 2.12A). Thus, IM expression is not sensitive to excitation pressure. In fact, the differences in excitation pressure during greening at 25/150 between *im* and wild-type cotyledons appear to be inversely related to the degree of stimulation of IM expression. Clearly, the putative role for IM in photoprotection by modulating excitation pressure during chloroplast biogenesis does not require maximal expression of IM. Constitutive levels of IM must be sufficient to keep the PQ pool oxidized during the first 6 h of greening.

Photostasis, that is, photoautotrophic energy balance, involves communication between chloroplasts and mitochondria through the integration of light-dependent, photosynthetic redox reactions with the light-independent respiratory redox reactions. These two redox compartments are linked metabolically through the complex C- and N-metabolic networks. IM exhibits 37 % sequence identity to mitochondrial AOX (Wu et al., 1999). Plant AOX expression is both developmentally regulated and stimulated by myriad abiotic stresses (Vanlerberghe and McIntosh., 1997; Arnholdt-Schmitt et al., 2006; Clifton et al., 2006; Umbach et al., 2006; McDonald, 2008). In contrast with IM, we show that AOX1a expression is sensitive to excitation pressure during greening of wild-type and *im* cotyledons (Figure 2.13B). Although minimal stimulation of AOX1a was

detected over the course of greening of the wild type at 25/50, 6 h of greening of the wild type at 25/150 induced a transient threefold stimulation of AOX1a expression, which returned to control levels upon completion of chloroplast biogenesis after 24 h of greening. By contrast, greening of *im* at 25/50 stimulated AOX1a expression approximately twofold, whereas greening at 25/150 stimulated AOX1a expression threefold (Figure 2.13B). Furthermore, this stimulation was not transient during greening of *im* cotyledons but remained high even after chloroplast biogenesis was completed after 24 h. The sensitivity of AOX1a to excitation pressure illustrates the important interplay between chloroplast and mitochondrial energy metabolism.

In summary, we report that the absence of IM is necessary but not sufficient to account for the variegated phenotype in *im* plants of *Arabidopsis*. We show that chloroplast energy imbalance as detected by increased excitation pressure through modulation of the redox state of the PQ pool governs variegation in *im*, *spotty*, *var1*, and *var2* seedlings. This is consistent with the model proposed by Rodermel and coworkers (Wu et al., 1999; Aluru et al., 2001, 2006, 2009; Aluru and Rodermel, 2004) for *im* seedlings as well as variegation in the *ghost* mutant of tomato (*Solanum lycopersicum*; Barr et al., 2004; Yu et al., 2007) whereby the presence of white sectors are due to chloroplast photo-oxidation. We agree with Miura et al. (2007) and Eckardt (2007) that variegation in *Arabidopsis* is a consequence of balance. However, the notion of an imbalance between D1 protein synthesis and degradation as suggested by Miura et al. (2007) fails to account for the heterogeneity in chloroplast development evident by the presence of white and green sectors in the *var2* mutant of *Arabidopsis*. We suggest that photosynthetic redox energy imbalance rather than D1 protein turnover governs the extent of variegation in *Arabidopsis* as indicated by modulation of excitation pressure in the chloroplast (Figures 2.8 and 2.13; see Supplemental Figure S2.5).

In our opinion, this provides the basis for a simple explanation for the variability not only in the extent but also in the exquisite patterns of variegation observed for *im*, *spotty*, *var1*, and *var2*. Leaf angle relative to incident light, leaf position relative to its nearest neighbors, leaf morphology, and leaf anatomy all dramatically attenuate light

capture and light propagation within a mature leaf. This results in a very heterogeneous distribution of light and, thus, gradients of photosynthetic activity within a leaf (Vogelmann et al., 1996). It seems reasonable to suggest that, for the same reasons, internal light will be attenuated during the emergence of cotyledons as well as during leaf initiation and expansion creating a heterogeneous distribution of excitation pressures internally that will affect heterogeneity in chloroplast biogenesis. Thus, green sectors observed in leaves of the variegated seedlings arise because chloroplasts present in those cells develop under sufficiently low excitation pressure ($1-qP \leq 0.2$; Figure 2.11C) during early chloroplast biogenesis such that the cellular antioxidant capacity and/or nonphotochemical quenching capacity is sufficient to protect against chloroplast photo-oxidation. Thus, under these conditions, chloroplast biogenesis in the first 12 h is able to proceed normally and leaf sectors will appear green. By contrast, the combination of either high irradiance at moderate temperature or moderate irradiance at low temperature will induce a variegated phenotype because the cellular antioxidant capacity and/or the non-photochemical quenching capacity is insufficient to counteract the production of ROS during biogenesis of the photosynthetic apparatus under these high excitation pressure conditions ($1-qP \geq 0.4$; Figures 2.11D and 2.12) and protect the developing chloroplast against photo-oxidation. Thus, in our opinion, regulation of leaf variegation by photosynthetic redox imbalance can account for the variable sectoring patterns as well as the variable extent of white sectors typically observed during leaf variegation in *im*, *spotty*, *var1*, and *var2*.

ACKNOWLEDGMENTS

This work was supported by the Natural Sciences and Engineering Research Council of Canada (NSERC; individual discovery grants to D.P.M. and N.P.A.H.) and by the U.S. Department of Energy (Energy Biosciences; Grant DF-FG02-94ER20147 to S.R.R.). We thank Richard Harris of the Biotron Experimental Climate Change Research Center for his technical assistance in the development of the imaging technique. D.R. was the recipient of an NSERC postgraduate scholarship (CGS-D). S.W. was supported by an NSERC University Summer Research Assistantship.

2.5 References

- Adams III, W.W., Demmig-Adams, B., Verhoeven, A.S., and Barker, D.H. (1995). 'Photoinhibition' during winter stress: involvement of sustained xanthophyll cycle-dependent energy dissipation. *Aust. J. Plant Physiol.* 22: 261–276.
- Aluru, M.R., Bae, H., Wu, D., and Rodermel, S.R. (2001). The *Arabidopsis immutans* mutation affects plastid differentiation and the morphogenesis of white and green sectors in variegated plants. *Plant Physiol.* 127: 67–77.
- Aluru, M.R., and Rodermel, S.R. (2004). Control of chloroplast redox by the IMMUTANS terminal oxidase. *Physiol. Plant.* 120: 4–11.
- Aluru, M.R., Yu, F., Fu, A., and Rodermel, S.R. (2006). *Arabidopsis* variegation mutants: New insights into chloroplast biogenesis. *J. Exp. Bot.* 57: 1871–1881.
- Aluru, M.R., Zola, J., Foudree, A., and Rodermel, S.R. (2009). Chloroplast photo-oxidation-induced transcriptome reprogramming in *Arabidopsis immutans* white leaf sectors. *Plant Physiol.* 150: 904–923.
- Arnholdt-Schmitt, B., Costab, J.H., and Fernandes de Melob, D. (2006). AOX – A functional marker for efficient cell reprogramming under stress? *Trends Plant Sci.* 11: 281–287.
- Bae, G., and Choi, G. (2008). Decoding of light signals by plant phytochromes and their interacting proteins. *Annu. Rev. Plant Biol.* 59: 281–311.
- Baker, N.R. (2008). Chlorophyll fluorescence: A probe of photosynthesis in vivo. *Annu. Rev. Plant Biol.* 59: 89–113.
- Barr, J., White, W.S., Chen, L., Bae, H., and Rodermel, S.R. (2004). The GHOST terminal oxidase regulates developmental programming in tomato fruit. *Plant Cell Environ.* 27: 840–852.
- Bellafiore, S., Barneche, F., Peltier, G., and Rochaix, J.-D. (2005). State transitions and light adaptation require chloroplast thylakoid protein kinase STN7. *Nature* 433: 892–895.

- Bennoun, P. (1982). Evidence for a respiratory chain in the chloroplast. *Proc. Natl. Acad. Sci. USA* 79: 4352–4356.
- Biswal, U.C., Biswal, B., and Raval, M.K. (2003). *Chloroplast Biogenesis: From Plastid to Gerontoplast*. (Dordrecht, The Netherlands: Kluwer Academic Publishers).
- Bonardi, V., Pesaresi, P., Becker, T., Schleiff, E., Wagner, R., Pfannschmidt, T., Jahns, P., and Leister, D. (2005). Photosystem II core phosphorylation and photosynthetic acclimation require two different protein kinases. *Nature* 437: 1179–1182.
- Bräutigam, K., Dietzel L, Kleine T, Ströher E, Wormuth D, Dietz KJ, Radke D, Wirtz M, Hell R, Dörmann P, Nunes-Nesi A, Schauer N, Fernie AR, Oliver SN, Geigenberger P, Leister D, Pfannschmidt T. (2009). Dynamic plastid redox signals integrate gene expression and metabolism to induce distinct metabolic states in photosynthetic acclimation in *Arabidopsis*. *Plant Cell* 21(9):2715-32
- Carol, P., Stevenson, D., Bisanz, C., Breitenbach, J., Sandmann, G., Mache, R., Coupland, G., and Kuntz, M. (1999). Mutations in the *Arabidopsis* gene *IMMUTANS* cause a variegated phenotype by inactivating a chloroplast terminal oxidase associated with phytoene desaturation. *Plant Cell* 11: 57–68.
- Christie, J.M. (2007). Phototropin blue-light receptors. *Annu. Rev. Plant Biol.* 58: 21–45.
- Clifton, R., Millar, H.A., and Whelan, J. (2006). Alternative oxidases in *Arabidopsis*: A comparative analysis of differential expression in the gene family provides new insights into function of non-phosphorylating bypasses. *Biochim. Biophys. Acta* 1757: 730–741.
- Cournac, L., Redding, K., Ravenel, J., Rumeau, D., Josse, E.M., Kuntz, M., and Peltier, G. (2000). Electron flow between photosystem II and oxygen in chloroplasts of photosystem I-deficient algae is mediated by a quinol oxidase involved in chlororespiration. *J. Biol. Chem.* 275: 17256–17262.
- Cruz, J.L., Mosquim, P.R., Pelacani, C.R., Araújo, W.L., and DaMatta, F.M. (2003). Photosynthesis impairment in cassava leaves in response to nitrogen deficiency. *Plant Soil* 257: 417–423.
- Dietz, K.J. (2008). Redox signal integration: from stimulus to networks and genes. *Physiol. Plant.* 133: 459–468.
- Dietz, K.J., Schreiber, U., and Heber, U. (1985). The relationship between the redox state of Q_A and photosynthesis in leaves at various carbon-dioxide, oxygen and light regimes. *Planta* 166: 219–226.
- Eberhard, S., Finazzi, G., and Wollman, F.-A. (2008). The dynamics of photosynthesis. *Annu. Rev. Plant Biol.* 42: 463–515.
- Eckardt, N.A. (2007). Thylakoid development from biogenesis to senescence, and ruminations on regulation. *Plant Cell* 19: 1135–1138.

- Ensminger, I., Busch, F., and Hüner, N.P.A. (2006). Photostasis and cold acclimation: Sensing low temperature through photosynthesis. *Physiol. Plant.* 126: 28–44.
- Escoubas, J.M., Lomas, M., LaRoche, J., and Falkowski, P.G. (1995). Light intensity regulation of *cab* gene transcription is signaled by the redox state of the plastoquinone pool. *Proc. Natl. Acad. Sci. USA* 92: 10237–10241.
- Falkowski, P.G., and Chen, Y.-B. (2003). Photoacclimation of light harvesting systems in eukaryotic algae. In *Advances in Photosynthesis and Respiration: Light-Harvesting Antennas in Photosynthesis*, Vol. 13, B.R. Green and W.W. Parsons, eds (Dordrecht, The Netherlands: Kluwer Academic Publishers), pp. 423–447.
- Fernández, A.P., and Strand, Å. (2008). Retrograde signalling and plant stress: Plastid signals initiate cellular stress responses. *Curr. Opin. Plant Biol.* 11: 509–513.
- Fu, A., Park, S., and Rodermel, S.R. (2005). Sequences required for the activity of IM (IMMUTANS), a plastid terminal oxidase. In vitro and in planta mutagenesis of iron-binding sites and a conserved sequence that corresponds to exon 8. *J. Biol. Chem.* 280: 42489–42496.
- Giraud, E., Ho, L.H.M., Clifton, R., Carroll, A., Estavillo, G., Tan, Y.-F., Howell, K.A., Ivanova, A., Pogson, B.J., Millar, A.H., and Whelan, J. (2008) The absence of ALTERNATIVE OXIDASE1a in *Arabidopsis* results in acute sensitivity to combined light and drought stress. *Plant Physiol.* 147: 595–610.
- Gray, G.R., Chauvin, L.-P., Sarhan, F., and Hüner, N.P.A. (1997) Cold acclimation and freezing tolerance. A complex interaction of light and temperature. *Plant Physiol.* 114: 467–474.
- Huang, C., He, W., Guo, J., Chang, X., Su, P., and Zhang, L. (2005) Increased sensitivity to salt stress in an ascorbate-deficient *Arabidopsis* mutant. *J. Exp. Bot.* 56: 3041–3049.
- Hüner, N.P.A., Öquist, G., and Sarhan, F. (1998) Energy balance and acclimation to light and cold. *Trends Plant Sci.* 3: 224–230.
- Hüner, N.P.A., Öquist, G., and Melis, A. (2003) Photostasis in plants, green algae and cyanobacteria: The role of light harvesting antenna complexes. In *Advances in Photosynthesis and Respiration: Light-Harvesting Antennas in Photosynthesis*, Vol. 13, B.R. Green and W.W. Parsons, eds (Dordrecht, The Netherlands: Kluwer Academic Publishers), pp. 401–421.
- Joët, T., Genty, B., Josse, E.M., Kuntz, M., Cournac, L., and Peltier, G. (2002) Involvement of a plastid terminal oxidase in plastoquinone oxidation as enhanced by expression of the *Arabidopsis thaliana* enzyme in tobacco. *J. Biol. Chem.* 277: 31623–31630.
- Josse, E.M., Alcaraz, J.P., Labouré, A.M., and Kuntz, M. (2003) In vitro characterization of a plastid terminal oxidase (IM). *Eur. J. Biochem.* 270: 3787–3794.

- Josse, E.M., Simkin, A.J., Gaffé, J., Labouré, A.M., Kuntz, M., and Carol, P. (2000). A plastid terminal oxidase associated with carotenoid desaturation during chromoplast differentiation. *Plant Physiol.* 123: 1427–1436.
- Kargul, J., and Barber, J. (2008). Photosynthetic acclimation: Structural reorganisation of light harvesting antenna – role of redox dependent phosphorylation of major and minor chlorophyll *a/b* binding proteins. *FEBS Lett.* 275: 1056–1068.
- Koussevitzky, S., Nott, A., Mockler, T.C., Hong, F., Sachetto-Martins, G., Surpin, M., Lim, J., Mittler, R., and Chory, J. (2007). Signals from chloroplasts converge to regulate nuclear gene expression. *Science* 316: 715–719.
- Kramer, D.M., Johnson, G., Kiirats, O., and Edwards, G.E. (2004). New fluorescence parameters for the determination of Q_A redox state and excitation energy fluxes. *Photosynth. Res.* 79: 209–218.
- Krause, G.H., and Weis, E. (1991). Chlorophyll fluorescence and photosynthesis: The basics. *Annu. Rev. Plant Physiol. Plant Mol. Biol.* 42: 313–349.
- Król, M., Hüner, N.P.A., and McIntosh, A. (1987). Chloroplast biogenesis at cold hardening temperatures. Development of photosystem I and photosystem II activities in relation to pigment accumulation. *Photosynth. Res.* 14: 97–112.
- Król, M., Ivanov, A.G., Jansson, S., Kloppstech, K., and Hüner, N.P.A. (1999). Greening under high light or cold temperature affects the level of xanthophyll-cycle pigments, early light inducible proteins, and light-harvesting polypeptides in wild-type barley and the chlorina f2 mutant. *Plant Physiol.* 120: 193–203.
- Laemmli, U. (1970). Cleavage of structural proteins during the assembly of the head of bacteriophage T4. *Nature* 227: 680–685.
- Li, Q.-H., and Yang, H.-Q. (2007). Cryptochrome signaling in plants. *Photochem. Photobiol.* 83: 94–101.
- Martínez-Zapater JM. (1993). Genetic analysis of variegated mutants in *Arabidopsis*. *Journal of Heredity* 84, 138–140.
- Maxwell, D.P., Falk, S., and Hüner, N.P.A. (1994). Growth at low temperature mimics high light acclimation in *Chlorella vulgaris*. *Plant Physiol.* 105: 535–543.
- Maxwell, D.P., Falk, S., and Hüner, N.P.A. (1995a). Photosystem II excitation pressure and development of resistance to photoinhibition. Light-harvesting complex II abundance and zeaxanthin content in *Chlorella vulgaris*. *Plant Physiol.* 107: 687–694.
- Maxwell, D.P., Laudénbach, D.E., and Hüner, N.P.A. (1995b). Redox regulation of light-harvesting complex II and cab mRNA abundance in *Dunaliella salina*. *Plant Physiol.* 109: 787–795.

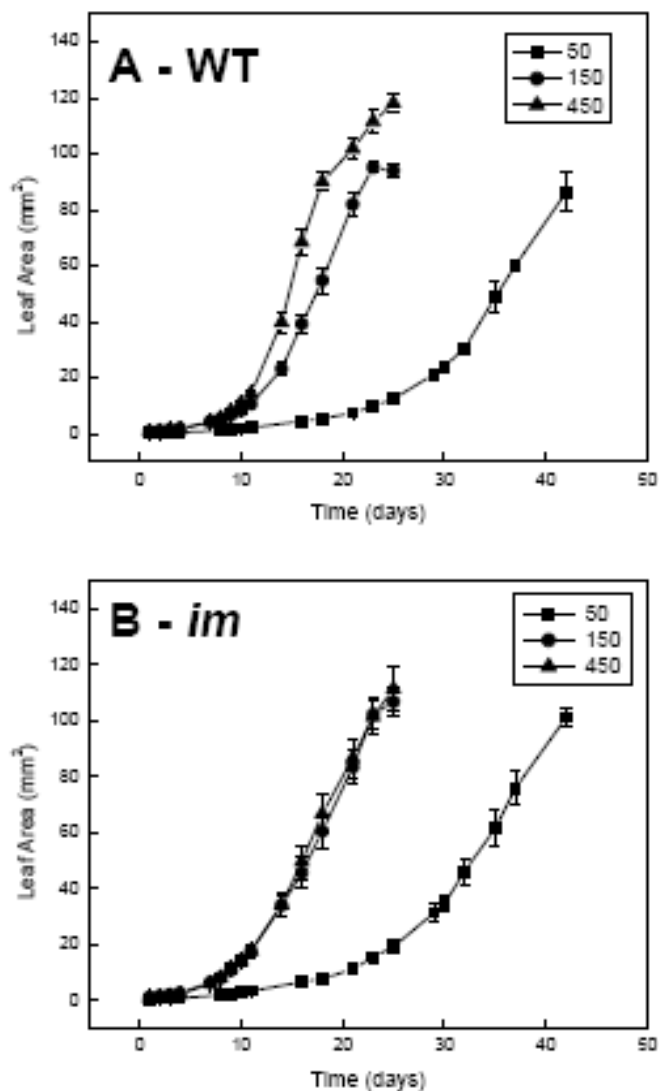
- Maxwell, D.P., Wang, Y., and McIntosh, L. (1999). The alternative oxidase lowers mitochondrial reactive oxygen production in plant cells. *Proc. Natl. Acad. Sci. USA* 96: 8271–8276.
- McCourt, P., and Keith, K. (1998). Sterile techniques in *Arabidopsis*. In *Arabidopsis Protocols*, J.M. Martinez-Zapater and J. Salinas, eds (Totowa, NJ: Humana Press), pp. 13–17.
- McDonald, A.E. (2008). Alternative oxidase: An inter-kingdom perspective on the function and regulation of this broadly distributed ‘cyanide resistant’ terminal oxidase. *Funct. Plant Biol.* 35: 535–552.
- Meskauskiene, R., Nater, M., Goslings, D., Kessler, F., op den Camp, R., and Apel, K. (2001). FLU: A negative regulator of chlorophyll biosynthesis in *Arabidopsis thaliana*. *Proc. Natl. Acad. Sci. USA* 98: 12826–12831.
- Minai, L., Wostrikoff, K., Wollman, F.-A., and Choquet, Y. (2006). Chloroplast biogenesis of photosystem II cores involves a series of assembly-controlled steps that regulate translation. *Plant Cell* 18: 159–175.
- Miskiewicz, E., Ivanov, A.G., Williams, J.P., Khan, M.U., Falk, S., and Hüner, N.P.A. (2000). Photosynthetic acclimation of the filamentous cyanobacterium, *Plectonema boryanum* UTEX 485, to temperature and light. *Plant Cell Physiol.* 41: 767–775.
- Miskiewicz, E., Ivanov, A.G., and Hüner, N.P.A. (2002). Stoichiometry of the photosynthetic apparatus and phycobilisome structure of the cyanobacterium *Plectonema boryanum* UTEX 485 are regulated by both light and temperature. *Plant Physiol.* 130: 1414–1425.
- Miura, E., Kato, Y., Matsushima, R., Albrecht, V., Laalami, S., and Sakamoto, W. (2007). The balance between protein synthesis and degradation in chloroplasts determines leaf variegation in *Arabidopsis yellow variegated* mutants. *Plant Cell* 19: 1313–1328.
- Mochizuki, N., Tanaka, R., Tanaka, A., Masuda, T., and Nagatani, A. (2008). The steady-state level of Mg-protoporphyrin IX is not a determinant of plastid-to-nucleus signaling in *Arabidopsis*. *Proc. Natl. Acad. Sci. USA* 105: 15184–15189.
- Moulin, M., McCormac, A., Terry, M.J., and Smith, A.G. (2008). Tetrapyrrole profiling in *Arabidopsis* seedlings reveals that retrograde plastid nuclear signaling is not due to Mg-protoporphyrin IX accumulation. *Proc. Natl. Acad. Sci. USA* 105: 15178–15183.
- Murchie, E.H., Pinto, M., and Horton, P. (2009). Agriculture and the new challenges for photosynthesis research. *New Phytol.* 181: 532–552.
- Niyogi, K.K. (2000). Safety valves for photosynthesis. *Curr. Opin. Plant Biol.* 3: 455–460.
- Noctor, G., De Paepe, R., and Foyer, C.H. (2007). Mitochondrial redox biology and homeostasis in plants. *Trends Plant Sci.* 12: 125–134.

- op den Camp, R., Przybyla, D., Ochsenbein, C., Laloi, C., Kim, C., Danon, A., Wagner, D., Hideg, E., Göbel, C., Feussner, I., Nater, M., and Apel, K. (2003). Rapid induction of distinct stress responses after the release of singlet oxygen in *Arabidopsis*. *Plant Cell* 15: 2320–2332.
- Palatnik, J.F., Tognetti, V.B., Poli, H.O., Rodríguez, R.E., Blanco, N., Gattuso, M., Hajirezaei, M.-R., Sonnewald, U., Valle, E.M., and Carrillo, N. (2003). Transgenic tobacco plants expressing antisense ferredoxin-NADP(H) reductase transcripts display increased susceptibility to photo-oxidative damage. *Plant J.* 35: 332–341.
- Peltier, G., and Cournac, L. (2002). Chlororespiration. *Annu. Rev. Plant Biol.* 53: 523–550.
- Pesaresi, P., Hertle, A., Pribil, M., Kleine, T., Wagner, R., Strissel, H., Ihnatowicz, A., Bonardi, V., Scharfenberg, M., Schneider, A., Pfannschmidt, T., and Leister, D. (2009). *Arabidopsis* STN7 kinase provides a link between short- and long-term photosynthetic acclimation. *Plant Cell* 21: 2402–2423.
- Pfannschmidt, T., Nilsson, A., and Allen, J.F. (1999). Photosynthetic control of chloroplast gene expression. *Nature* 397: 625–628.
- Pfannschmidt, T. (2003). Chloroplast redox signals: How photosynthesis controls its own genes. *Trends Plant Sci.* 8: 33–41.
- Pfannschmidt, T., Bräutigam, K., Wagner, R., Dietzel, L., Schröter, Y., Steiner, S., and Nykytenko, A. (2009). Potential regulation of gene expression in photosynthetic cells by redox and energy state: approaches towards better understanding. *Ann. Bot. (Lond.)* 103:599–607.
- Pham, D.L., Xu, C., and Prince, J.L. (2000). Current methods in medical image segmentation. *Annu. Rev. Biomed. Eng.* 2: 315–337.
- Philippar, K., Geis, T., Ilkavets, I., Oster, U., Schwenkert, S., Meurer, J., and Soll, J. (2007). Chloroplast biogenesis: The use of mutants to study the etioplast - chloroplast transition. *Proc. Natl. Acad. Sci. USA* 104: 678–683.
- Porra, R.J., Thompson, W.A., and Kreidemann, P.E. (1989). Determination of accurate extinction coefficients and simultaneous equations for assaying chlorophylls a and b extracted with different solvents: Verification of the concentration of chlorophyll standards by atomic absorption spectroscopy. *Biochim. Biophys. Acta* 975: 384–394.
- Rédei, G.P. (1963). Somatic instability caused by a cysteine-sensitive gene in *Arabidopsis*. *Science* 139: 767–769.
- Rédei, G.P. (1975). *Arabidopsis* as a genetic tool. *Annu. Rev. Genet.* 9: 111–127.
- Röbbelen, G. (1968). Genbedingte Rotlichtempfindlichkeit der Chloroplastendifferenzierung bei *Arabidopsis*. *Planta* 80: 237–254.
- Rochaix, J.-D. (2004). Genetics of the biogenesis and dynamics of the photosynthetic machinery in eukaryotes. *Plant Cell* 16: 1650–1660.

- Rockwell, N.C., Su, Y.-S., and Lagarias, J.C. (2006). Phytochrome structure and signaling mechanisms. *Annu. Rev. Plant Biol.* 57: 837–858.
- Rodermel, S.R. (2001). Pathways of plastid to nucleus signaling. *Trends Plant Sci.* 6: 471–478.
- Rodermel, S.R. (2002). *Arabidopsis* variegation mutants. In *The Arabidopsis Book*, C.R. Somerville and E.R. Meyerowitz, eds (Rockville, MD: American Society of Plant Biologists), pp. 1–28.
- Rosso, D., Ivanov, A.G., Fu, A., Geisler-Lee, J., Hendrickson, L., Geisler, M., Stewart, G., Król, M., Hurry, V., Rodermel, S.R., Maxwell, D.P., and Hüner, N.P.A. (2006). IMMUTANS does not act as a stress-induced safety valve in the protection of the photosynthetic apparatus of *Arabidopsis* during steady-state photosynthesis. *Plant Physiol.* 142: 1–12.
- Ruckle, M.E., DeMarco, S.M., and Larkin, R.M. (2007). Plastid signals remodel light signaling networks and are essential for efficient chloroplast biogenesis in *Arabidopsis*. *Plant Cell* 19: 3944–3960.
- Sakamoto, W., Miyagishima, S., and Jarvis, P. (2008). Chloroplast biogenesis: Control of plastid development, protein import, division and inheritance. In *The Arabidopsis Book*, C.R. Somerville and E.M. Meyerowitz, eds (Rockville, MD: American Society of Plant Biologists), doi/10.1199/tab.0110, <http://www.aspb.org/publications/arabidopsis/>.
- Schreiber, U., Bilger, W., and Neubauer, C. (1994). Chlorophyll fluorescence as a non-intrusive indicator for rapid assessment of in vivo photosynthesis. In *Ecophysiology of Photosynthesis*, E. Schulze and M.M. Caldwell, eds (Berlin: Springer-Verlag), pp. 49–70.
- Sezgin, M., and Sankur, B. (2004). Survey over image thresholding techniques and quantitative performance evaluation. *J. Electron. Imaging* 13: 146–165.
- Shahbazi, M., Gilbert, M., Labouré, A., and Kuntz, M. (2007). The dual role of the plastid terminal oxidase (PTOX) in tomato. *Plant Physiol.* 145: 691–702.
- Stepien, P., and Johnson, G.N. (2009). Contrasting responses of photosynthesis to salt stress in the glycophyte *Arabidopsis thaliana* and the halophyte *Thellungiella halophila*. Role of the plastid terminal oxidase as an alternative electron sink. *Plant Physiol.* 149: 1154–1165.
- Strand, Å., Asami, T., Alonso, J., Ecker, J.R., and Chory, J. (2003). Chloroplast to nucleus communication triggered by accumulation of Mg-protoporphyrin-IX. *Nature* 421: 79–83.
- Streb, P., Josse, E.-M., Gallouet, E., Baptist, F., Kuntz, M., and Cornic, G. (2005). Evidence for alternative electron sinks to photosynthetic carbon assimilation in the high mountain plant species *Ranunculus glacialis*. *Plant Cell Environ.* 28: 1123–1135.

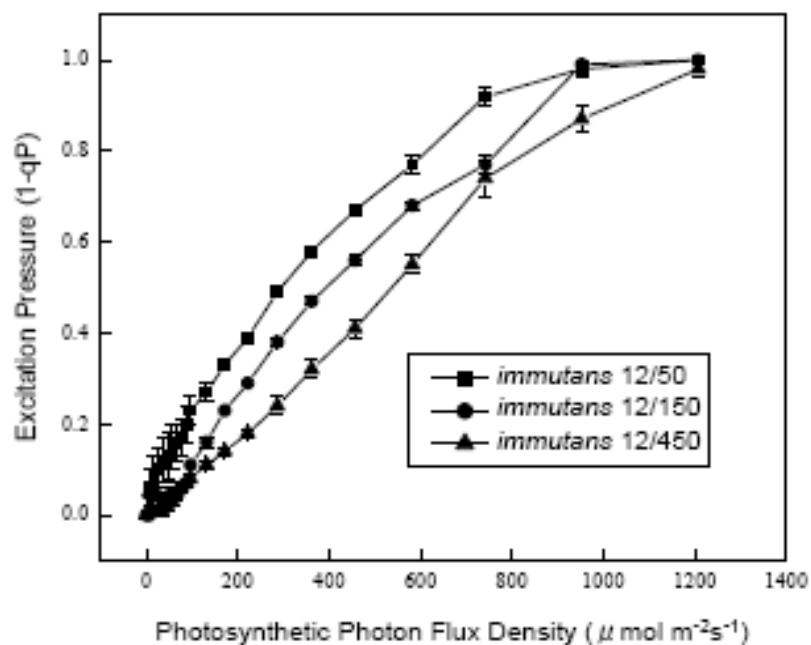
- Sun, S.-Y., Chao, D.Y., Li, X.-M., Shi, M., Gao, J.-P., Zhu, M.-Z., Yang, S.L., and Lin, H.-X. (2009). OsHAL3 mediates a new pathway in the light-regulated growth of rice. *Nat. Cell Biol.* 11: 845–851.
- Tobin, E.M., and Silverthorne, J. (1985). Light regulation of gene expression in higher plants. *Annu. Rev. Plant Physiol.* 36: 569–593.
- Umbach, A.L., Ng, V.S., and Siedow, J.N. (2006). Regulation of plant alternative oxidase activity: A tale of two cysteines. *Biochim. Biophys. Acta* 757: 135–142.
- Vanlerberghe, G.C., and McIntosh, L. (1997). Alternative oxidase: From gene to function. *Annu. Rev. Plant Physiol. Plant Mol. Biol.* 48: 703–734.
- Vogelmann, T.C., Nishio, J.N., and Smith, W.K. (1996). Leaves and light capture: light propagation and gradients of carbon fixation within leaves. *Trends Plant Sci.* 1: 65–70.
- Wetzel, C.M., Jiang, C.Z., Meehan, L.J., Voytas, D.F., and Rodermel, S.R. (1994). Nuclear-organelle interactions: The *immutans* variegation mutant of *Arabidopsis* is plastid autonomous and impaired in carotenoid biosynthesis. *Plant J.* 6: 161–175.

2.6 Supplemental Figures and Tables



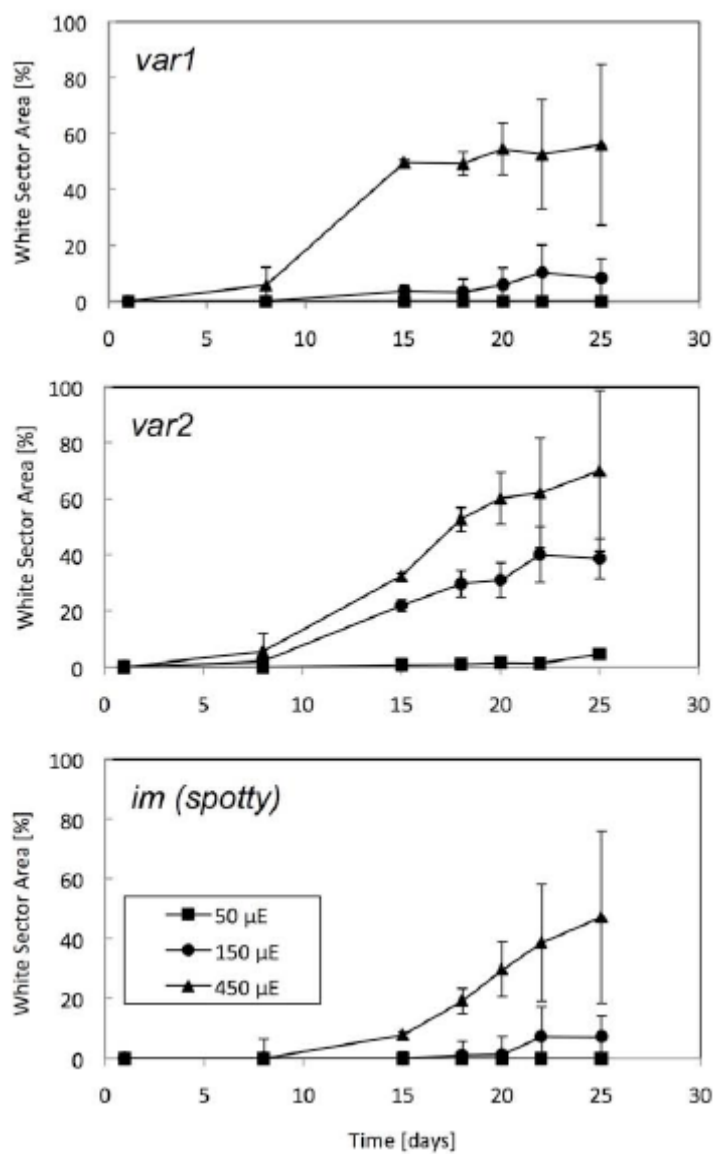
Supplemental Figure S 2.1 Growth Kinetics of WT and *im* Seedlings

Growth was measured as total leaf area (mm²) as a function of time for both WT (A) and *im* (B). Leaf area measurements were initiated 7 days after seeding at 5 μmol photons m⁻²s⁻¹ at 25 °C to prevent the onset of white sectors in the cotyledons. Both genotypes were grown at 25 °C and an irradiance of either 50, 150, or 450 μmol photons m⁻²s⁻¹. All plants were grown with an 8/16 h day/night cycle. Data represent the means ± SE from 10 different plants per treatment.



Supplemental Figure S 2.2 Acclimation of *im* to HEP at Low Temperature

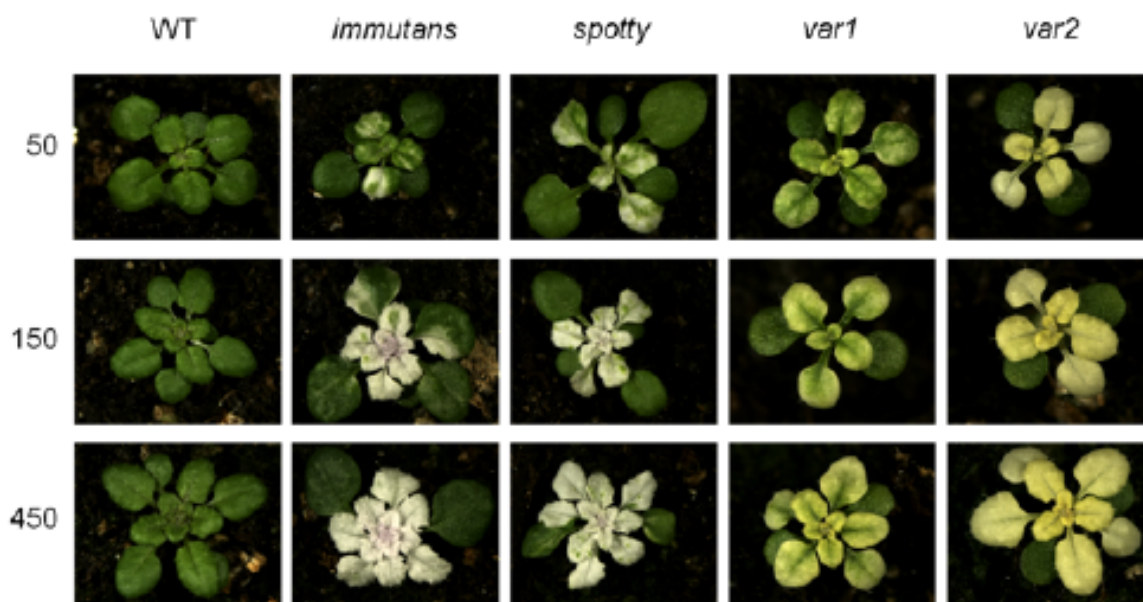
The effect of growth irradiance on the light response curves for excitation pressure for *im* plants. Seedlings were grown under a short day photoperiod (8h) at 12°C and an irradiance of either 50, 150 or 450 $\mu\text{mol photons m}^{-2} \text{s}^{-1}$. Excitation pressure was measured at the respective growth temperature.



Supplemental Figure S 2.3 Extent of Variegation of the *var1*, *var2* and *im (spotty)*

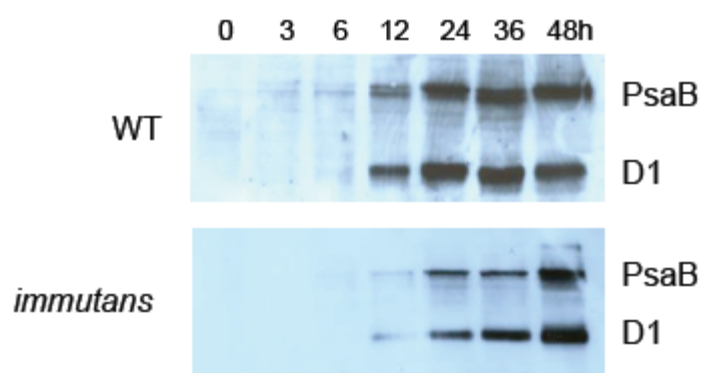
Mutants of *Arabidopsis*

Plants were grown at 25 °C and at either 50, 150 or 450 $\mu\text{mol photons m}^{-2}\text{s}^{-1}$. Variegation was quantified by determining percentage of white sectors as detailed in “Materials and Methods”.



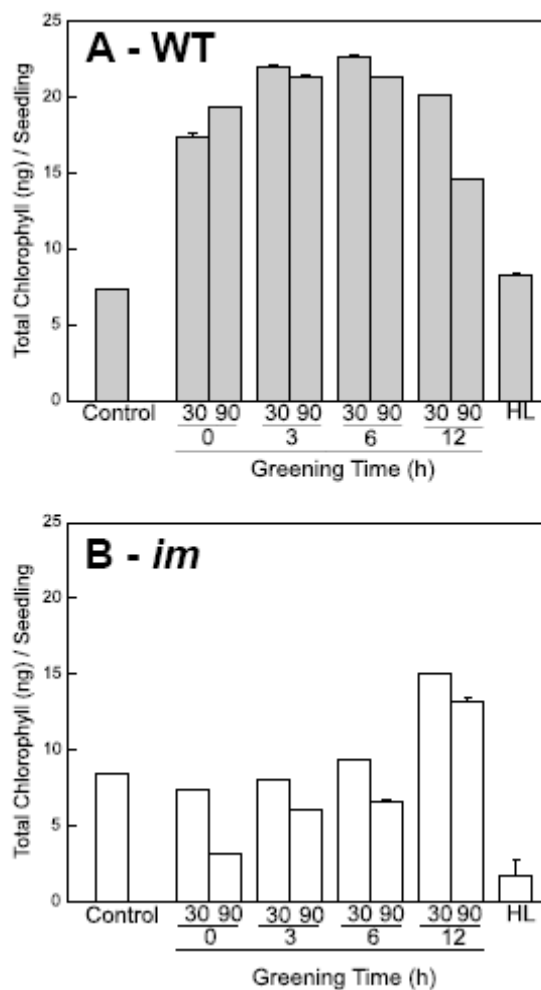
Supplemental Figure S 2.4 Variegation Mutant Phenotypes at Low Temperature

Representative photographs of WT, *im*, *spotty*, *var1* and *var2* seedlings. All seedlings were grown under short day conditions (8h light/16 h dark) at 12°C and an irradiance of either 50, 150 or 450 $\mu\text{mol photons m}^{-2} \text{s}^{-1}$.



**Supplemental Figure S 2.5 The Biogenesis of Photosystem II and Photosystem I
Reaction Centers**

Accumulation of peptides associated with photosystem I (PsaB) and photosystem II (D1) were measured in extracts of cotyledons of both WT and *im* plants. Tissue was harvested as a function of time after etiolated seedlings were shifted to the light as described in detail in the "Materials and Methods".



Supplemental Figure S 2.6 The Effects of a HL Pulse on Greening in WT and *im* Cotyledons

Conditions are as for Figure 11 except that the duration of the high light pulse was for either 30 min or 90 min. (A) WT and (B) *im*.

CHAPTER 3

3 ***ARABIDOPSIS* MUTANTS *ATD2* AND *CHS5* DISPLAY LEAF VARIATION IN RESPONSE TO EXCITATION PRESSURE DESPITE A LACK OF INVOLVEMENT IN PHOTOSYNTHETIC ELECTRON TRANSPORT**

3.1 *Introduction*

All higher plants possess a complex photosynthetic apparatus located in their chloroplasts, which originated from prokaryotic ancestors and partially retained its autonomous genome. Since this genome encodes only 80-100 out of the 2500-3500 proteins found in these plastids (Aluru et al, 2006; Peltier et al, 2002) the remainder of the proteins are encoded in the nucleus. The spatial separation of gene expression requires perpetual communication between these two organelles, both anterograde (nucleus to plastid) and retrograde (plastid to nucleus), to successfully synchronize both loci of gene expression in order to develop and maintain a functional chloroplast (Koussevitzky et al, 2007, Fernández and Strand 2008; Pfannschmidt and Yang 2012). Any energy imbalances in the PETC require a remodeling of the chloroplast in order to avoid photo-oxidative stress, caused by high PS II excitation pressure (EP). When light intensity increases suddenly, the relatively slow rate of electron transport cannot keep up with the rapid photochemical processes involved in light absorption, rendering the reaction centers of PS II closed, a stress condition called EP (Hüner et al. 1998, Ensminger et al. 2006).

The first defense mechanism against short term HEP-stress is energy dissipation as heat and that is performed by a process called non-photochemical quenching (NPQ) during which carotenoids absorb excess light energy and utilize it to reversibly change their epoxidation state and emit the energy that cannot be quenched photochemically as heat (Król et al. 1999; Wilson et al. 2003). If there is too much light energy absorbed, so that photochemistry and NPQ cannot quench it fast enough and the PS II reaction

centers cannot transfer their electrons to plastoquinone (PQ) fast enough due to a lack of available oxidized PQ, the excited chlorophyll molecules produce singlet oxygen, a highly reactive and unstable reactive oxygen species (ROS) (op den Camp et al, 2003) with detrimental effects on pigments, lipids, and proteins (mainly within PS II) (Apel & Hirt 2004). The same phenomenon of energy imbalance can be mimicked without any increase in light intensity by either low temperature (Maxwell et al, 1995), salt stress (Huang et al, 2005) or nutrient deficiencies (Cruz et al 2003) as both decrease the rate at which metabolism is able to utilize photosynthetically generated electrons (Hüner et al, 1998).

Apart from NPQ as a measure of photo-protection, the light harvesting antennae can be remodeled to effectively reduce the absorptive cross-section of PS II (Maxwell et al, 1995; Escoubas et al, 1995), or alternative electron sinks (e.g. PTOX) can be activated (Bennoun et al. 1982; Carol et al, 1999). To alleviate photo-oxidative damage there is a variety of ROS scavenging enzymes (Suzuki et al, 2012), proteases to remove photo-inactivated PS II (Zhang et al, 2010) and increased PS II de-novo synthesis to avoid photoinhibition (Pfannschmidt and Yang 2012).

Variegated plants are defined as “any plant that develops patches of different colors in its vegetative parts” (Kirk & Tilney-Bassett 1978). The most common variegation we find, especially in *Arabidopsis*, is green – white and green – yellow; the green sectors contain apparently normal chloroplasts and the yellow or white sectors contain impaired plastids lacking chlorophyll and/or carotenoids (Yu et al. 2007). Variegated sectors are alive, but are not sufficiently photosynthetically active to sustain themselves and hence act as sink tissues (Aluru et al, 2001). Some variegated mutants contain genetically heterogeneous plastid or mitochondrion populations where the genomes of some organelles carry mutations preventing a proper chloroplast development in some sectors, while other sectors develop normally. Other variegated plants possess a homogenous genotype, carrying mutations in their nucleus, which raises the question of why some sectors turn green and some stay white (Rodermel, 2002). In the previous chapter of this thesis we demonstrated, that in the *im* variegated mutant of *Arabidopsis*,

high PS II excitation pressure led to photo-oxidative damage during early stages (3-6 h) of greening, presumably due to the lack of the IM protein as both a safety –valve for excess electrons in PQH₂ and as an electron donor for the synthesis of photo-protective carotenoids (Rosso, Bode et al. 2009). The differentiation into white and green sectors appears to be derived from a different micro-environment that the pro-plastids are exposed to during a sensitive transition phase, when they develop into green chloroplasts. This micro-environment can contain differential degrees of EP due to partial shading of the entire cell by other cells or even just chloroplasts shading each other. In addition, EP can be modulated by differential sink demands that distinct cells display, for example during different stages of their development, which might allow some cells with low EP to undergo a normal greening process, while other cells with HEP develop defective chloroplasts.

Furthermore we provided a preview on some additional variegated mutants (*spotty*, *var1*, *var2*) demonstrating, that just like in *im* the extent of their variegation depended not only on the intensity of irradiance during their growth but also temperature. Thus we proposed that it is neither light nor temperature per se regulating variegation in these mutants, but PS II excitation pressure is responsible for the extent of leaf sectoring. In addition to presenting the full set of quantification data of these mutants in this manuscript, we added two more, previously unmentioned variegated mutants: *atd2* and *chs5*. While *spotty* constitutes another allele of PTOX knockout *im*, as it was first isolated by Rédei (1963) and Röbbelen (1968), *var1* and *var2* constitute two distinct isoforms of subunits from a thylakoidal FtsH metallo-protease (*ftsH5* and *ftsH2*, respectively) responsible for the removal of photo-damaged PS II reaction centers (Zhang et al, 2010). Both, *var1* and *var2* plants were created by Martínez-Zapater in 1993. All of the above mentioned gene-products are involved in PET and located in the thylakoid. *atd2* on the other hand was created by van der Graaff (1997) and the mutation affects the protein (5-phosphoribosyl-1-pyrophosphate) amidotransferase2, an enzyme catalyzing the first committed step of de-novo purine biosynthesis. The affected enzyme is predominantly expressed in leaves while another isoform (*atd1*) can still

produce purine in roots and flowers (van der Graaff et al, 2004). Thus, *adt2* is not linked to PET. *chs5* was created by Schneider et al in 1994 but not much is known of the location of the mutation. However, the phenotype was described as chlorotic when grown under low temperature conditions (Schneider et al 1994).

Since *im*, *spotty*, *var1* and *var2* are all mutations impaired in mechanisms preventing or alleviating the effects of HEP as parts of the photosynthetic apparatus, it seems reasonable that the extent of variegation in these mutants is controlled by EP. Hence, we hypothesize that EP does not control variegation in *atd2* and *chs5* since the mutations leading to the variegated phenotype are not intrinsically involved in PET.

For this experiment we germinated the variegated mutant plants under very low light conditions at room temperature (25 °C and 5 $\mu\text{mol photons m}^{-2}\text{s}^{-1}$) for a week, keeping excitation pressure low, in order to avoid photo-oxidative damage during germination. After one week we shifted the seedlings to growth regimes that induce increasing degrees of EP using various growth irradiances (50, 150 and 450 $\mu\text{mol photons m}^{-2}\text{s}^{-1}$) at a growth temperature of either 25 °C or 12 °C (25/50, 25/150, 25/450, 12/50, 12/150 and 12/450) and measured the extent of leaf variegation over the period of vegetative growth. If it is light intensity governing the extent of variegation, then growing the plants at lower temperature should not have an effect on leaf sectoring and vice versa. Yet, if lowering the growth temperature has the same effect on variegation as increasing light intensity, then this would be a strong indication that the true regulator in these mutants is indeed HEP.

3.2 *Material and Methods*

3.2.1 *Plant Growth*

Seeds of *Arabidopsis thaliana* (ecotype Columbia) wild type and the variegated mutants *im* (CS3157; AT4G22260), *var1* (CS271; AT5G42270), and *var2* (CS271; AT2G30950), *atd2* (CS114; AT4G34740), *chs5* (CS8004) were obtained from the ABRC (Columbus, OH), and *spotty* was generated as described previously (Wetzel et al., 1994). The seeds were sterilized with 20 % (v/v) bleach and 0.05 % (v/v) Tween 20 and germinated on moist and autoclaved soil under controlled environment conditions at 25 °C with a photosynthetic photon flux density of 5 $\mu\text{mol photons m}^{-2} \text{s}^{-1}$ for 1 week. Plants were then thinned to one plant per pot and grown at either 25 or 12 °C with increasing irradiance of either 50, 150, or 450 $\mu\text{mol photons m}^{-2} \text{s}^{-1}$. All plants were grown with an 8/16-h day/night cycle to prevent the early induction of flowering.

3.2.2 *Determination of Growth Rate*

Growth of both wild-type and *im* plants was quantified by measuring total leaf area as a function of time. Leaf area was measured using a dissecting microscope (SteReo Lumar V12; Zeiss; Oberkochen; Germany) at various levels of magnification attached to a CCD camera (Retiga 1300 monochrome 10 bit; Qimaging; Surrey; Canada). Digital photos were taken, and leaf area was analyzed using imaging analysis software (Northern Eclipse Image Analysis Software 7.0; Empix Imaging; Mississauga; Canada). Leaf area was measured by tracing and measuring the area of each leaf per plant. The image analysis software was calibrated with an object of known size for each level of magnification, and the number of pixels was divided by the appropriate conversion factor. Exponential growth rates of *Arabidopsis* leaf expansion were calculated by linear regression analysis of ln-transformed data of leaf area (mm^2) versus time.

3.2.3 *Quantification of Variegation*

The extent of leaf variegation in *im* seedlings was estimated non-destructively from images captured by a CCD camera (Retiga 1300 monochrome 10 bit; Qimaging; Surrey; Canada) attached to a dissecting microscope (SteReo Lumar V12; Zeiss; Oberkochen;

Germany) at various levels of magnification as required. The camera was oriented directly over the center of the plant and the magnification selected on the dissecting microscope ensured that an image of the entire plant was captured for each measurement. Digital photos were analyzed using imaging analysis software (Northern Eclipse Image Analysis Software 7.0; Empix Imaging Mississauga; Canada). The image analysis software was calibrated with an object of known size for each magnification, and the number of pixels was divided by the appropriate conversion factor. Images were then converted to grayscale, thereby creating a binary partitioning of the image intensities. An intensity value was determined, called the threshold value in order to separate green versus white sectors (Pham et al., 2000; Sezgin and Sankur, 2004). Threshold analysis was performed on each image captured to ensure that all green sectors could be clearly resolved from all white sectors irrespective of magnification. Total leaf area was measured by tracing and then calculating the area of each leaf per plant. Subsequently, the total area of white sectors per leaf was calculated and then divided by the total area of the leaf to determine the percentage of white sectors for each leaf examined. Statistical significance was determined by a one-way ANOVA at a 95 % confidence interval, followed by a Bonferroni test to test for differences between group means (Microcal Origin Lab 7.5; Origin Lab).

3.3 **Results:**

3.3.1 **Plant Growth Kinetics:**

Plant growth was measured over time using digital images quantifying the total leaf area of all plants grown under each light and temperature regime (Figure 3.2). Wild-type plants, as well as *im*, *spotty* and *atd2* displayed a logarithmic growth rate constant of ca 0.10 mm²/day when grown at 25/50, while *var1*, *var2* and *chs5* grew marginally slower under the same growth regime (0.09, 0.09 and 0.08 mm²/day, respectively) (Table 3.1, Figure 3.2). Plants grown at 25/150 all roughly doubled their growth rates compared to 25/50 with the exception of *atd2*, which only increased its growth rate by 30 %. A further increase in growth irradiance did not have the same effect though, since plant growth appeared already light saturated at 150 μmol m⁻² s⁻¹ and plants grown at 25/450 did not display a significant increase over plants grown at 25/150 (Table 3.1, Figure 3.2).

Table 3.1: Logarithmic Growth Rate Constants. The effects of differential growth irradiance (photosynthetic photon flux density; PPF) and Temperature (°C) on the growth rates (mm²/day) of the various variegated mutants and wild-type *Arabidopsis* was quantified using logarithmic growth rate constants. Exponential growth rates were calculated by linear regression analysis of ln-transformed data of leaf area (mm²) over time.

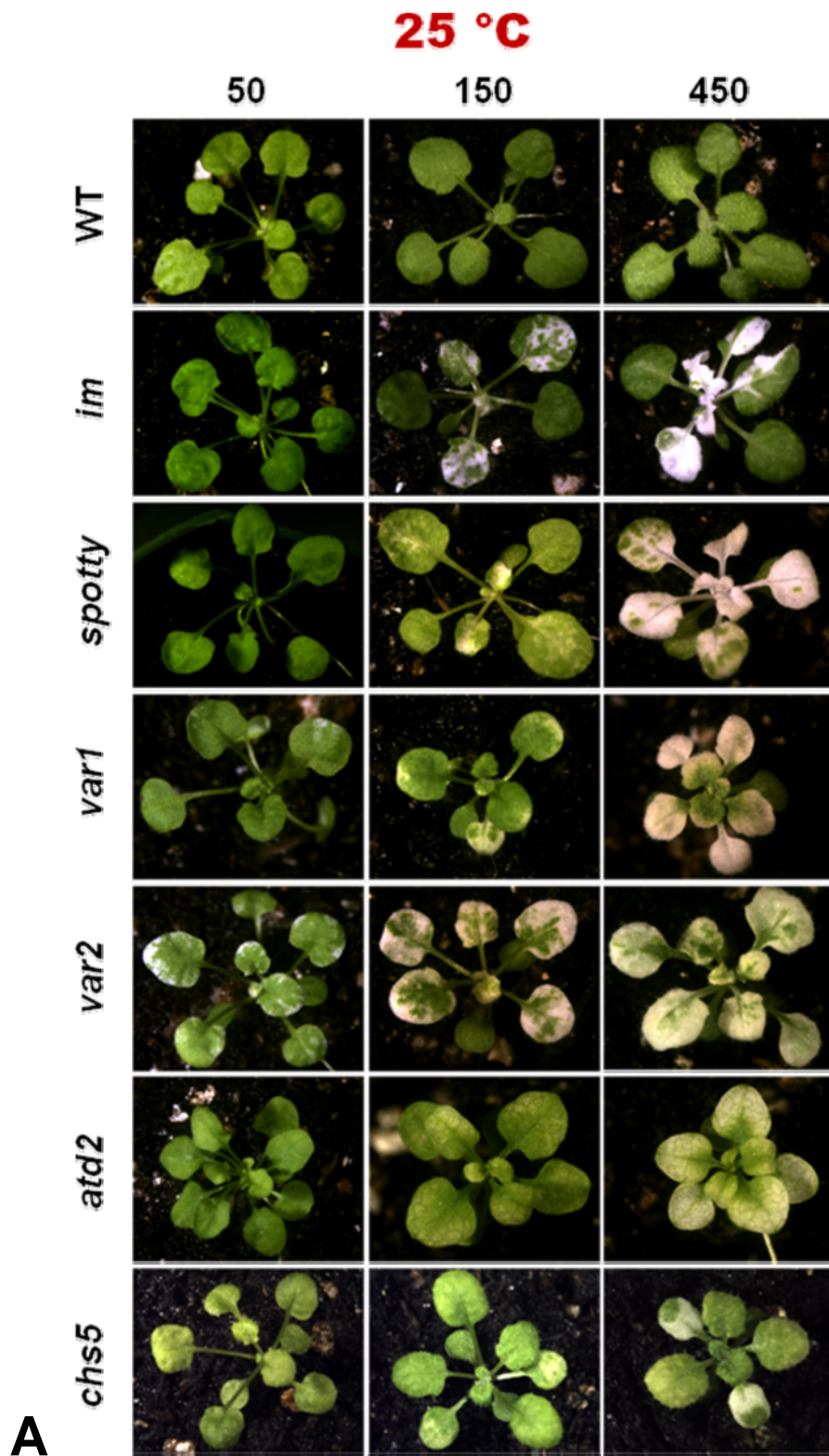
25 °C

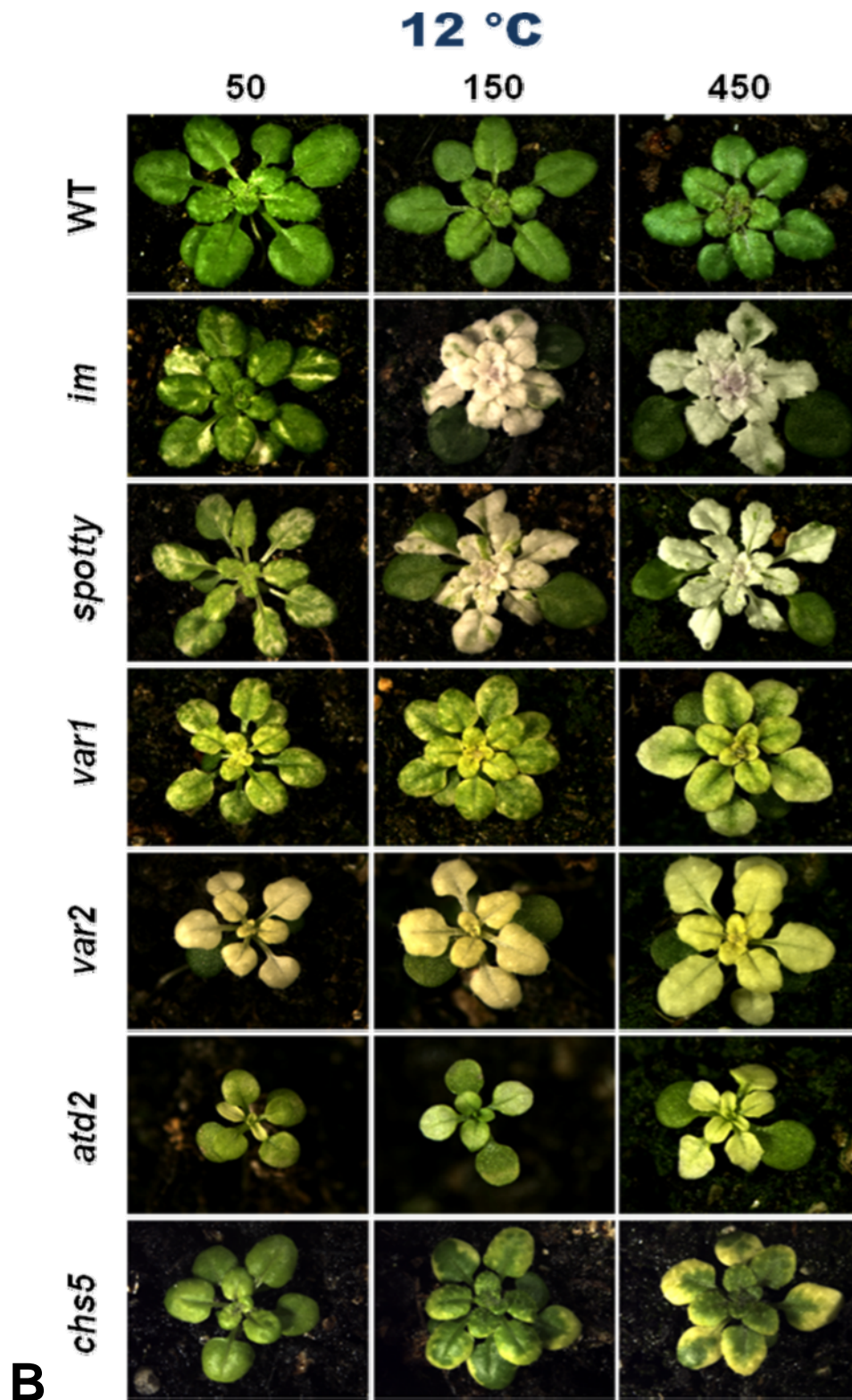
PPFD ($\mu\text{mol m}^{-2} \text{s}^{-1}$)	logarithmic growth rate constants (mm ² /day)						
	WT	<i>im</i>	<i>spotty</i>	<i>var1</i>	<i>var2</i>	<i>atd2</i>	<i>chs5</i>
50	0.10	0.10	0.10	0.09	0.09	0.10	0.08
150	0.21	0.21	0.21	0.17	0.17	0.13	0.16
450	0.23	0.24	0.22	0.15	0.16	0.13	0.17

12 °C

PPFD ($\mu\text{mol m}^{-2} \text{s}^{-1}$)	logarithmic growth rate constants (mm ² /day)						
	WT	<i>im</i>	<i>spotty</i>	<i>var1</i>	<i>var2</i>	<i>atd2</i>	<i>chs5</i>
50	0.07	0.06	0.06	0.04	0.03	0.03	0.05
150	0.11	0.06	0.07	0.05	0.04	0.04	0.07
450	0.12	0.09	0.10	0.06	0.06	0.04	0.13

Figure 3.1: Representative images of variegated *Arabidopsis* mutants. *Arabidopsis thaliana* wild-type and the variegated mutants *im*, *spotty*, *var1*, *var2*, *atd2* and *chs5* were grown under different light intensities (50, 150 and $\mu\text{mol m}^{-2} \text{s}^{-1}$) at either 25 °C **(A)** 12 °C **(B)** and photographs were taken at comparable developmental stages.

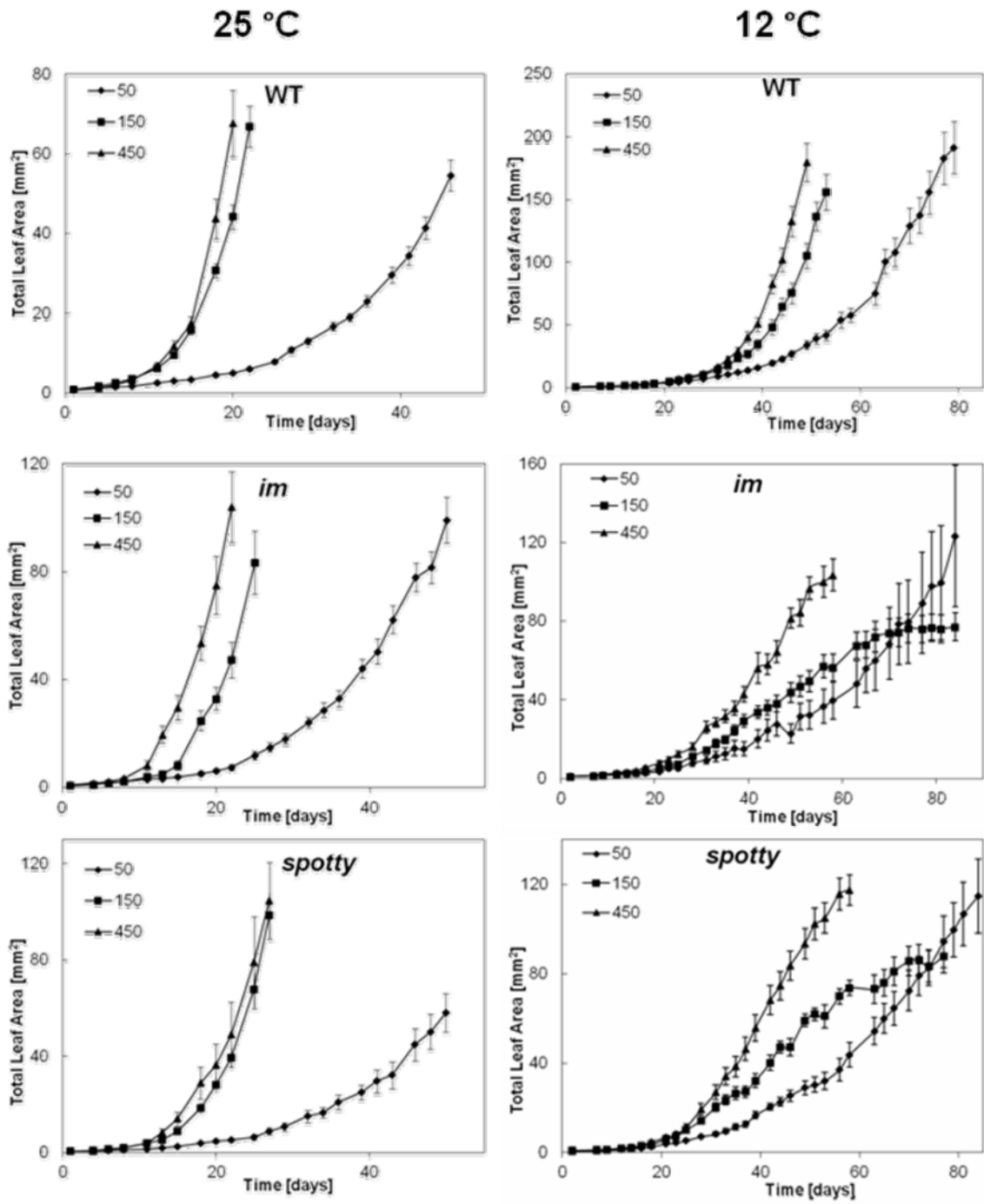


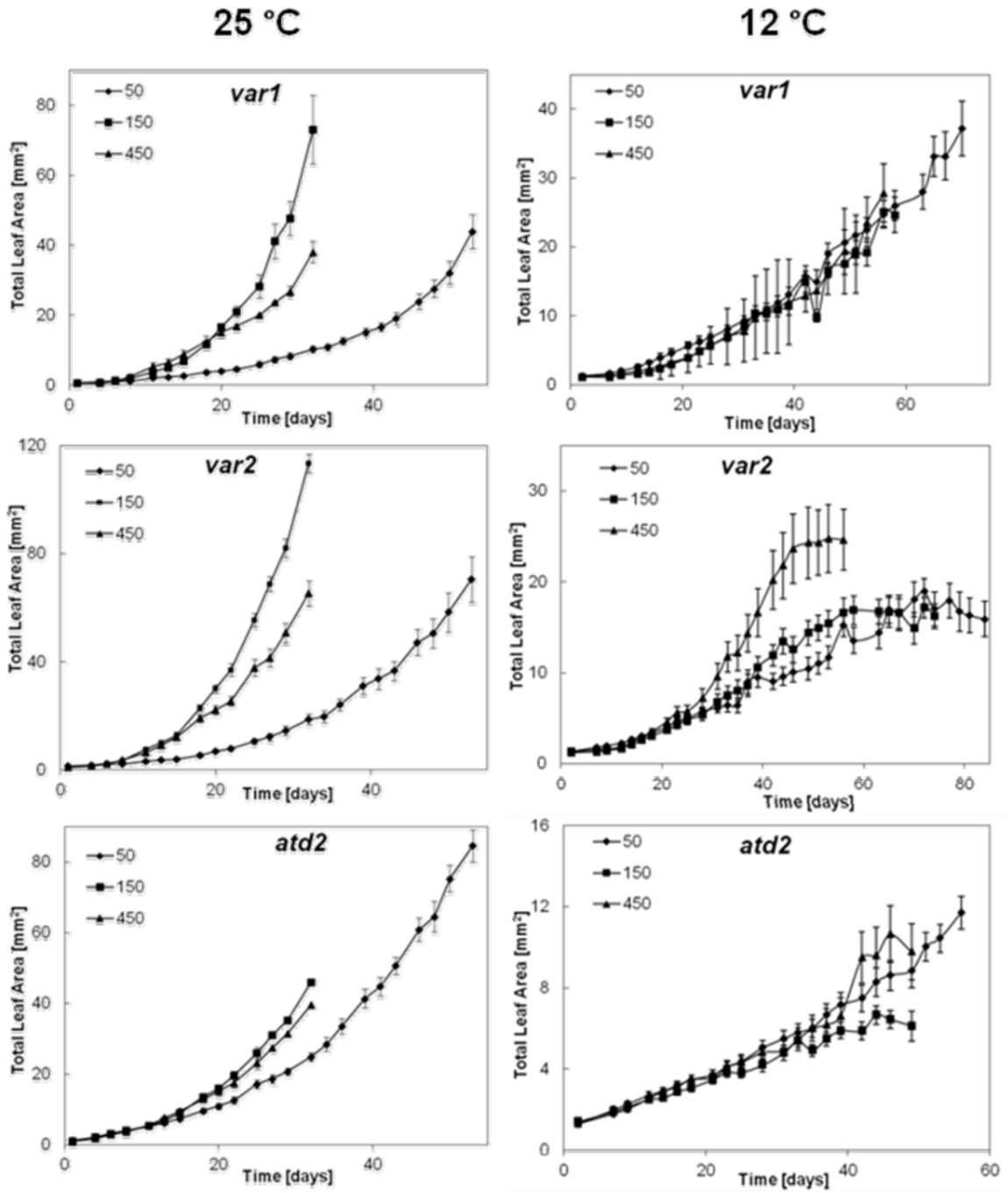


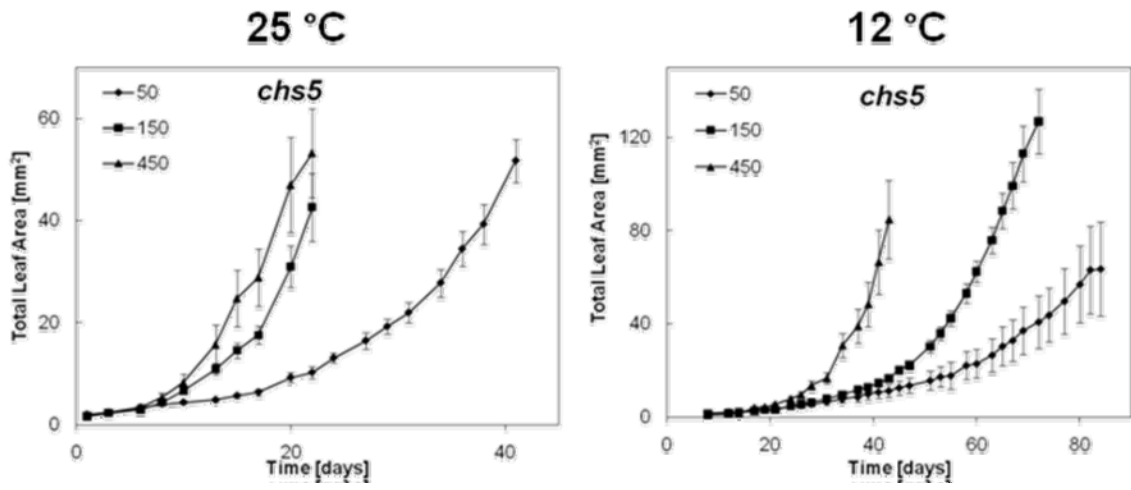
Plants grown at 12 °C showed overall reduced growth rates compared to the plants grown at 25 °C with all the genotypes monitored. At 50 $\mu\text{mol m}^{-2} \text{s}^{-1}$ the wild-type displayed a 30 % reduction in growth rate at 12 °C compared with 25°C and the mutant plants decreased their growth rates even more: *im* and *spotty*: 40 %, *var1*: 55 %, *var2*: 66 %, *atd2*: 70 % and *chs5*: 38 %. Wild-type plants showed increased growth rates from 12/50 to 12/150 by 57 % and *chs5* increased by 40 % but none of the other mutants showed any major differences between those two growth conditions. Thus, the growth of the plants at low temperature appeared to decrease sensitivity of the growth rates of all genotypes towards changes in growth light intensities. While growth rates in the wild-type plants were light saturated at 12/150, some mutants showed increased growth rates at 12/450 compared to 12/150, thus, *im* and *var2* increased their growth rates by 50 % each, while *spotty* and *chs5* increased their growth rates by 43 % and 71 % respectively (Table 3.1). Interestingly, we observed that, when kept under at low temperature regime, the growth rates of *var1* and *atd2* did not show any sensitivity to the light intensity the plants were grown at.

When the variegated mutants *var1*, *var2*, *atd2* and *chs5* were grown at low temperature, not only did they not display a decrease in growth rate, but they also had a drastically reduced total leaf area. In contrast, wild-type, *im* and *spotty* plants did eventually reach the final size of their counterparts grown at 25 °C (Figure 3.2).

Figure 3.2: *Arabidopsis* Mutant Growth Curves. The growth of *Arabidopsis* variegated mutant and wild-type (WT) plants grown at different light (50, 150, 450 $\mu\text{mol photons m}^{-2} \text{s}^{-1}$) and temperature (12 and 25 °C) regimes was quantified over time utilizing digital images. The data shows representative results from two independent experiments and each data point represents the average from 5-15 individual plants $\pm\text{SE}$.





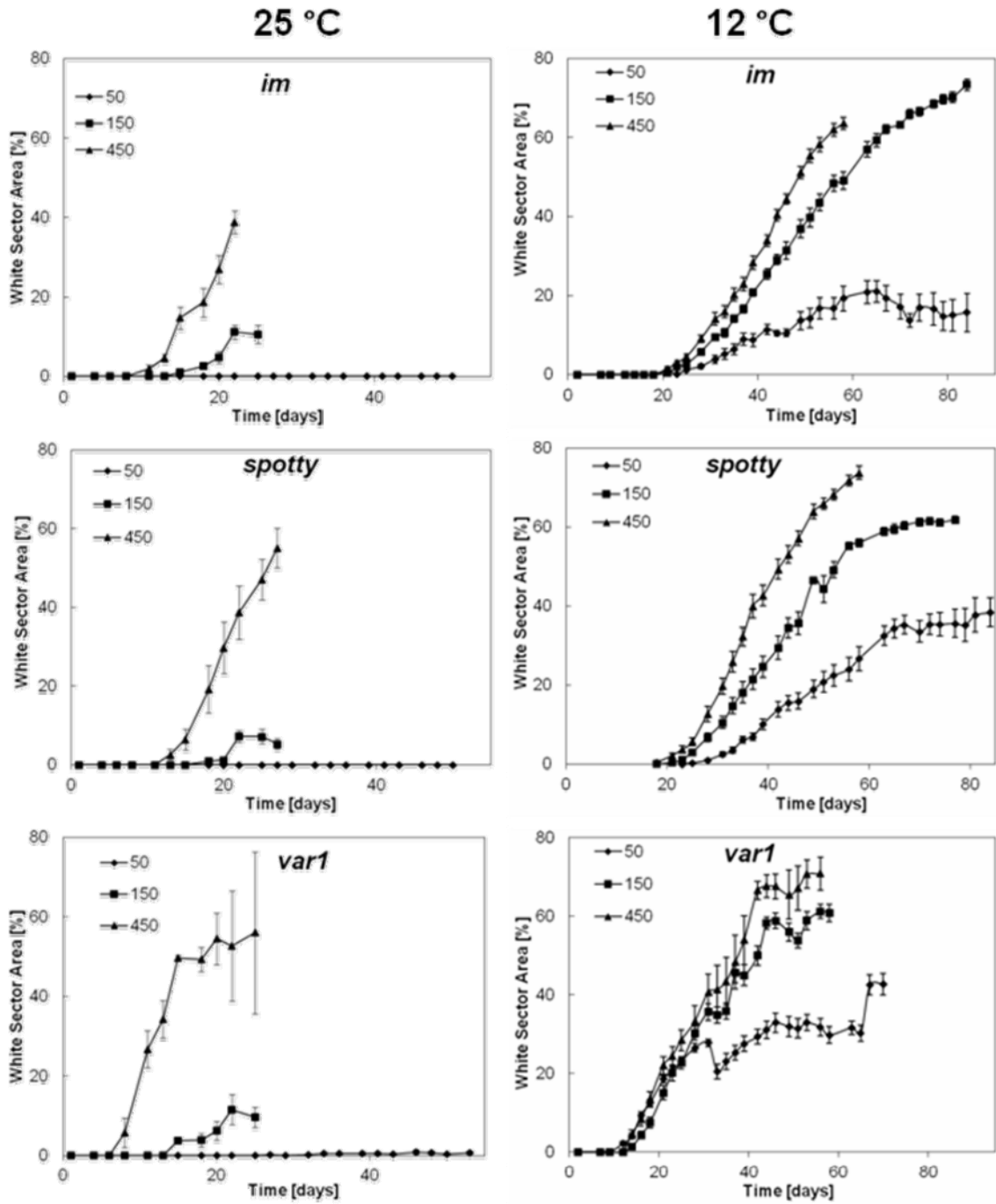


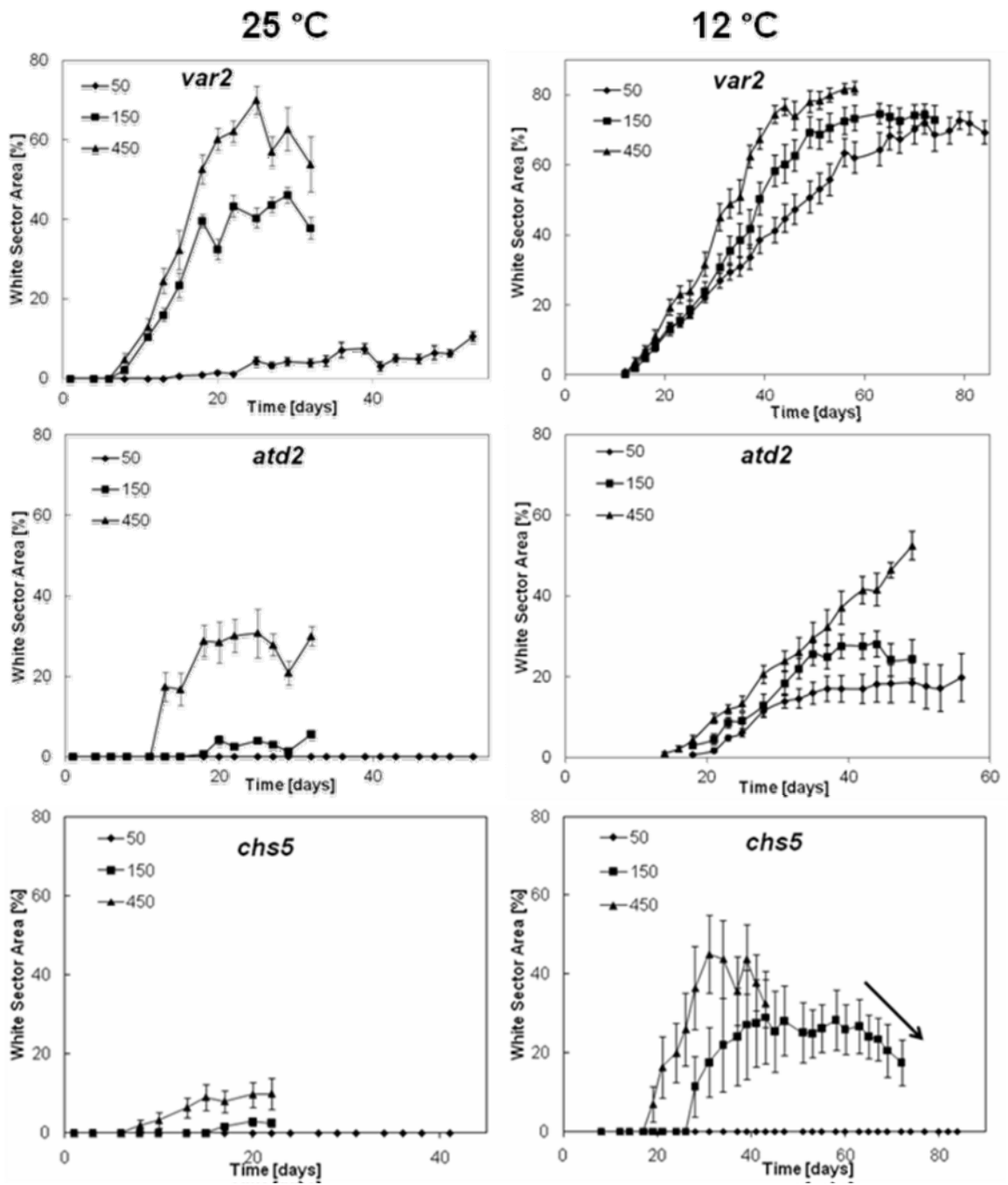
3.3.2 *Effects of Growth Irradiance and Temperature on Variegation*

As our previous research (Rosso et al., 2006; Rosso, Bode et al., 2009) had shown, both *spotty* and *im* displayed the all green phenotype in cotyledons and first true leaves when plants were grown at moderate temperature (25 °C) and very low irradiance (5 $\mu\text{mol m}^{-2} \text{s}^{-1}$) for 7 days after germination (Figure 3.1). Interestingly, all other *Arabidopsis* mutants that were examined (*var1*, *var2*, *atd2* and *chs5*) also displayed an all green phenotype in their cotyledons, but not in their first true leaves (Figure 3.1). In order to determine whether growth irradiance and growth temperature governs the extent of variegation in *var1*, *var2*, *atd2* and *chs5* the way it does in *im* and *spotty*, the seedlings were then shifted to various growth regimes exposing the plants to increasing levels of irradiance (50, 150 or 450 $\mu\text{mol m}^{-2} \text{s}^{-1}$) at either 25 (25/50; 25/150; 25/450) or 12 °C (12/50; 12/150; 12/450). Regardless which growth regime each mutant was exposed to, the all green phenotype of the cotyledons or first true leaves persisted throughout the development of all the mutants.

Along with total leaf area, the kinetics of variegation were quantified as percentage of white sector area in comparison to total leaf area every second or third day throughout the plant's development. All measurements were performed non-destructively utilizing digital imaging as described in Material and Methods. The most striking variegation result was its complete absence throughout the entire period of vegetative plant development in *im*, *spotty*, *atd2* and *chs5* when these mutants were grown at 25/50 (Figure 3.1 and Figure 3.3 (left column: diamonds)). We reported this before for *im* (Rosso et al. 2006, Rosso, Bode et al., 2009) and while the lack of variegation made *im*, *spotty* and *chs5* indistinguishable in phenotype from the wild-type, *atd2* was visibly different from both wild-type and the other mutants due to its dwarfed growth habit with smaller and thinner leaves, shorter petioles and complete lack of trichomes. Only *var2* displayed any significant degree of variegation when grown at 25/50 (Figure 3.1; Figure 3.3, left column).

Figure 3.3: Quantification of Variegation in *im*, *spotty*, *var1*, *var2*, *atd2* and *chs5*. The extent of leaf variegation in the various mutant lines of *Arabidopsis* grown at different light (50, 150, 450 $\mu\text{mol photons m}^{-2} \text{s}^{-1}$) and temperature (12 and 25 °C) regimes was quantified over time as the percentage of total leaf area that was white. The data shows representative results from two independent experiments and each data point represents the average from 5-15 individual plants \pm SE.





Most mutant plants grown at 25/150 started to show their white sectors after ~15 days after their shift from 25/5, with the exception of *var2* which started variegating after ~10 days (Figure 3.3, left column: squares). The maximum extent of variegation at 25/150 varied from 3 % in *chs5*, over 6-7 % in *atd2* and *spotty* up to 11-12 % in *im* and *var1*, while only *var2* reached up to 44 %. Growth at 25/450 induced the development of white sectors in all mutants 2-5 days earlier than growth at 25/150 and each mutant displayed a higher degree of variegation when grown at 25/450 than at 25/150 (Figure 3.1; Figure 3.3; left column: triangles). *im* seedlings exhibited up to 39 %, *spotty*: 55 %, *var1*: 56 %, *var2*: 63 %, *atd2*: 31 % and *chs5*: 10 % maximum variegation, when they were grown at 25/450.

As we previously demonstrated for *im* and *spotty* (Rosso, Bode et al., 2009), the exposure of the seedlings to low temperature ought to increase the extent of white leaf sectors at each given growth light intensity if excitation pressure ultimately controls variegation in these mutants. As expected, the time it took the seedlings after the shift to their respective growth light at low temperature to develop variegated sectors increased ~5-10 days, depending on the mutant line (Figure 3.1; Figure 3.3, right column). Strikingly all but one mutant (i.e. *chs5*) variegated even at low light intensity, when grown at 12 °C with *im* reaching a maximum percentage of white sector area of up to 17 %, *spotty*: 38 %, *var1*: 43 %, *var2*: 73 % and *atd2*: 20 %. While each mutant exhibited a higher quantity of maximum variegation at 12/150 (*im*: 73 %, *spotty*: 62 %, *var1*: 61 %, *var2*: 74 %, *atd2*: 37 %, *chs5*: 28 %) than it displayed at either 12/50 or at 25/150, a further increase in growth light intensity at low temperature did not lead to a significant increase in white sector area in the plants, as variegation appeared light saturated at $150 \mu\text{mol m}^{-2} \text{s}^{-1}$ at low temperature. The only exception to that was *atd2*, which reached its maximum level of variegation at 12/450 (52 %).

In summary we can state that the extent of variegation in all monitored mutant lines was increased with an increase in light intensity and at each level of light intensity the extent of variegation was greater at lower than at moderate temperature. Thus it

appears that the degree to which a plant is variegated depends on an interplay of both, light and temperature.

3.3.3 ***Patterns of Leaf Variegation in Different Arabidopsis Mutants:***

While the objective of this experiment was to quantify the extent of variegation, it has to be stated that different mutants display different patterns of variegation which affected the measurements. While *im*, *spotty*, *var1* and *var2* display a mostly chaotic pattern of distinctly separate sectors of green and variegated areas, *atd2* developed white sectors gradually from the leaf margin towards the mostly green centre of the leaf while maintaining mostly green leaf veins, which is called a reticulate type of variegation. White sectors in *chs5* grew either from the leaf margin towards the base of the leaf, or vice versa, from the base towards the tip (Figure 3.4). In both *atd2* and *chs5* the gradual appearance of white sectors as opposed to the strict separation of the sectors in the other mutants impairs the precision of their quantification. The mutant lines *var1* and *var2* on the other hand, unlike *im* and *spotty*, still possess carotenoids in their variegated sectors giving them a yellowish-orange color which impedes the imaging software's ability to distinguish between the different sectors. These issues are reflected in the larger error bars in Figure 3.3 when the percentage of white area is quantified for these mutants.

In addition to the constraints given above, *chs5* did not develop any variegation at 25/50 after 41 days at this growth regime but began to lose its green color in all parts of its true leaves (Figure 3.4A). Furthermore, *chs5* seemed to be the only mutant I observed that decreased its extent of variegation during later stages of its development. These mutant plants grown at either 12/150 or 12/450 decreased their percentage of white sectors due to the fact that past the time point 40 days after the shift from 25/5, only the green sectors seemed to be growing (Figure 3.4B). It appeared as if *chs5* grown at 12/150 or 12/450 lost its susceptibility to light and temperature in regard to variegation.

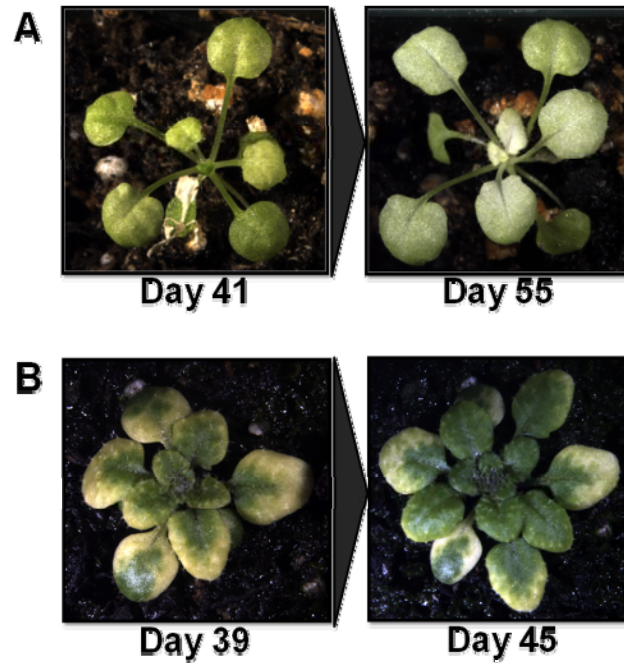


Figure 3.4 Development in Phenotype of the *Arabidopsis chs5* Mutant

(A) When *chs5* was grown at an irradiance of $50 \mu\text{mol m}^{-2} \text{s}^{-1}$ at 25°C plants did not variegate but started becoming paler when grown past 40 days under this regime. The photographs show the same plant with a 14 days difference in growth time. **(B)** When *chs5* was grown at an irradiance of $450 \mu\text{mol m}^{-2} \text{s}^{-1}$ at 12°C the degree of variegation declined over time. The photographs show the same plant with only a 6 day difference in growth time.

3.4 Discussion:

All the mutant plants we examined displayed an increased extent of variegation with an increase in growth irradiance and an increased extent of variegation when growth temperature was lowered, regardless of the light condition the plants were grown under. This is strong evidence that it is indeed not light intensity or temperature *per se* that govern variegation in these mutants, but EP. Thus, EP must be the true regulator of leaf sectoring in all variegated mutants that we have tested, regardless of the origin and site of the mutation responsible for the variegated phenotype.

We demonstrated before that IM plays a role as an alternative electron sink for PQ which seems to be essential very early during chloroplast development. This notion was recently supported by Fu and co-workers (2012) when they rescued the *im* variegated phenotype by targeting different mitochondrial alternative oxidases (*aox1a* and *aox2*) to the chloroplast demonstrating that they can functionally substitute for IM. Much like *im* and *spotty*, *var1* and *var2* are directly involved in the EP-stress response by removing photo-damaged D1 proteins, which are part of the PS II reaction center (Zhang et al, 2010). Thus, it appears plausible that these mutants are particularly susceptible to HEP: *im* and *spotty* are lacking the ability to actively decrease EP by oxidizing PQH₂ and subsequently opening up closed PS II reaction centers and moreover they are lacking photo-protective carotenoids which could prevent HEP. While *var1* and *var2* are not involved in prevention of an excessive accumulation of closed PS II reaction centers, they are both crucial for coping with the damage inflicted by HEP, so new and functional D1 proteins can replace their photo-oxidized counterparts. Yet, *atd2* and *chs5* have no known function linking them to the prevention or alleviation of HEP stress and while we don't know about the mutation responsible for the phenotype in *chs5*, we know that *atd2* is impaired in purine biosynthesis in the leaves, a process with no direct link to PET. The effects of the *atd2* deletion obviously go far beyond the variegated phenotype. The leaves of the *atd2* plants do not fully develop and apart from the defects described above, they're lacking palisade cells and the vasculature is underdeveloped (Yu et al,

2007). Presumably these defects are caused by low levels of purine in the leaves, which is necessary not only for DNA replication during mitosis and hence for leaf growth, but also for the generation of all mRNAs. Thus, it is conceivable that chloroplast biogenesis, amongst other developmental processes, is sensitive to the insufficient abundance of this nucleotide. Since *atd1*, an isoform of *atd2*, is mainly expressed in roots and flowers (van der Graaff et al., 2004), purine needs to be imported to the leaves from these parts of the plant in order to assure basal levels of overall transcription. Nevertheless, despite the vast defects in this mutant related to transcription and DNA replication, there is a clear correlation between its extent of variegation and EP. This might be explained by a general decrease in transcription in the mutant cell, preventing rapid de novo synthesis of photo-oxidative damaged thylakoid proteins, rendering the chloroplast defective and colorless, but it has also been suggested that this mutant is impaired in plastid signaling, implying a dual role for *atd2* (van der Graaff et al, 2004).

We have no information on the gene locus in the *chs5* mutant so any statements about the origin of the EP susceptibility would be pure speculation. Yet our data indicates that the chlorotic sectors are indeed susceptible to HEP rather than merely chilling sensitive (Figure 3.3), as it was suggested by Schneider et al (1995). Also, it appears that *chs5* is slightly less sensitive to HEP than other mutants, since its phenotype is less variegated than others at any given light intensity and regardless of growth temperature it does not variegate at low light intensities. Additionally, when grown at 12/150 for longer than 60 days, its white sector area decreases, as after a certain developmental stage the white sectors slowly start to recede and all the new leaves growing develop an all green phenotype. Thus, *chs5* is the first mutant we observed where variegation decreases after a certain age. However, all green plants grown at 25/50 lose their green coloring when grown for longer than 40 days (Figure 3.4A) a phenomenon that cannot be explained merely by susceptibility to HEP since it doesn't occur at higher levels of irradiance or at lower growth temperature. Instead, this bleaching effect appears to be rooted in the development of the leaves, considering that it cannot be observed for

most of the plant's vegetative growth period. However, further experiments are needed to elucidate this peculiar phenomenon.

In conclusion we are surprised to report that all variegated plants we examined displayed variegation controlled by EP rather than light or temperature, regardless of the type of mutation present. These results strengthen our previous hypothesis that the respective mutations are necessary but not sufficient to explain the occurrence of white sectors in variegated plants. We hypothesize that there is a threshold of EP above which the plant needs the gene products which are absent in our variegated mutants, in order to ensure the development of functional and fully pigmented chloroplasts. Hence, if this threshold is exceeded in the absence of the necessary gene products, the plant starts to display variegation. While *im*, *spotty*, *var1* and *var2* appear to display a cell autonomous plastid development with white sector cells giving rise to white sectors and being strictly separated from green sectors, the distinction is less clear in *atd2* and *chs5*, suggesting a different reason for the sectoring in these mutants. In order to explain the extent and patterns of variegation in *atd2* and *chs5*, a better molecular understanding of the mutations is necessary in order to address the defects in chloroplast biogenesis exhibited by these two mutants.

ACKNOWLEDGEMENT: I am very grateful to David Scaduto for his extensive help in quantifying the variegation and growing the mutant plants.

3.5 *References:*

- Aluru, M.R., Bae, H., Wu, D., and Rodermel, S.R. (2001). The *Arabidopsis immutans* mutation affects plastid differentiation and the morphogenesis of white and green sectors in variegated plants. *Plant Physiol.* 127: 67–77.
- Aluru M.R., Yu F., Fu A., Rodermel S.R. (2006). *Arabidopsis* variegation mutants: new insights into chloroplast biogenesis. *J. Exp. Bot.* 57 (9): 1871-1881
- Apel, K.; Hirt, H. (2004) Reactive oxygen species: metabolism, oxidative stress, and signal transduction. *Annu Rev Plant Biol*, 55: 373-399
- Bennoun, P. (1982). Evidence for a respiratory chain in the chloroplast. *Proc. Natl. Acad. Sci. USA* 79: 4352–4356.
- Carol, P., Stevenson, D., Bisanz, C., Breitenbach, J., Sandmann, G., Mache, R., Coupland, G., and Kuntz, M. (1999). Mutations in the *Arabidopsis* gene *IMMUTANS* cause a variegated phenotype by inactivating a chloroplast terminal oxidase associated with phytoene desaturation. *Plant Cell* 11: 57–68.
- Cruz, J.L., Mosquim, P.R., Pelacani, C.R., Araújo, W.L., and DaMatta, F.M. (2003). Photosynthesis impairment in cassava leaves in response to nitrogen deficiency. *Plant Soil* 257: 417–423.
- Ensminger, I., Busch, F., and Hüner, N.P.A. (2006). Photostasis and cold acclimation: Sensing low temperature through photosynthesis. *Physiol. Plant.* 126: 28–44
- Escoubas, J.M., Lomas, M., LaRoche, J., and Falkowski, P.G. (1995). Light intensity regulation of *cab* gene transcription is signaled by the redox state of the plastoquinone pool. *Proc. Natl. Acad. Sci. USA* 92: 10237–10241.
- Fernández, A.P., and Strand, Å . (2008). Retrograde signaling and plant stress: Plastid signals initiate cellular stress responses. *Curr. Opin. Plant Biol.* 11: 509–513.
- Fu, A.; Liu, H.; Yu, F.; Kambakam, S.; Luan, S.; Rodermel, S.R. (2012). Alternative oxidases (AOX1a and AOX2) can functionally substitute for plastid terminal oxidase in *Arabidopsis* chloroplasts. *Plant Cell* 24(4):1579-95
- Huang, C., He, W., Guo, J., Chang, X., Su, P., and Zhang, L. (2005). Increased sensitivity to salt stress in an ascorbate-deficient *Arabidopsis* mutant. *J. Exp. Bot.* 56: 3041–3049.
- Hüner, N.P.A., Öquist, G., and Sarhan, F. (1998). Energy balance and acclimation to light and cold. *Trends Plant Sci.* 3: 224–230.
- Kirk J.T.O. & Tilney-Bassett R.A.E. (1978) *The Plastids*, 2nd edn. Elsevier/North-Holland, Amsterdam, the Netherlands

- Koussevitzky, S., Nott, A., Mockler, T.C., Hong, F., Sachetto-Martins, G., Surpin, M., Lim, J., Mittler, R., and Chory, J. (2007). Signals from chloroplasts converge to regulate nuclear gene expression. *Science* 316: 715–719.
- Król, M., Ivanov, A.G., Jansson, S., Kloppstech, K., and Hüner, N.P.A. (1999). Greening under high light or cold temperature affects the level of xanthophyll-cycle pigments, early light inducible proteins, and light-harvesting polypeptides in wild-type barley and the chlorina f2 mutant. *Plant Physiol.* 120: 193–203.
- Martínez-Zapater JM. (1993). Genetic analysis of variegated mutants in *Arabidopsis*. *Journal of Heredity* 84, 138–140.
- Maxwell, D.P., Laudenbach, D.E., and Hüner, N.P.A. (1995). Redox regulation of light-harvesting complex II and cab mRNA abundance in *Dunaliella salina*. *Plant Physiol.* 109: 787–795.
- op den Camp, R., Przybyla, D., Ochsenbein, C., Laloi, C., Kim, C., Danon, A., Wagner, D., Hideg, E., Göbel, C., Feussner, I., Nater, M., and Apel, K. (2003). Rapid induction of distinct stress responses after the release of singlet oxygen in *Arabidopsis*. *Plant Cell* 15: 2320–2332.
- Peltier J, Emanuelsson O, Kalume DE, Ytterberg J, Frisco G, Rudella A, Liberias DA, Soderberg L, Roepstorff P, von Heijne G. 2002. Central functions of the luminal and peripheral thylakoid proteome of *Arabidopsis* determined by experimentation and genome-wide prediction. *Plant Cell* 14:211-236.
- Pfannschmidt, T.; Yang, C. (2012) The hidden function of photosynthesis: a sensing system for environmental conditions that regulates plant acclimation responses
- Pham, D.L., Xu, C., and Prince, J.L. (2000). Current methods in medical image segmentation. *Annu. Rev. Biomed. Eng.* 2: 315–337.
- Rédei, G.P. (1963) Somatic instability caused by a cysteine-sensitive gene in *Arabidopsis*. *Science* **139**, 767–769.
- Röbbelen, G. (1968) Genbedingte Rotlicht-Empfindlichkeit der Chloroplastendifferenzierung bei *Arabidopsis*. *Planta* 80, 237–254.
- Rodermel, S. (1999) Subunit control of Rubisco biosynthesis: a relic of an endosymbiotic past? *Photosynthesis Research* 59:105-123.
- Rodermel, S.R. (2002). *Arabidopsis* variegation mutants. In *The Arabidopsis Book*, C.R. Somerville and E.R. Myerowitz, eds (Rockville, MD: American Society of Plant Biologists), pp. 1–28.
- Rosso, D., Ivanov, A.G., Fu, A., Geisler-Lee, J., Hendrickson, L., Geisler, M., Stewart, G., Król, M., Hurry, V., Rodermel, S.R., Maxwell, D.P., and Hüner, N.P.A. (2006). IMMUTANS does not act as a stress-induced safety valve in the protection of the photosynthetic apparatus of *Arabidopsis* during steady-state photosynthesis. *Plant Physiol.* 142: 1–12.

- Rosso, D.; Bode, R.; Li, W.; Król, M.; Saccon, D.; Wang, S.; Schillaci, L.A.; Rodermel, S.R.; Maxwell, D.P.; Hüner, N.P.A. (2009). Photosynthetic Redox Imbalance Governs Leaf Sectoring in the *Arabidopsis thaliana* Variegation Mutants *immutans*, *spotty*, *var1*, and *var2*. *Plant Cell*, Vol. 21(11): 3473–3492
- Schneider, J.C.; Hugly, S.; Somerville, CR (1994). Chilling sensitive mutants of *Arabidopsis*. *Weeds World* 1: 2-6.
- Sezgin, M., and Sankur, B. (2004). Survey over image thresholding techniques and quantitative performance evaluation. *J. Electron. Imaging* 13: 146–165.
- Suzuki, N.; Koussevitzky, S.; Mittler, R.; Miller, G. (2012). ROS and redox signalling in the response of plants to abiotic stress. *Plant Cell Environ.* 35(2):259-70
- van der Graaff, E.; Lamers, G.; Den Dulk-Ras, A.; Hooykaas, P.J.J. (1997). Developmental mutants of *Arabidopsis thaliana* obtained after gene tagging with an activator T-DNA construct. 8TH INTERNATIONAL CONFERENCE ON *ARABIDOPSIS* RESEARCH
- van der Graaff, E.; Hooykaas, P.; Lein, W.; Lerchl, J.; Kunze, G.; Sonnewald, U.; Boldt, R. 2004. Molecular analysis of "de novo" purine biosynthesis in solanaceous species and in *Arabidopsis thaliana*. *Front Biosci.* 1;9:1803-16.
- Wetzel, C.M., Jiang, C.Z., Meehan, L.J., Voytas, D.F., and Rodermel, S.R. (1994). Nuclear-organelle interactions: The *immutans* variegation mutant of *Arabidopsis* is plastid autonomous and impaired in carotenoid biosynthesis. *Plant J.* 6: 161–175.
- Wilson, K.E., Król, M., and Hüner, N.P.A. (2003). Temperature-induced greening of *Chlorella vulgaris*. The role of the cellular energy balance and zeaxanthin-dependent nonphotochemical quenching. *Planta* 217: 616–627.
- Yu, F.; Fu, A.; Aluru M.; Park, S.; Xu, Y.; Liu, H.; Liu, X.; Foudree, A.; Nambogga M.; Rodermel, S.R. (2007). Variegation mutants and mechanisms of chloroplast biogenesis. *Plant, Cell and Environment* 30: 350–365
- Zhang, D.; Kato, Y; Zhang, L; Fujimoto, M; Tsutsumi, N; Sodmergen; Sakamoto, W. (2010) The FtsH Protease Heterocomplex in *Arabidopsis*: Dispensability of Type-B Protease Activity for Proper Chloroplast Development. *Plant Cell* 22: 3710–3725.

CHAPTER 4

4 SHORT TERM EFFECTS OF CHANGES IN EXCITATION PRESSURE ON GLOBAL GENE EXPRESSION IN *ARABIDOPSIS THALIANA*

4.1 *Introduction:*

A plant's ability to cope with external stress depends to a large part on its ability to respond to environmental cues with a change in gene expression. The spatial disparity between the sensors receiving these stimuli, which are located in numerous compartments of the cell, and the loci of gene expression (i.e. nucleus, plastids, and mitochondria) must be bridged by signaling pathways. Retrograde signaling from the chloroplast to the nucleus has been explained through the transfer of information in the form of metabolites (Bräutigam et al. 2009), reactive oxygen species (ROS) (Miller et al., 2010), pigment biosynthesis (Kindgren et al. 2011; Woodson et al. 2011) and the redox state of the photosynthetic electron transport chain (PETC) (Pogson et al. 2008; Koussevitzky et al., 2007). There is no strict separation between these signaling factors since it is the components of the PETC that produce the ROS at both the oxygen evolving complex of photosystem II (PS II) (singlet oxygen) and the NADP⁺ reducing-side of photosystem I (PS I) (hydrogen peroxide), when excessively reduced. Some pigments are used for light harvesting in order to fuel the PETC, some are quenching excessively absorbed light energy, and metabolites are produced utilizing the chemical energy (i.e. NADPH and ATP) created by the reduction potential of PET.

One very sensitive retrograde regulator is believed to be the relative redox state of plastoquinone, since its electron transport capacity is limited by the rate of diffusion throughout the thylakoid membrane and hence it reflects the rate at which PSII reaction centers are opened (Hüner et al. 1998).

Photosynthetic stress in plants manifests itself in a strong reduction of the PETC in the thylakoid membranes of the chloroplasts which leads to a formation of reactive oxygen

species (ROS) and hence promotes oxidative damage. The relative reduction state of the PETC is reflected in the relative closure of PS II reaction centers which can be measured in-vivo as excitation pressure utilizing chlorophyll a fluorescence (Dietz et al. 1985; Krause & Weis 1991; Hüner et al. 1998). One cause for photosynthetic stress can be excess light, since the intensity of irradiance in nature can vary by several orders of magnitude within very short periods of time and the rate of processing the excess energy via photochemistry falls several orders of magnitude below the rate of light absorption by the photosystems. The same effect is achieved by a sudden drop in temperature, which will decelerate the biochemistry of the PETC, yet leave the rate of light absorption unaltered, because the photochemistry is driven by temperature-independent photophysical processes. Thus a sudden decrease in temperature can mimic the effects of high levels of irradiance on the PETC and so can various other environmental factors (i.e. salt stress, lack of nutrients, drought), which decrease the metabolic capacity to consume electrons from the PETC rendering its components predominantly reduced. The strong reduction of Q_A , the first stable quinone electron acceptor of PSII is called excitation pressure (Dietz et al., 1985; Hüner et al., 1998) and reflects a strong reduction of the entire PETC.

Photoautotroph organisms have many mechanisms of altering their phenotype as a result of high excitation pressure. Green algae alter the amount of pigments associated with the photosystems (Escoubas et al. 1995) or their epoxidation state (Wilson et al. 2003), as well as the amount of light harvesting complexes and their distribution amongst PSII and PSI can be manipulated (Maxwell et al. 1995). Winter varieties of wheat and rye on the other hand adjust their carbon sink capacities, for example by the means of increased sugar production and/or modified growth rates or patterns (Hüner et al 1998, Dahal et al 2012), Many plant species utilize an alternative electron sink in the PETC in form of a plastid terminal oxidase (Rosso et al. 2009, McDonald et al. 2011). In order for any of these acclimation strategies to be carried out, there needs to be a sensitive and fast communication between the PETC sensing the stress and the nucleus, providing the adequate genetic program to be set into motion. This study focuses on the

signaling capacities of the PETC, in particular PQH₂ and PSII. In order to reduce the PETC, *Arabidopsis thaliana* plants grown under oxidizing conditions (low light and ambient temperature) were either shifted to high light (HL) or low temperature (LT). With the purpose of capturing the primary signaling targets of PQH₂ and PS II and to avoid secondary regulatory effects, the gene expression was monitored one hour into the shift, utilizing whole genome gene expression microarrays. Additionally, gene expression is measured in plants treated with the specific chemical inhibitors. 3-(3,4-dichlorophenyl)-1,1-dimethylurea (DCMU) and 2,5-dibromo-3-methyl-6-isopropyl-p-benzoquinone (DBMIB) which possess the ability to block the PETC at Q_A of PS II and the PQ binding site of the Cytochrome b₆f complex, respectively, and hence render the PQ pool either entirely oxidized (+DCMU) or reduced (+DBMIB).

4.2 **Material and Methods:**

4.2.1 **Plant Growth**

Arabidopsis thaliana (Columbia) seeds were surface sterilized with 20% (v/v) bleach and 0.05% (v/v) Tween 20, sown on moistened and autoclaved soil and imbibed at 4 °C in the dark for three days. On the third day the seeds were shifted to a growth cabinet (GCW15, Environmental Growth Chambers, Chagrin Falls, Ohio) where they were exposed to 25°C and 50 $\mu\text{mol photons m}^{-2}\text{s}^{-1}$ (25/50) with a 8h/16h (light/dark) photoperiod until mid log-phase of vegetative growth (i.e. 51 days under the given growth conditions) and watered every second day with half strength Hoagland's solution. After 51 days the plants were treated and then shock-frozen in liquid nitrogen and stored at -80 °C until further processing.

All subsequent treatments were performed four hours into the photoperiod and lasted one hour. Control plants (25/50) were shifted to either 25 °C with 750 $\mu\text{mol photons m}^{-2}\text{s}^{-1}$ (HL) or 5 °C with 50 $\mu\text{mol photons m}^{-2}\text{s}^{-1}$ (LT), respectively. During both inhibitor treatments, control plants (25/50) were incubated with the respective inhibitor for one hour, after infiltration using the original growth conditions in the presence (25 °C/50 $\mu\text{mol photons m}^{-2}\text{s}^{-1}$) and absence of light (25 °C, darkness) to subtract pleiotropic effects of the inhibitors. Detached leaves were vacuum infiltrated with either H₂O for control, 10 μM 3-(3,4-dichlorophenyl)-1,1-dimethylurea (DCMU) or 6 μM 2,5-dibromo-3-methyl-6-isopropyl-p-benzoquinone (DBMIB) and incubated for one hour, then immediately frozen in liquid nitrogen and stored at -80°C until further processing.

4.2.2 **Chlorophyll a Fluorescence**

Plants were dark adapted for 20 minutes in order to perform steady state fluorescence measurements using a Heinz Walz Imaging PAM (Effeltrich, Germany). The dark-adapted plants (control, HL and LT) and detached leaves (H₂O, DBMIB and DCMU infiltrated) were pulsed with an 800 ms pulse of saturating blue light ($\lambda = 470 \text{ nm}$; 6000 $\mu\text{mol photons m}^{-2} \text{ s}^{-1}$), supplied by the Imaging PAM photodiode (IMAG-L; Heinz Walz) as a light source. Photochemical quenching was calculated as qP (Schreiber et al., 1994) and

the relative reduction state of PSII or excitation pressure was estimated as $1-qP$ (Dietz *et al.*, 1985; Hüner *et al.*, 1998, 2003) and used as an estimate for the relative reduction state of PQ.

Statistical differences were assessed using a one-way ANOVA ($P=0.05$) coupled with a Bonferroni test to determine significant differences between group means (Microcal Origin Lab 7.5; Origin Lab).

4.2.3 P700 Measurements

The redox state of P700 was monitored under ambient O_2 and CO_2 conditions on detached leaves in-vivo using a PAM 101 modulated fluorometer using a dual wavelength emitter-detector ED-P700DW unit and PAM-102 units (Heinz Walz, Germany). Far-red light was provided by a FL-101 light source ($\lambda_{max} = 715$ nm, 10 W m^{-2} , Schott filter RG 715) and used to fully oxidize P700 to $P700^+$. Subsequent single turnover (ST, 14 μs) multiple turnover (MT, 50 ms) saturating light flashes were applied with XMT-103 and XST-103 power control units, respectively, in order to reduce P700. The redox state of $P700/P700^+$ was assessed as the change of absorbance at 820 nm and the signals were recorded using an oscilloscope card (PC-SCOPE T6420, Intelligente Messtechnik GmbH, Backnang, Germany) installed in an IBM-PC. The peak area under the oxidation curve following the ST and MT flashes and the stationary $P700^+$ represents intersystem electron flow and is used as a measure of efficacy and efficiency of DBMIB and DCMU.

4.2.4 RNA Extraction

Leaf material of three plants from each growth condition was pooled into one sample, ground to a fine powder using liquid nitrogen and RNA was extracted using the RNeasy Plant Minikit (Qiagen). Residual DNA was digested on-column utilizing the matching RNase free DNase kit (Qiagen). Three biological replications were performed, for each experimental condition.

4.2.5 ***RNA Quality Assessment, Probe Preparation and GeneChip Hybridization***

The following steps were performed by David Carter in the London Regional Genomics Center at the Robarts Research Institute (London, Canada).

The quality of the extracted RNA was examined using the Agilent 2100 Bioanalyzer (Agilent Technologies Inc., Palo Alto, CA) and the RNA 6000 Nano kit (Caliper Life Sciences, Mountain View, CA). Biotinylated complementary RNA (cRNA) was generated from 500 ng of total RNA following the Affymetrix GeneChip 3' IVT Express Kit Manual (Affymetrix, Santa Clara, CA).

https://www.affymetrix.com/user/login.jsp?toURL=/support/file_download.affx?onloadforward=/support/downloads/manuals/3_ivt_express_kit_manual.pdf

A total of 10 µg labeled cRNA was hybridized to the Affymetrix Arabidopsis ATH1 Genome Arrays for 16 hours at 45°C as described in the Affymetrix GeneChip 3' IVT Express Kit Manual (Affymetrix, Santa Clara, CA). The first step of GeneChip staining was performed by using Streptavidin-Phycoerythrin, the second step by an antibody solution and then finally another Streptavidin-Phycoerythrin solution, with all liquid handling performed by a GeneChip Fluidics Station 450. GeneChips were then scanned with the Affymetrix GeneChip Scanner 3000 7G (Affymetrix, Santa Clara, CA) using Command Console v1.1.

I performed the following data analysis:

Probe level (.CEL file) data were generated using the Affymetrix Command Console v1.1. Probes were summarized to the gene level data in Partek Genomics Suite v6.5 (Partek, St. Louis, MO) using the RMA algorithm (Irizarry *et. al.*, 2003). Partek was used to determine gene level ANOVA p-values, fold changes and false discovery rate (FDR).

4.2.6 ***Quantitative Real-Time RT-PCR:***

First strand cDNA was generated using the High Capacity cDNA Reverse Transcription Kit (Applied Biosystems, CA). Real-time PCR was then performed using TaqMan Gene Expression Assays (Applied Biosystems, CA) for each of the displayed genes (Table S4.1) 15 ng of cDNA and the 7900HT Real-Time PCR System (Applied Biosystems, Foster City,

CA, USA) using the standard run conditions recommended by the manufacturer (50 °C: 2 min; 95 °C: 10 min; 40 x (95 °C: 15 s; 60 °C: 1 min)). The total reaction volume was 20 µl and the relative cDNA levels were calculated using the relative standard curve method according to the manufacturer's recommendations. The expression of each gene was normalized to the expression of *act2*.

4.2.7 Functional Analysis of Differentially Regulated Genes:

The MapMan program (Thimm et al., 2004) was used in order to classify and display genes into metabolic pathway groups and to quantify the genes active in cellular responses.

4.3 Results:

4.3.1 Chlorophyll *a* Fluorescence (Excitation pressure and P700)

In order to assess whether the experimental treatments generated the desired increase in EP, chlorophyll *a* fluorescence measurements were performed in-vivo on the plants. Both the HL and LT treated plants showed the same significant 4-fold increase in closed PS II reaction centers (Figure 4.1). On the other hand, both of the inhibitor treatments appeared to equally close all PS II reaction centers ($1 - qP = 1.0$) (Figure 4.1). The absolute values for EP varied depending on whether it was measured as $1 - qP$ (Dietz *et al.*, 1985; Schreiber *et al.*, 1994; Hüner *et al.*, 1998) or $1 - qL$ (Kramer *et al.*, 2004; Baker, 2008), but the trends remained the same (Figure 4.1; see Supplemental Figure S4.1).

To address the efficiency of the two inhibitors, the linear electron transport in plants treated with either DBMIB or DCMU was additionally tested utilizing P700 measurements as described in the Methods. The traces show that in the control plants, which were infiltrated with water for one hour, intersystem electron transport was unimpaired (Figure 4.2). After oxidizing P700 to P700⁺ with far red light the A_{820} increased due to the incapability of PS II to provide electrons in order to reduce P700 under this selective light condition. Once a single- and a multiple turnover saturating light flash was applied, PS II produced electrons and transported them to PS I which is visible in the sudden decrease in A_{820} , representing the reduction of P700⁺ to P700. Yet, in the traces shown for plants that were infiltrated with either DCMU or DBMIB for the same time period as the water control, these peaks of decrease in A_{820} after the application of various saturating light flashes were not present. Even though PS II was producing electrons as a response to the saturating light, they could not be transported to PS I in order to reduce P700⁺ anymore, due to the effects of the two inhibitors (Figure 4.2).

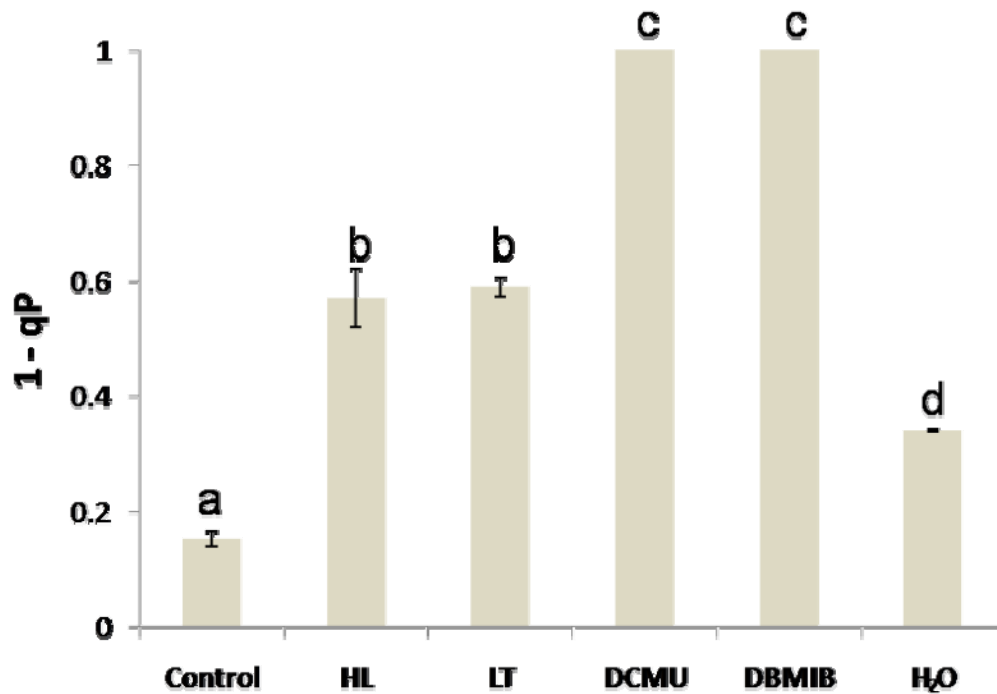


Figure 4.1 Quantification of Excitation Pressure in *Arabidopsis* Leaves after Various Stress Treatments

Excitation Pressure was measured as 1-qP in all treatments. Control plants and plants infiltrated with DCMU, DBMIB and water were measured at 25°C and 50 $\mu\text{mol photons m}^{-2}\text{s}^{-1}$, while plants exposed to HL and LT were measured at 25°C and 750 $\mu\text{mol photons m}^{-2}\text{s}^{-1}$ and 5°C and 50 $\mu\text{mol photons m}^{-2}\text{s}^{-1}$ respectively. Data represent the mean \pm SE calculated from three to six different plants per treatment. Letters represent statistically significant differences between means at the 95% confidence interval.

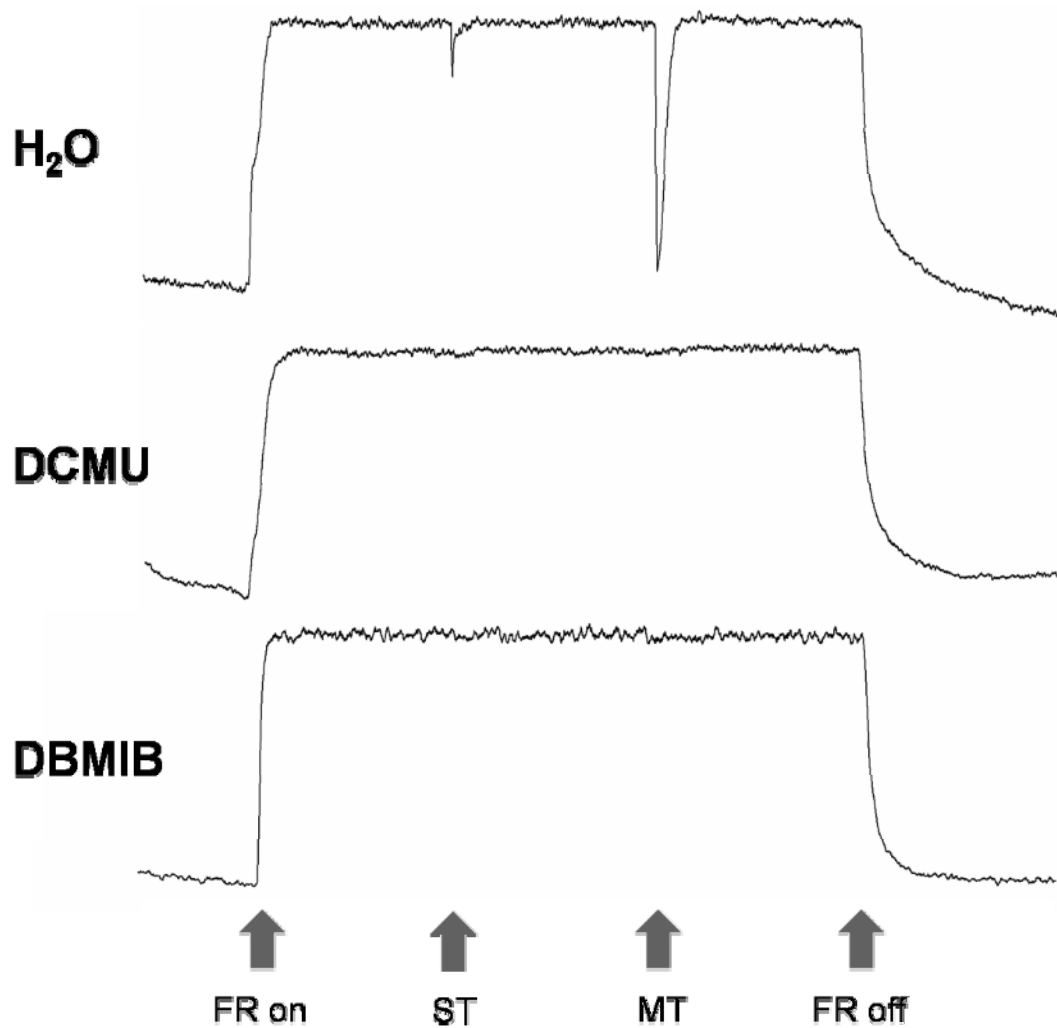


Figure 4.2 Intersystem Electron Transport in Response to Inhibitor Treatment

P700 traces measured as ΔA_{820} in detached leaves that were vacuum infiltrated with either DBMIB, DCMU or water and incubated for one hour at 25°C and 50 $\mu\text{mol photons m}^{-2}\text{s}^{-1}$. After a steady-state level of P700⁺ was achieved by illumination with far-red light (FR) a saturating white light single turnover flash (ST) and a multiple turnover (MT) flash pulse was applied. Each trace shows a representative result chosen from 3 individual measurements from 3 distinct plants.

4.3.2 *Determination of Differential Gene Expression*

The biologically significant cut-off level for gene expression on all microarrays of treated plants in comparison to their respective control was chosen at 1.5 fold while the statistical significance level was chosen as $P = 0.01$. While choice of fold-change cut-off levels did affect the total number of genes found differentially expressed, the ratios between up- and down-regulated genes and the intersections between the compared treatments remained the same, indicating that the choice of a cut-off level of 1.5 fold does not skew the results in any particular direction (Fig S4.2 C,D,E and Fig S4.3 A-F). This was confirmed by examining the distribution of the differentially regulated genes at different fold change cut-off levels (1.5x, 2.0x, 2.5x and 3.0x) on a functional level throughout the major metabolic pathways, using MapMan (Thimm et al., 2004). The results confirm that the even distribution of genes regulated by either HEP, PQH₂ or PS II amongst primary metabolic pathways is not altered when different cut-off levels are applied (Fig. S4.4).

4.3.3 *High-Light and Low-Temperature Shift Experiments*

The shift to both HL and LT resulted in the radical reprogramming of gene expression including both up-regulated and down-regulated genes, when compared to the control. Out of the 22,800 probes monitored, ca. 19.9 % were differentially expressed as a result of the HL treatment, or, more precisely, 2073 transcripts were up-regulated and 2456 were down-regulated. This is in congruency with previous experiments performed by Ruckle et al. (2012) which found that 20 % of the Arabidopsis transcriptome is regulated by light.

Plants that underwent the LT treatment expressed ca. 29.2 % of the genes differentially, that reflected 2493 up-regulated and 4174 down-regulated transcripts (Figure 4.3A and S4.2).

Interestingly, approximately 10.9 % of all measured transcripts showed the same altered gene expression in both, the HL and LT treatment (Figure 4.3). These 817 up-regulated and 1672 down-regulated genes constitute the genes that under a traditional

experimental setup are identified as HEP-regulated genes (Maxwell et al, 1998; Ndong et al, 2001) and will hereafter be referred to as such.

The following mRNAs that are associated with light signaling were affected by the HL treatment: *lhcb2.3*: -14.6x; *lhcb4.2*: -7.9x; *lhcb6*: -3.1x; *lhca6*: -2.6x; *lhca4*: -2.6x; *lhcb3*: -2.0x; *lhcb5*: -1.8x; *lhca1*: -1.6x; *lhcb2.1*: -1.6x; *lhca2*: -1.5x; *elip1* 9.6x; *elip2*: 7.1x (LT: *elip2*: 6.2x); *petE* (plastocyanin) -4.3x (LT: *petE*: -1.9).

Several transcripts that are known to be cold-induced, such as the cold regulated (*cor*) genes and the *cbf* transcription factors were all up-regulated in our LT shift experiment (*cor15a*: 2.1x; *cor15b*: 2.5x; *cor47*: 6.2x; *cbf1*: 8.4x; *cbf2*: 9.8x; *cbf3/dreb1a*: 10.4x; *cbf4*: 2.3x). Additionally to the LT treatment, *cbf3/dreb1a* was found up-regulated in the HL treatment (4.9x) making it a HEP regulated transcript, and the PQH₂ (5.2x) regulated genes, while *cbf1* was also up-regulated by PQH₂ (2.5x), but not by HEP.

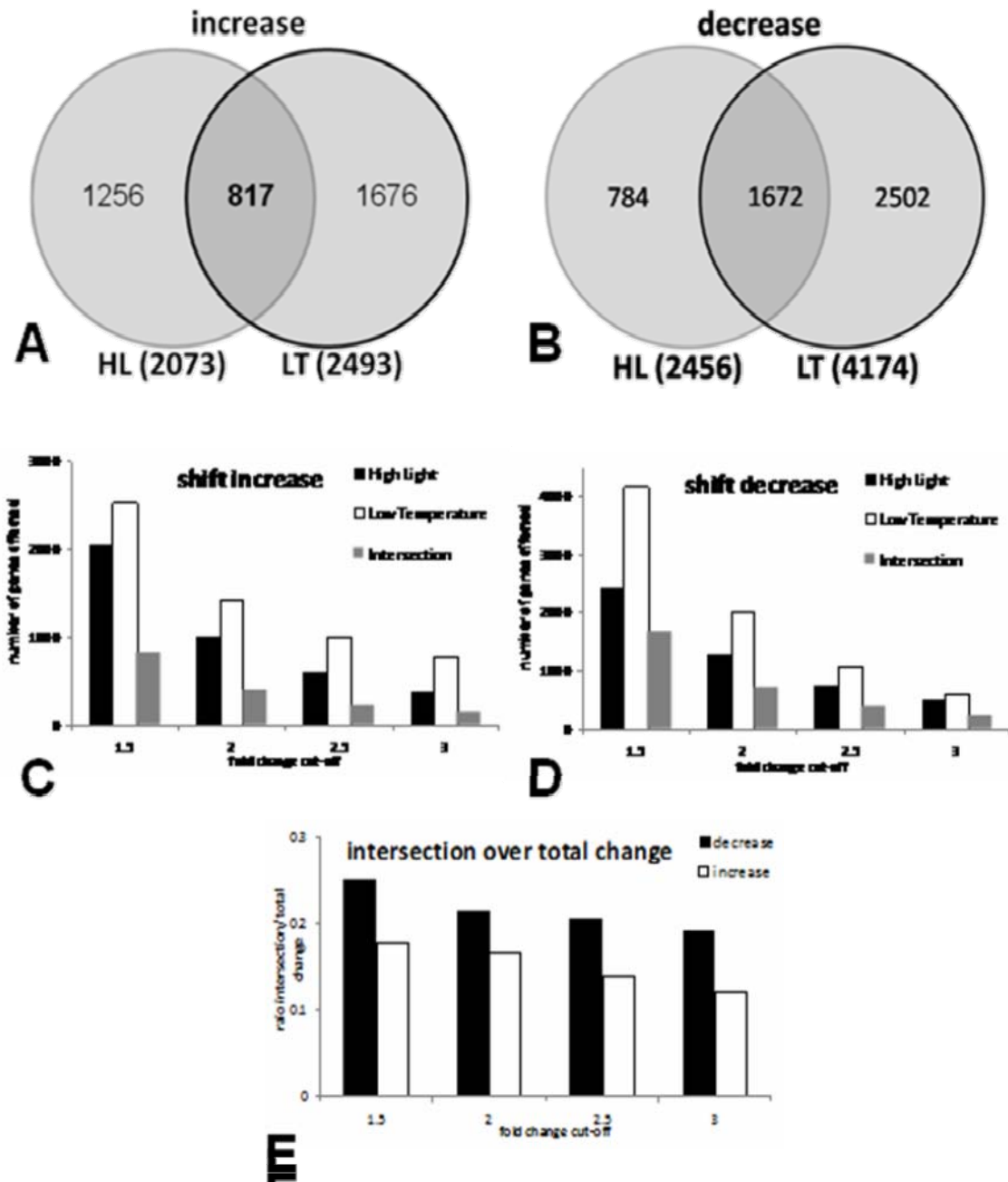


Figure 4.3 Number of Genes Regulated by HL and LT

Venn diagram of genes **(A)** up- and **(B)** down-regulated in total after shift to high light (HL) and low temperature (LT) in comparison to control plants (25/50) at a fold change level of greater than 1.5x. C+D: Total number of genes **(C)** up- or **(D)** down-regulated by HL and LT and both together at different fold change cut-off levels. **(E)** Ratio of genes that are altered by both HL and LT over total number of genes altered by either HL or LT.

4.3.4 *The Effects of Chemical Inhibitors on Gene Expression*

In order to distinguish which genes are regulated by the PQ-pool and which ones were altered due to the infiltration process or to possible unspecific effects of the inhibitors, plants were infiltrated with DCMU, DBMIB and water, respectively, and then incubated for one hour in either growth light conditions ($50 \mu\text{mol photons m}^{-2}\text{s}^{-1}$) or in the darkness. An ANOVA was performed in order to create gene lists comparing the inhibitor and water infiltration effects in the light to their effects in the dark. The resulting lists of genes altered only by infiltration with either inhibitor in the light was compared to the list of genes altered by H₂O infiltration only in the light and duplicates were removed in order to create lists of genes that are truly regulated by either DCMU or DBMIB. Both inhibitors were used at the minimal concentrations, necessary for inhibiting the PETC in this experiment, to avoid pleiotropic effects on gene expression.

The infiltration with the inhibitors resulted in a more specific change of gene expression. While ca. 9.3 % of all genes (1057 up-regulated and 1071 down-regulated) were differentially expressed after the DBMIB inhibition, only ca. 3.1 % of the monitored transcripts (285 up-regulated and 420 down-regulated) were altered as a response to the DCMU inhibition (Figure 4.4 and S4.3).

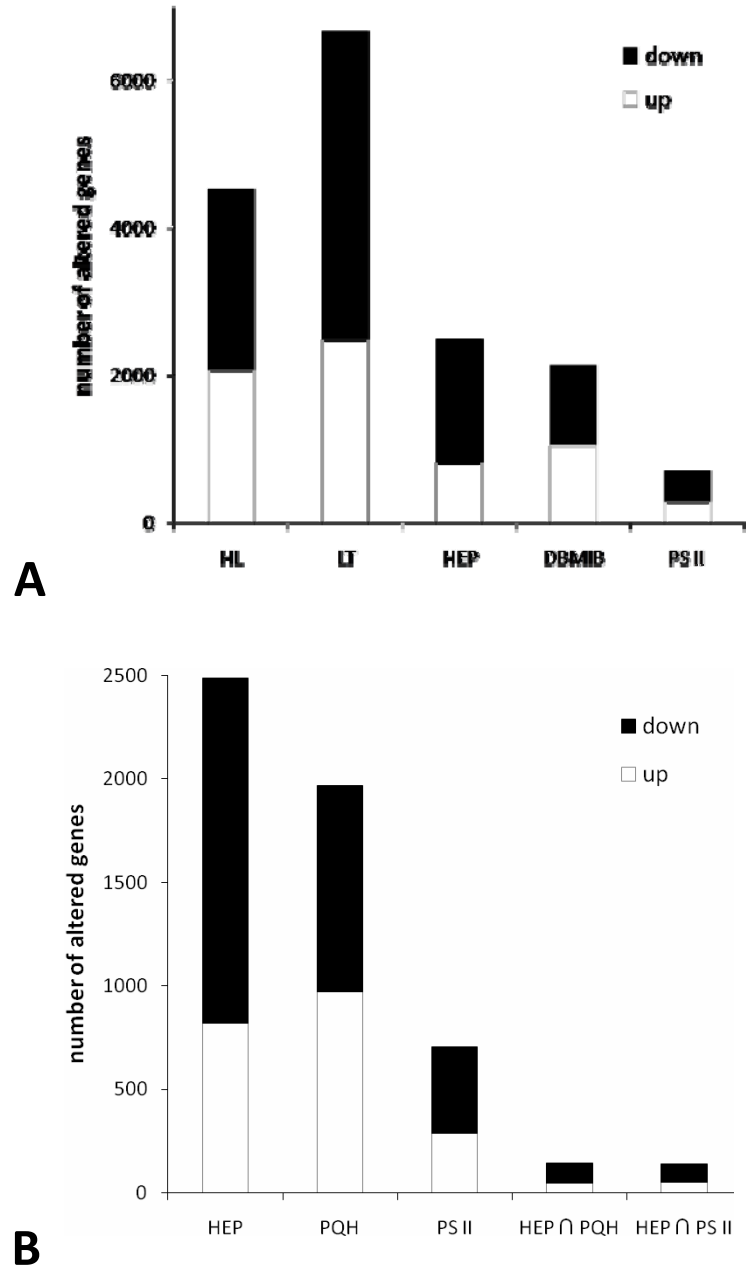


Figure 4.4 Comparison of Differentially Expressed Genes in Different Groups

Number of genes altered in each treatment compared to its respective control condition and comparisons of different treatments. **(A)** HL = High Light; LT = Low Temperature; HEP = genes that are equally regulated by high light and low temperature; DBMIB & PS II = genes regulated by either DBMIB or PS II **(B)** PQH₂ = genes regulated by plastoquinol; ∩ = intersection between two gene lists. The black part of the bars represents down-regulated genes and the white part represents the up-regulated genes. Genes were considered altered at a fold change level of 1.5x and P = 0.01.

4.3.5 **Contribution of PQH₂ and PS II to Gene Expression**

Since the PQ-pool was already fairly oxidized during the control growth conditions (1-qP \approx 0.15, Figure 4.1) and couldn't be much further oxidized by DCMU, the major effect of the addition of this inhibitor was to close the reaction centers of PS II. DBMIB on the other hand closed all the reaction centers of PS II and completely reduced the PQ-pool at the same time. So in order to single out the list of genes that was purely regulated by the reduced PQ pool, the list of DCMU regulated genes was subtracted from the list of DBMIB regulated genes (Figure 4.4). Due to the small overlap of genes regulated by DCMU and DBMIB, the number of genes truly regulated by the reduced PQ pool was still about 8.6 %, with 970 up-regulated and 1000 down-regulated transcripts (Figure 4.4; see Supplemental Figure S4.2).

In order to distinguish which genes were regulated by true PS II excitation pressure that is the redox state of Q_A⁻, the gene expression data from DCMU treated plants was determined. Since DCMU closes all PS II reaction centers, the genes regulated purely by DCMU can be inferred to be regulated by PS II and will from here on be referred to as such.

Some genes that have been previously described to be active in plastid signaling, such as *gun5* (Koussevitzky et al. 2007) and *stn7* (Pesaresi et al. 2010) were up-regulated by PQH₂ (ca 1.8 fold and ca 2.0 fold, respectively), but not in any of the other treatments.

4.3.6 **Comparison of HEP, PQH₂ and PS II as Redox Sensors of Gene Expression**

When considering the transcripts that were differentially expressed as a result of both the HL and the LT treatment (HEP regulated genes) and then comparing them to the PS II regulated genes, there is only an overlap of 5.5 % (51 up- and 86 down-regulated genes) between the two groups. The comparison of the HEP treatment list with the PQH₂ regulated genes results in an overlap of 5.7 % (47 up-regulated and 95 down-regulated genes)(Figure 4.4).

4.3.7 **Functional Analysis (MapMan):**

The genes that were differentially regulated as a result of HEP stress (i.e. in both the HL and LT treatment), appeared to be distributed over all of the most important metabolic processes, regardless of their cellular localization, with distinct accumulation of altered genes in various photosynthesis associated pathways (i.e. light reactions, photorespiration, tetrapyrrole synthesis) and mitochondrial electron transport (Figure 4.5A; see Supplemental Table S4.2).

The genes that appeared to be regulated by PQH₂ (Fig 4.4B; see Supplemental Table S4.3) equally appear in all major metabolic pathways and even though, by numbers, they made up for about 79 % of the HEP genes, they did not, for the most part, match the HEP regulated transcripts. In fact, when looking at photosynthesis related processes (Figure 4.5A,B, top right) it became apparent that HEP seems to inhibit gene expression, while PQH₂ increases transcript abundance, sometimes for the same genes (e.g. *lhcb6*, *lpa2*, *lhcb4.2*, *lhca6*, *atpd*, *ted4*) and only *aocat2* seemed to be up-regulated by both regulators (see Supplemental Table S4.2 and Table S4.3).

The impact of PS II on regulating gene expression in the major metabolic pathways was less than either HEP or PQH₂. But it can be stated that, contrary to the latter two gene regulators, there appears to be no apparent concentration of regulated transcripts in the photosynthesis related pathways of genes controlled by PS II (Figure 4.5C; see Supplemental Table S4.4).

The analysis of cellular responses with MapMan yielded similar findings. In spite of the different total number of regulated genes, all three regulators modulated the gene expression involved with most cellular response processes (Fig 4.6A-C). In fact, when looking at the main categories, the ratios between all three regulators seem similar and the true differences only arise in detailed differentiation of abiotic stresses and ROS sensing mechanisms. Interestingly, in none of the examined datasets could we find altered transcripts associated to a heme- or a light response. Unlike HEP and PS II, PQH₂ seemed to additionally lack a response linked to touch/wounding, glutaredoxin and

peroxiredoxin. PS II, on the other hand, did not induce a dismutase/catalase response, which could be found in both HEP and PQH₂.

Figure 4.5. MapMan Display of Major Metabolic Pathways. MapMan software (Thimm et al., 2004) was used to display significant changes in transcript abundance of genes associated with major metabolic pathways. **(A)** illustrates the differentially expressed genes that were affected by HEP. **(B)** shows the genes that were regulated by PQH₂ and **(C)** displays the genes that were differentially expressed by PS II. Red squares represent down-regulated transcripts, blue squares represent up-regulated transcripts, while white squares represent transcripts that remained unaltered in comparison to the control.

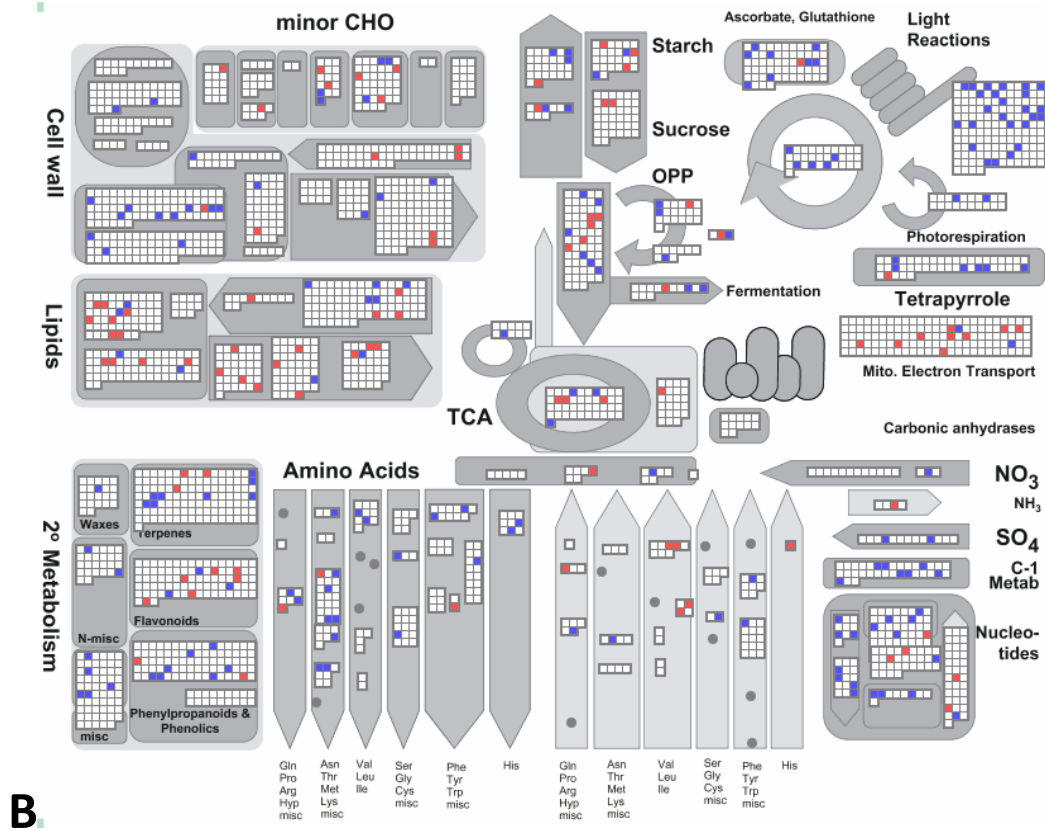
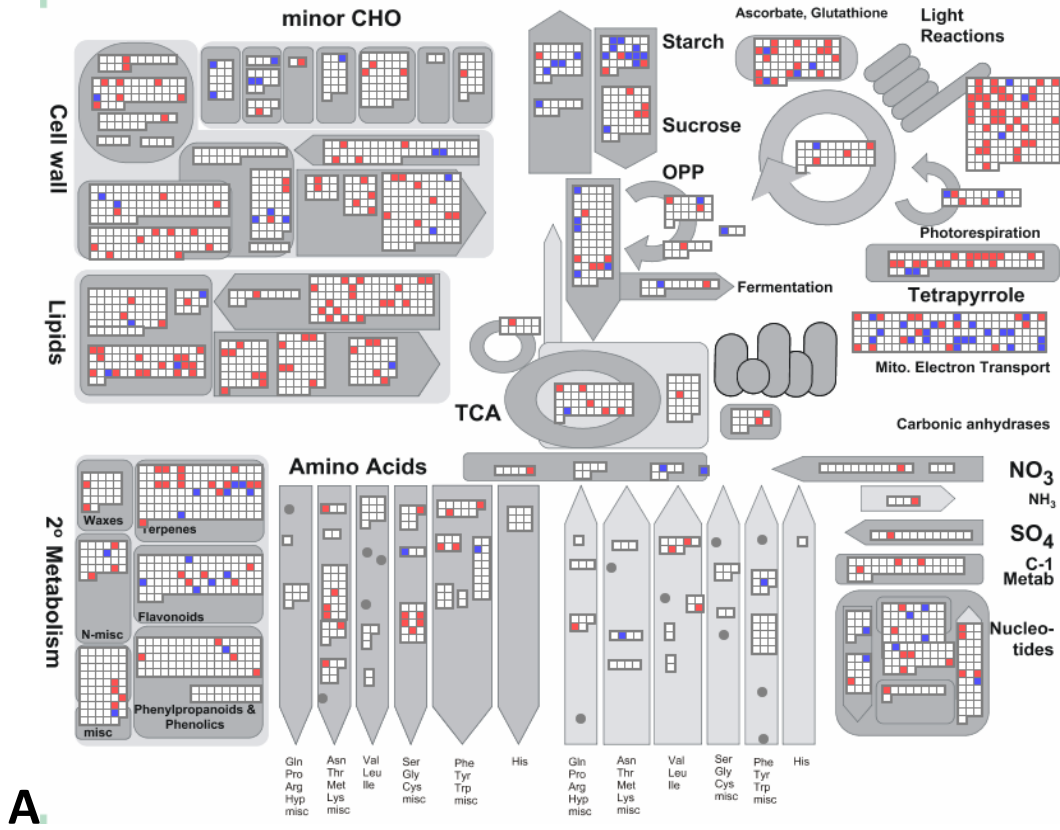
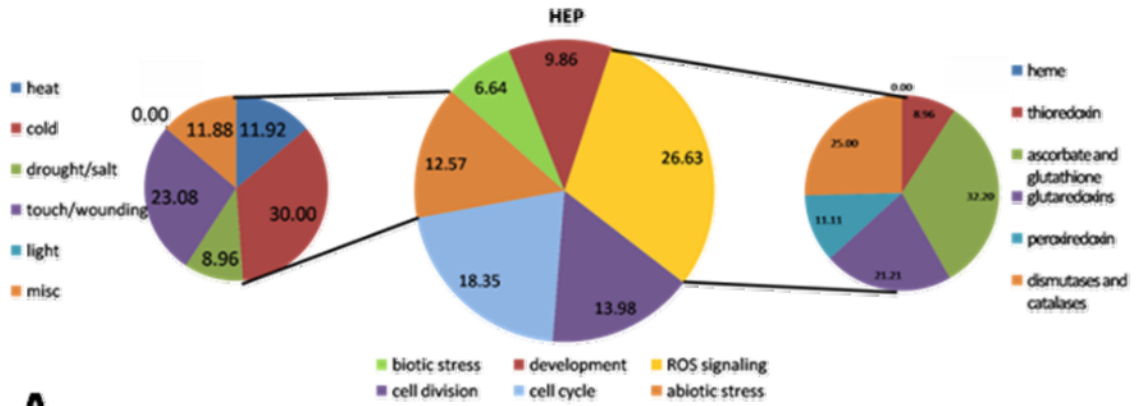
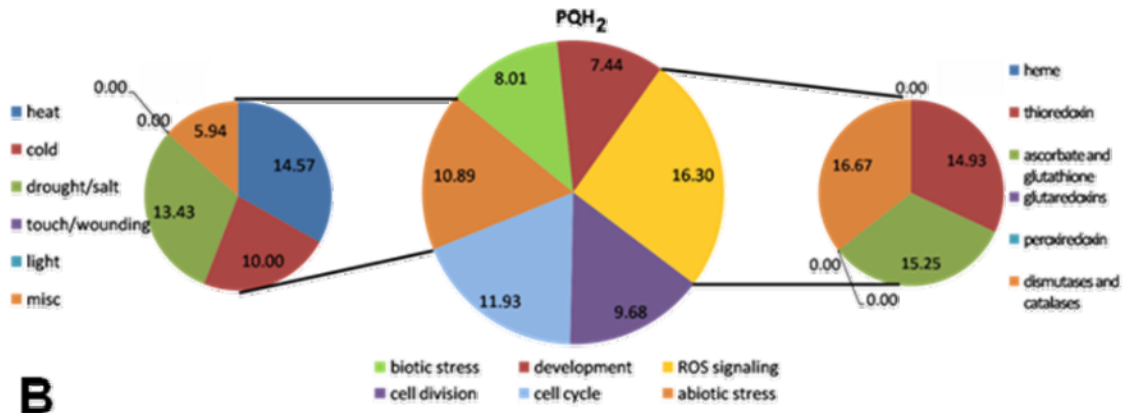


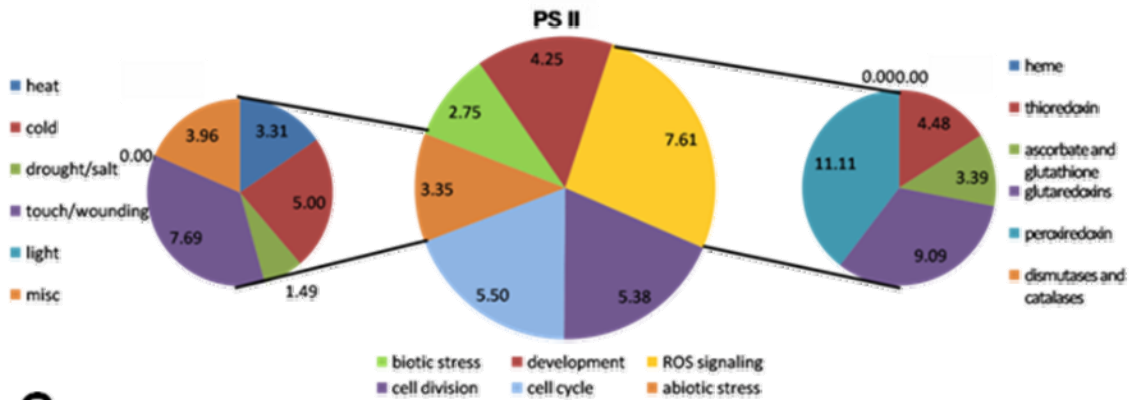
Figure 4.6. Display of Cellular Responses. MapMan software (Thimm et al., 2004) was used to display an overview of significant changes in transcript abundance of genes associated with Cellular Responses, showing the percentage of genes altered in each category. **(A)** illustrates the differentially expressed genes that were regulated by HEP, **(B)** shows the genes that were regulated by PQH₂ and **(C)** displays the genes that were differentially expressed by only DCMU and hence represent closed PSII reaction centers.



A



B



C

4.3.8 ***Real-time RT-PCR:***

After verifying the purity and integrity of the extracted RNA on the “Bioanalyzer”, quantitative real-time RT-PCR was performed in order to validate the microarray expression analysis for the transcripts for (*spa1*, *dreb1a*, *nda1* and *tub8*) (see Supplemental Figure S4.5). All four transcripts showed the same trend in both the Affymetrix ATH-1 microarray and the qPCR experiment for the majority of experimental treatments.

4.4 *Discussion:*

Previous research had shown that PS II EP acts as a global cellular energy sensor that affects far more than merely photosynthetic processes. For example HEP is able to regulate the growth pattern of a whole plant as well as altering mitochondrial electron transport and playing an important role in chloroplast development (Hüner et al., 1998, Rosso, Bode et al, 2009). It is also able to regulate the expression of genes which are entirely unrelated to photosynthesis and the chloroplast (e.g. wheat aluminum induced transcript, *wali7* or the mitochondrial alternative oxidase *aox1a* in *Arabidopsis*) (Ndong et al. 2001; Rosso, Bode et al. 2009), but the full extent of this phenomenon remained unknown. Moreover, excitation pressure effects were traditionally researched by modulation of light and temperature (Maxwell et al. 1995, Gray et al. 1997, Rosso, Bode et al. 2009), as it was assumed that *in-vivo* the intersystem electron transport components act as one signal, since their relative reduction states are connected and hence reflect each other.

Nevertheless, more recent investigations have demonstrated that redox signals from the PETC can arise at least at three different sites: PS II, the PQ-pool and the reducing side of PS I (reviewed in Fernandez & Strand 2008). *In-vivo*, a sudden increase in light intensity or a decrease in temperature will render the entire PETC in a reduced state causing each of these three sensors to signal that they are reduced. This, and the fact that light and temperature are, apart from their effects on the PETC, strong abiotic signals that can be sensed in various parts of the plant cell, can explain the large change in gene expression in the HL and LT treatments.

Only the addition of the specific electron transport inhibitors DCMU and DBMIB makes it possible to investigate the individual roles of PS II and PQ in retrograde signaling, even though this experimental setup precludes definite statements about PS I signaling.

DCMU binds to the Q_A binding site of PS II, thus inhibiting electron transfer between PS II and PQ, leaving PS II fully reduced (Figure 4.1), while both PQ and PSI and all downstream factors remain entirely oxidized. DBMIB on the other hand binds to the PQ

binding site of cytochrome b_6f , thus blocking the electron transfer between PQ and the cytochrome b_6f complex and hence results in a fully reduced PS II and PQ while still leaving PSI and subsequent downstream factors (i.e. NADP^+) oxidized.

The ratio of genes differentially expressed by all treatments, HL and LT (see Supplemental Figure S4.2 C-E) and both inhibitors (see Supplemental Figure S4.3) stays roughly the same, regardless of the fold change level that is used to determine which genes are altered in their expression and which ones are not. This shows that choosing either cut-off level does not bias the experiment in either direction.

The most striking result of this investigation was the huge impact of both HL and LT on overall gene expression (Figure 4.3 + 4.4) and their large overlap of genes that are regulated in the same way by both factors. All of these genes would have been annotated as EP or redox regulated, using traditional light-temperature experimental setups. Yet our results show clearly that in spite of an almost equally large number of PQH_2 regulated genes, there is very little in common between these two groups and only 7 % of the PQH_2 regulated genes were also found in the HEP group.

Previous experiments investigating photosynthetic redox signaling were predominantly performed by utilizing *lhcb1* or *rbcS* as reporter transcripts (Piippo et al. 2006; Kindgren et al. 2012; Ruckle et al. 2012), yet it has to be stated that our experiments did not result in a differential expression of either one of these transcripts, even though many other light harvesting complex transcripts of both PS II and PS I were affected (HEP: *lhca6*, *lhcb4*, *lhcb6* are down-regulated; PQH_2 : *lhca1*, *lhca3*, *lhca5*, *lhca6*, *lhcb2.1*, *lhcb4*, *lhcb2.3*; are up-regulated; PS II: no *lhcb*'s were affected). The reason for that is the comparatively short exposure (1h) of the plants to the respective stress condition used to catch primary transcript targets of redox signaling. This suggests that both *rbcS* and *lhcb1* are not regulated per se through any reduced component of the PETC, but rather through one or more secondary events that are regulated by the PETC.

It is also astonishing how few genes, in comparison, are solely regulated by PS II, which might be partially explained due to the fact that the redox state of PQH_2 and PS II are

inseparable from each other *in-vivo* and there is little need for two independent redox sensors. Another explanation might be the high turnover rate of PS II, rendering it too unstable as a reliable sensor.

One explanation for the disparity between the genes regulated by HEP and the genes that have been identified as truly regulated through PS II and PQH₂, might be the differential degree of reduction applied through the experimental setup. While HL and LT are very effective reductants of the PETC, they only close ca. 60 % of all PS II reaction centers ($1-qP \approx 0.6$; Figure 4.1), the inhibitors fully inhibit linear electron transport ($1-qP = 1.0$; Figure 4.1), presumably creating a more severe and slightly different stress condition, to which the plant might require an alternative strategy of reaction. Another possible scenario could be that the pleiotropic effects that both HL and LT indubitably have, might override some of the redox signals of the PETC.

As for the functional analysis, it is to be stated that even though PS II appears to regulate only a fraction of the genes compared to PQH₂ and HEP, in all cases it becomes apparent that the genes involved are not merely involved with photosynthesis or closely related chloroplast processes, but all regulators affect many distinct pathways of metabolism in different parts of the cell. This holds true for not only the major metabolic pathways (Figure 4.5) but also the cellular responses (Figure 4.6). This is not surprising since the PETC acts as an energy sensor for the chloroplast which is tightly connected to the energy status of the entire cell (Hüner et al. 1998). This means that changes in the reduction state of the PETC will affect all other cellular compartments apart from the chloroplast, which ultimately receive their chemical energy through photosynthesis. For example we were recently able to demonstrate that a change in excitation pressure affects the alternative oxidase of the mitochondria (Rosso, Bode et al, 2009), suggesting that a strong reduction of the PETC will alter mitochondrial retrograde signaling and electron transport as well.

Our findings are not congruent with Piippo *et al.* (2006) who suggested that the redox state of the PQ pool is of minor importance for nuclear gene regulation, at least during early stages of chloroplast signaling. In contrast we found that 8.6 % of the monitored

genes responded to a reduced PQ pool suggesting, that PQ might be one of the major players in photosynthetic redox signaling.

We conclude, that redox signaling of the PETC exists most likely as a synergistic and complex network of sensors and signal transducers that are partially integrated and redundant. Yet there are various sensors within the thylakoid membrane that affect distinct target genes that are not regulated by another sensor, or not altered the same way by other sensors. Both PS II and PQH₂ are important components of this sensing/signaling machinery considering that together they regulate up to 11.7 % (PS II: 3.1 %; PQH₂: 8.6 %) of the entire genome, but they can only account for ca 11 % of the HEP effects. The remaining 89 % of HEP induced gene regulation are most likely due to other factors, such as PS I, NADPH⁺ or downstream metabolites which can fine tune excitation pressure signaling and possibly override the indubitably significant effects of PQH₂ and PS II.

ACKNOWLEDGEMENT:

We are grateful to David Carter at the London Regional Genomics Center (Robarts Research Institute, London, Ontario, Canada; <http://www.lrgc.ca>) for processing all the micro-array chips and providing the license and training for the use of Partek. Research was supported by grants to NPAH from NSERC, CFI and the CRC program.

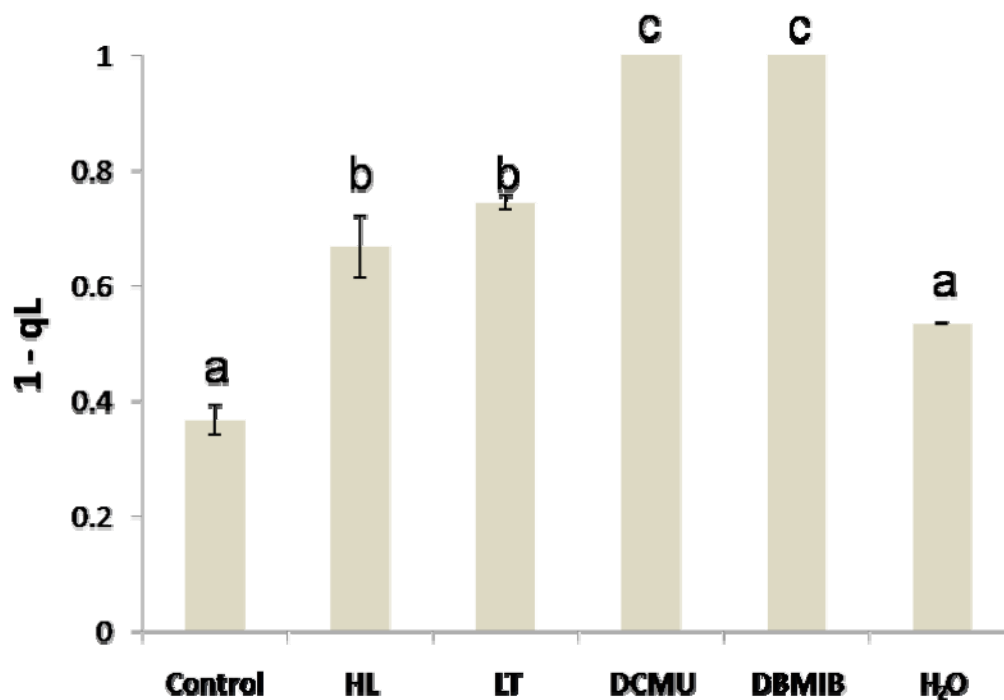
4.5 *References:*

- Bräutigam, K., Dietzel, L., Kleine, T., Ströher, E., Wormuth, D., Dietz, K.J., Radke, D., Wirtz, M., Hell, R., Dörmann, P., Nunes-Nesi, A., Schauer, N., Fernie, A.R., Oliver, S.N., Geigenberger, P., Leister, D., and Pfannschmidt, T. (2009). Dynamic plastid redox signals integrate gene expression and metabolism to induce distinct metabolic states in photosynthetic acclimation in *Arabidopsis*. *Plant Cell*. 21: 2715–2732.
- Dahal, K., Kane, K., Gadapati, W., Webb, E., Savitch, L.V., Singh, J., Sharma, P., Sarhan, F., Longstaffe, F.J., Grodzinski, B., and Hüner, N.P.A. (2012). The effects of phenotypic plasticity on photosynthetic performance in winter rye, winter wheat and *Brassica napus*. *Phys. Plant*. 144: 169–188.
- Dietz, K.J., Schreiber, U., and Heber, U. (1985). The relationship between the redox state of QA and photosynthesis in leaves at various carbon-dioxide, oxygen and light regimes. *Planta* 166: 219–226.
- Escoubas, J.M., Lomas, M., LaRoche, J., and Falkowski, P.G. (1995). Light intensity regulation of cab gene transcription is signaled by the redox state of the plastoquinone pool. *Proc. Natl. Acad. Sci. USA* 92: 10237–10241.
- Fernández, P.A., and Strand, Å. (2008). Retrograde signaling and plant stress: plastid signals initiate cellular stress responses. *Curr Opin Plant Biol*. 11:509–513.
- Hüner, N.P.A., Öquist, G., and Sarhan, F. (1998). Energy balance and acclimation to light and cold. *Trends Plant Sci*. 3: 224–230.
- Hüner, N.P.A., Öquist, G., and Melis, A. (2003). Photostasis in plants, green algae and cyanobacteria: The role of light harvesting antenna complexes. In *Advances in Photosynthesis and Respiration: Light-Harvesting Antennas in Photosynthesis*, Vol. 13, B.R. Green and W.W. Parsons, eds (Dordrecht, The Netherlands: Kluwer Academic Publishers), pp. 401–421.
- Irizarry, R.A., Bolstad, B.M., Collin, F., Cope, L.M., Hobbs, B., Terence, P., and Speed, T.P. (2003) Summaries of Affymetrix GeneChip probe level data. *Nucleic Acids Research* 31(4): 15
- Gill, S.S., Tuteja, N. (2010) Reactive oxygen species and antioxidant machinery in abiotic stress tolerance in crop plants. *Plant Phys Biochem* 48: 909-930

- Gray, G.R., Chauvin, L-P., Sarhan, F., and Hüner, N.P.A. (1997). Cold Acclimation and Freezing Tolerance (A Complex Interaction of Light and Temperature). *Plant Physiol.* 114(2): 467-474.
- Gray, G.R., and Heath, D. (2005). A global reorganization of the metabolome in *Arabidopsis* during cold acclimation is revealed by metabolic fingerprinting. *Phys Plant.* 124: 236–248.
- Hosack, D.A., Dennis, G., Sherman, B.T., Lane, H.C., and Lempicki, R.A. (2003). Identifying biological themes within lists of genes with EASE. *Genome Biology* 2003, 4: R70
- Ivanov, A.G., Morgan, R.M., Gray, G.R., Velitchkova, M.Y. and Huner, N.P.A. (1998) Temperature/light dependent development of selective resistance to photoinhibition of photosystem I. *FEBS Lett.* 430: 288–292.
- Kindgren, P., Eriksson, M.-J., Benedict, C., Mohapatra, A., Gough, S.P., Hansson, M., Kieselbach, T., and Strand, A. (2011). A novel proteomic approach reveals a role for Mg-protoporphyrin IX in response to oxidative stress. *Physiol Plant.* 141: 310–320.
- Kindgren, P., Kremnev, D., Blanco, N.E., de Dios Barajas López, J., Fernández, A.P., Tellgren-Roth, C., Small, I., and Strand, Å. (2012). The plastid redox insensitive 2 mutant of *Arabidopsis* is impaired in PEP activity and high light-dependent plastid redox signalling to the nucleus. *Plant J.* 70(2): 279-91.
- Koussevitzky, S., Nott, A., Mockler, T.C., Hong, F., Sachetto-Martins, G., Surpin, M., Lim, J., Mittler, R., and Chory, J. (2007). Signals from Chloroplasts Converge to Regulate Nuclear Gene Expression. *Science.* 316: 715-719
- Kramer, D.M., Johnson, G., Kiirats, O., and Edwards, G.E. (2004). New fluorescence parameters for the determination of QA redox state and excitation energy fluxes. *Photosynth. Res.* 79: 209–218.
- Krause, G.H., and Weis, E. (1991). Chlorophyll fluorescence and photosynthesis: the basics. *Annu. Rev. Plant Physiol. Plant Mol. Biol.* 42: 313–349.
- McDonald, A.E., Ivanov, A.G., Bode, R., Maxwell, D.P., Rodermeil, S.R., and Hüner, N.P.A. (2011). Flexibility in photosynthetic electron transport: The physiological role of plastoquinol terminal oxidase (PTOX). *Biochim. Biophys. Acta:* 1807: 954–967.
- Maxwell, D.P., Laudenbach, D.E., and Hüner, N.P.A. (1995). Redox Regulation of Light-Harvesting Complex II and *cab* mRNA Abundance in *Dunaliella salina*. *Plant Physiol.* 109: 787-795.
- Miller, G., Suzuki, N., Ciftci-Yilmaz, S., and Mittler, R. (2010). Reactive oxygen species homeostasis and signaling during drought and salinity stresses. *Plant Cell and Environ.* 33: 453–467.
- Ndong, C., Danyluk, J., Hüner, N.P., and Sarhan, F. (2001). Survey of gene expression in winter rye during changes in growth temperature, irradiance or excitation pressure. *Plant Mol Biol.* 45(6): 691-703

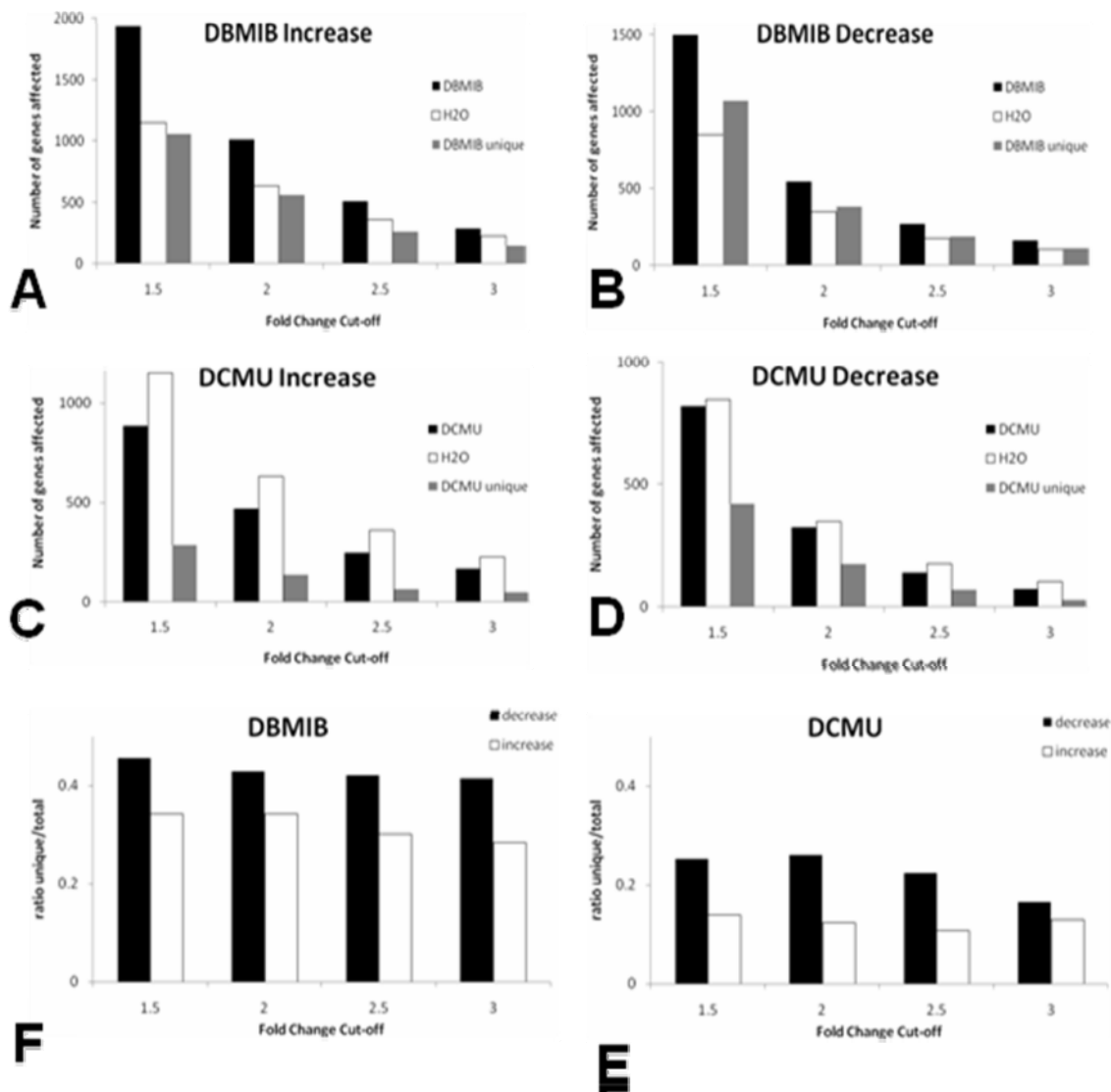
- Pesaresi, P., Hertle, A., Pribil, M., Schneider, A., Kleine, T., and Leister, D. (2010). Optimizing photosynthesis under fluctuating light. The role of the Arabidopsis STN7 kinase. *Plant Signaling & Behaviour*. 5: 21-25.
- Piippo, M., Allahverdiyeva, Y., Paakkanen, V., Suoranta, U-M., Battchikova, N., and Aro, E-M. (2006). Chloroplast-mediated regulation of nuclear genes in Arabidopsis thaliana in the absence of light stress. *Physiol Genomics*. 25: 142-152.
- Pogson, B.J., Woo, N.S., Forster, B., and Small, I.D. (2008). Plastid signalling to the nucleus and beyond. *Trends Plant Sci*. 13(11), 602–609.
- Rosso, D., Bode, R., Li, W., Krol, M., Saccon, D., Wang, S., Schillaci, L.A., Rodermel, S.R., Maxwell, D.P., and Hüner, N.P.A. (2009). Photosynthetic Redox Imbalance Governs Leaf Sectoring in the Arabidopsis thaliana Variegation Mutants immutans, spotty, var1, and var2. *Plant Cell*. 21(11):3473-92
- Ruckle, M.E., Burgoon, L.D., Lawrence, L.A., Sinkler, C.A., and Larkin, R.M. (2012). Plastids Are Major Regulators of Light Signaling in Arabidopsis. *Plant Phys*. 159: 366–390.
- Schreiber, U., Bilger, W., and Neubauer, C. (1994). Chlorophyll fluorescence as a non-intrusive indicator for rapid assessment of in vivo photosynthesis. In *Ecophysiology of Photosynthesis*, E. Schulze and M.M. Caldwell, eds (Berlin: Springer-Verlag), pp. 49–70.
- Thimm, O., Bläsing, O., Gibon, Y., Nagel, A., Meyer, S., Krüger, P., Selbig, J., Müller, L.A., Rhee, S.Y., and Stitt, M. (2004). MAPMAN: a user-driven tool to display genomics data sets onto diagrams of metabolic pathways and other biological processes. *Plant J*. 37(6):914-39.
- Wilson, K.E., Krol, M., and Hüner, N.P.A. (2003). Temperature-induced greening of *Chlorella vulgaris*. The role of the cellular energy balance and zeaxanthin-dependent nonphotochemical quenching. *Planta*. 217: 616–627.
- Woodson, J.D., Perez-Ruiz, J.M., and Chory, J. (2011). Heme synthesis by plastid ferrochelatase I regulates nuclear gene expression in plants. *Curr. Biol*. 21: 897–903.

4.6 Supplemental Figures



Supplemental Figure S 4.1 Quantification of Excitation Pressure in Plants after Various Stress Treatments

Excitation Pressure was measured as 1-qL (B) in all treatments. Control plants and plants infiltrated with DCMU, DBMIB and water were measured at 25°C and 50 $\mu\text{mol photons m}^{-2}\text{s}^{-1}$, while plants exposed to HL and LT were measured at 25°C and 750 $\mu\text{mol photons m}^{-2}\text{s}^{-1}$ and 5°C and 50 $\mu\text{mol photons m}^{-2}\text{s}^{-1}$ respectively. Data represent the mean \pm SE calculated from three to six different plants per treatment. Letters represent statistically significant differences between means at the 95% confidence interval.



Supplemental Figure S 4.2 Number of Genes Regulated by Inhibitors

Comparison of genes up- (A,C) and down-regulated (B,D) considering different fold-change cut-off levels, after treatment with the inhibitors DBMIB (A,B) and DCMU (C,D) in comparison to control plants treated with water. E,F: Ratio of genes that are up- and down-regulated uniquely by DBMIB (E) and DCMU (F) over total number of genes altered by each inhibitor itself and the water control in total.

Figure S4.3 MapMan Display of Major Metabolic Pathways. MapMan display of profiling data. MapMan software (Thimm et al., 2004) was used to display significant changes in transcript abundance of genes associated with major metabolic pathways, A illustrates the differentially expressed genes which were affected by HL. B shows the genes that were regulated by LT. Red squares represent down-regulated transcripts, blue squares represent up-regulated transcripts, while white squares represent transcripts that remained unaltered.

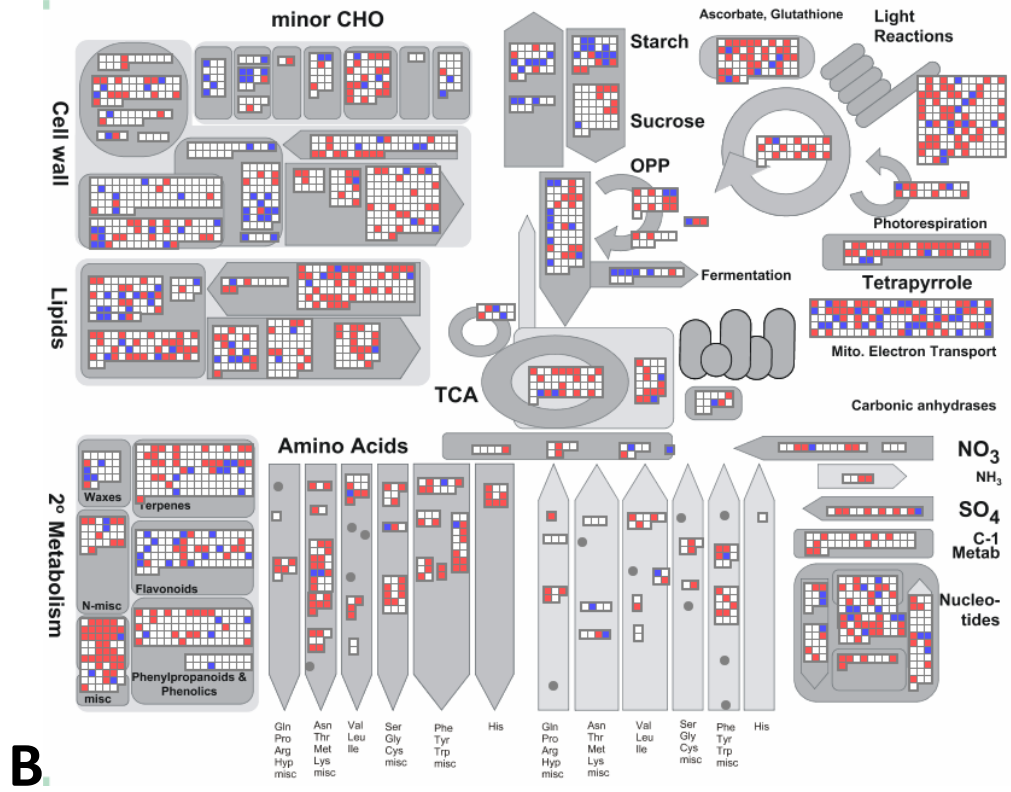
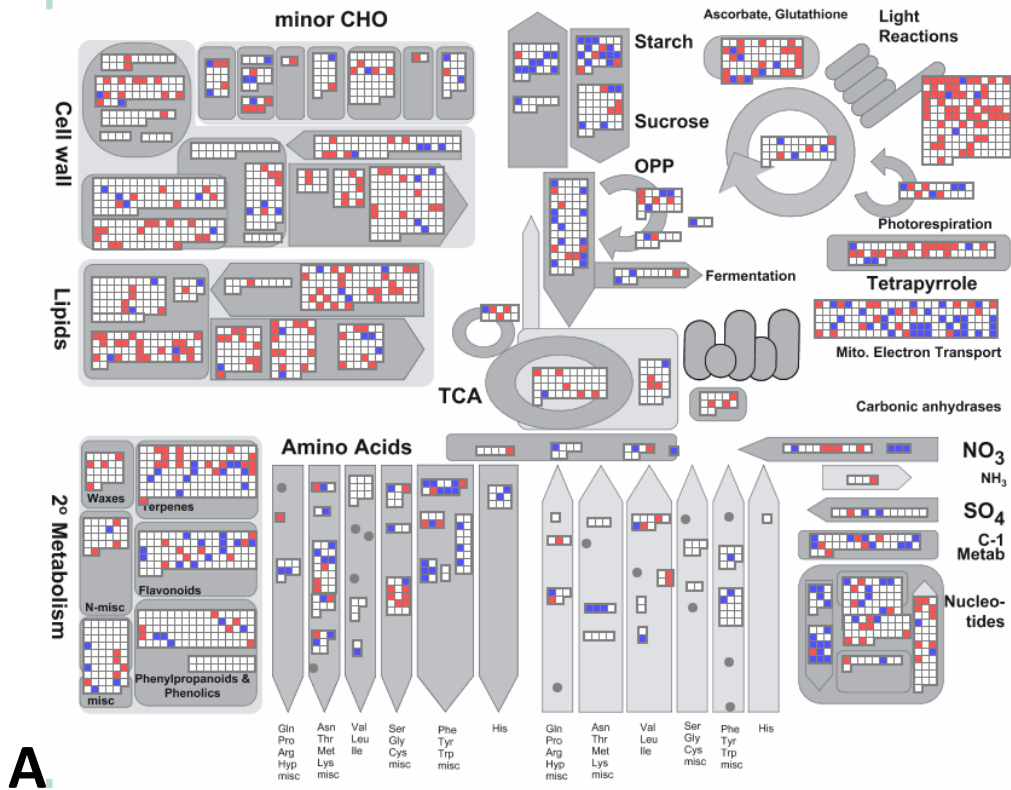
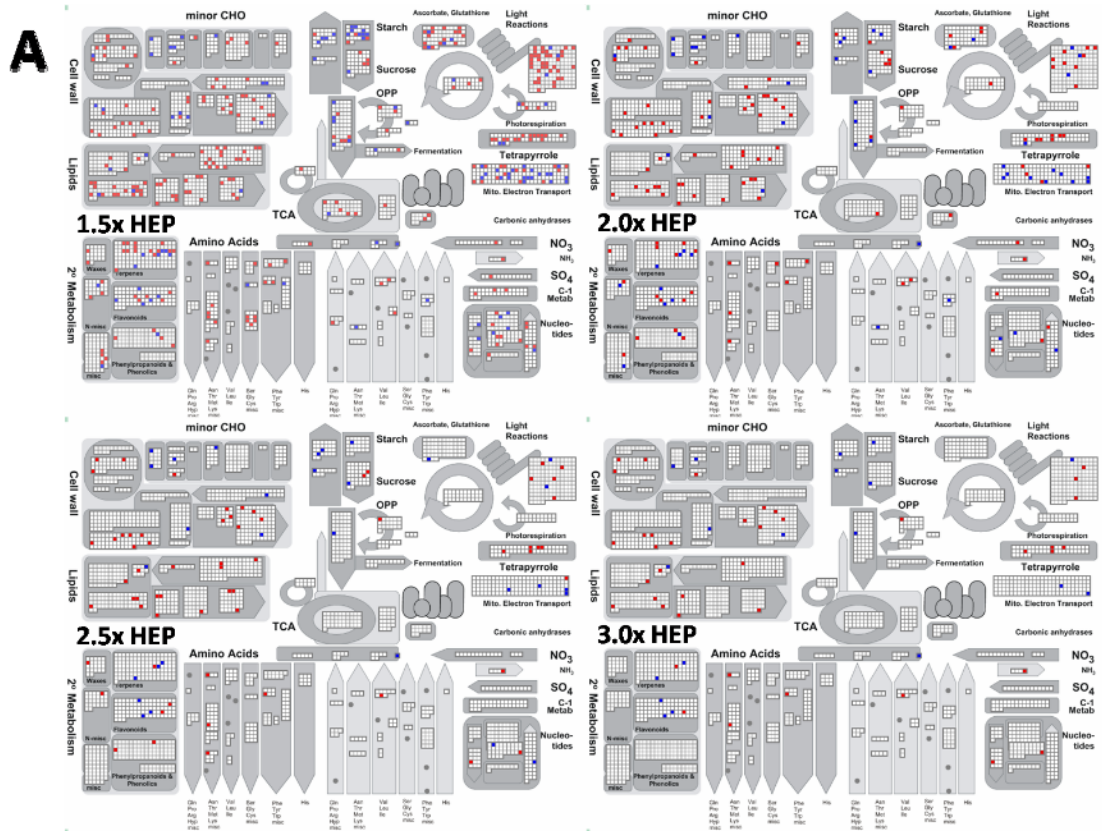
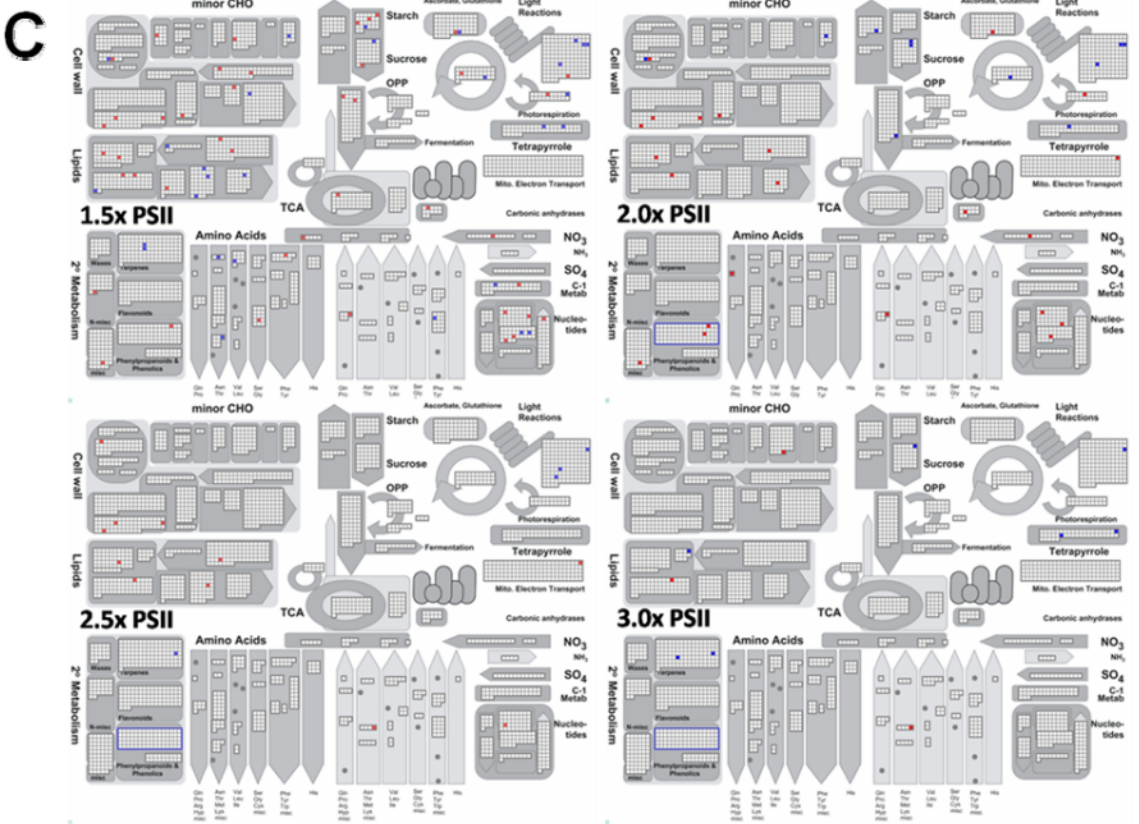
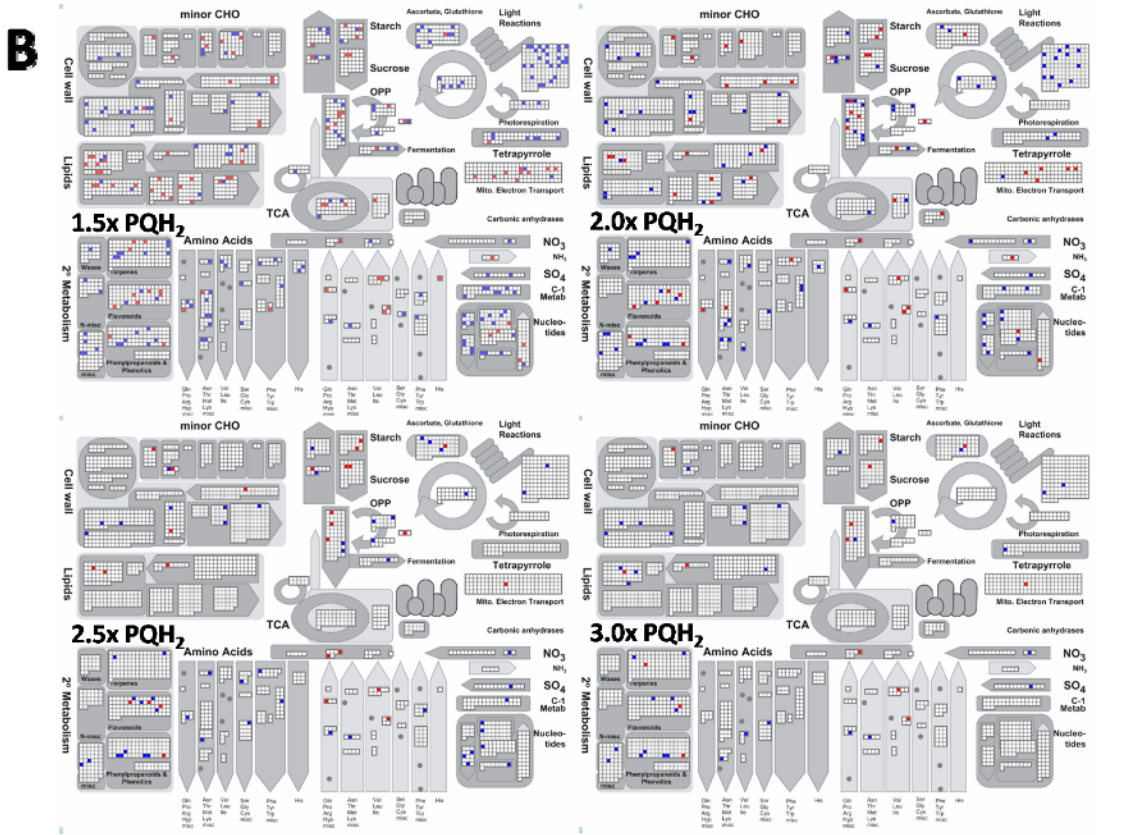
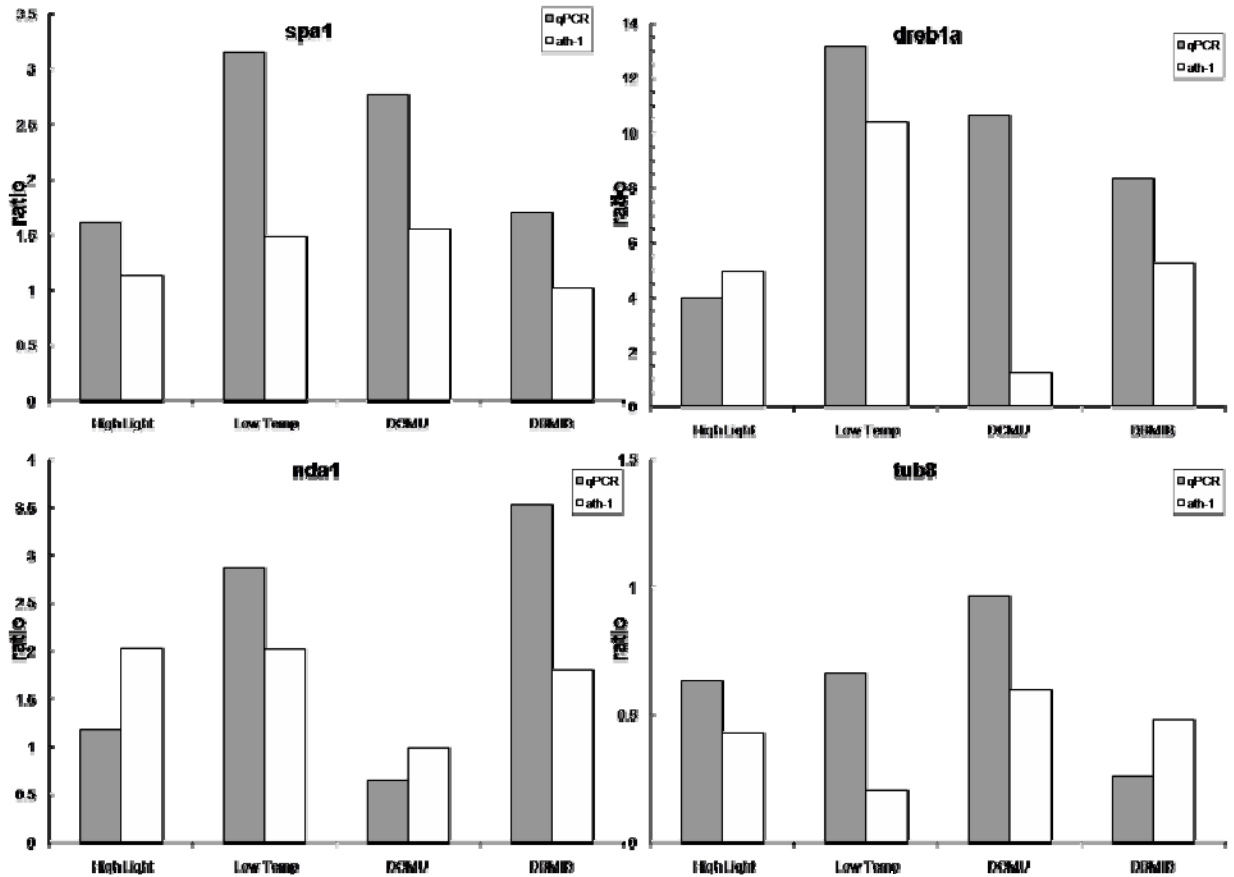


Figure S4.4 MapMan Display of Major Metabolic Pathways at Various Cut-Off Levels. MapMan display of genes involved in the major metabolic pathways, up- and down-regulated at different fold-change cut-off levels. $P = 0.01$. **(A)** genes regulated by HEP, **(B)** genes regulated by PQH₂, **(C)** genes regulated by PS II.







Supplemental Figure S 4.5 Comparison of qRT-PCR and Microarray Expression Data

Gene expression ratios of *spa1* (NM_130197), *dreb1a* (NM_118680), *nda1* (NM_100592) and *tub8* (NM_122291) assessed by both, microarray (ath-1) and quantitative real-time PCR (qPCR). Ratios were calculated by dividing the absolute expression value of each gene after each treatment by its absolute expression value in respective control treatment.

4.7

Supplemental Tables

Supplemental Table S 4.1 Real-time assay IDs. List of transcripts and their “TaqMan Assay ID” used for Real-time qPCR.

Gene Name/ Transcript ID	TaqMan Assay ID
<i>DREB1A</i> / NM_118680	At02238412_s1
<i>NDA1</i> / NM_100592	At02262067_g1
<i>TUB8</i> / NM_122291	At02337298_g1
<i>SPA1</i> / NM_130197	At02263713_g1
<i>ACT2</i> / NM_112764	At02335270_gH

Supplemental Table S 4.2 Expression Data of a Subset of Genes Regulated by HEP and Involved in Major Metabolic Pathways (according to MapMan). Genes were considered up- or down-regulated when their fold-change value exceeded at least 1.5x or -1.5x ($P = 0.01$) in both experimental conditions (HL and LT) when compared to the control plants.

Affymetrix ID's	Locus ID's	Annotation	Up-/Down-regulated
Cell Wall			
253808_at	at4g28300	hydroxyproline-rich glycoprotein family protein	down
258455_at	at3g22440	hydroxyproline-rich glycoprotein family protein	down
266460_at	at2g47930	AGP26; ARABINOGALACTAN PROTEIN 26	down
259664_at	at1g55330	AGP21	down
247189_at	at5g65390	AGP7	down
249037_at	at5g44130	FLA13; FASCICLIN-LIKE ARABINOGALACTAN PROTEIN 13 PRECURSOR	up
247638_at	at5g60490	FLA12	down
266588_at	at2g14890	AGP9; ARABINOGALACTAN PROTEIN 9	down
266552_at	at2g46330	AGP16; ARABINOGALACTAN PROTEIN 16	down
253723_at	at4g29240	leucine-rich repeat family protein / extensin family protein	down
257246_at	at3g24130	pectinesterase family protein	up
258369_at	at3g14310	ATPME3; pectinesterase	down
258193_at	at3g29090	ATPME31; pectinesterase family protein	up
259034_at	at3g09410	pectinacylesterase family protein	down
254573_at	at4g19420	pectinacylesterase family protein	down
255433_at	at4g03210	XTH9; XYLOGLUCAN ENDOTRANGLUCOSYLASE/HYDROLASE 9	down
255822_at	at2g40610	ATEXPA8; ARABIDOPSIS THALIANA EXPANSIN A8	down
267158_at	at2g37640	EXP3	down
266215_at	at2g06850	EXGT-A1; ENDOXYLOGLUCAN TRANSFERASE	down
265443_at	at2g20750	ATEXPB1; ARABIDOPSIS THALIANA EXPANSIN B1	down
266790_at	at2g28950	ATEXPA6; ARABIDOPSIS THALIANA EXPANSIN A6	down
247162_at	at5g65730	xyloglucan:xyloglucosyl transferase, putative	down
261226_at	at1g20190	ATEXPA11; ARABIDOPSIS THALIANA EXPANSIN 11	down
257071_at	at3g28180	ATCSLC04; CELLULOSE-SYNTHASE LIKE C4	down
262109_at	at1g02730	ATCSLD5; 1,4-beta-D-xylan synthase/ cellulose synthase	down
250505_at	at5g09870	CESA5; CELLULOSE SYNTHASE 5	up
265824_at	at2g35650	ATCSLA07; CELLULOSE SYNTHASE LIKE	up
265175_at	at1g23480	ATCSLA03; CELLULOSE SYNTHASE-LIKE A3	down
254185_at	at4g23990	ATCSLG3; cellulose synthase/ transferase	up
250015_at	at5g18070	DRT101; DNA-DAMAGE-REPAIR/TOLERATION 101	down
261211_at	at1g12780	UGE1; UDP-D-glucose/UDP-D-galactose 4-epimerase 1	down
263221_at	at1g30620	MUR4; MURUS 4; UDP-arabinose 4-epimerase	up
267429_at	at2g34850	MEE25; maternal effect embryo arrest 25); UDP-glucose 4-epimerase	up

251855_at	at3g54690	sugar isomerase (SIS) domain-containing protein / CBS domain-containing protein	down
261373_at	at1g53000	cytidylyltransferase family	down
246184_at	at5g20950	glycosyl hydrolase family 3 protein	down
252445_at	at3g47000	glycosyl hydrolase family 3 protein	down
258774_at	at3g10740	ASD1; ALPHA-L-ARABINOFURANOSIDASE 1	down
247266_at	at5g64570	XYL4; xylan 1,4-beta-xylosidase	down
248622_at	at5g49360	BXL1; BETA-XYLOSIDASE 1	down
250444_at	at5g10560	glycosyl hydrolase family 3 protein	down
251982_at	at3g53190	pectate lyase family protein	down
257651_at	at3g16850	glycoside hydrolase family 28 protein / polygalacturonase (pectinase) family protein	down
258719_at	at3g09540	pectate lyase family protein	up
250669_at	at5g06870	PGIP2; POLYGALACTURONASE INHIBITING PROTEIN	down
254221_at	at4g23820	glycoside hydrolase family 28 protein	down
261834_at	at1g10640	polygalacturonase	down
258552_at	at3g07010	pectate lyase family protein	down
265350_at	at2g22620	lyase	down
251831_at	at3g55140	pectate lyase family protein	down
260727_at	at1g48100	glycoside hydrolase family 28 protein / polygalacturonase (pectinase) family protein	up
Carbohydrates			
264511_at	at1g09350	AtGols3; Arabidopsis thaliana galactinol synthase	up
251642_at	at3g57520	AtSIP2; Arabidopsis thaliana seed imbibition	up
263136_at	at1g78580	ATTPS1; TREHALOSE-6-PHOSPHATE SYNTHASE	up
263452_at	at2g22190	catalytic/ trehalose-phosphatase	up
254321_at	at4g22590	at4g22590: trehalose-6-phosphate phosphatase, putative at4g22592:	up
	at4g22592	CPuORF27; Conserved peptide upstream open reading frame 27	
264339_at	at1g70290	ATTPS8; alpha,alpha-trehalose-phosphate synthase	down
248398_at	at5g51970	sorbitol dehydrogenase, putative	down
254707_at	at4g18010	AT5PTASE2; MYO-INOSITOL POLYPHOSPHATE 5-PHOSPHATASE 2	up
251319_at	at3g61610	aldose 1-epimerase family protein	down
262519_at	at1g17160	pfkB-type carbohydrate kinase family protein	down
250186_at	at5g14500	aldose 1-epimerase family protein	down
255281_at	at4g04970	GSL1; GLUCAN SYNTHASE-LIKE 1	down
Sucrose/Starch			
262174_at	at1g74910	ADP-glucose pyrophosphorylase family protein	down
261642_at	at1g27680	APL2; ADPGLC-PPASE LARGE SUBUNIT; glucose-1-phosphate adenylyltransferase	up
261191_at	at1g32900	starch synthase, putative	up
249785_at	at5g24300	SSI1; SUPPRESSOR OF SALICYLIC ACID INSENSITIVITY 1; starch synthase/transferase, transferring glycosyl groups	up
263912_at	at2g36390	SBE2.1; starch branching enzyme 2.1; 1,4-alpha-glucan branching enzyme	up
255016_at	at4g10120	ATSPS4F; sucrose-phosphate synthase/ transferase	up
248029_at	at5g55700	BAM4; BETA-AMYLASE 4	up
248997_at	at5g45300	BMV2; BETA-AMYLASE 2	up

245346_at	at4g17090	CT-BMY; CHLOROPLAST BETA-AMYLASE	up
266357_at	at2g32290	BAM6; BETA-AMYLASE 6	up
261754_at	at1g76130	AMY2; ALPHA-AMYLASE-LIKE 2	up
256746_at	at3g29320	glucan phosphorylase, putative	down
252468_at	at3g46970	PHS2; ALPHA-GLUCAN PHOSPHORYLASE 2	up
246829_at	at5g26570	ATGWD3; carbohydrate kinase/ catalytic/ phosphoglucan, water dikinase	up
262784_at	at1g10760	SEX1; STARCH EXCESS 1; alpha-glucan, water dikinase	up
251110_at	at5g01260	glycoside hydrolase starch-binding domain-containing protein	up
246508_at	at5g16150	PGLCT; PLASTIDIC GLC TRANSLOCATOR	down
248886_at	at5g46110	APE2; ACCLIMATION OF PHOTOSYNTHESIS TO ENVIRONMENT 2; antiporter/ triose-phosphate transmembrane transporter	down
260107_at	at1g66430	pfkB-type carbohydrate kinase family protein	down
262038_at	at1g35580	CINV1; cytosolic invertase 1; beta-fructofuranosidase	down
260969_at	at1g12240	ATBETAFRUCT4; beta-fructofuranosidase/ hydrolase	down
265118_at	at1g62660	beta-fructosidase; BFRUCT3	down
245998_at	at5g20830	SUS1; SUCROSE SYNTHASE 1	up
Glycolysis/Gluconeogenesis/Oxidative Phosphorylation			
258849_at	at3g03250	UGP; UDP-glucose pyrophosphorylase	up
263921_at	at2g36460	fructose-bisphosphate aldolase, putative	down
264668_at	at1g09780	2,3-biphosphoglycerate-independent phosphoglycerate mutase, putative	up
264907_at	at2g17280	phosphoglycerate/bisphosphoglycerate mutase family protein	up
247534_at	at5g61580	PFK4; PHOSPHOFRUCTOKINASE 4	down
255365_at	at4g04040	MEE51; maternal effect embryo arrest 51; diphosphate-fructose-6- phosphate 1-phosphotransferase	down
256836_at	at3g22960	PKP-ALPHA; pyruvate kinase	down
248283_at	at5g52920	PKP-BETA1; PLASTIDIC PYRUVATE KINASE BETA SUBUNIT 1	down
260653_at	at1g32440	PKp3; plastidial pyruvate kinase 3	up
247983_at	at5g56630	PFK7; PHOSPHOFRUCTOKINASE 7	up
249694_at	at5g35790	G6PD1; GLUCOSE-6-PHOSPHATE DEHYDROGENASE 1	down
245977_at	at5g13110	G6PD2; GLUCOSE-6-PHOSPHATE DEHYDROGENASE 2	up
249733_at	at5g24400	emb2024; embryo defective 2024; 6-phosphogluconolactonase	down
260967_at	at1g12230	transaldolase, putative	down
265649_at	at2g27510	ATFD3; ferredoxin 3;	up
248138_at	at5g54960	PDC2 pyruvate decarboxylase-2	up
245742_at	at1g44170	ALDH3H1; ALDEHYDE DEHYDROGENASE 3H1	down
263986_at	at2g42790	CSY3; citrate synthase 3	down
Lipids			
255692_at	at4g00400	GPAT8; glycerol-3-phosphate acyltransferase 8	down
252953_at	at4g38570	PIS2; PROBABLE CDP-DIACYLGLYCEROL-INOSITOL 3- PHOSPHATIDYLTRANSFERASE 2	down
245533_at	at4g15130	CCT2; choline-phosphate cytidyltransferase	down
257175_s_at	at3g23480 at3g23470	at3g23480: cyclopropane fatty acid synthase-related at3g23470: cyclopropane-fatty-acyl-phospholipid synthase	up
253701_at	at4g29890	choline monooxygenase, putative (CMO-like)	down
267280_at	at2g19450	TAG1; TRIACYLGLYCEROL BIOSYNTHESIS DEFECT 1	down

248050_at	at5g56100	glycine-rich protein / oleosin	down
246201_at	at4g36750	quinone reductase family protein	down
264037_at	at2g03750	sulfotransferase family protein	down
261771_at	at1g76150	ATECH2; maoC-like dehydratase domain-containing protein	down
253909_at	at4g27270	quinone reductase family protein	up
258467_at	at3g06060	short-chain dehydrogenase/reductase (SDR) family protein	down
261492_at	at1g14290	SBH2; SPHINGOID BASE HYDROXYLASE 2	down
258911_at	at3g06470	GNS1/SUR4 membrane family protein	down
249799_at	at5g23670	LCB2; protein binding / serine C-palmitoyltransferase	up
261076_at	at1g07420	SMO2-1; STEROL 4-ALPHA-METHYL-OXIDASE 2-1	down
254333_at	at4g22753	SMO1-3; STEROL 4-ALPHA METHYL OXIDASE 1-3	up
254860_at	at4g12110	SMO1-1; STEROL-4ALPHA-METHYL OXIDASE 1-1	down
254280_at	at4g22756	SMO1-2; STEROL C4-METHYL OXIDASE 1-2	up
262722_at	at1g43620	UDP-glucose:sterol glucosyltransferase, putative	up
255797_at	at2g33630	3-beta hydroxysteroid dehydrogenase/isomerase family protein	down
260550_at	at2g43420	3-beta hydroxysteroid dehydrogenase/isomerase family protein	down
252542_at	at3g45770	oxidoreductase, zinc-binding dehydrogenase family protein	up
250253_at	at5g13640	ATPDAT; phosphatidylcholine-sterol O-acyltransferase	down
254547_at	at4g19860	lecithin:cholesterol acyltransferase family protein / LACT family protein	up
260957_at	at1g06080	ADS1; DELTA 9 DESATURASE 1	down
246613_at	at5g35360	CAC2; acetyl-CoA carboxylase/ biotin carboxylase	up
250125_at	at5g16390	CAC1; CHLOROPLASTIC ACETYLCOENZYME A CARBOXYLASE 1	up
250470_at	at5g10160	beta-hydroxyacyl-ACP dehydratase, putative	up
266035_at	at2g05990	MOD1; MOSAIC DEATH 1; enoyl-[acyl-carrier-protein] reductase (NADH)/ enoyl-[acyl-carrier-protein] reductase/ oxidoreductase	up
261722_at	at1g08510	FATB; fatty acyl-ACP thioesterases B	up
250114_s_at	at5g16370 at5g16340	at5g16370: AAE5; ACYL ACTIVATING ENZYME 5 at5g16340: AMP-binding protein, putative	down
249638_at	at5g36880	acetyl-CoA synthetase, putative / acetate-CoA ligase, putative	up
261801_at	at1g30520	AAE14; Acyl-Activating Enzyme 14	up
267606_at	at2g26640	KCS11; 3-KETOACYL-COA SYNTHASE 11	up
250891_at	at5g04530	KCS19; 3-KETOACYL-COA SYNTHASE 19	up
261570_at	at1g01120	KCS1; 3-KETOACYL-COA SYNTHASE 1	up
253285_at	at4g34250	KCS16; 3-KETOACYL-COA SYNTHASE 16	up
254102_at	at4g25050	ACP4; acyl carrier protein 4	down
259095_at	at3g05020	ACP1; acyl carrier protein 1	down
258485_at	at3g02630	acyl-(acyl-carrier-protein) desaturase, putative	down
258086_at	at3g25860	LTA2; dihydrolipoyllysine-residue acetyltransferase	up
266904_at	at2g34590	transketolase family protein	down
262733_s_at	at1g28660 at1g28670	at1g28660: lipase, putative at1g28670: ARAB-1; carboxylesterase	up
263987_at	at2g42690	lipase, putative	up
250008_at	at5g18630	lipase class 3 family protein	down
263359_at	at2g15230	ATLIP1; Arabidopsis thaliana lipase 1	down

258374_at	at3g14360	lipase class 3 family protein	up
246507_at	at5g16120	hydrolase, alpha/beta fold family protein	down
266983_at	at2g39400	hydrolase, alpha/beta fold family protein	down
253220_s_at	at4g34930 at4g34920	at4g34930: 1-phosphatidylinositol phosphodiesterase-related at4g34920: 1-phosphatidylinositol phosphodiesterase-related	up
252950_at	at4g38690	1-phosphatidylinositol phosphodiesterase-related	down
259708_at	at1g77420	hydrolase, alpha/beta fold family protein	down
254351_at	at4g22300	SOBER1; SUPPRESSOR OF AVRST-ELICITED RESISTANCE 1; carboxylesterase	down
246124_at	at5g20060	phospholipase/carboxylesterase family protein	down
266500_at	at2g06925	PLA2-ALPHA; phospholipase A2	down
247176_at	at5g65110	ACX2; ACYL-COA OXIDASE 2	down
246304_at	at3g51840	ACX4; ACYL-COA OXIDASE 4	down
265843_at	at2g35690	ACX5; ACYL-COA OXIDASE 5	down
258315_at	at3g16175	thioesterase family protein	down
253759_at	at4g29010	AIM1; ABNORMAL INFLORESCENCE MERISTEM; enoyl-CoA hydratase	up
249895_at	at5g22500	FAR1; FATTY ACID REDUCTASE 1; fatty acyl-CoA reductase (alcohol-forming)	down
TCA Cycle			
262908_at	at1g59900	AT-E1 ALPHA; oxidoreductase, acting on the aldehyde or oxo group of donors, disulfide as acceptor / pyruvate dehydrogenase (acetyl-transferring)	down
256160_at	at1g30120	PDH-E1 BETA; PYRUVATE DEHYDROGENASE E1 BETA	down
261920_at	at1g65930	isocitrate dehydrogenase, putative / NADP+ isocitrate dehydrogenase, putative	up
247060_at	at5g66760	SDH1-1; ATP binding / succinate dehydrogenase	down
265456_at	at2g46505	SDH4; succinate dehydrogenase (ubiquinone)	down
248461_s_at	at2g47510 at5g50950	at2g47510: FUM1; FUMARASE 1 at5g50950: fumarate hydratase, putative	down
263663_at	at1g04410	malate dehydrogenase, cytosolic, putative	down
246396_at	at1g58180	BCA6; carbonic anhydrase family protein	down
265170_at	at1g23730	BCA3; BETA CARBONIC ANHYDRASE 4	down
Mitochondrial Electron Transport			
253230_at	at4g34700	complex 1 family protein / LVR family protein	down
244902_at	atmg0065	NAD4L; Encodes NADH dehydrogenase subunit 4L	down
256267_at	at3g12260	complex 1 family protein / LVR family protein	down
252326_at	at3g48680	GAMMA CAL2; GAMMA CARBONIC ANHYDRASE-LIKE 2	down
247330_at	at5g63510	GAMMA CAL1; GAMMA CARBONIC ANHYDRASE LIKE 1	down
257337_at	atmg0006	NAD5; Mitochondrial NADH dehydrogenase subunit 5	down
247011_at	at5g67590	FRO1; FROSTBITE1; NADH dehydrogenase (ubiquinone)	down
257338_s_at	atmg00513 at2g07711	atmg00513: NAD5 Mitochondrial NADH dehydrogenase subunit 5 at2g07711: pseudogene, similar to NADH dehydrogenase subunit 5	down
254378_at	at4g21810	DER2.1; DERLIN-2.1	down
244920_s_at	at2g07751 atmg00990	at2g07751: NADH-ubiquinone oxidoreductase chain 3, putative atmg00990: NADH dehydrogenase subunit	down
244943_at	atmg0007	NAD9; NADH dehydrogenase subunit 9	down
252959_at	at4g38640	choline transporter-related	down

249959_at	at5g18800	NADH-ubiquinone oxidoreductase 19 kDa subunit (NDUFA8) family protein	down
256057_at	at1g07180	NDA1; ALTERNATIVE NAD(P)H DEHYDROGENASE 1	down
256209_at	at1g50940	ETFALPHA; electron transfer flavoprotein alpha); FAD binding / electron carrier	down
258452_at	at3g22370	AOX1A; ALTERNATIVE OXIDASE 1A	down
260129_at	at1g36380	unknown protein	down
266045_s_at	atmg00220 at2g07727	atmg00220: Symbols: COB; Mitochondrial apocytochrome b (cob) gene encodes a subunit of the ubiquinol-cytochrome c oxidoreductase at2g07727: cytochrome b (MTCYB) (COB) (CYTB)	down
255011_at	at4g10040	CYTC-2; cytochrome c-2	down
244945_at	atmg0011	CCB206; Encodes a mitochondria-encoded cytochrome c biogenesis protein	down
263510_s_at	atmg00900 at2g07771 at2g07681	atmg00900: CCB256 cytochrome c biogenesis orf256 at2g07771: cytochrome c biogenesis protein-related at2g07681: cytochrome c biogenesis protein, putative	down
263509_s_at	atmg00730 at2g07687	atmg00730: COX3 Encodes cytochrome c oxidase subunit 3. at2g07687: cytochrome c oxidase subunit 3	down
247865_at	at5g57815	cytochrome c oxidase subunit 6b, putative	down
257333_at	atmg0136	COX1; cytochrome c oxidase subunit 1	down
244950_at	atmg0016	COX2; cytochrome c oxidase subunit 2	down
265227_s_at	atmg01280 at2g07695	atmg01280: ORF291; encodes a cytochrome c oxidase subunit II at2g07695: cytochrome c oxidase subunit II, putative	down
265227_s_at	atmg01280 at2g07695	atmg01280: ORF291; encodes a cytochrome c oxidase subunit II at2g07695: cytochrome c oxidase subunit II, putative	down
258987_at	at3g08950	electron transport SCO1/SenC family protein	down
254120_at	at4g24570	DIC2; mitochondrial substrate carrier family protein	down
263874_at	at2g21870	unknown protein	down
250863_at	at5g04750	F1F0-ATPase inhibitor protein, putative	down
256679_at	at3g52300	ATPQ; ATP SYNTHASE D CHAIN, MITOCHONDRIAL	down
265228_s_at	atmg01190 at2g07698	atmg01190: ATP1; ATPase subunit 1 at2g07698: ATP synthase alpha chain, mitochondrial, putative	down
248825_at	at5g47030	ATP synthase delta' chain, mitochondrial	up
244901_at	atmg0064	ORF25; encodes a plant b subunit of mitochondrial ATP synthase based on structural similarity and the presence in the F(0) complex	down
255594_at	at4g01660	ATABC1; ARABIDOPSIS THALIANA ABC TRANSPORTER 1	down
Redox - Ascorbate/Glutathion			
262637_at	at1g06640	2-oxoglutarate-dependent dioxygenase, putative	down
249523_at	at5g38630	ACYB-1; carbon-monoxide oxygenase	down
260545_at	at2g43350	ATGPX3; GLUTATHIONE PEROXIDASE 3	down
263534_at	at2g24940 at2g24945	at2g24940: AtMAPR2; Arabidopsis thaliana membrane-associated progesterone binding protein at2g24945: unknown protein	down
261011_at	at1g26340	CB5-A; CYTOCHROME B5 ISOFORM A	up
248682_at	at5g48810	CB5-D; CYTOCHROME B5 ISOFORM D	down
264383_at	at2g25080	ATGPX1; GLUTATHIONE PEROXIDASE 1	down
245238_at	at4g25570	ACYB-2; carbon-monoxide oxygenase	down
255078_at	at4g09010	APX4; ASCORBATE PEROXIDASE 4	down
246030_at	at5g21105	L-ascorbate oxidase/ copper ion binding / oxidoreductase	down
259707_at	at1g77490	TAPX; THYLAKOIDAL ASCORBATE PEROXIDASE	down

246051_at	at5g28840	GME; GDP-D-MANNOSE 3',5'-EPIMERASE	up
253307_at	at4g33670	L-galactose dehydrogenase (L-GalDH)	down
249585_at	at5g37830	OXP1; OXOPROLINASE 1; 5-oxoprolinase (ATP-hydrolyzing)/ hydrolase	down
257252_at	at3g24170	ATGR1; glutathione-disulfide reductase	up
254270_at	at4g23100	GSH1; GLUTAMATE-CYSTEINE LIGASE	down
261530_at	at1g63460	glutathione peroxidase, putative	down
254890_at	at4g11600	ATGPX6; GLUTATHIONE PEROXIDASE 6	up
251205_at	at3g63080	ATGPX5; glutathione peroxidase 5	down
Photosynthesis			
259491_at	at1g15820	LHCB6; LIGHT HARVESTING COMPLEX PSII SUBUNIT 6	down
251082_at	at5g01530	LHCB4; chlorophyll A-B binding protein CP29	down
259970_at	at1g76570	chlorophyll A-B binding family protein	up
258993_at	at3g08940	LHCB4.2; light harvesting complex PSII	down
248409_at	at5g51545	LPA2; low psii accumulation2	down
264837_at	at1g03600	photosystem II family protein	down
251701_at	at3g56650	thylakoid lumenal 20 kDa protein	down
245368_at	at4g15510	photosystem II reaction center PsbP family protein	down
256979_at	at3g21055	PSBTN; photosystem II subunit T	down
252130_at	at3g50820	PSBO2; PHOTOSYSTEM II SUBUNIT O-2; oxygen evolving/ poly(U) binding	down
261388_at	at1g05385	photosystem II 11 kDa protein-related	down
245195_at	at1g67740	PSBY	down
262632_at	at1g06680	PSBP-1; PHOTOSYSTEM II SUBUNIT P-1; poly(U) binding	down
244964_at	atcg00580	PSBE; PSII cytochrome b559	down
245047_at	atcg00020	PSBA; chlorophyll binding protein D1, photosystem II reaction center core	up
267569_at	at2g30790	PSBP-2; photosystem II subunit P-2	down
245050_at	atcg00070	PSBK; PSII K protein	down
255248_at	at4g05180	PSBQ-2; calcium ion binding	down
247073_at	at5g66570	PSBO1; PS II OXYGEN-EVOLVING COMPLEX 1)	down
254398_at	at4g21280	PSBQ-1; oxygen-evolving enhancer protein 3, chloroplast, putative	down
265149_at	at1g51400	photosystem II 5 kD protein	down
251784_at	at3g55330	PPL1; PsbP-like protein 1	down
256015_at	at1g19150	LHCA6; chlorophyll binding	down
255457_at	at4g02770	PSAD-1; photosystem I subunit D-1	down
254790_at	at4g12800	PSAL; photosystem I subunit L	down
263114_at	at1g03130	PSAD-2; photosystem I subunit D-2	down
258285_at	at3g16140	PSAH-1; photosystem I subunit H-1	down
265287_at	at2g20260	PSAE-2; photosystem I subunit E-2	down
266716_at	at2g46820	PSI-P; PHOTOSYSTEM I P SUBUNIT; DNA binding	down
262557_at	at1g31330	PSAF; photosystem I subunit F	down
245000_at	atcg00210	YCF6; hypothetical protein	up
255046_at	at4g09650	ATPD; ATP SYNTHASE DELTA-SUBUNIT GENE	down
261769_at	at1g76100	PETE1; PLASTOCYANIN 1	down
253391_at	at4g32590	ferredoxin-related	down

264179_at	at1g02180	ferredoxin-related	down
247131_at	at5g66190	FNR1; FERREDOXIN-NADP(+)-OXIDOREDUCTASE 1	down
259210_at	at3g09150	GUN3; HY2; ELONGATED HYPOCOTYL 2 phytochromobilin:ferredoxin oxidoreductase	down
255617_at	at4g01330	ATP binding / kinase/ protein kinase/ protein serine/threonine kinase/ protein tyrosine kinase	down
244936_at	atcg01100	NDHA; NADH dehydrogenase ND1	down
245417_at	at4g17360	formyltetrahydrofolate deformylase	up
248802_at	at5g47435	formyltetrahydrofolate deformylase, putative	down
260309_at	at1g70580	AOAT2; ALANINE-2-OXOGLUTARATE AMINOTRANSFERASE 2	up
266517_at	at2g35120	glycine cleavage system H protein, mitochondrial, putative	down
260164_at	at1g79870	oxidoreductase family protein	down
245015_at	atcg00490	RBCL; large subunit of RUBISCO	up
261197_at	at1g12900	GAPA-2; GLYCERALDEHYDE 3-PHOSPHATE DEHYDROGENASE A SUBUNIT 2	down
247278_at	at5g64380	fructose-1,6-bisphosphatase family protein	down
247523_at	at5g61410	RPE; ribulose-phosphate 3-epimerase	down
260370_at	at1g69740	HEMB1; metal ion binding / porphobilinogen synthase	down
246033_at	at5g08280	HEMC; HYDROXYMETHYLBILANE SYNTHASE	down
245042_at	at2g26540	HEMD; uroporphyrinogen-III synthase	down
255826_at	at2g40490	HEME2; uroporphyrinogen decarboxylase	down
257219_at	at3g14930	HEME1; uroporphyrinogen decarboxylase	down
255402_at	at4g03205	hemf2; coproporphyrinogen III oxidase, putative / coproporphyrinogenase, putative	down
255537_at	at4g01690	PPOX; protoporphyrinogen oxidase	down
248920_at	at5g45930	CHLI2, MAGNESIUM CHELATASE I2	down
261695_at	at1g08520	CHLD; ATP binding / magnesium chelatase/ nucleoside-triphosphatase/ nucleotide binding	down
254105_at	at4g25080	CHLM; magnesium-protoporphyrin IX methyltransferase	down
251664_at	at3g56940	CRD1; COPPER RESPONSE DEFECT 1	down
253871_at	at4g27440	PORB; PROTOCHLOROPHYLLIDE OXIDOREDUCTASE B	down
248197_at	at5g54190	PORA; oxidoreductase/ protochlorophyllide reductase	down
245242_at	at1g44446	CH1; CHLORINA 1; chlorophyllide a oxygenase	down
267617_at	at2g26670	TED4; REVERSAL OF THE DET PHENOTYPE 4; heme oxygenase (decyclizing)	down
249091_at	at5g43860	ATCLH2; chlorophyllase	up
262536_at	at1g17100	SOUL heme-binding family protein	up
Amino Acids			
252415_at	at3g47340	ASN1; GLUTAMINE-DEPENDENT ASPARAGINE SYNTHASE 1	down
255552_at	at4g01850	SAM-2; S-ADENOSYLMETHIONINE SYNTHETASE 2	down
258322_at	at3g22740	HMT3; homocysteine S-methyltransferase	down
258417_at	at3g17365	catalytic/ methyltransferase	down
248402_at	at5g52100	crr1; chlororespiration reduction 1; dihydrodipicolinate reductase	down
258977_s_at	at3g02020 at5g14060	at3g02020: AK3; ASPARTATE KINASE 3 at5g14060: CARAB-AK-LYS; amino acid binding / aspartate kinase	down
255778_at	at1g18640	PSP; 3-PHOSPHOSERINE PHOSPHATASE	down
260309_at	at1g70580	AOAT2; ALANINE-2-OXOGLUTARATE AMINOTRANSFERASE 2	up

245286_at	at4g14880	OASA1; O-ACETYL SERINE (THIOL) LYASE (OAS-TL) ISOFORM A1	down
251322_at	at3g61440	CYSC1; CYSTEINE SYNTHASE C1	down
251487_at	at3g59760	OASC; O-ACETYL SERINE (THIOL) LYASE ISOFORM C	down
260566_at	at2g43750	OASB (O-ACETYL SERINE (THIOL) LYASE B	down
246701_at	at5g28020	CYSD2; CYSTEINE SYNTHASE D2	down
265382_at	at2g16790	shikimate kinase family protein	down
258281_at	at3g26900	shikimate kinase family protein	down
260360_at	at1g69370	CM3; chorismate mutase 3	down
250407_at	at5g10870	ATCM2; chorismate mutase 2	down
266671_at	at2g29690	ASA2; ANTHRANILATE SYNTHASE 2	up
267001_at	at2g34470	UREG; UREASE ACCESSORY PROTEIN G	down
257173_at	at3g23810	SAHH2; S-ADENOSYL-L-HOMOCYSTEINE (SAH) HYDROLASE 2	up
245168_at	at2g33150	PKT3; PEROXISOMAL 3-KETOACYL-COA THIOLASE 3	down
256965_at	at3g13450	DIN4; DARK INDUCIBLE 4; 3-methyl-2-oxobutanoate dehydrogenase	down
253279_at	at4g34030	MCCB; 3-METHYLCROTONYL-COA CARBOXYLASE	down
248207_at	at5g53970	aminotransferase, putative	up
256765_at	at3g22200	POP2; POLLEN-PISTIL INCOMPATIBILITY 2; 4-aminobutyrate:pyruvate transaminase	down
260309_at	at1g70580	AOAT2; ALANINE-2-OXOGLUTARATE AMINOTRANSFERASE 2	up
246597_at	at5g14760	AO; L-ASPARTATE OXIDASE	up
Nitrogen-/Sulfur-/C-1			
247908_at	at5g57440	GS1; catalytic/ hydrolase	down
250032_at	at5g18170	GDH1; GLUTAMATE DEHYDROGENASE 1	down
256835_at	at3g22890	APS1; ATP SULFURYLASE 1	down
263601_s_at	at4g34570 at2g16370	at4g34570: THY-2; thymidylate synthase at2g16370: THY-1; THYMIDYLATE SYNTHASE 1	down
245115_at	at2g41530	SFGH; S-FORMYLGLUTATHIONE HYDROLASE	down
261864_s_at	at1g50480 at2g12280 at2g12200	at1g50480: THFS; 10-FORMYLTETRAHYDROFOLATE SYNTHETASE at2g12280: ligase, putative at2g12200: ligase, putative	down
Nucleotides			
257702_at	at3g12670	emb2742; embryo defective 2742; CTP synthase/ catalytic	up
253252_at	at4g34740	ATASE2; GLN PHOSPHORIBOSYL PYROPHOSPHATE AMIDOTRANSFERASE 2	up
256461_s_at	at1g36280 at4g18440	at1g36280: adenylosuccinate lyase, putative at4g18440: adenylosuccinate lyase, putative	down
261013_at	at1g26440	Symbols: ATUPSS; ARABIDOPSIS THALIANA UREIDE PERMEASE 5	down
267132_at	at2g23420	NAPRT2; NICOTINATE PHOSPHORIBOSYLTRANSFERASE 2	up
250413_at	at5g11160	APT5; Adenine phosphoribosyltransferase 5	up
259224_at	at3g07800	thymidine kinase, putative	down
254069_at	at4g25434	ATNUDT10; Arabidopsis thaliana Nudix hydrolase homolog 10	up
246126_at	at5g20070	ATNUDX19; ARABIDOPSIS THALIANA NUDIX HYDROLASE HOMOLOG 19	up
258998_at	at3g01820	adenylate kinase family protein	up
258885_at	at3g10030	aspartate/glutamate/uridylylate kinase family protein	down
251426_at	at3g60180	uridylylate kinase, putative / uridine monophosphate kinase, putative / UMP kinase, putative	down
253697_at	at4g29700	type I phosphodiesterase/nucleotide pyrophosphatase family protein	down

261258_at	at1g26640	aspartate/glutamate/uridylate kinase family protein	down
263601_s_at	at4g34570 at2g16370	at4g34570: THY-2; thymidylate synthase 2 at2g16370: THY-1; THYMIDYLATE SYNTHASE 1	down
263180_at	at1g05620	URH2; URIDINE-RIBOHYDROLASE 2	down
247275_at	at5g64370	BETA-UP; beta-ureidopropionase	down
253212_s_at	at4g34890 at4g34900	at4g34890: XDH1; XANTHINE DEHYDROGENASE 1 at4g34900: XDH2; XXANTHINE DEHYDROGENASE 2	down
250318_at	at5g12200	dihydropyrimidinase / DHPase / dihydropyrimidine amidohydrolase / hydantoinase (PYD2)	down
253679_at	at4g29610	cytidine deaminase, putative / cytidine aminohydrolase, putative	up
Secondary Metabolism			
255732_at	at1g25450	KCS5; 3-KETOACYL-COA SYNTHASE 5	down
245199_at	at1g67730	YBR159; ketoreductase/ oxidoreductase	down
266279_at	at2g29290	tropinone reductase, putative	down
251658_at	at3g57020	strictosidine synthase family protein	up
262173_at	at1g74920	ALDH10A8; 3-chloroallyl aldehyde dehydrogenase/ oxidoreductase	down
257177_at	at3g23490	CYN; CYANASE; DNA binding / cyanate hydratase/ hydro-lyase	down
260387_at	at1g74100	SOT16; SULFOTRANSFERASE 16; desulfoglucosinolate sulfotransferase/ sulfotransferase	down
250589_at	at5g07700	MYB76; myb domain protein 76; DNA binding / transcription factor	down
263153_s_at	at1g54010 at1g54000	at1g54010: myrosinase-associated protein, putative at1g54000: myrosinase-associated protein, putative	down
246880_s_at	at5g26000 at5g25980	at5g26000: TGG1; THIOGLUCOSIDE GLUCOHYDROLASE 1 at5g25980: TGG2; GLUCOSIDE GLUCOHYDROLASE 2	down
249942_at	at5g22300	NIT4; NITRILASE 4	up
266099_at	at2g38040	CAC3; acetyl-CoA carboxylase	down
267377_at	at2g26250	KCS10; 3-KETOACYL-COA SYNTHASE 10	down
264963_at	at1g60600	ABC4; ABERRANT CHLOROPLAST DEVELOPMENT 4; 1,4-dihydroxy-2- naphthoate octaprenyltransferase/ prenyltransferase	down
260236_at	at1g74470	geranylgeranyl reductase	down
245281_at	at4g15560	CLA1; CLOROPLASTOS ALTERADOS 1; 1-deoxy-D-xylulose-5-phosphate synthase	down
246198_at	at4g36810	GGPS1; GERANYLGERANYL PYROPHOSPHATE SYNTHASE 1	down
248690_at	at5g48230	ACAT2; ACETOACETYL-COA THIOLASE 2	down
254845_at	at4g11820	MVA1; acetyl-CoA C-acetyltransferase/ hydroxymethylglutaryl-CoA synthase	down
259983_at	at1g76490	HMG1; HYDROXY METHYLGLUTARYL COA REDUCTASE 1	down
266414_at	at2g38700	MVD1; MEVALONATE DIPHOSPHATE DECARBOXYLASE 1	down
250117_at	at5g16440	IPP1; ISOPENTENYL DIPHOSPHATE ISOMERASE 1	down
262526_at	at1g17050	SPS2; Solanesyl diphosphate synthase	up
266958_at	at2g34630	GPS1; geranyl diphosphate synthase, putative	up
245301_at	at4g17190	FPS2; FARNESYL DIPHOSPHATE SYNTHASE 2	down
248718_at	at5g47770	FPS1; FARNESYL DIPHOSPHATE SYNTHASE 1	down
253394_at	at4g32770	VTE1; VITAMIN E DEFICIENT 1; tocopherol cyclase	up
258708_at	at3g09580	amine oxidase family protein	down
254020_at	at4g25700	BETA-OHASE 1; BETA-HYDROXYLASE 1; carotene beta-ring hydroxylase	up
246411_at	at1g57770	amine oxidase family	up

263122_at	at1g78510	SPS1; solanesyl diphosphate synthase 1	up
256994_s_at	at3g25830 at3g25820	at3g25830: ATTPS-CIN; terpene synthase-like sequence-1,8-cineole at3g25820: ATTPS-CIN; terpene synthase-like sequence-1,8-cineole	down
253879_s_at	at4g27560 at4g27570	at4g27560: glycosyltransferase family protein at4g27570: glycosyltransferase family protein	up
260982_at	at1g53520	chalcone-flavanone isomerase-related	down
265929_s_at	at2g18560 at2g18570	at2g18560: UDP-glucuronosyl/UDP-glucosyl transferase family protein at2g18570: UDP-glucuronosyl/UDP-glucosyl transferase family protein	down
266643_s_at	at2g29730 at2g29710	at2g29730: UGT71D1; UDP-GLUCOSYL TRANSFERASE 71D1 at2g29710: UDP-glucuronosyl/UDP-glucosyl transferase family protein	down
261048_at	at1g01420	UGT72B3; UDP-GLUCOSYL TRANSFERASE 72B3	up
254835_s_at	at4g12320 at4g12310	at4g12320: CYP706A6 at4g12310: CYP706A5	up
253195_at	at4g35420	dihydroflavonol 4-reductase family / dihydrokaempferol 4-reductase family	down
252123_at	at3g51240	F3H; FLAVANONE 3-HYDROXYLASE	up
251402_at	at3g60290	oxidoreductase	down
265200_s_at	at2g36800 at2g36790	at2g36800: DOGT1; DON-GLUCOSYLTRANSFERASE 1 at2g36790: UGT73C6; UDP-glucosyl transferase 73C6	up
252199_at	at3g50270	transferase family protein	down
266578_at	at2g23910	cinnamoyl-CoA reductase-related	up
251144_at	at5g01210	transferase family protein	down
252183_at	at3g50740	UGT72E1; UDP-glucosyl transferase 72E1	down
253017_at	at4g37970	CAD6; CINNAMYL ALCOHOL DEHYDROGENASE 6	down

Supplemental Table S 4.3 Expression Data of a Subset of Genes Regulated by PQH₂ and Involved in Major Metabolic Pathways (according to MapMan). Genes were considered up- or down-regulated when their fold-change value exceeded at least 1.5x or -1.5x ($P = 0.01$) in the DBMIB treatment but not the DCMU treatment when compared to the control plants.

Affymetrix ID's	Locus ID's	Annotation	Up-/Down-regulated
Cell Wall			
251395_at	at2g45470	FLA8; FASCICLIN-LIKE ARABINOGALACTAN PROTEIN 8	up
256673_at	at3g52370	FLA15; FASCICLIN-LIKE ARABINOGALACTAN PROTEIN 15 PRECURSOR	up
261363_at	at1g41830	SKS6; SKU5-SIMILAR 6; pectinesterase	up
258764_at	at3g10720	pectinesterase, putative	up
266735_at	at2g46930	pectinacylesterase, putative	up
254578_at	at4g19410	pectinacylesterase, putative	down
259034_at	at3g09410	pectinacylesterase family protein	up
259033_at	at3g09405	CONTAINS InterPro DOMAIN/s: Pectinacylesterase	up
246403_at	at1g57590	carboxylesterase	up
255524_at	at4g02330	ATPMEPCR; pectinesterase	up
253372_at	at4g33220	ATPME44 enzyme inhibitor/ pectinesterase	up
263841_at	at2g36870	xyloglucan:xyloglucosyl transferase, putative	up
252997_at	at4g38400	ATEXLA2; ARABIDOPSIS THALIANA EXPANSIN-LIKE A2	up
253040_at	at4g37800	xyloglucan:xyloglucosyl transferase, putative	up
263565_at	at2g15390	FUT4; fucosyltransferase	up
250892_at	at5g03760	ATCSLA09; mannan synthase/ transferase	up
260592_at	at1g55850	ATCSLE1; cellulose synthase/ transferase	down
251945_at	at3g53520	UXS1; UDP-GLUCURONIC ACID DECARBOXYLASE 1	down
261624_at	at1g02000	GAE2 ; UDP-D-GLUCURONATE 4-EPIMERASE 2	down
256575_at	at3g14790	RHM3; RHAMNOSE BIOSYNTHESIS 3; UDP-L-rhamnose synthase/ catalytic	down
250444_at	at5g10560	glycosyl hydrolase family 3 protein	up
245196_at	at1g67750	pectate lyase family protein	up
262060_at	at1g80170	polygalacturonase, putative / pectinase, putative	up
251645_at	at3g57790	glycoside hydrolase family 28 protein	down
253326_at	at4g33440	glycoside hydrolase family 28 protein	down
Carbohydrates			
263320_at	at2g47180	AtGolS1; Arabidopsis thaliana galactinol synthase 1	down
263019_at	at1g23870	ATTPS9; transferase, transferring glycosyl groups	down
250607_at	at5g07370	ATIPK2A; INOSITOL POLYPHOSPHATE KINASE 2 ALPHA	down
266693_at	at2g19800	MIOX2; MYO-INOSITOL OXYGENASE 2;	down
252934_at	at4g39120	IMPL2; MYO-INOSITOL MONOPHOSPHATASE LIKE 2	up
263705_at	at1g31190	IMPL1; MYO-INOSITOL MONOPHOSPHATASE LIKE 1	up
266087_at	at2g37790	aldo/keto reductase family protein	up

247929_at	at5g57330	aldose 1-epimerase family protein	up
261136_at	at1g19600	pfkB-type carbohydrate kinase family protein	down
262519_at	at1g17160	pfkB-type carbohydrate kinase family protein	down
254223_at	at4g23730	aldose 1-epimerase family protein	up
250297_at	at5g11980	conserved oligomeric Golgi complex component-related	down
Sucrose/Starch			
264476_at	at1g77130	PGSIP2; PLANT GLYCOGENIN-LIKE STARCH INITIATION PROTEIN 2	up
263544_at	at2g21590	APL4; glucose-1-phosphate adenyltransferase	up
261642_at	at1g27680	APL2; ADPGLC-PPASE LARGE SUBUNIT	up
250029_at	at5g18200	UTP:galactose-1-phosphate uridylyltransferase	down
245904_at	at5g11110	ATSPS2F; SUCROSE PHOSPHATE SYNTHASE 2F	down
246076_at	at5g20280	ATSPS1F; sucrose phosphate synthase 1F	up
263954_at	at2g35840	sucrose-phosphatase 1 (SPP1)	up
248029_at	at5g55700	BAM4; BETA-AMYLASE 4	down
266357_at	at2g32290	BAM6; BETA-AMYLASE 6	up
250007_at	at5g18670	BMV3; beta-amylase	down
251110_at	at5g01260	glycoside hydrolase starch-binding domain-containing protein	down
248886_at	at5g46110	APE2 ; ACCLIMATION OF PHOTOSYNTHESIS TO ENVIRONMENT 2	up
263250_at	at2g31390	pfkB-type carbohydrate kinase family protein	down
248381_at	at5g51830	pfkB-type carbohydrate kinase family protein	down
Glycolysis/Gluconeogenesis/Oxidative Phosphorylation			
260207_at	at1g70730	phosphoglucomutase, cytoplasmic, putative	up
262806_at	at1g20950	pyrophosphate-dependent 6-phosphofructose-1-kinase-related	up
250917_at	at5g03690	fructose-bisphosphate aldolase, putative	down
262944_at	at1g79550	PGK; phosphoglycerate kinase	down
264645_at	at1g08940	phosphoglycerate/bisphosphoglycerate mutase family protein	down
264907_at	at2g17280	phosphoglycerate/bisphosphoglycerate mutase family protein	up
247338_at	at5g63680	pyruvate kinase, putative	down
252300_at	at3g49160	pyruvate kinase family protein	down
246412_at	at5g17530	phosphoglucosamine mutase family protein	up
264386_at	at1g12000	pyrophosphate-dependent 6-phosphofructose-1-kinase, putative	up
260653_at	at1g32440	PKp3; plastidial pyruvate kinase 3	up
249694_at	at5g35790	G6PD1; glucose-6-phosphate dehydrogenase	up
245977_at	at5g13110	G6PD2; glucose-6-phosphate dehydrogenase	down
249732_at	at5g24420	glucosamine/galactosamine-6-phosphate isomerase-related	up
259098_at	at3g04790	ribose 5-phosphate isomerase-related	up
255230_at	at4g05390	ATRFNR1; ROOT FNR 1; ferredoxin-NADP+ reductase/ oxidoreductase	down
261806_at	at1g30510	ATRFNR2 ;ROOT FNR 2; ferredoxin-NADP+ reductase/ oxidoreductase	up
250094_at	at5g17380	pyruvate decarboxylase family protein	down
253083_at	at4g36250	ALDH3F1; Aldehyde Dehydrogenase 3F1	up
252372_at	at3g48000	ALDH2B4; ALDEHYDE DEHYDROGENASE 2B4	up
250498_at	at5g09660	PMDH2; peroxisomal NAD-malate dehydrogenase 2	up
Lipids			

259113_at	at3g05510	phospholipid/glycerol acyltransferase family protein	down
262583_at	at1g15110	phosphatidyl serine synthase family protein	down
255692_at	at4g00400	GPAT8; glycerol-3-phosphate acyltransferase 8	up
254998_at	at4g09760	choline kinase, putative	up
260244_at	at1g74320	choline kinase, putative	down
254360_at	at4g22340	phosphatidate cytidyltransferase	down
251819_at	at3g55030	PGPS2; phosphatidylglycerolphosphate synthase 2	down
255681_at	at4g00550	DGD2; UDP-galactosyltransferase	down
259070_at	at3g11670	DGD1; DIGALACTOSYL DIACYLGLYCEROL DEFICIENT 1	down
264523_at	at1g10030	ERG28; Arabidopsis homolog of yeast ergosterol28	up
249947_at	at5g19200	short-chain dehydrogenase/reductase (SDR) family protein	down
254306_at	at4g22330	ATCES1; catalytic/ hydrolase, acting on C-N (but not peptide) bonds, in linear amides	down
257038_at	at3g19260	LOH2; LAG ONE HOMOLOGUE 2	down
249840_at	at5g23450	ATLCBK1; A. THALIANA LONG-CHAIN BASE (LCB) KINASE 1	down
254333_at	at4g22753	SMO1-3; STEROL 4-ALPHA METHYL OXIDASE 1-3	up
260957_at	at1g06080	ADS1; DELTA 9 DESATURASE 1	down
258269_at	at3g15690	biotin carboxyl carrier protein of acetyl-CoA carboxylase-related	up
262176_at	at1g74960	FAB1; FATTY ACID BIOSYNTHESIS 1	up
263432_at	at2g22230	beta-hydroxyacyl-ACP dehydratase, putative	up
249869_at	at5g23050	AAE17; ACYL-ACTIVATING ENZYME 17	down
262414_at	at1g49430	LACS2; LONG-CHAIN ACYL-COA SYNTHETASE 2	up
260531_at	at2g47240	LACS1; long-chain-fatty-acid--CoA ligase family protein	up
253840_at	at4g27780	ACBP2; ACYL-COA BINDING PROTEIN ACBP 2	down
259159_at	at3g05420	ACBP4; ACYL-COA BINDING PROTEIN 4	down
262733_s_at	at1g28660 at1g28670	at1g28660: lipase, putative at1g28670: ARAB-1; carboxylesterase/hydrolase	down
260833_at	at1g06800	lipase class 3 family protein	down
251191_at	at3g62590	lipase class 3 family protein	down
246507_at	at5g16120	hydrolase, alpha/beta fold family protein	down
254846_at	at4g11830	PLDGAMMA2; phospholipase D	down
258430_at	at3g16785	PLDP1; PHOSPHOLIPASE D P1	down
255852_at	at1g66970	SVL2 (SHV3-LIKE 2); glycerophosphodiester phosphodiesterase/ kinase	up
259169_at	at3g03520	phosphoesterase family protein	down
246304_at	at3g51840	ACX4; ACYL-COA OXIDASE 4	down
258524_at	at3g06810	IBR3; IBA-RESPONSE 3; acyl-CoA dehydrogenase/ oxidoreductase	down
245249_at	at4g16760	ACX1; ACYL-COA OXIDASE 1	down
254776_at	at4g13360	catalytic	up
TCA Cycle			
256160_at	at1g30120	PDH-E1 BETA; PYRUVATE DEHYDROGENASE E1 BETA	up
261165_at	at1g34430	EMB3003; embryo defective 3003	up
263117_at	at1g03040	basic helix-loop-helix (bHLH) family protein	down
258439_at	at3g17240	mtLPD2; LIPOAMIDE DEHYDROGENASE 2	down
253954_at	at4g26970	aconitate hydratase/ copper ion binding	down

260615_at	at1g53240	malate dehydrogenase (NAD), mitochondrial	up
250929_at	at5g03290	NAD+ isocitrate dehydrogenase, putative	down
Mitochondrial Electron Transport			
266835_at	at2g29990	NDA2; ALTERNATIVE NAD(P)H DEHYDROGENASE 2	down
256057_at	at1g07180	NDA1; ALTERNATIVE NAD(P)H DEHYDROGENASE 1)	up
249158_at	at5g43430	ETFBETA; electron carrier	down
260536_at	at2g43400	ETFQO; electron-transfer flavoprotein:ubiquinone oxidoreductase	down
246944_at	at5g25450	ubiquinol-cytochrome C reductase complex 14 kDa protein, putative	down
262591_at	at1g15220	CCMH; oxidoreductase	down
246309_at	at3g51790	ATG1; ARABIDOPSIS TRANSMEMBRANE PROTEIN G1P-RELATED 1	down
263509_s_at	atmg00730 at2g07687	atmg00730: COX3 Encodes cytochrome c oxidase subunit 3. at2g07687: cytochrome c oxidase subunit 3	down
257333_at	atmg01360	COX1; cytochrome c oxidase subunit 1	down
247746_at	at5g58970	ATUCP2; UNCOUPLING PROTEIN 2	up
265228_s_at	atmg01190 at2g07698	atmg01190: ATP1; ATPase subunit 1 at2g07698: ATP synthase alpha chain, mitochondrial, putative	down
Redox - Ascorbate/Glutathion			
256892_at	at3g19000	oxidoreductase, 2OG-Fe(II) oxygenase family protein	up
260545_at	at2g43350	ATGPX3; GLUTATHIONE PEROXIDASE 3	up
263534_at	at2g24940 at2g24945	at2g24940: AtMAPR2; Arabidopsis thaliana membrane-associated progesterone binding protein 2 at2g24945: unknown protein	up
262616_at	at1g06620	2-oxoglutarate-dependent dioxygenase, putative	up
258695_at	at3g09640	APX2; ASCORBATE PEROXIDASE 2	down
252862_at	at4g39830	L-ascorbate oxidase, putative	up
246021_at	at5g21100	L-ascorbate oxidase, putative	up
251860_at	at3g54660	ATGR2; GLUTATHIONE REDUCTASE	up
261530_at	at1g63460	glutathione peroxidase, putative	up
Photosynthesis			
259491_at	at1g15820	LHCB6, CP24; LIGHT HARVESTING COMPLEX PSII SUBUNIT 6	up
267002_s_at	at2g34430 at2g34420	at2g34430: LHB1B1; chlorophyll binding at2g34420: LHB1B2; chlorophyll binding	up
263345_s_at	at2g05070 at2g05100	at2g05070: LHCB2.2; chlorophyll binding at2g05100: LHCB2.1; chlorophyll binding	up
258239_at	at3g27690	LHCB2.3; chlorophyll binding	up
258993_at	at3g08940	LHCB4.2; light harvesting complex PSII); chlorophyll binding	up
248409_at	at5g51545	LPA2 ; low PSII accumulation2	up
251701_at	at3g56650	thylakoid luminal 20 kDa protein	up
259981_at	at1g76450	oxygen-evolving complex-related	up
253790_at	at4g28660	PSB28; PHOTOSYSTEM II REACTION CENTER PSB28 PROTEIN	up
262612_at	at1g14150	oxygen evolving enhancer 3 (PsbQ) family protein	up
245213_at	at1g44575	NPQ4; NONPHOTOCHEMICAL QUENCHING; chlorophyll binding / xanthophyll binding	up
251031_at	at5g02120	OHP; ONE HELIX PROTEIN	up
266979_at	at2g39470	PPL2; PsbP-like protein 2	up
267526_at	at2g30570	PSBW; PHOTOSYSTEM II REACTION CENTER W	up
251814_at	at3g54890	LHCA1; chlorophyll binding	up

245806_at	at1g45474	LHCA5; pigment binding	up
256015_at	at1g19150	LHCA6; chlorophyll binding	up
265033_at	at1g61520	LHCA3; chlorophyll binding	up
256309_at	at1g30380	PSAK; photosystem I subunit K	up
259840_at	at1g52230	PSAH2; PHOTOSYSTEM I SUBUNIT H2	up
255046_at	at4g09650	ATPD; ATP SYNTHASE DELTA-SUBUNIT GENE	up
253391_at	at4g32590	ferredoxin-related	up
247816_at	at5g58260	subunit of NDH-N of NAD(P)H:plastoquinone dehydrogenase complex	up
262288_at	at1g70760	CRR23; chlororespiratory reduction 23	up
260036_at	at1g68830	STN7; Stt7 homolog STN7; kinase/ protein kinase	up
257004_s_at	at3g14130 at3g14150	at3g14130: (S)-2-hydroxy-acid oxidase, peroxisomal at3g14150: (S)-2-hydroxy-acid oxidase, peroxisomal, putative	up
260309_at	at1g70580	AOAT2; ALANINE-2-OXOGLUTARATE AMINOTRANSFERASE 2	up
251218_at	at3g62410	CP12-2; protein binding	up
247278_at	at5g64380	fructose-1,6-bisphosphatase family protein	up
259098_at	at3g04790	ribose 5-phosphate isomerase-related	up
255720_at	at1g32060	PRK; PHOSPHORIBULOKINASE	up
254502_at	at4g20130	PTAC14; PLASTID TRANSCRIPTIONALLY ACTIVE14	up
261307_at	at1g48520	GATB; GLU-ADT SUBUNIT B;	up
250243_at	at5g13630	GUN5; GENOMES UNCOUPLED 5	up
246870_at	at5g26030	FC1; ferrochelatase 1	up
267617_at	at2g26670	TED4; REVERSAL OF THE DET PHENOTYPE 4	up
245027_at	at2g26550	HO2; HEME OXYGENASE 2	up
257003_at	at3g14110	FLU; FLUORESCENT IN BLUE LIGHT	up
267342_at	at2g44520	COX10; cytochrome c oxidase 10	down
Amino Acids			
265965_at	at2g37500	arginine biosynthesis protein ArgJ family	up
250403_at	at5g10920	argininosuccinate lyase, putative	up
262582_at	at1g15410	aspartate-glutamate racemase family	down
247218_at	at5g65010	ASN2; ASPARAGINE SYNTHETASE 2	up
252974_at	at4g38800	ATMTN1; catalytic/ methylthioadenosine nucleosidase	down
259343_s_at	at3g03780 at5g17920	at3g03780: AtMS2; 5-methyltetrahydropteroyltriglutamate-homocysteine S-methyltransferase at5g17920: ATMS1; 5-methyltetrahydropteroyltriglutamate-homocysteine S-methyltransferase	up
267233_s_at	at2g43910 at2g43920	at2g43910: thiol methyltransferase, putative at2g43920: thiol methyltransferase, putative	up
248576_at	at5g49810	MMT; S-adenosylmethionine-dependent methyltransferase	up
251948_at	at3g53580	diaminopimelate epimerase family protein	up
258977_s_at	at3g02020 at5g14060	at3g02020: AK3 (ASPARTATE KINASE 3); aspartate kinase at5g14060: CARAB-AK-LYS; amino acid binding / aspartate kinase	up
262841_at	at1g14810	semialdehyde dehydrogenase family protein	up
251536_at	at3g58610	ketol-acid reductoisomerase	up
247158_at	at5g65780	ATBCAT-5; branched-chain-amino-acid transaminase	up
260309_at	at1g70580	AOAT2; ALANINE-2-OXOGLUTARATE AMINOTRANSFERASE 2	up

259094_at	at3g04940	CYSD1; CYSTEINE SYNTHASE D1	up
252900_at	at4g39540	shikimate kinase family protein	up
266608_at	at2g35500	shikimate kinase-related	up
247864_s_at	at1g25155 at5g57890 at1g25083 at1g24909 at1g24807 at1g25220	anthranilate synthase beta subunits, putative	up
259486_at	at1g15710	prephenate dehydrogenase family protein	down
258457_at	at3g22425	IGPD; imidazoleglycerol-phosphate dehydratase	up
260172_s_at	at5g10330 at1g71920	HPA1; HISTIDINOL PHOSPHATE AMINOTRANSFERASE 1; histidinol-phosphate transaminase	up
250385_at	at5g11520	ASP3; ASPARTATE AMINOTRANSFERASE 3	down
260309_at	at1g70580	AOAT2; ALANINE-2-OXOGLUTARATE AMINOTRANSFERASE 2	up
257315_at	at3g30775	ERD5; EARLY RESPONSIVE TO DEHYDRATION 5; proline dehydrogenase	down
255065_s_at	at4g08870 at4g08900	arginase, putative	up
257173_at	at3g23810	SAHH2; S-ADENOSYL-L-HOMOCYSTEINE (SAH) HYDROLASE 2	up
258527_at	at3g06850	BCE2; dihydrolipoamide branched chain acyltransferase	down
245168_at	at2g33150	PKT3; PEROXISOMAL 3-KETOACYL-COA THIOLASE 3	down
263118_at	at1g03090	MCCA; methylcrotonoyl-CoA carboxylase	down
252570_at	at3g45300	IVD; ISOVALERYL-COA-DEHYDROGENASE	down
262712_at	at1g16460	ATRDH2; ARABIDOPSIS THALIANA RHODANESE HOMOLOGUE 2	up
263714_at	at2g20610	SUR1; SUPERROOT 1; S-alkylthiohydroximate lyase/ carbon-sulfur lyase/ transaminase	up
254776_at	at4g13360	catalytic	up
260814_at	at1g43710	emb1075; embryo defective 1075; carboxy-lyase	down
Nitrogen-/Sulfur-/C-1			
259681_at	at1g77760	NIA1; NITRATE REDUCTASE 1	up
250580_at	at5g07440	GDH2; GLUTAMATE DEHYDROGENASE 2	down
255785_at	at1g19920	APS2; sulfate adenyllyltransferase	up
252870_at	at4g39940	AKN2; APS-kinase 2; adenyllylsulfate kinase	up
253558_at	at4g31120	SKB1; SHK1 BINDING PROTEIN 1; protein methyltransferase	up
263601_s_at	at4g34570 at2g16370	at4g34570: THY-2; thymidylate synthase 2 at2g16370: THY-1 (THYMIDYLATE SYNTHASE 1); dihydrofolate reductase/ thymidylate synthase	up
246800_at	at5g26780	SHM2; SERINE HYDROXYMETHYLTRANSFERASE 2	up
255685_s_at	at4g00600 at4g00620	tetrahydrofolate dehydrogenase/cyclohydrolase, putative	up
267187_s_at	at3g59970 at2g44160	at3g59970: MTHFR1; METHYLENETETRAHYDROFOLATE REDUCTASE 1 at2g44160: MTHFR2; METHYLENETETRAHYDROFOLATE REDUCTASE 2	up
251759_at	at3g55630	ATDFD; A. THALIANA DHFS-FPGS HOMOLOG D; tetrahydrofolylpolyglutamate synthase	up
247409_at	at5g62980	dihydroneopterin aldolase, putative chr5:25276034-25277266 FORWARD	up
Nucleotides			
256002_at	at1g29900	CARB; CARBAMOYL PHOSPHATE SYNTHETASE B	up
255529_at	at4g02120	CTP synthase, putative	up

257702_at	at3g12670	emb2742; embryo defective 2742; CTP synthase/ catalytic	up
264675_at	at1g09830	phosphoribosylamine--glycine ligase; PUR2	up
251830_at	at3g55010	PUR5; ATP binding / phosphoribosylformylglycinamide cyclo-ligase	up
251599_at	at3g57610	ADSS; ADENYLOSUCCINATE SYNTHASE	up
260294_at	at1g63660	GMP synthase (glutamine-hydrolyzing), putative	up
246281_at	at4g36940	NAPRT1; NICOTINATE PHOSPHORIBOSYLTRANSFERASE 1	up
264439_at	at1g27450	APT1; ADENINE PHOSPHORIBOSYL TRANSFERASE 1	up
251920_at	at3g53900	UMP pyrophosphorylase, putative	up
249318_at	at5g40870	AtUK/UPRT1; Uridine kinase/Uracil phosphoribosyltransferase 1	up
267533_at	at2g42070	ATNUDX23; ARABIDOPSIS THALIANA NUDIX HYDROLASE HOMOLOG 23	up
252507_at	at3g46200	ATNUDT9; Arabidopsis thaliana Nudix hydrolase homolog 9	down
248923_at	at5g45940	atnudt11; Arabidopsis thaliana Nudix hydrolase homolog 11	up
265958_at	at2g37250	ADK; ADENOSINE KINASE	down
258885_at	at3g10030	aspartate/glutamate/uridylate kinase family protein	down
254958_at	at4g11010	NDPK3; NUCLEOSIDE DIPHOSPHATE KINASE 3	up
263601_s_at	at4g34570 at2g16370	at4g34570: THY-2; Thymidylate synthase 2 at2g16370: THY-1; THYMIDYLATE SYNTHASE 1	up
250181_at	at5g14460	pseudouridine synthase/ transporter	up
258106_at	at3g23580	RNR2A; RIBONUCLEOTIDE REDUCTASE 2A	up
250034_at	at5g18280	ATAPY2; ARABIDOPSIS THALIANA APYRASE 2	down
258567_at	at3g04080	ATAPY1; APYRASE 1; ATPase/ calmodulin binding / nucleotide diphosphatase	down
253678_at	at4g29600	cytidine deaminase, putative / cytidine aminohydrolase, putative	up
Secondary Metabolism			
264147_at	at1g02205	CER1; ECERIFERUM 1; octadecanal decarbonylase	up
252092_at	at3g51420	SSL4; STRICTOSIDINE SYNTHASE-LIKE 4	up
256246_at	at3g66658	ALDH22a1; Aldehyde Dehydrogenase 22a1	up
255438_at	at4g03070	AOP1; oxidoreductase	up
263477_at	at2g31790	UDP-glucuronosyl/UDP-glucosyl transferase family protein	up
260387_at	at1g74100	SOT16; SULFOTRANSFERASE 16	up
253534_at	at4g31500	CYP83B1; CYTOCHROME P450 MONOOXYGENASE 83B1	up
263714_at	at2g20610	SUR1; SUPERROOT 1; S-alkylthiohydroximate lyase/ carbon-sulfur lyase/ transaminase	up
246539_at	at5g15460	MUB2; MEMBRANE-ANCHORED UBIQUITIN-FOLD PROTEIN 2	down
254156_at	at4g24490	protein prenyltransferase	down
267220_at	at2g02500	ISPD; 2-C-methyl-D-erythritol 4-phosphate cytidyltransferase	up
252996_s_at	at4g38460	GGR; geranylgeranyl reductase	up
259983_at	at1g76490	HMG1; HYDROXY METHYLGLUTARYL COA REDUCTASE 1	down
249688_at	at5g36160	aminotransferase-related	up
258755_at	at3g11945	ATHST; homogentisate solanesyltransferase	up
260821_at	at1g06820	CRTISO; CAROTENOID ISOMERASE	up
250095_at	at5g17230	phytoene synthase (PSY)	up
259092_at	at3g04870	ZDS; ZETA-CAROTENE DESATURASE	up
247936_at	at5g57030	LUT2; LUTEIN DEFICIENT 2; lycopene epsilon cyclase	up

250794_at	at5g05270	chalcone-flavanone isomerase family protein	up
251923_at	at3g53880	aldo/keto reductase family protein	down
255703_at	at4g00040	chalcone and stilbene synthase family protein	down
263135_at	at1g78550	oxidoreductase, 2OG-Fe(II) oxygenase family protein	down
255622_at	at4g01070	GT72B1; UDP-glucosyltransferase	down
251402_at	at3g60290	oxidoreductase	up
266875_at	at2g44800	oxidoreductase, 2OG-Fe(II) oxygenase family protein	up
265200_s_at	at2g36800 at2g36790	at2g36800: DOGT1; DON-GLUCOSYLTRANSFERASE 1 at2g36790: UGT73C6; UDP-glucosyl transferase 73C6	down
256454_at	at1g75280	isoflavone reductase, putative	down
252199_at	at3g50270	transferase family protein	up
260260_at	at1g68540	oxidoreductase family protein	up
251144_at	at5g01210	transferase family protein	down
258037_at	at3g21230	4CL5; 4-coumarate:CoA ligase 5	up
251295_at	at3g62000	O-methyltransferase family 3 protein	up
250149_at	at5g14700	cinnamoyl-CoA reductase-related	up
261899_at	at1g80820	CCR2; CINNAMOYL COA REDUCTASE	up
258023_at	at3g19450	ATCAD4; cinnamyl-alcohol dehydrogenase	up
259911_at	at1g72680	ATCAD1; cinnamyl-alcohol dehydrogenase, putative	down

Supplemental Table S 4.4 Expression Data of a Subset of Genes Regulated by PS II and Involved in Major Metabolic Pathways (according to MapMan). Genes were considered up- or down-regulated when their fold-change value exceeded at least 1.5x or -1.5x ($P = 0.01$) in response to only DCMU when compared to the control plants.

Affymetrix ID's	Locus ID's	Annotation	Up-/Down-regulated
Cell Wall			
265536_at	at2g15880	leucine-rich repeat family protein / extensin family protein	1
265114_at	at1g62440	LRX2; LEUCINE-RICH REPEAT/EXTENSIN 2	-1
253608_at	at4g30290	XTH19; XYLOGLUCAN ENDOTRANSGLUCOSYLASE/HYDROLASE 19	-1
245325_at	at4g14130	XTR7; XYLOGLUCAN ENDOTRANSGLYCOSYLASE 7	-1
247162_at	at5g65730	xyloglucan:xyloglucoyl transferase, putative	-1
245228_at	at3g29810	COBL2; COBRA-LIKE PROTEIN 2 PRECURSOR	-1
265103_at	at1g31070	UDP-N-acetylglucosamine pyrophosphorylase-related	-1
252121_at	at3g51160	MUR1; MURUS 1; GDP-mannose 4,6-dehydratase	-1
258774_at	at3g10740	ASD1; ALPHA-L-ARABINOFURANOSIDASE 1	-1
251864_at	at3g54920	PMR6; powdery mildew resistant 6; lyase/ pectate lyase	1
Carbohydrates			
256633_at	at3g28340	GATL10; Galacturonosyltransferase-like 10	-1
249925_at	at5g19150	carbohydrate kinase family	-1
263183_at	at1g05570	CALS1; CALLOSE SYNTHASE 1; 1,3-beta-glucan synthase/ transferase	1
Sucrose/Starch			
256861_at	at3g23920	BAM1; BETA-AMYLASE 1	-1
258109_at	at3g23640	HGL1; heteroglycan glucosidase 1	-1
261754_at	at1g76130	AMY2; ALPHA-AMYLASE-LIKE 2	-1
263322_at	at2g04270	RNEE/G; RNASE E/G-LIKE; endoribonuclease	1
251935_at	at3g54090	pfkB-type carbohydrate kinase family protein	1
253980_at	at4g26620	sucrase-related	-1
Glycolysis/Gluconeogenesis/Oxidative Phosphorylation			
253404_at	at4g32840	PFK6; PHOSPHOFRUCTOKINASE 6	-1
258588_s_at	at3g04120	GAPC1; GLYCERALDEHYDE-3-PHOSPHATE DEHYDROGENASE C SUBUNIT 1	-1
261506_at	at1g71697	ATCK1; CHOLINE KINASE 1	-1
253578_at	at4g30340	ATDGK7; Diacylglycerol kinase 7	-1
Lipids			
247783_at	at5g58800	quinone reductase family protein	-1
250662_at	at5g07010	ST2A; SULFOTRANSFERASE 2A; hydroxyjasmonate sulfotransferase/ sulfotransferase	-1
264442_at	at1g27480	lecithin:cholesterol acyltransferase family protein / LACT family protein	1
258250_at	at3g15850	FAD5; FATTY ACID DESATURASE 5	1
251736_at	at3g56130	biotin/lipoyl attachment domain-containing protein	-1
266319_s_at	at3g10280,at2g46720	at3g10280: KCS14; 3-KETOACYL-COA SYNTHASE 14 at2g46720: KCS13; 3-KETOACYL-COA SYNTHASE 13	-1

250199_at	at5g14180	MPL1; MYZUS PERSICAE-INDUCED LIPASE 1	-1
253220_s_at	at4g34930,at4g34920	at4g34930: 1-phosphatidylinositol phosphodiesterase-related at4g34920: 1-phosphatidylinositol phosphodiesterase-related	1
254893_at	at4g11830	PLDGAMMA2; phospholipase D	1
252343_at	at3g48610	phosphoesterase family protein	1
253492_at	at4g31810	enoyl-CoA hydratase/isomerase family protein	1
TCA-Cycle			
264871_at	at1g24180	IAR4; oxidoreductase, acting on the aldehyde or oxo group of donors, disulfide as acceptor	-1
264313_at	at1g70410	BCA4; carbonic anhydrase, putative / carbonate dehydratase, putative	-1
Redox - Ascorbate/Glutathion			
257252_at	at3g24170	ATGR1; glutathione-disulfide reductase	-1
246785_at	at5g27380	GSH2; GLUTATHIONE SYNTHETASE 2	1
Photosynthesis			
256979_at	at3g21055	PSBTN; photosystem II subunit T	1
263442_at	at2g28605	Encodes a PsbP domain-OEC23 like protein localized in thylakoid (peripheral-luminal side)	1
244972_at	atcg00680)	PSBB encodes for CP47, subunit of the photosystem II reaction center.	1
245000_at	atcg00210)	YCF6 hypothetical protein	1
255617_at	at4g01330	ATP binding / kinase/ protein kinase/ protein serine/threonine kinase/ protein tyrosine kinase	-1
263761_at	at2g21330	fructose-bisphosphate aldolase, putative	-1
264069_at	at2g28000	CPN60A; CHAPERONIN-60ALPHA	1
258359_s_at	at3g14415,at3g14420	at3g14415: (S)-2-hydroxy-acid oxidase, peroxisomal, putative at3g14420: (S)-2-hydroxy-acid oxidase, peroxisomal, putative	-1
253387_at	at4g33010	AtGLDP1; Arabidopsis thaliana glycine decarboxylase P-protein 1	1
246033_at	at5g08280	HEMC; HYDROXYMETHYLBILANE SYNTHASE	1
264820_at	at1g03475	LIN2; LESION INITIATION 2; coproporphyrinogen oxidase	1
Amino Acids			
250484_at	at5g10240	ASN3; ASPARAGINE SYNTHETASE 3	1
254535_at	at4g19710	AK-HSDH II; bifunctional aspartate kinase/homoserine dehydrogenase, putative / AK-HSDH, putative	1
264525_at	at1g10060	ATBCAT-1; branched-chain amino acid aminotransferase 1 / branched-chain amino acid transaminase 1 (BCAT1)	1
246701_at	at5g28020	CYSD2; CYSTEINE SYNTHASE D2	-1
263897_at	at2g21940	shikimate kinase, putative	-1
248879_at	at5g46180	DELTA-OAT; ornithine-oxo-acid transaminase	-1
253492_at	at4g31810	enoyl-CoA hydratase/isomerase family protein	1
250090_at	at5g17330	GAD; calmodulin binding / glutamate decarboxylase	-1
Nitrogen-/Sulfur-/C-1			
256524_at	at1g66200	ATGSR2; copper ion binding / glutamate-ammonia ligase	-1
253387_at	at4g33010	AtGLDP1; Arabidopsis thaliana glycine decarboxylase P-protein 1	1
245115_at	at2g41530	SFGH; S-FORMYLGLUTATHIONE HYDROLASE	-1
Nucleotides			
254328_at	at4g22570	APT3; ADENINE PHOSPHORIBOSYL TRANSFERASE 3	-1
263167_at	at1g03030	phosphoribulokinase/uridine kinase family protein	-1

246126_at	at5g20070	ATNUDX19; ARABIDOPSIS THALIANA NUDIX HYDROLASE HOMOLOG 19	1
247376_at	at5g63310	NDPK2; NUCLEOSIDE DIPHOSPHATE KINASE 2	1
255089_at	at4g09320	NDPK1; ATP binding / nucleoside diphosphate kinase	1
251961_at	at3g53620	AtPPa4; Arabidopsis thaliana pyrophosphorylase 4	-1
261579_at	at1g01050	AtPPa1; Arabidopsis thaliana pyrophosphorylase 1	-1
258162_at	at3g17810	dihydroorotate dehydrogenase family protein / dihydroorotate oxidase family protein	-1
Secondary Metabolism			
257177_at	at3g23490	CYN; CYANASE; DNA binding / cyanate hydratase/ hydro-lyase	-1
252678_s_at	at3g44300,at3g44310	at3g44300: NIT2; nitrilase 2 at3g44310: NIT1; indole-3-acetonitrile nitrilase	-1
246778_at	at5g27450	MK; MEVALONATE KINASE	1
251118_at	at3g63410	APG1; ALBINO OR PALE GREEN MUTANT 1; 2-methyl-6-phytyl-1,4-benzoquinone methyltransferase	1
255787_at	at2g33590	cinnamoyl-CoA reductase family	-1

Chapter 5

5 EFFECTS OF LONG TERM ACCLIMATION TO EXCITATION PRESSURE ON GLOBAL GENE EXPRESSION IN *ARABIDOPSIS THALIANA*

5.1 *Introduction*

The previous chapter of this thesis dealt with the gene expression patterns of plants that were exposed to short term high photosystem II (PS II) excitation pressure (HEP) stress, whereas this chapter is focused on the effect of long term acclimation to HEP on whole genome gene expression in Arabidopsis plants grown under different light and temperature regimes promoting varying degrees of HEP.

HEP is a physiological stress condition that reflects a strongly reduced photosynthetic electron transport chain (PETC). HEP is defined as the strong reduction of Q_A the first stable electron acceptor of PS II (Hüner et al 1998; Hüner et al 2003; Ensminger et al. 2006; Wilson et al. 2006) and can hence be quantified in-vivo by chlorophyll a fluorescence as 1-qP (Schreiber et al., 1994). During photostasis the PETC is mostly oxidized and the rate at which light energy is absorbed by the photosystems is in balance with the rate of electron transport and the rate that the plant's metabolism consumes these electrons (Ensminger et al. 2006). In nature, light intensity commonly increases by several orders of magnitude within very short periods of time and this increases the rate of energy absorption drastically while leaving electron transport and consumption by metabolism almost unaltered (Hüner & Grodzinski 2011). This leads to HEP and ultimately to the generation of reactive oxygen species (ROS) at both PS II and PS I, which further leads to oxidative damage within the thylakoids and ultimately cell death (Kim et al. 2012). The same stress condition can be mimicked by low temperature while the light intensity remains unaltered. Upon exposure to low temperature the rate of electron transport and metabolism are lowered which results in a comparable strong reduction of the PETC and hence HEP induced photo-oxidation (Hüner et al, 1998; Ensminger et al, 2006).

Considering that 95 % of all 3000 chloroplast proteins are encoded in the nucleus (Koussevitzky et al. 2007), it is assumed that the chloroplast coordinates nuclear gene expression via retrograde regulation (Escoubas et al. 1995; Piippo et al. 2006; Fernández & Strand 2008; Pesaresi et al. 2010; Foudree et al. 2010; Woodson et al. 2011). This retrograde signaling allows the plant not only to remodel the PETC, but to govern phenotypic plasticity of the entire plant in order to acclimate to stress. Hence the chloroplast possesses a dual function of being the primary energy producer and sensor of change in the environment (Hüner et al. 1998; Wilson et al. 2006; Murchie et al. 2009).

In order to cope with this destructive stress condition, photoautotroph organisms have developed a wide array of acclimation strategies. Green algae, such as *Dunaliella tertiolecta*, *Dunaliella salina* and *Chlorella vulgaris* develop the same HEP phenotype when grown either at high light and ambient temperature or ambient light and low temperature. The HEP phenotype is visible as a yellow culture compared to the dark green color of the low EP phenotype. This yellow color is due to a reduced total chlorophyll content per cell, a high chlorophyll a/b ratio, reduced light harvesting proteins, and an increase in abundance and epoxidation state of photoprotective carotenoids. In short, these organisms decrease the capacity of the PETC to absorb light by decreasing the size of light harvesting antennae (Maxwell et al. 1995; Escoubas et al. 1995; Wilson et al. 2003).

Winter varieties of grass plants such as wheat and rye, but also *Brassica napus* seem to have adapted a different strategy: plants acclimated to HEP display a dwarf phenotype compared to non acclimated plants and they possess a higher biomass due to increased specific leaf area, reducing the quantity of light energy the leaves are absorbing. On the other hand the plants up-regulate their photosynthetic rate, by increasing carbon assimilation in the Calvin-Benson Cycle, sucrose and starch production and respiration in order to process the electrons generated by PS II (Dahal *et al.*, 2012a; 2012b).

In *Arabidopsis thaliana* it was shown within an array of variegated mutants that HEP governs the extent of leaf variegation to the degree that variegation could be fully

suppressed in some cases, when the plants were grown under extremely low excitation pressure (Rosso, Bode et al, 2009). These mutants, namely *im*, *spotty*, *var1* and *var2* are lacking either the plant terminal oxidase (PTOX; *im* and *spotty*), or different subunits of a FtsH protease (*var1* and *var2*). PTOX constitutes an alternative electron sink for the PETC (McDonald et al, 2011) while the FtsH protease is involved in the turnover of damaged PS II reaction centers, processes designed to prevent or alleviate oxidative damage caused by HEP early during leaf development and hence they represent different mechanisms of *Arabidopsis* to acclimate to HEP.

Several parts of the PETC have been postulated as sensors of HEP in retrograde signaling (i.e. PS II, PQH₂ and various factors on the acceptor side of PS I) and because they are all interconnected, their relative redox states reflect each other (Ndong et al. 2001; Pogson et al. 2008; Koussevitzky et al., 2007). Many putative mediators of signal transduction have been described, such as ROS generated at both PS II (singlet oxygen) and PS I (H₂O₂) (Suzuki et al, 2012), metabolites (Bräutigam et al, 2009) and intermediates of chlorophyll biosynthesis (Kindgren et al. 2011; Woodson et al. 2011). All of these factors are eventually recognized by signaling proteins like for instance STN7, EXECUTER and the GUN proteins, which integrate different signals and forward them to the nucleus, where they interact with transcription factors (e.g. ABI4) to promote the required adjustment in gene expression (see review by Fernández and Strand 2008). The extent of each sensors effect on global gene expression remains ambiguous though and it is not fully understood how the different sensors affect discrete genes when their signals are passed on by the same signaling peptides. Furthermore it needs to be addressed what the differences are in signaling and gene expression in response to either short term HEP exposure or acclimation to HEP.

In the present experimental design, we aimed to assess the transcriptional changes of the entire *Arabidopsis* genome in plants acclimated to HEP, in contrast to the last chapter of this thesis, which was intended to elucidate the response of the transcriptome to short term HEP stress. Hence we grew *Arabidopsis* plants to mid log phase of their vegetative growth at varying levels of light intensity (50 and 450 μmol

photons $\text{m}^{-2}\text{s}^{-1}$) at two different growth temperatures (12 and 25 °C), thus creating growth regimes promoting varying degrees of excitation pressure. The changes in global gene expression were monitored utilizing an *Arabidopsis* whole genome microarray (Affymetrix).

5.2 **Material and Methods:**

5.2.1 **Plant Growth**

Arabidopsis thaliana (Columbia) seeds were treated with 20% (v/v) bleach and 0.05% (v/v) Tween 20 for surface sterilization, sown on moistened and autoclaved soil and imbibed at 4 °C in the dark for three days. On the third day the seeds were shifted to a growth cabinet (GCW15, Environmental Growth Chambers, Chagrin Falls, Ohio) where they were exposed to their respective growth temperature of either 25 or 12 °C and light intensity of either 50 or 450 $\mu\text{mol photons m}^{-2}\text{s}^{-1}$ (25/50; 25/450; 12/50 and 12/450) with a 8h/16h (light/dark) photoperiod until mid log-phase of vegetative growth, in order to assure that plants were at a comparable developmental age. Plants were watered every second day with half strength Hoagland's solution. On the last day the plants were harvested during mid-photoperiod, rapidly frozen in liquid nitrogen and stored at -80 °C until further processing.

5.2.2 **Chlorophyll a Fluorescence**

Light response curves for excitation pressure were generated using an Imaging PAM Chlorophyll Fluorometer (Heinz Walz). Samples were dark adapted for 20 min prior to all measurements. All fluorescence measurements were performed on the plant's leaves at their respective growth temperature (either 12 or 25 °C). The fluorescence parameters were calculated after Schreiber et al. (1994). After dark adaptation, the leaves were exposed to a short (800 ms) pulse of saturating blue light ($6000 \mu\text{mol photons m}^{-2}\text{s}^{-1}$; $\lambda = 470 \text{ nm}$) provided by the Imaging PAM photodiode (IMAG-L; Heinz Walz). Excitation pressure was calculated as 1-qP (Dietz et al., 1985; Hüner et al., 1998, 2003).

5.2.3 **RNA Extraction**

Leaf material of three plants from each growth condition was pooled into one sample, ground to a fine powder using liquid nitrogen and RNA was extracted using the RNeasy Plant Minikit (Qiagen). Residual DNA was digested on-column utilizing the matching RNase free DNase kit (Qiagen).

5.2.4 ***RNA Quality Assessment, Probe Preparation and GeneChip Hybridization***

The following steps were performed by David Carter in the London Regional Genomics Center at the Robarts Research Institute (London, Canada).

The quality of the extracted RNA was examined using the Agilent 2100 Bioanalyzer (Agilent Technologies Inc., Palo Alto, CA) and the RNA 6000 Nano kit (Caliper Life Sciences, Mountain View, CA). Biotinylated complementary RNA (cRNA) was generated from 500 ng of total RNA following the Affymetrix GeneChip 3' IVT Express Kit Manual (Affymetrix, Santa Clara, CA).

https://www.affymetrix.com/user/login.jsp?toURL=/support/file_download.affx?onloadforward=/support/downloads/manuals/3_ivt_express_kit_manual.pdf

A total of 10 µg labeled cRNA was hybridized to the Affymetrix Arabidopsis ATH1 Genome Arrays for 16 hours at 45°C as described in the Affymetrix GeneChip 3' IVT Express Kit Manual (Affymetrix, Santa Clara, CA). The first step of GeneChips staining was performed by using Streptavidin-Phycoerythrin, the second step by an antibody solution and then finally another Streptavidin-Phycoerythrin solution, with all liquid handling performed by a GeneChip Fluidics Station 450. GeneChips were then scanned with the Affymetrix GeneChip Scanner 3000 7G (Affymetrix, Santa Clara, CA) using Command Console v1.1.

The following data analysis was performed by me:

Probe level (.CEL file) data were generated using the Affymetrix Command Console v1.1. Probes were summarized to the gene level data in Partek Genomics Suite v6.5 (Partek, St. Louis, MO) using the RMA algorithm (Irizarry *et al.*, 2003). Partek was used to determine gene level ANOVA p-values, fold changes and false discovery rate (FDR).

5.2.5 Quantitative Real-time RT-PCR:

First strand cDNA was generated using the High Capacity cDNA Reverse Transcription Kit (Applied Biosystems, CA). Real-time PCR was then performed using TaqMan Gene Expression Assays (Applied Biosystems, CA) for each of the displayed genes (Table S4.1). A total of 15 ng of cDNA and the 7900HT Real-Time PCR System (Applied Biosystems, Foster City, CA, USA) using the standard run conditions recommended by the manufacturer (50 °C: 2 min; 95°C: 10 min; 40 x [95 °C: 15 s; 60 °C: 1 min]). The total reaction volume was 20 µl and the relative cDNA levels were calculated using the relative standard curve method according to the manufacturer's recommendations. The expression of each gene was normalized to the expression of *act2*.

5.2.6 Functional Analysis of Differentially Regulated Genes:

The MapMan program (Thimm et al., 2004) was used in order to classify and display genes into metabolic pathway groups and to identify the transcription factors involved.

5.3 Results:

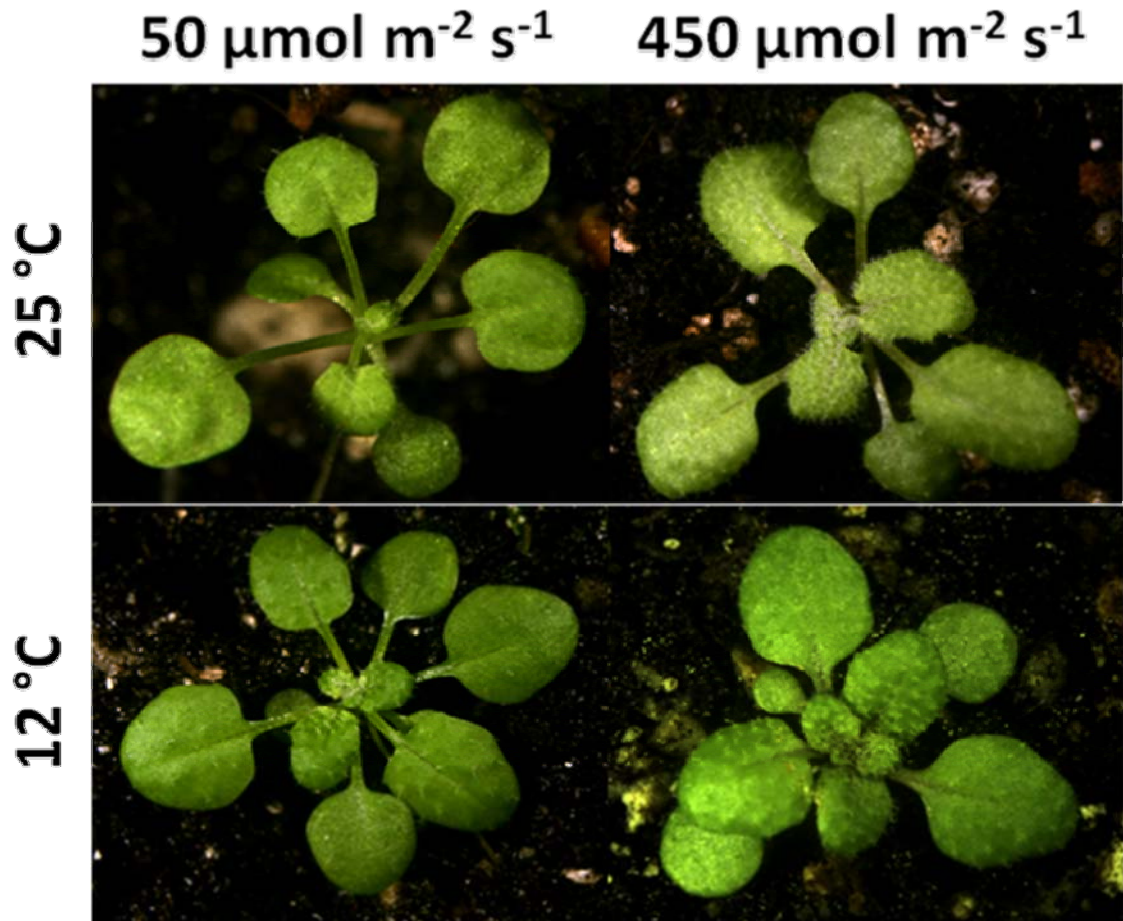


Figure 5.1 Representative Photographs of Arabidopsis Acclimated to Various Light and Temperature Regimes

Plants were grown to mid-log phase of vegetative growth at their respective growth regime in order to have them at a comparable developmental age. Photos display representative plants from each growth regime.

5.3.1 *Acclimation to HEP*

The phenotypes of plants acclimated to different levels of HEP induced by growth under varying levels of light and temperature is displayed in Figure 5.1. With increasing EP the petioles tend to get a little shorter and the leaf color changes, due to slightly decreased levels of chlorophyll per leaf area and reduced chlorophyll *a/b* ratios as reported previously by Rosso and colleagues (2006). All of these phenotypic effects appear more pronounced at 12 °C than at 25 °C and with increased growth irradiance.

Since excitation pressure (1-qP) is an estimate for the proportion of closed PS II reaction centers, it reflects the relative redox state of the entire PETC and is hence sensitive to both light and temperature. The excitation pressure light response curves of the plants grown at different light and temperature regimes (Figure 5.2) indicated that these plants were actually acclimated to their respective growth condition. Plants grown under higher light conditions displayed decreased susceptibility to EP at increasing levels of irradiance so that a higher light intensity was needed in order to close the reaction centers of PS II. Additionally, plants had acclimated to their respective growth temperature, since the EP was comparable between plants grown at 12 °C and at 25 °C, when they were grown at the same light intensity. At a measuring light intensity of 500 $\mu\text{mol m}^{-2} \text{s}^{-1}$, plants grown at either 12/50 or at 25/50 had a comparable proportion of closed PS II reaction centers (37.4 % and 35.0 ± 3.8 % respectively), while plants grown at 12/450 and 25/450 displayed only 15.2 ± 1.5 % and 18.4 ± 0.7 % respectively of closed PS II reaction centers (Figure 5.2).

We previously demonstrated that non-acclimated plants display significantly higher degrees of EP at a lower measuring temperature (Rosso, Bode et al., 2009) when grown under the same light regime. Yet, the light response curves of these acclimated plants showed no apparent difference of EP in plants grown under different temperature but equal light regimes. This indicated a successful acclimation of these plants to their respective growth regimes at various levels of excitation pressure.

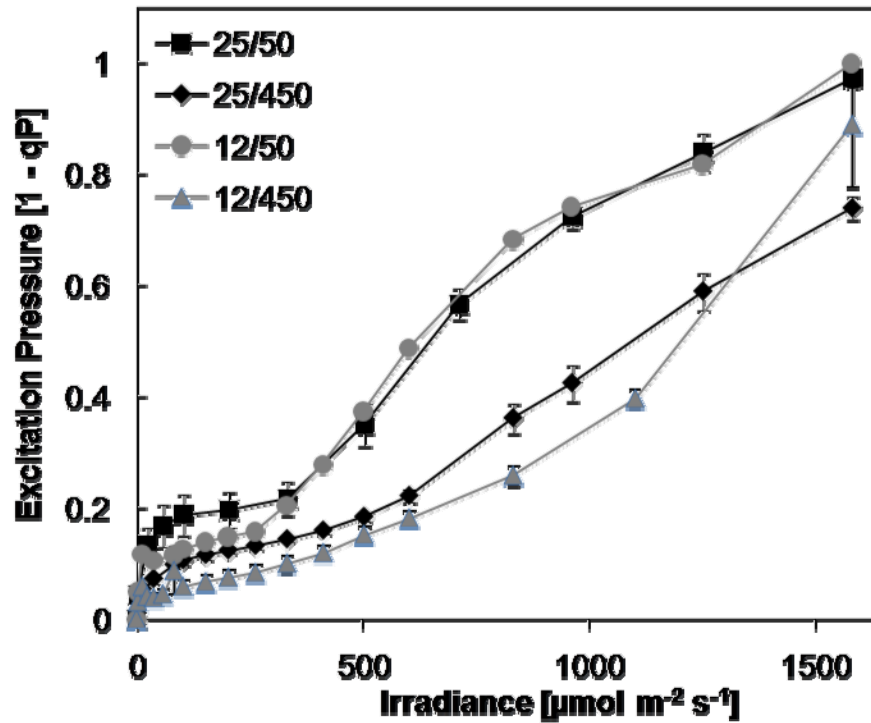


Figure 5.2 The Effects of Growth Irradiance and Temperature on Excitation Pressure and Photoacclimation

Excitation pressure (1-qP) light response curves were performed for *Arabidopsis* leaves grown under varying growth temperature light regimes (25/50 (black squares), 25/450 (black diamonds), 12/50 (grey circles) and 12/450 (grey triangles)). Measurements were performed on attached leaves at the respective growth temperature of the plant, with increasing irradiance from 0 to 1550 $\mu\text{mol photons m}^{-2} \text{s}^{-1}$. Plants were grown with an 8/16-h day/night cycle, and attached leaves were measured 4 h into the photoperiod. Data represent the mean \pm SE calculated from 2 - 4 measurements per plant in 3 - 5 different plants per treatment (except, 12/50 where, due to technical difficulties, only one plant could be measured, hence there is no SE).

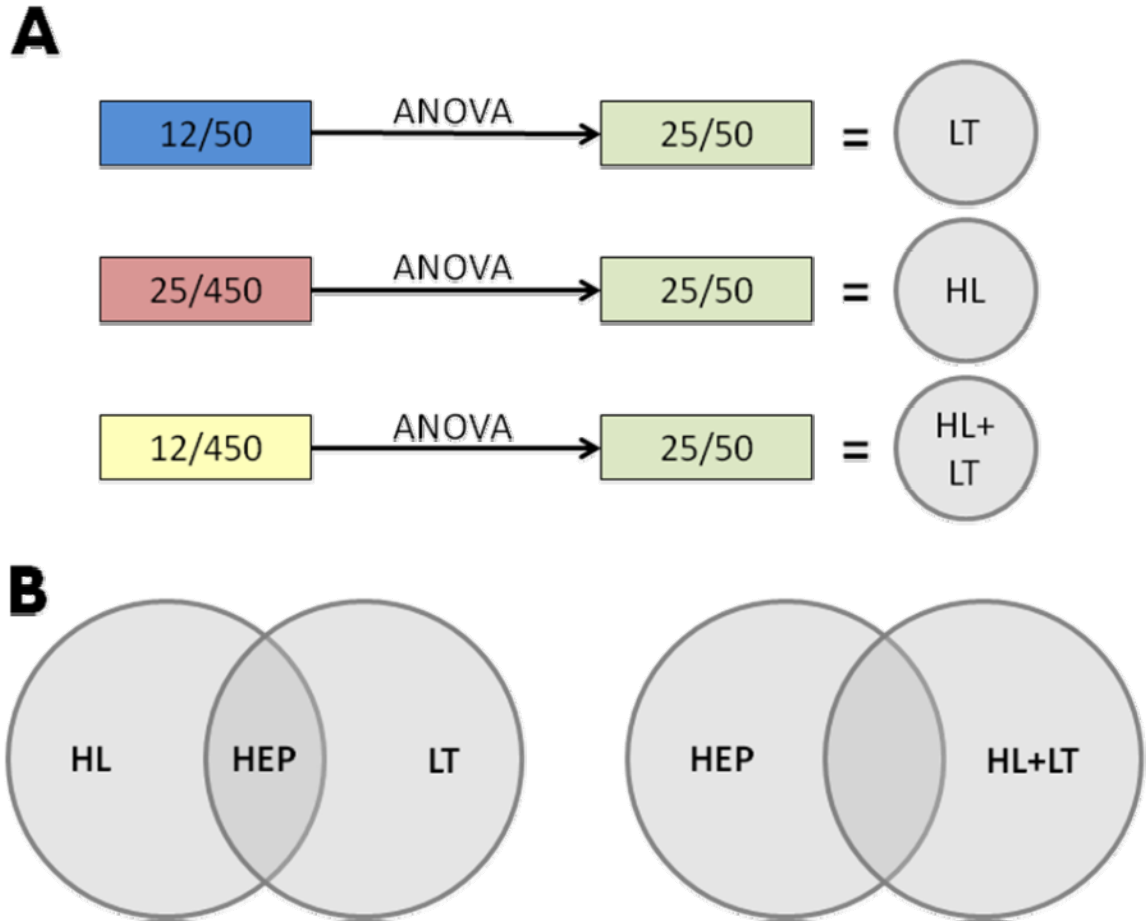


Figure 5.3 Determination of Differential Gene Expression

(A) A two-way ANOVA was performed between the microarray gene expression data from the plants grown at 12 °C and 50 $\mu\text{mol photons m}^{-2} \text{s}^{-1}$ (12/50) and the control plants grown under 25 °C and 50 $\mu\text{mol photons m}^{-2} \text{s}^{-1}$ (25/50); the resulting gene list was considered to be regulated by acclimation to low temperature (LT). The same process was applied to plants grown under 25 °C and 450 $\mu\text{mol photons m}^{-2} \text{s}^{-1}$ (high light; HL) and plants grown under 12°C and 450 $\mu\text{mol photons m}^{-2} \text{s}^{-1}$ (high light and low temperature; HL/LT). Transcripts were considered changed at a fold change value of 1.5x and $P \leq 0.01$.

(B) Transcripts that were altered in the same manner due to both lower growth temperature LT and higher growth irradiance (HL) were considered to be regulated by high excitation pressure (HEP). As a control the HEP list was compared to genes regulated by high light and low temperature at the same time (HL/LT).

5.3.2 ***Differential Gene Expression in Plants Acclimated to Various Growth Regimes***

In order to distinguish genes that are differentially expressed as a result of acclimation to HEP from differential gene expression due to acclimation to different light and temperature conditions, we used plants grown at low excitation pressure conditions (25/50) as our control group. We then compared plants that were grown at higher levels of EP, due to the same temperature, but higher irradiance (25/450), the same level of irradiance but lower temperature (12/50) and both, lower temperature and higher irradiance (12/450), to the control group using two-way ANOVAs. (Figure 5.3A). Only genes that increased or decreased their expression levels with a fold-change value ≥ 1.5 and $P \leq 0.01$ were considered differentially expressed. This resulted in three separate gene lists that were differentially expressed due to acclimation to either low temperature (LT), high light (HL) or both (HL+LT) (Figure 5.3A). Genes that were expressed differentially and in the same manner by both, HL and LT were considered to be altered through acclimation to HEP directly, rather than HL or LT individually. HEP genes were compared to HL+LT in order to verify, whether the genes identified as acclimation HEP are truly found regulated in the plants grown under the highest degree of excitation pressure (Figure 5.3B).

Acclimation to HL resulted in 12 % of the monitored transcriptome being alternatively expressed with 1282 up- and 1547 down-regulated genes (Figure 5.4), including, as expected, various light harvesting genes (i.e. *lhcb2.3*: down; *lhcb6*: down; *lhcb4.3*: up; *lhca6*: down; *lhcb4.2*: down), transcripts for subunits of both, PS II and PS I, Calvin-Benson cycle enzymes and many more photosynthesis associated mRNAs. Acclimation to LT resulted in 10 % of all genes being regulated differentially, with 1162 up- and 1127 down-regulated genes. Apart from a range of photosynthetic genes several genes associated with response to cold temperatures were found changed (i.e. *cor47*: up; *cor15A*: up; *cor15B*: up; *cor414-tm1*: up; *cbf1*: up; *cbf2*: up; *cbf3*: up; *cbf-b*: down; *ice1*: up). As expected, HL+LT resulted in the largest change in gene expression in comparison

to the control with ca. 16 % of the genome altered (1764 up- and 1931 down-regulated) (Figure 5.4).

Approximately 3 % of all mRNAs were expressed differentially as a result of acclimation to both HL and LT in the same way (344 up- and 391 down-regulated) (Figure 5.4). This set of genes was designated as HEP genes. About 79 % of these HEP acclimation genes were also found changed in the plants grown under the highest degree of excitation pressure (12/450) corroborating the validity of the HEP gene group. Interestingly we again found several light-regulation associated components of the PETC changed, such as subunits of PS II (i.e. *lhcb4.3*: up; *psbp2*: down;), as well as PS I (*lhca6*: down; *psad2*: down) and the Cytochrome b_6f complex (*petg*: down), but also components of the thylakoidal ATPase (*atpa*: down; *atph*: up). In addition, some of the transcripts associated with regulation by cold temperature were found in this HEP acclimation group (i.e. *cbf-b*: down; *cor15A*: up; *cor15B*: down), indicating that many of these transcripts that have previously been described as either light or temperature dependent, are indeed regulated by the redox state of the PETC or EP.

In the previous chapter of this thesis we determined that ca 11 % of the entire *Arabidopsis* genome is changed due to short term (1h) HEP stress. What proportion of the HEP stress gene group was still present in the gene group acclimated to HEP? To answer this question we made a comparison between the list of genes that were involved in HEP stress with the gene group associated with acclimation to HEP. Out of the 735 genes that were differentially expressed as a result of acclimation to HEP, almost one third (224 transcripts) were already present in the HEP stress response (Figure 5.5).

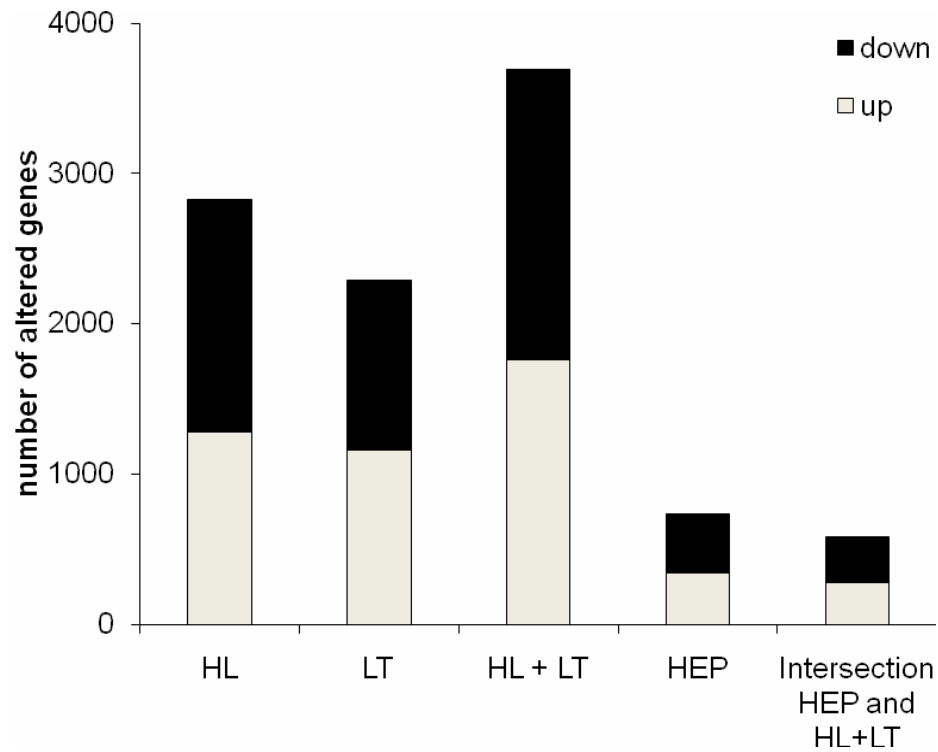


Figure 5.4 Comparison of Differentially Expressed Genes Between Different Groups
 Number of genes altered in plants grown at high light (HL), in plants grown at low temperature (LT), in plants grown at high light and low temperature at the same time (HL+LT), the list of common genes (HEP) between HL and LT and the intersection of genes regulated by HL+LT and HEP. The black part of the bars represents down-regulated genes and the white part represents the up-regulated genes. Genes were considered changed at a fold change value $\geq 1.5x$ and $P \leq 0.01$.

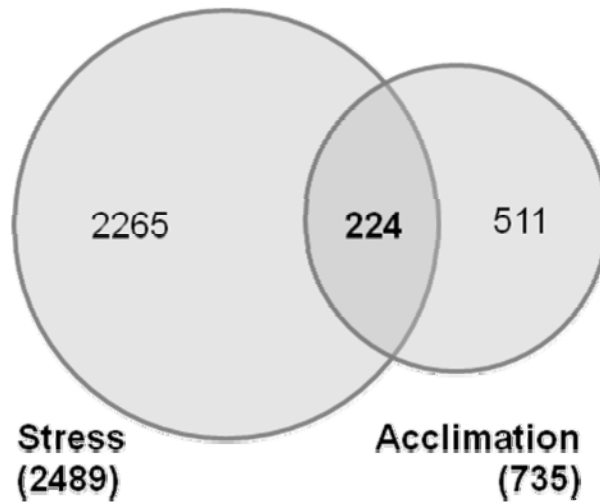


Figure 5.5 Common Gene Expression in HEP Stress and Acclimation

Venn Diagramm comparison of genes differentially regulated by short term (1h) HEP stress and long term HEP acclimation. Genes were considered changed at a fold change value $\geq 1.5x$ and $P \leq 0.01$.

5.3.3 **Real-Time RT-PCR**

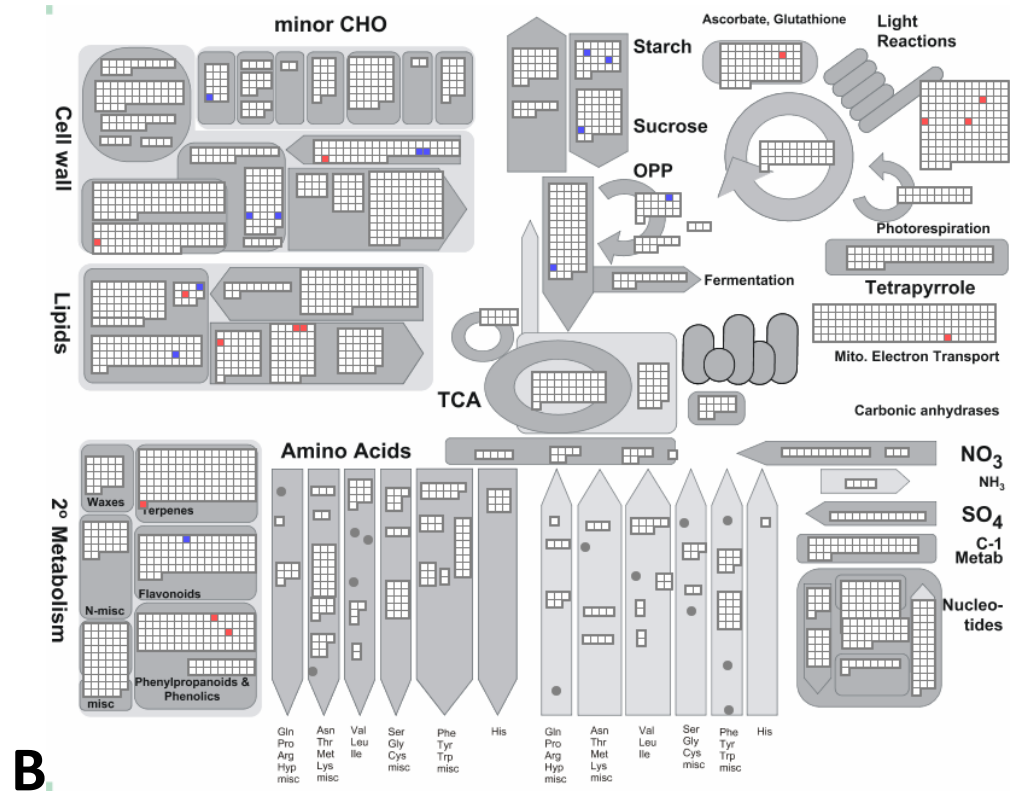
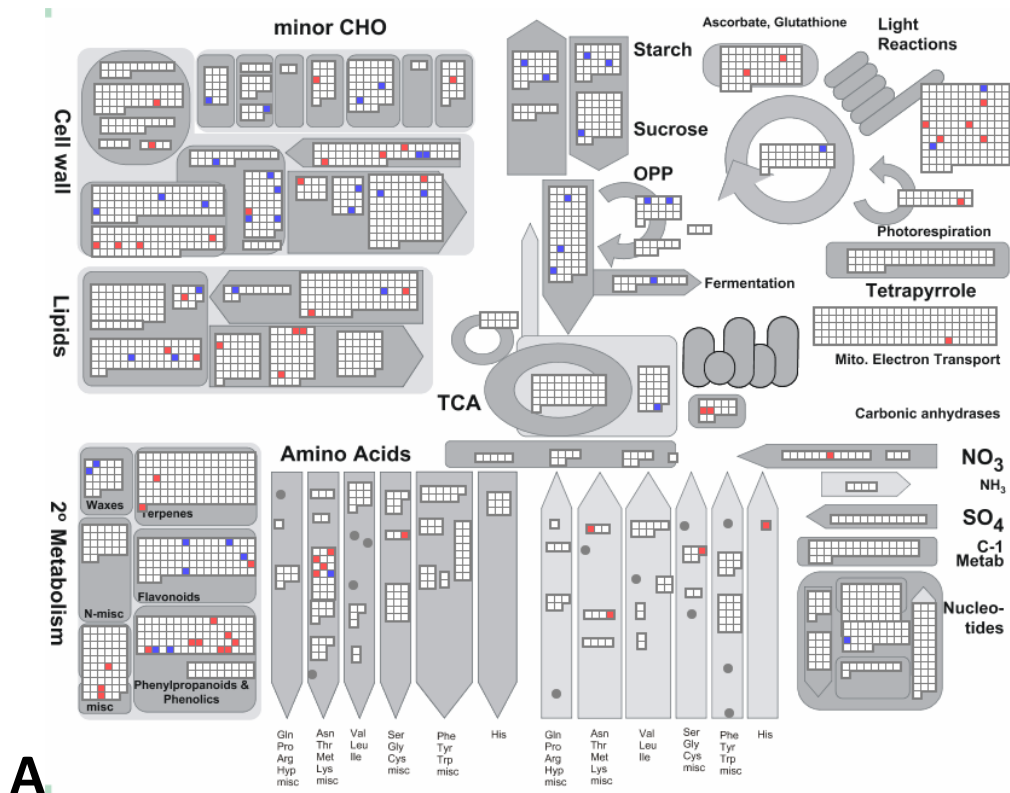
Quantitative real-time RT-PCR was performed in order to verify the microarray expression analysis for the transcripts for *spa1*, *dreb1a*, *nda1* and *tub8* (see Supplemental Figure S5.1). The same trends were found between the expression ratios of qPCR and the Affymetrix ATH1 microarray data, when the different experimental conditions were compared to the control plants, in almost all treatments that were tested. These results substantiate the validity of the microarrays.

5.3.4 **Functional Characterisation of Gene Expression:**

The set of genes that were responsible for the acclimation to HEP displayed very little accumulation of altered transcripts related to any particular metabolic pathway when it was plotted using MapMan. Interestingly, it seems that particularly processes associated with energy metabolism, that is: Krebs cycle, mitochondrial electron transport, and most processes involved in photosynthesis (i.e. photorespiration, Calvin-Benson cycle, tetrapyrrole metabolism, light reactions) appear mostly unchanged (Figure 5.6A). Out of the 136 genes associated with light reactions, only eight were affected by acclimation to HEP; *lhcb4.3* and *atph* were up-regulated, while the rest of the eight regulated light reaction genes (*psbp-2*, *lhca6*, *psad-2*, *petg* and *atpa*) were all down-regulated. Additionally two oxygen scavenging transcripts were down-regulated. While lipid metabolism, cell wall biogenesis, various secondary metabolism pathways, and starch and sucrose metabolism were affected, there was no apparent accumulation of altered transcripts within either one of these groups. Unlike lipid metabolism, cell wall biogenesis and the secondary metabolism pathways, where both up- and down-regulation of transcripts could be observed we could only detect up-regulated transcripts in starch and sucrose metabolism.

Figure 5.6. MapMan Display of Gene Expression Data. MapMan software (Thimm et al., 2004) was used to display significant changes in transcript abundance of genes associated with major metabolic pathways. **(A)** shows the differentially expressed genes which represent the acclimation to HEP. **(B)** shows the genes that were regulated by both HEP acclimation and short term HEP stress.

Red squares represent down-regulated transcripts, blue squares represent up-regulated transcripts, while white squares represent transcripts that remained unaltered.



When comparing the MapMan overview of major metabolic pathways for the genes that were differentially regulated as a response to HEP stress and acclimation to HEP, it becomes apparent that out of the 224 genes hardly any were involved in chloroplast related processes, be it light reactions (apart from: *lhca6*, *psbp-2*, *psad-2*; all down-regulated), Calvin cycle, photorespiration or tetrapyrrole metabolism (Figure 5.6B). In fact, it seems that genes from this group did not accumulate in any of the major metabolic pathways. While some pathways, such as cell wall biogenesis, lipid metabolism, starch and sucrose metabolism and light reactions only had a small amount of genes differentially regulated, other pathways, such as all amino acid anabolism and catabolism, nucleotide metabolism, the Krebs cycle, N-, S- and C₁ - metabolism were entirely unaffected. The majority of the 224 genes present in both the HEP acclimation and stress group were not represented on the major metabolism chart (Figure 5.6B).

Furthermore, MapMan was used to assess which genes out of these two groups constituted known transcription factors. Within the HEP acclimation genes 79 differentially regulated transcription factors (31 up- and 48 down-regulated) from various families could be found (Table 5.1). Apart from 15 altered putative and unclassified transcription factors the families with the most altered transcripts (>2) were the “Basic Helix-Loop-Helix family” (8), “C2H2 zinc finger family” (7), “MYB-related transcription factor family” (5), “MYB domain transcription factor family” (4), “Heat-shock transcription factor family” (4), “Homeobox transcription factor family” (4), “C2C2(Zn) CO-like, Constans-like zinc finger family” (3) and the “Pseudo ARR transcription factor family” (3).

Exploring the list of 224 genes that was differentially regulated by both HEP stress and acclimation, there were still 28 differentially expressed transcription factors found with 17 down- and 11 up-regulated (Table 5.2). While the “MYB-related transcription factor family” had already 4 altered transcripts 1 hour into the HEP stress, none of the “MYB domain transcription factor family” transcripts were activated or repressed during this early stage. The only two other notable families with >2 members altered were

“C2C2(Zn) CO-like, Constans-like zinc finger family” (3) and “Pseudo ARR transcription factor family” (3).

Table 5.1 Transcription Factors Changed by Acclimation to HEP. List of transcription factors and their families according to MapMan, that are either up- or down-regulated (≥ 1.5 x, $P \leq 0.01$) by acclimation to HEP in *A. thaliana*.

Family	Locus Tag	Name/Description	Up/Down
ABI3/VP1-related B3-domain-containing transcription factor family	at2g46870	Symbols: NGA1 NGA1 (NGATHA1); transcription factor	down
AP2/EREBP, APETALA2/Ethylene-responsive element binding protein family	at1g68840	Symbols: RAV2, RAP2.8, TEM2 RAV2 (REGULATOR OF THE ATPASE OF THE VACUOLAR MEMBRANE); DNA binding / transcription factor/ transcription repressor	down
	at2g39250	Symbols: SNZ SNZ (SCHNARCHZAPFEN); DNA binding / transcription factor	down
ARR	at2g25180	ARR12 (ARABIDOPSIS RESPONSE REGULATOR 12); transcription factor/ two-component response regulator	down
Basic Helix-Loop-Helix family	at2g20180	PIL5 (PHYTOCHROME INTERACTING FACTOR 3-LIKE 5); DNA binding / phytochrome binding / transcription factor	down
	at1g73830	Symbols: BEE3 BEE3 (BR ENHANCED EXPRESSION 3); DNA binding / transcription factor	up
	at5g39860	Symbols: PRE1 PRE1 (PACLOBUTRAZOL RESISTANCE1); DNA binding / transcription factor	down
	at5g04150	Symbols: BHLH101 BHLH101; DNA binding / transcription factor	down
	at3g47640	basic helix-loop-helix (bHLH) family protein	down
	at5g54680	Symbols: ILR3 ILR3 (iaa-leucine resistant3); DNA binding / transcription factor	down
	at1g51140	basic helix-loop-helix (bHLH) family protein	down
	at1g18400	Symbols: BEE1 BEE1 (BR Enhanced Expression 1); transcription factor	up
bZIP transcription factor family	at3g10800	Symbols: BZIP28 BZIP28; DNA binding / transcription factor	down
	at5g24800	Symbols: ATBZIP9, BZO2H2, BZIP9 BZIP9 (BASIC LEUCINE ZIPPER 9); DNA binding / protein heterodimerization/ transcription factor	down
C2C2(Zn) CO-like, Constans-like zinc finger family	at2g47890	zinc finger (B-box type) family protein	up
	at1g28050	zinc finger (B-box type) family protein	up
	at5g48250	zinc finger (B-box type) family protein	up
C2C2(Zn) DOF zinc finger family	at1g29160	Dof-type zinc finger domain-containing protein	up
C2H2 zinc finger family	at3g50700	Symbols: AtIDD2 AtIDD2 (Arabidopsis thaliana Indeterminate(ID)-Domain 2); nucleic acid binding / transcription factor/ zinc ion binding	up
	at1g67030	Symbols: ZFP6 ZFP6 (ZINC FINGER PROTEIN 6); nucleic acid binding / transcription factor/ zinc ion binding	down
	at4g17810	nucleic acid binding / transcription factor/ zinc ion binding	down
	at2g29660	zinc finger (C2H2 type) family protein	down
	at3g58070	Symbols: GIS GIS (GLABROUS INFLORESCENCE STEMS); nucleic acid binding / transcription factor/ zinc ion binding	up
	at1g04990	zinc finger (CCCH-type) family protein	up
	at4g05330	Symbols: AGD13 AGD13 (ARF-GAP domain 13); ARF GTPase activator/ zinc ion binding	up
CCAAT box binding factor family, HAP2	at1g30500	Symbols: NF-YA7 NF-YA7 (NUCLEAR FACTOR Y, SUBUNIT A7); specific transcriptional repressor/ transcription factor	down
G2-like transcription factor family, GARP	at2g40970	myb family transcription factor	down

	at3g10760	myb family transcription factor	down
Homeobox transcription factor family	at2g22800	Symbols: HAT9 HAT9; DNA binding / transcription factor	down
	at5g47370	Symbols: HAT2 HAT2; DNA binding / transcription factor/ transcription repressor	down
	at1g75410	Symbols: BLH3 BLH3 (BEL1-LIKE HOMEODOMAIN 3); DNA binding / transcription factor	down
	at4g40060	Symbols: ATHB-16 ATHB16 (ARABIDOPSIS THALIANA HOMEODOMAIN PROTEIN 16); sequence-specific DNA binding / transcription activator/ transcription factor	down
MADS box transcription factor family	at2g03710	Symbols: SEP4, AGL3 SEP4 (SEPALLATA 4); DNA binding / transcription factor	down
	at5g10140	Symbols: FLC, FLF, AGL25 FLC (FLOWERING LOCUS C); specific transcriptional repressor/ transcription factor	down
MYB domain transcription factor family	at4g37260	Symbols: MYB73, ATMYB73 MYB73 (MYB DOMAIN PROTEIN 73); DNA binding / transcription factor	up
	at1g22640	Symbols: ATMYB3, MYB3 MYB3 (MYB DOMAIN PROTEIN 3); DNA binding / transcription factor	down
	at5g07690	Symbols: MYB29, ATMYB29, PMG2 ATMYB29 (ARABIDOPSIS THALIANA MYB DOMAIN PROTEIN 29); DNA binding / transcription factor	down
	at5g59780	Symbols: MYB59, ATMYB59-3 MYB59 (MYB DOMAIN PROTEIN 59); DNA binding / transcription factor	down
MYB-related transcription factor family	at5g47390	myb family transcription factor	down
	at1g71030	Symbols: ATMYBL2, MYBL2 MYBL2 (ARABIDOPSIS MYB-LIKE 2); DNA binding / transcription factor	down
	at1g74840	myb family transcription factor	down
	at1g18330	Symbols: EPR1 EPR1 (EARLY-PHYTOCHROME- RESPONSIVE1); DNA binding / transcription factor	down
	at1g19000	myb family transcription factor	down
GRAS transcription factor family	at1g63100	scarecrow transcription factor family protein	up
Heat-shock transcription factor family	at2g26150	Symbols: ATHSFA2, HSFA2 ATHSFA2; DNA binding / transcription factor	down
	at5g43840	Symbols: AT-HSFA6A, HSFA6A AT-HSFA6A; DNA binding / transcription factor	down
	at1g67970	Symbols: AT-HSFA8, HSFA8 AT-HSFA8; DNA binding / transcription factor	up
	at5g62020	Symbols: AT-HSFB2A, HSFB2A AT-HSFB2A; DNA binding / transcription factor	down
Triple-Helix transcription factor family	at1g76880	trihelix DNA-binding protein, putative	up
WRKY domain transcription factor family	at2g37260	Symbols: TTG2, ATWRKY44, WRKY44, DSL1 TTG2 (TRANSPARENT TESTA GLABRA 2); transcription factor	up
Auxin/IAA family	at4g32280	Symbols: IAA29 IAA29 (INDOLE-3-ACETIC ACID INDUCIBLE 29); transcription factor	down
	at4g14550	Symbols: IAA14, SLR IAA14 (INDOLE-3-ACETIC ACID INDUCIBLE 14); protein binding / transcription factor	down
ELF3	at2g25930	Symbols: ELF3, PYK20 ELF3 (EARLY FLOWERING 3); protein C-terminus binding / transcription factor	up
B3 transcription factor family	at3g53310	transcriptional factor B3 family protein	down
	at4g01580, at3g18960	at4g01580: transcriptional factor B3 family protein at3g18960: transcriptional factor B3 family protein	up
Global transcription factor group	at5g14270	Symbols: ATBET9 ATBET9 (Arabidopsis thaliana Bromodomain and Extraterminal Domain protein 9); DNA binding	up
DNA synthesis/chromatin structure:histone	at5g02560	Symbols: HTA12 HTA12; DNA binding	down
PHD finger transcription factor	at3g14980	PHD finger transcription factor, putative	up
Pseudo ARR transcription factor family	at5g24470	Symbols: APRR5, PRR5 APRR5 (ARABIDOPSIS PSEUDO-RESPONSE REGULATOR 5); transcription regulator/ two-component response regulator	up

	at5g60100	Symbols: APRR3, PRR3 APRR3 (ARABIDOPSIS PSEUDO-RESPONSE REGULATOR 3); transcription regulator/ two-component response regulator	up
	at5g61380	Symbols: TOC1, APRR1, PRR1 TOC1 (TIMING OF CAB EXPRESSION 1); transcription regulator/ two-component response regulator	up
General Transcription	at2g22840	Symbols: AtGRF1 AtGRF1 (GROWTH-REGULATING FACTOR 1); transcription activator	up
	at4g37740	Symbols: AtGRF2 AtGRF2 (GROWTHREGULATING FACTOR 2); transcription activator	up
SNF7	at5g44560	Symbols: VPS2.2 VPS2.2	up
Putative transcription regulator	at1g44770	unknown protein	down
	at2g45820	DNA-binding protein, putative	down
	at2g41870	remorin family protein	down
	at4g01780, at3g48670	at4g01780: XH/XS domain-containing protein at3g48670: XH/XS domain-containing protein / XS zinc finger domain-containing protein	up
	at5g54930	AT hook motif-containing protein	up
	at3g61260	DNA-binding family protein / remorin family protein	down
Unclassified	at1g76590	zinc-binding family protein	up
	at5g61190	zinc finger protein-related	up
	at1g51200	zinc finger (AN1-like) family protein	down
	at2g33845	DNA-binding protein-related	down
	at4g27000	Symbols: ATRBP45C ATRBP45C; RNA binding	down
	at4g30410	transcription factor	down
	at3g53460	Symbols: CP29 CP29; RNA binding / poly(U) binding	up
	at2g34620	mitochondrial transcription termination factor-related / mTERF-related	down
	at5g12440	nucleic acid binding / nucleotide binding / zinc ion binding	up

Table 5.2 Transcription Factors Changed by Both Short Term and Long Term Exposure to HEP. Intersection of *A. thaliana* Transcription Factors, according to MapMan, that are either up- or down-regulated (≥ 1.5 x, $P \leq 0.01$) by both acclimation to HEP and HEP short term stress (1h).

Family	Locus Tag	Name/Description	Up/Down
AP2/EREBP, APETALA2/Ethylene-responsive element binding protein family	at1g68840	Symbols: RAV2, RAP2.8, TEM2 RAV2 (REGULATOR OF THE ATPASE OF THE VACUOLAR MEMBRANE); DNA binding / transcription factor/ transcription repressor	down
Basic Helix-Loop-Helix family	at2g20180	PIL5 (PHYTOCHROME INTERACTING FACTOR 3-LIKE 5); DNA binding / phytochrome binding / transcription factor	down
	at5g04150	Symbols: BHLH101 BHLH101; DNA binding / transcription factor	down
C2C2(Zn) CO-like, Constans-like zinc finger family	at2g47890	zinc finger (B-box type) family protein	up
	at1g28050	zinc finger (B-box type) family protein	up
	at5g48250	zinc finger (B-box type) family protein	up
C2H2 zinc finger family	at1g67030	Symbols: ZFP6 ZFP6 (ZINC FINGER PROTEIN 6); nucleic acid binding / transcription factor/ zinc ion binding	down
MYB-related transcription factor family	at5g47390	myb family transcription factor	down
	at1g71030	Symbols: ATMYBL2, MYBL2 MYBL2 (ARABIDOPSIS MYB-LIKE 2); DNA binding / transcription factor	down
	at1g19000	myb family transcription factor	down
	at1g22640	Symbols: ATMYB3, MYB3 MYB3 (MYB DOMAIN PROTEIN 3); DNA binding / transcription factor	down
G2-like transcription factor family, GARP	at2g40970	myb family transcription factor	down
ARR	at2g25180	ARR12 (ARABIDOPSIS RESPONSE REGULATOR 12); transcription factor/ two-component response regulator	down
Heat-shock transcription factor family	at1g67970	HSFA8 AT-HSFA8; DNA binding / transcription factor	up
ELF3	at2g25930	Symbols: ELF3, PYK20 ELF3 (EARLY FLOWERING 3); protein C-terminus binding / transcription factor	up
Aux/IAA family	at4g32280	Symbols: IAA29 IAA29 (INDOLE-3-ACETIC ACID INDUCIBLE 29); transcription factor	down
	at4g14550	Symbols: IAA14, SLR IAA14 (INDOLE-3-ACETIC ACID INDUCIBLE 14); protein binding / transcription factor/ transcription repressor	down
Global transcription factor group	at5g14270	ATBET9 (Arabidopsis thaliana Bromodomain and Extraterminal Domain protein 9); DNA binding	up
DNA synthesis/chromatin structure:histone	at5g02560	Symbols: HTA12 HTA12; DNA binding	down
Pseudo ARR transcription factor family	at5g24470	Symbols: APRR5, PRR5 APRR5 (ARABIDOPSIS PSEUDO-RESPONSE REGULATOR 5); transcription regulator/ two-component response regulator	up
	at5g60100	Symbols: APRR3, PRR3 APRR3 (ARABIDOPSIS PSEUDO-RESPONSE REGULATOR 3); transcription regulator/ two-component response regulator	up
	at5g61380	TOC1 (TIMING OF CAB EXPRESSION 1); transcription regulator/ two-component response regulator	up
Unclassified	at1g76590	zinc-binding family protein	up
	at4g30410	transcription factor	down
	at2g34620	mitochondrial transcription termination factor-related / mTERF-related	down
Putative transcription regulator	at1g44770	unknown protein	down
	at2g41870	remorin family protein	down
	at5g54930	AT hook motif-containing protein	up

5.4 Discussion:

Chapter 2 of this thesis demonstrates the sensitivity of excitation pressure towards both light and temperature. Plants acclimated to warmer, more moderate temperature regimes (i.e. 25 °C) or lower light levels are more susceptible to HEP at increasing light intensities and lower temperatures (Rosso, Bode et al. 2009). The plants in this experiment, however, when grown at a lower temperature (12 °C), did not appear to suffer elevated EP, when compared to the plants grown at higher temperatures at the same light intensity. Moreover, at both high and low growth temperatures, plants that were grown at HL (450 $\mu\text{mol photons m}^{-2} \text{s}^{-1}$) displayed less susceptibility to elevated EP, than plants grown at lower light intensity (50 $\mu\text{mol photons m}^{-2} \text{s}^{-1}$). At a measuring light intensity of 500 $\mu\text{mol photons m}^{-2} \text{s}^{-1}$ plants grown at higher light intensities (450 $\mu\text{mol photons m}^{-2} \text{s}^{-1}$) displayed approximately half the amount of PS II reaction centers closed compared to plants grown at lower light intensity (50 $\mu\text{mol photons m}^{-2} \text{s}^{-1}$) when EP was measured at their respective growth temperature of either 12 or 25 °C.

A major problem for plants suffering HEP stress is oxidative damage promoted by ROS generated at both PS II and PS I. Thus we noted with interest, that there was no induction of ROS scavenging enzyme transcripts (Figure 5.6A), in fact *apx3* and *gpx1* were down-regulated in response to HEP acclimation, again indicating that these plants were not under acute oxidative stress. This leads us to the conclusion that these plants were adequately acclimated to their respective growth regime and are in fact each in a different state of photostasis.

Looking at the level of whole genome gene expression, it appears that while the acclimation to lower temperature causes about 10 % of the genome to be altered, acclimation to HL requires ca. 12, while acclimation to pure HEP merely requires a fraction of these genes (a total of 3 % of the whole genome) to be differentially expressed (Figure 5.4). This number appears very small, when considering that the HEP stress response from Chapter 3 of this thesis resulted in a change of ca 11 % of the entire transcriptome. Yet it is remarkable that roughly one third of all the genes

regulated through acclimation to HEP was already regulated in the same manner merely 1h after the first stress response (Figure 5.5).

Even though we do not possess the full time course of gene expression regulated by HEP, we do have the two extreme time points on either side of the course, the first response (i.e. one hour after application of HEP) and the fully acclimated state. While there was a drastic response to HEP stress, presumably for chloroplast remodeling and modification of the plants entire metabolism and growth habit in order to acclimate to the new environment, comparatively smaller change in gene expression seems to be necessary to maintain that acclimated state. The fact that 30 % of the genes are shared between HEP stress and acclimation suggests that these genes are necessary for the upkeep of acclimation and that the acclimation response and the stress response overlap in time and function.

Similar to the results in our stress experiment in Chapter 4, the two genes that have been previously used as reporters in many redox signaling studies, *lhcb1* and *rbcS* (Piippo et al. 2006; Kindgren et al. 2012; Ruckle et al. 2012), were not found to be alternatively expressed as a result of acclimation to HEP. This makes us question the effectiveness of these two transiently up-regulated transcripts as reporters for redox signaling, since they don't appear to be regulated by either primary redox signaling (see chapter 4) nor do they persist to be regulated into the acclimated state.

It seems striking that hardly any alterations seem to happen in the PETC or elsewhere in the chloroplast suggesting that just like *Brassica napus*, winter rye and barley (Dahal et al. 2012a), *Arabidopsis* does not primarily acclimate to HEP through chloroplast remodeling processes. A variety of different metabolic pathways appear affected on a transcript level (e.g. lipid metabolism, cell wall biogenesis, minor carbohydrates and various secondary metabolism pathways), but there was no accumulation of altered transcripts in any particular metabolic pathway. Yet, while these pathways almost seem to display stochastically up- and down-regulated transcripts, some other pathways dealing with the major carbohydrates, namely starch and sucrose metabolism, glycolysis and oxidative phosphorylation were consistently up-regulated. This is in congruency

with the findings of Schmitz et al. (2012) who reported that major carbohydrates are important during high light acclimation, not only to utilize excess electrons that are photosynthetically generated, but they are hypothesized to act as novel components in retrograde signaling.

It has to be stated though, that functional extrapolations of gene expression data have to be viewed skeptically, since changes on a transcript level do not necessarily translate into changes in protein abundance or functionality (Dahal et al. 2012a). Further factors, such as rate of translation and post-translational modifications have to be considered, before functional predictions can be made. Moreover, the small number of genes found by MapMan corresponding to the major metabolic pathways (108 genes out of 735 genes regulated by acclimation to HEP) indicate that the HEP-acclimated state might not require drastic modifications in any particular aspect of metabolism and that once the stress situation is handled, very few adjustments are necessary in order to maintain photostasis.

Considering the notable number of transcription factors affected by acclimation to HEP (Table 5.1), it becomes apparent that development and general chromatin accessibility play a significant role. Four different homeobox genes (*hat4*, *hat9*, *blh3* and *athb16*) regulate the plants morphogenesis and could account for the phenotype. In addition there was a remarkable number of transcription factors altered in response to HEP acclimation that are associated with circadian processes (*prr1*, *prr3*, *prr5*, *elf3* and *flc*) most of which were already present after the 1h HEP stress was applied (Table 5.2). Another transcript of interest, that was found in both the plants that were acclimated to HEP and the plants that were stressed by HEP, is a member from the AP2/EREBP family (*rav2*), that was hypothesized to be targeted to the chloroplast and be involved in chloroplast retrograde signaling (Dietz et al. 2010).

In summary we conclude that acclimation to HEP is a process that unlike the HEP stress response, does not manifest itself by drastic changes in transcript levels of major metabolic processes and while photosynthetic processes are mostly unaffected and the starch/sucrose production and consumption appear enhanced, the key to acclimation

seems to be a more subtle and general alteration of most of the major metabolic pathways, which only requires minimal long term changes in gene expression. The differentially regulated transcription factors suggest a further element of developmental alterations during the plant's morphogenesis in order to alleviate HEP. The fact that a large percentage (one third) of all genes necessary for acclimation are immediately activated after the first exposure to HEP, shows that while acclimation to HEP and the stress response to HEP are distinct processes, they do temporally overlap.

ACKNOWLEDGEMENTS:

We are grateful to David Carter at the London Regional Genomics Center (Robarts Research Institute, London, Ontario, Canada; <http://www.lrgc.ca>) for processing all the micro-array chips and providing the license and training for the use of Partek.

5.5 References:

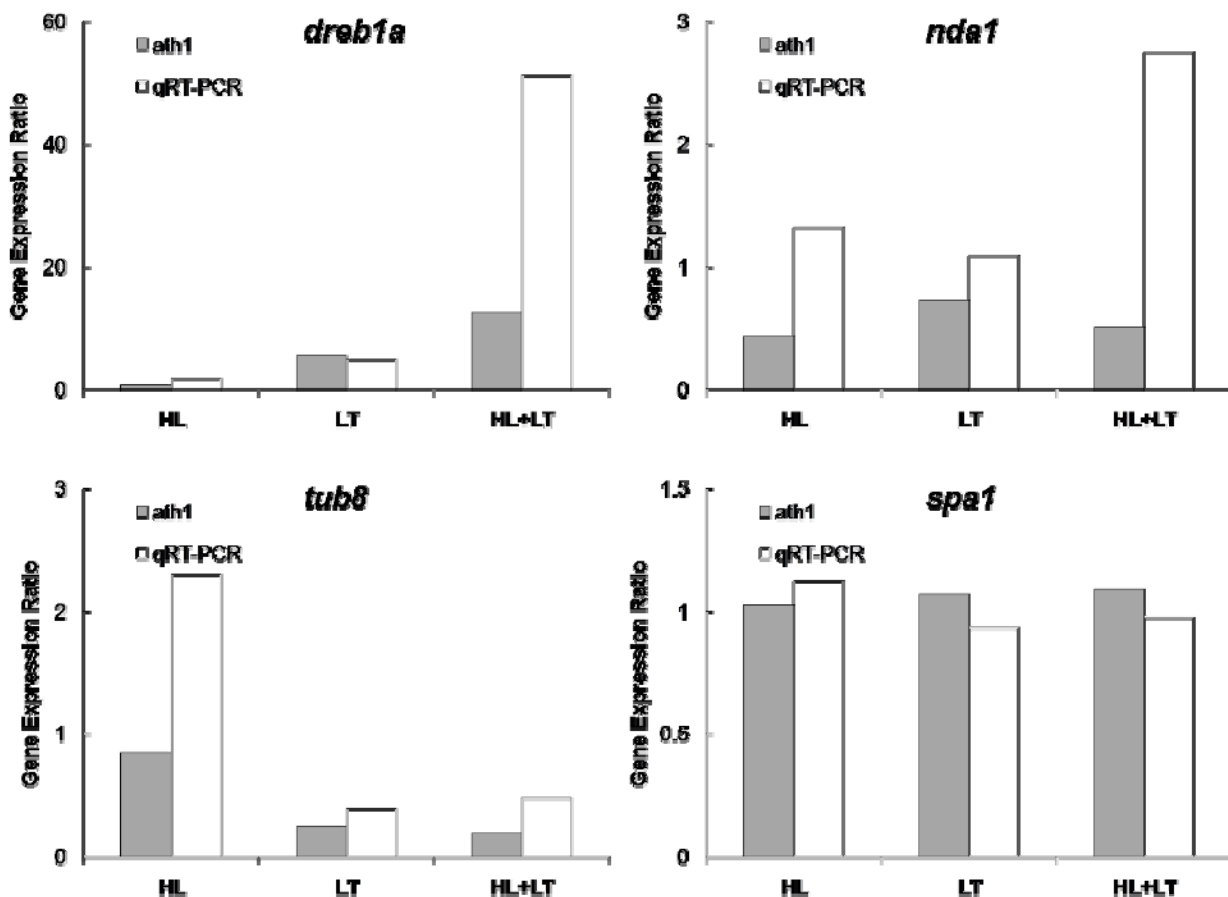
- Bräutigam, K., Dietzel, L., Kleine, T., Ströher, E., Wormuth, D., Dietz, K.J., Radke, D., Wirtz, M., Hell, R., Dörmann, P., Nunes-Nesi, A., Schauer, N., Fernie, A.R., Oliver, S.N., Geigenberger, P., Leister, D., and Pfannschmidt, T. (2009). Dynamic plastid redox signals integrate gene expression and metabolism to induce distinct metabolic states in photosynthetic acclimation in *Arabidopsis*. *Plant Cell*. 21: 2715–2732.
- Dahal, K., Kane, K., Gadapati, W., Webb, E., Savitch, L.V., Singh, J., Sharma, P., Sarhan, F., Longstaffe, F.J., Grodzinski, B., and Hüner, N.P.A. (2012a). The effects of phenotypic plasticity on photosynthetic performance in winter rye, winter wheat and *Brassica napus*. *Phys. Plant*. 144: 169–188.
- Dahal, K., Gadapati, W., Savitch, L.V., Singh, J., and Hüner, N.P.A. (2012b). Cold acclimation and BnCBF17-over-expression enhance photosynthetic performance and energy conversion efficiency during long-term growth of *Brassica napus* under elevated CO₂ conditions. *Planta*. (*in press*).
- Dietz, K.J., Schreiber, U., and Heber, U. (1985). The relationship between the redox state of Q_A and photosynthesis in leaves at various carbon-dioxide, oxygen and light regimes. *Planta*. 166: 219–226.
- Dietz, K.J., Vogel, M.O., and Viehhauser, A. (2010). AP2/EREBP transcription factors are part of gene regulatory networks and integrate metabolic, hormonal and environmental signals in stress acclimation and retrograde signaling. *Protoplasma*. 245(1-4): 3-14.
- Ensminger, I., Busch, F., and Hüner, N.P.A. (2006). Photostasis and cold acclimation: sensing low temperature through photosynthesis. *Physiol. Plant*. 126: 28-44.
- Escoubas, J.M., Lomas, M., LaRoche, J., and Falkowski, P.G. (1995). Light intensity regulation of *cab* gene transcription is signaled by the redox state of the plastoquinone pool. *Proc. Natl. Acad. Sci. USA* 92: 10237–10241.
- Fernández, P.A., and Strand, Å. (2008). Retrograde signaling and plant stress: plastid signals initiate cellular stress responses. *Curr Opin Plant Biol*. 11: 509–513.
- Foudree, A., Aluru, M., and Rodermel, S. (2010). PDS activity acts as a rheostat of retrograde signaling during early chloroplast biogenesis. *Plant Signal Behav*. 5(12): 1629-32.
- Hüner, N.P.A., Öquist, G., and Sarhan, F. (1998). Energy balance and acclimation to light and cold. *Trends Plant Sci*. 3: 224–230.

- Hüner, N.P.A., Öquist, G., and Melis, A. (2003). Photostasis in plants, green algae and cyanobacteria: The role of light harvesting antenna complexes. In *Advances in Photosynthesis and Respiration: Light-Harvesting Antennas in Photosynthesis*, Vol. 13, B.R. Green and W.W. Parsons, eds (Dordrecht, The Netherlands: Kluwer Academic Publishers), pp. 401–421.
- Hüner, N.P.A. and Grodzinski, B. (2011). "Photosynthesis and photoautotrophy" in *Comprehensive Biotechnology*, ed. M. Moo-Young (Elsevier) vol. 1, 315–322.
- Irizarry, R.A., Bolstad, B.M., Collin, F., Cope, L.M., Hobbs, B., Terence, P., and Speed, T.P. (2003). Summaries of Affymetrix GeneChip probe level data. *Nucleic Acids Research* 31(4): 15.
- Ivanov, A.G., Morgan, R.M., Gray, G.R., Velitchkova, M.Y., and Hüner, N.P.A. (1998). Temperature/light dependent development of selective resistance to photoinhibition of photosystem I. *FEBS Lett.* 430: 288–292.
- Kim, C., Meskauskiene, R., Zhang, S., Lee, K.P., Lakshmanan, A.M., Blajicka, K., Herrfurth, C., Feussner, I., and Apel, K. (2012). Chloroplasts of Arabidopsis are the source and a primary target of a plant-specific programmed cell death signaling pathway. *Plant Cell. In press.*
- Kindgren, P., Eriksson, M.-J., Benedict, C., Mohapatra, A., Gough, S.P., Hansson, M., Kieselbach, T., and Strand, A. (2011). A novel proteomic approach reveals a role for Mg-protoporphyrin IX in response to oxidative stress. *Physiol Plant.* 141: 310–320.
- Kindgren, P., Kremnev, D., Blanco, N.E., de Dios Barajas López, J., Fernández, A.P., Tellgren-Roth C., Small, I., and Strand, Å. (2012). The plastid redox insensitive 2 mutant of Arabidopsis is impaired in PEP activity and high light-dependent plastid redox signalling to the nucleus. *Plant J.* 70(2):279-91.
- Koussevitzky, S., Nott, A., Mockler, T.C., Hong, F., Sachetto-Martins, G., Surpin, M., Lim, J., Mittler, R., and Chory, J. 2007. Signals from Chloroplasts Converge to Regulate Nuclear Gene Expression. *Science.* 316: 715-719.
- Kramer, D.M., Johnson, G., Kiirats, O., and Edwards, G.E. (2004). New fluorescence parameters for the determination of QA redox state and excitation energy fluxes. *Photosynth. Res.* 79: 209–218.
- Krause, G.H., and Weis, E. (1991). Chlorophyll fluorescence and photosynthesis: the basics. *Annu. Rev. Plant Physiol. Plant Mol. Biol.* 42: 313–349.
- McDonald, A.E., Ivanov, A.G., Bode, R., Maxwell, D.P., Rodermel, S.R., and Hüner, N.P.A. (2011). Flexibility in photosynthetic electron transport: The physiological role of plastoquinol terminal oxidase (PTOX). *Biochim. Biophys. Acta:* 1807: 954–967.
- Maxwell, D.P., Laudenbach, D.E., and Hüner, N.P.A. (1995). Redox Regulation of Light-Harvesting Complex II and cab mRNA Abundance in *Dunaliella salina*. *Plant Physiol.* 109: 787-795.
- Miller .G., Suzuki, N., Ciftci-Yilmaz, S., and Mittler, R. (2010). Reactive oxygen species homeostasis and signaling during drought and salinity stresses. *Plant Cell and Environ.* 33: 453–467.
- Murchie, E.H., Pinto, M., and Horton, P. (2009). Agriculture and the new challenges for photosynthesis research. *New Phytol.* 181: 532–552.

- Ndong, C., Danyluk, J., Hüner, N.P., and Sarhan, F. (2001). Survey of gene expression in winter rye during changes in growth temperature, irradiance or excitation pressure. *Plant Mol Biol.* 45(6): 691-703
- Pesaresi, P., Hertle, A., Pribil, M., Schneider, A., Kleine, T., and Leister, D. (2010). Optimizing photosynthesis under fluctuating light: The role of the Arabidopsis STN7 kinase. *Plant Signaling & Behaviour.* 5: 21-25.
- Piippo, M., Allahverdiyeva, Y., Paakkanen, V., Suoranta, U-M., Battchikova, N., and Aro, E-M. (2006). Chloroplast-mediated regulation of nuclear genes in Arabidopsis thaliana in the absence of light stress. *Physiol Genomics.* 25: 142-152.
- Pogson, B.J., Woo, N.S., Forster, B. and Small, I.D. (2008) Plastid signalling to the nucleus and beyond. *Trends Plant Sci.* 13(11), 602–609.
- Rosso, D., Bode, R., Li, W., Krol, M., Saccon, D., Wang, S., Schillaci, L.A., Rodermel, S.R., Maxwell, D.P., and Hüner, N.P.A. (2009). Photosynthetic Redox Imbalance Governs Leaf Sectoring in the *Arabidopsis thaliana* Variegation Mutants immutans, spotty, var1, and var2. *Plant Cell* 21(11):3473-92
- Rosso, D., Ivanov, A.G., Fu, A., Geisler-Lee, J., Hendrickson, L., Geisler, M., Stewart, G., Krol, M., Hurry, V., Rodermel, S.R., Maxwell, D.P., and Hüner, N.P.A. (2006). IMMUTANS does not act as a stress-induced safety valve in the protection of the photosynthetic apparatus of Arabidopsis during steady-state photosynthesis. *Plant Physiol.* 142(2):574-85.
- Ruckle, M.E., Burgoon, L.D., Lawrence, L.A., Sinkler, C.A., and Larkin, R.M. (2012). Plastids Are Major Regulators of Light Signaling in Arabidopsis. *Plant Phys.* 159: 366–390.
- Schmitz, J., Schöttler, M.A., Krueger, S., Geimer, S., Schneider, A., Kleine, T., Leister, D., Bell, K., Flügge, U.I., and Häusler, R.E. (2012). Defects in leaf carbohydrate metabolism compromise acclimation to high light and lead to a high chlorophyll fluorescence phenotype in *Arabidopsis thaliana*. *BMC Plant Biology.* 12: 8
- Schreiber, U., Bilger, W., and Neubauer, C. (1994). Chlorophyll fluorescence as a non-intrusive indicator for rapid assessment of in vivo photosynthesis. In *Ecophysiology of Photosynthesis*, E. Schulze and M.M. Caldwell, eds (Berlin: Springer-Verlag), pp. 49–70.
- Suzuki, N., Koussevitzky, S., Mittler, R., Miller, G. (2012). ROS and redox signalling in the response of plants to abiotic stress. *Plant Cell Environ.* 35(2): 259-70
- Thimm, O., Bläsing, O., Gibon, Y., Nagel, A., Meyer, S., Krüger, P., Selbig, J., Müller, L.A., Rhee, S.Y., and Stitt, M. (2004). MAPMAN: a user-driven tool to display genomics data sets onto diagrams of metabolic pathways and other biological processes. *Plant J.* 37(6): 914-39.
- Wilson, K.E., Krol, M., and Hüner, N.P.A. (2003). Temperature-induced greening of *Chlorella vulgaris*. The role of the cellular energy balance and zeaxanthin-dependent nonphotochemical quenching. *Planta.* 217: 616–627.
- Wilson, K.E., Ivanov, A.G., Öquist, G., Grodzinski, B., Sarhan, F., and Hüner, N.P.A. (2006). Energy balance, organellar redox status and acclimation to environmental stress. *Can. J. Bot.* 84: 1355-1370.
- Woodson, J.D., Perez-Ruiz, J.M., and Chory, J. (2011). Heme synthesis by plastid ferrochelatase I regulates nuclear gene expression in plants. *Curr. Biol.* 21: 897–903.

Zhong, R., Lee, C., Zhou, J., McCarthy, R.L., and Ye, Z.H. (2008). A battery of transcription factors involved in the regulation of secondary cell wall biosynthesis in *Arabidopsis*. *Plant Cell*. 20(10): 2763-82.

5.6 Supplemental Figures

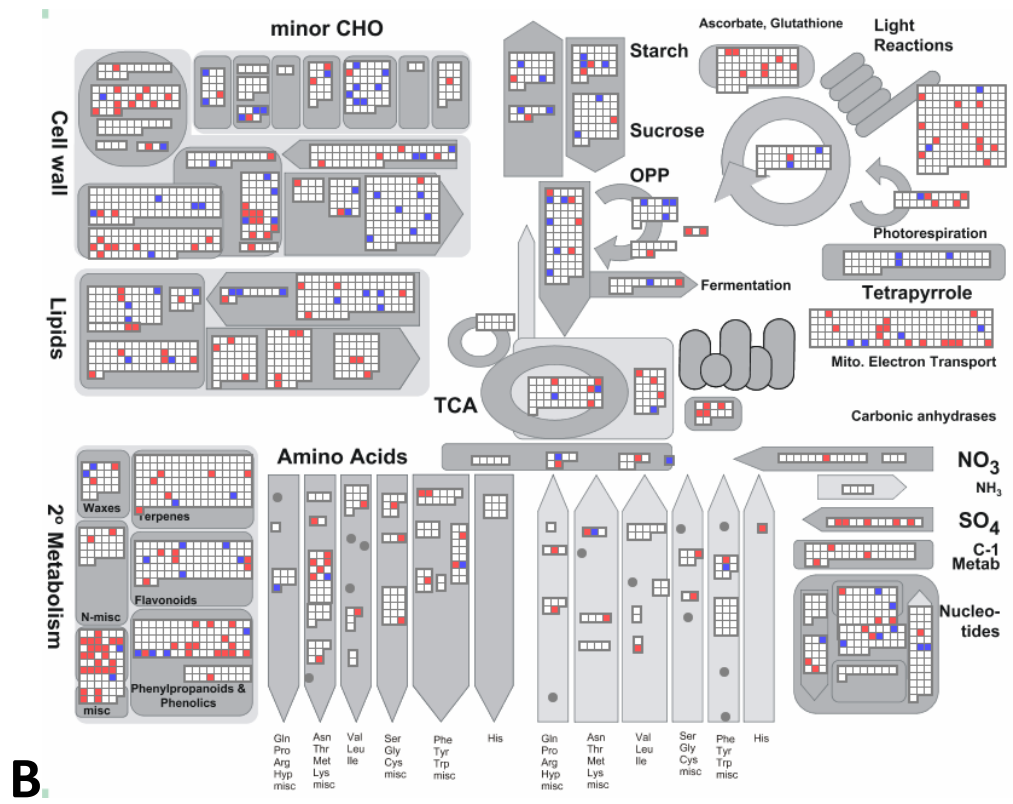
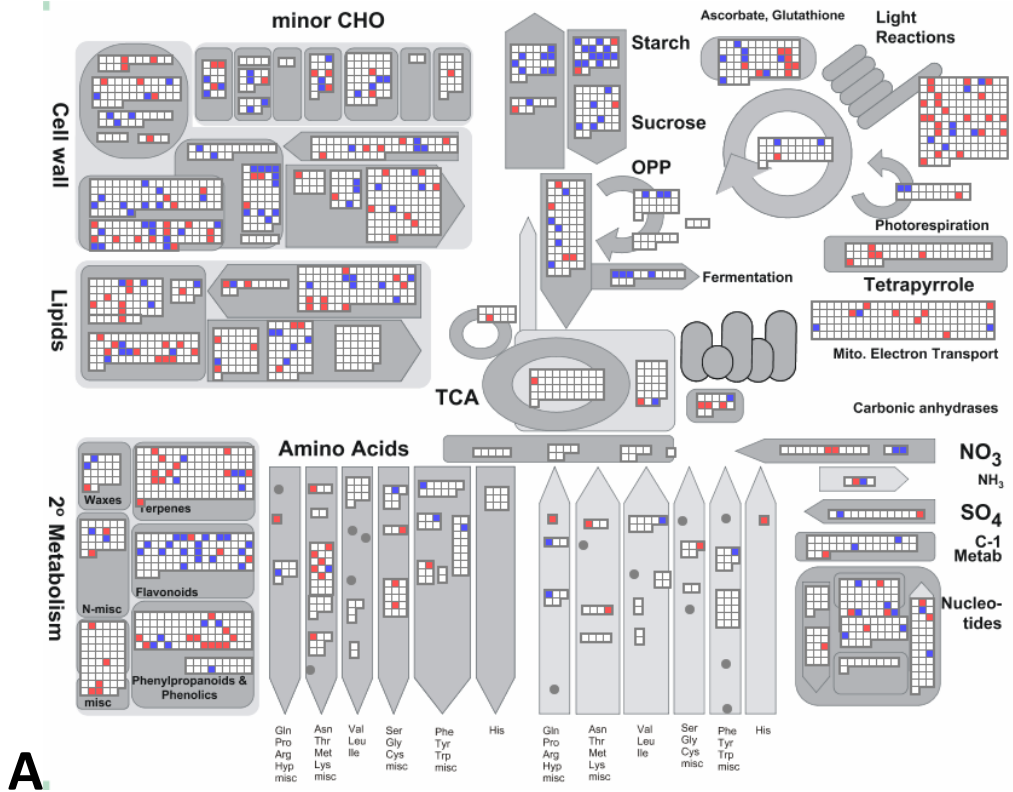


Supplemental Figure S 5.1 Comparison of qRT-PCR and Microarray Expression Data.

Gene expression ratios of *spa1* (NM_130197), *dreb1a* (NM_118680), *nda1* (NM_100592) and *tub8* (NM_122291) assessed by both, microarray (ath-1) and quantitative real-time PCR (qRT-PCR). Ratios were calculated by dividing the average expression value of each gene in the plants grown at various light and temperature regimes (25/450 = HL; 12/50 = LT; 12/450 = HL+LT) by the expression value of the same gene in the control plants (25/50).

Figure S5.2. MapMan Display of Gene Expression Data. MapMan software (Thimm et al., 2004) was used to display significant changes in transcript abundance of genes associated with major metabolic pathways. **(A)** shows the differentially expressed genes which represent the acclimation to High Light (HL). **(B)** shows the differentially expressed genes which represent the acclimation to Low Temperature (LT).

Red squares represent down-regulated transcripts, blue squares represent up-regulated transcripts, while white squares represent transcripts that remained unaltered.



CHAPTER 6

6 CONCLUSIONS:

Previous research on the function of IM had shown that, when expressed heterologously in *E. coli*, IM was able to reduce PQH₂ specifically. In context with the finding that IM has a 37 % identical DNA sequence with the mitochondrial AOX, the hypothesis was formed that IM might function as the elusive PTOX of the chlororespiratory pathway (Wu et al, 1999; Josse et al, 2003). Moreover it was known that IM also plays a role in carotenoid biosynthesis (Wetzel et al, 1994). The enzyme PDS, which catalyzes the crucial desaturation of the colorless precursor phytoene to ζ-carotene, donates the electrons it has accepted from this reaction to the PQ pool. If there is not a sufficient amount of oxidized PQ at hand PDS cannot produce the photo-protective carotenoids at conditions of HEP, when they are most needed and the role of IM was to oxidize PQH₂ during conditions of photosynthetic stress (Aluru et al 2006). Yet experiments with the IM knockout mutant *im* and two different IM over-expressing lines (Rosso et al, 2006) demonstrated that IM does not act as a stress-induced safety valve for a strongly reduced PQ-pool in fully expanded leaves that are photosynthetically competent.

Results from chapter 2 clearly demonstrated that even though IM might not be a safety valve in fully expanded leaves, it can function as a crucial alternative electron sink during the initial assembly of the photosynthetic apparatus in early stages (3-6 h) of chloroplast development. If IM is not present during this time window, the chloroplast becomes susceptible to HEP induced photo-oxidation, because it does not produce enough protective carotenoids to ensure the development of a functional photosynthetic apparatus. This study showed as well, that the photo-bleaching of the white sectors is not a simple irradiance effect, because plants grown at low temperature showed a significant increase in variegation and it is therefore the redox state of intersystem electron transport that regulates the extent of variegation in both *im* and *spotty*. We

could show for the first time ever that IM has indeed a function as a crucial safety valve for electrons in intersystem electron transport, since it significantly decreases excitation pressure. We could further demonstrate that it displays its safety valve capacity not as a response to stress, as it has been previously proposed (Niyogi, 2000, Peltier and Cournac, 2002), but during early chloroplast biogenesis, when the components of the PETC are being assembled. This finding is also another strong indicator that IM is the elusive PTOX enzyme, a notion that was further corroborated in a recent report by Fu and co-workers (2012), who demonstrated that the mitochondrial analogue of PTOX, AOX could save the variegated phenotype in *im* when it was targeted to the chloroplast instead.

The variegated mutants *var1* and *var2* display variegation in response to a gene defect affecting a FtsH metalloprotease complex anchored in the thylakoid membrane. Similar to IM this protease is photo-protective, as it removes photo-damaged reaction centers of PS II making room for new functional proteins (Miura et al, 2007) and both mutants have been described as sensitive to light intensity (Martínez-Zapater, 1993). Hence we predicted to find the extent of their leaf variegation also to be controlled by EP. After the publication of chapter 2, Zhang et al (2010) found that the extent of variegation is also dependent on the total amount of FtsH protease present in the thylakoids. They agree with our proposed threshold model, stating that variegation depends not only on the lack of the protein in the thylakoid, but on HEP induced photo-oxidation during very early stages of chloroplast development. I propose that variegation is determined very early during thylakoid assembly in both *var1* and *var2*, the same way it is in *im*.

Although we know that *atd2* has a deficiency in an isoform of an enzyme crucial for purine biosynthesis, not much is known about the remaining variegated mutant *chs5* (van der Graaf et al. 2004, Schneider et al, 1994). Looking at the development of *atd2* leaves, which grow without trichomes, stay very small with thin leaves lacking much differentiated tissue and display an incompletely developed vascular system, it appears that *atd2* simply does not fully develop in many respects, presumably due to a lack in purine. The purine, which is produced by *atd1*, mainly in the roots and flowers needs to

be imported to the leaves and it appears as if there is only enough to develop the primary features, which enable the plant to survive. I hypothesize that the presence of HEP necessitates a higher production rate of mRNAs in order to replenish photo-oxidized components of the thylakoids and the low supply of purine in *atd2* does not allow for a sufficient accumulation of transcripts to support chloroplast development under these conditions.

This was the first time it could be demonstrated that the control of variegation by excitation pressure extends far beyond the elements of the PETC and based on these results, I hypothesize that HEP governs the extent of white sector formation in all variegated mutants, regardless what the mutation is, that evokes the variegated phenotype in the first place.

Previous research had shown that PQH₂ acts as an important sensor of a strongly reduced PETC, be it in response to increased irradiance, low temperature, or specific inhibitors, which chemically alter the reduction state of the PQ pool. It was shown that PQH₂ changes nuclear gene expression inducing the remodeling of the chloroplast in order to re-establish photostasis (Maxwell et al, 1995; Escoubas et al, 1995; Hüner et al 1998; Wilson et al, 2003; Ensminger et al, 2006). Further research could demonstrate, that the redox state of PETC regulates far more processes than merely photosynthesis, in fact significant regulation of all types of cellular metabolic processes has been observed (Ndong et al, 2001; Bräutigam et al, 2009). We know now that it is not only PQH₂ which contributes to retrograde signaling from the chloroplast and a variety of sensors of chloroplast energy (im-)balance have been identified, such as PS II, reactive oxygen species, the proton motive force of the trans-thylakoid proton gradient and various elements on the acceptor site of PS I (Figure 6.1). The results in chapter 4 of this thesis demonstrate, the significance of both PS II and PQH₂ as sensors for nuclear gene expression, for many cellular and in particular metabolic processes, which goes against the findings of Piippo et al (2006), who stated that the redox state of PQ is of “minimal or no importance” during early stress signaling. Yet I do agree with their conclusion stating that reducing molecules at the acceptor site of PS I and the ratios of

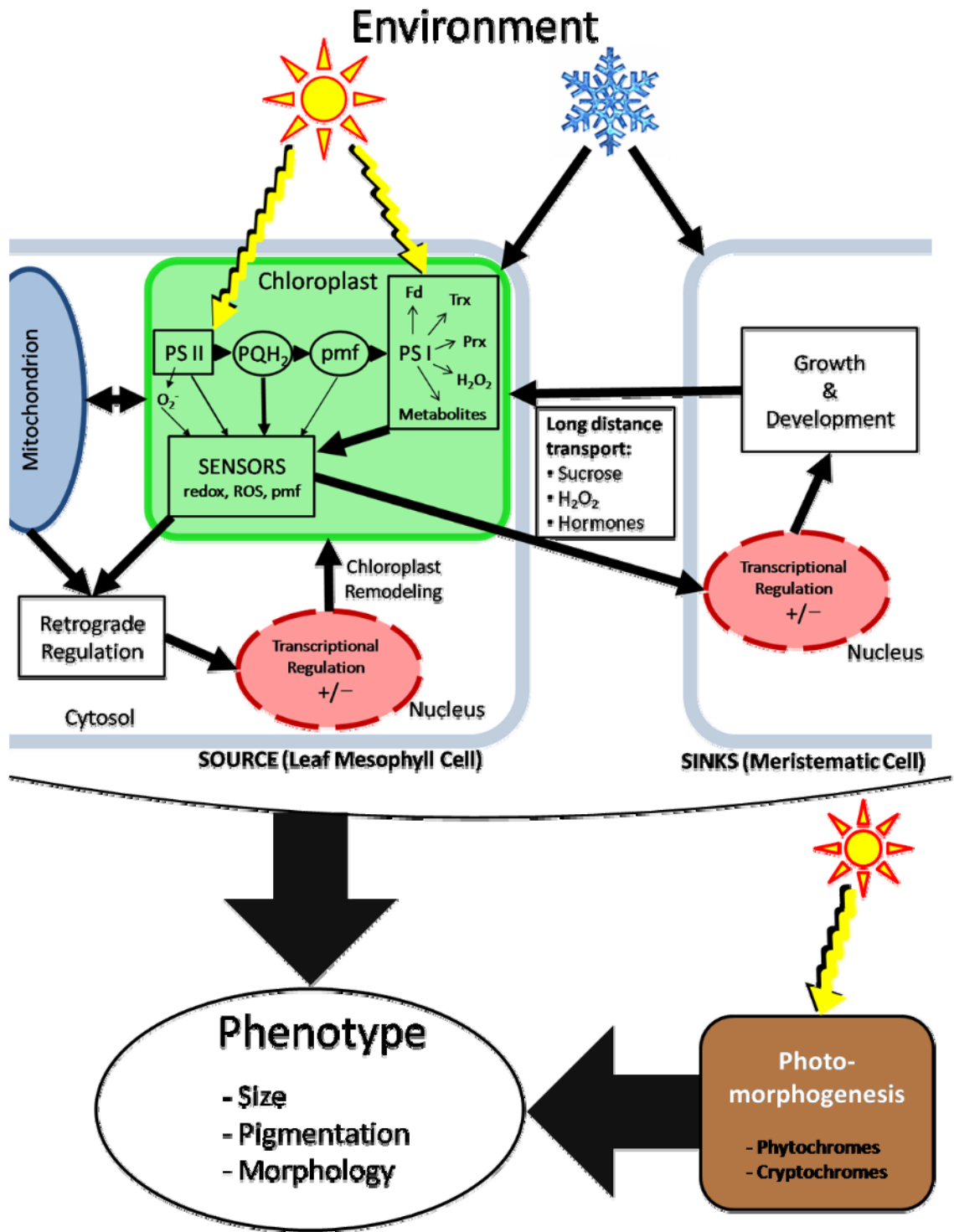
NADPH/NADP⁺ and ATP/ADP most likely contribute to chloroplast stress signaling in more significant ways than PQH₂ or PS II do, based on my findings that the latter two combined only make up for a mere 12 % of all altered transcript during the HEP stress response.

In chapter 5, I demonstrated that the HEP acclimation response was clearly distinct from the short term stress response, since there was not only a largely different set of genes changed than in the stress response, but also the type of genes affected were different. The short-term stress response resulted in a widespread reprogramming of genes associated with a large variety of metabolic pathways, including, but not restricted to photosynthetic genes, which is in agreement with metabolomic studies performed by Bräutigam et al (2009). The long-term acclimation response on the other hand induced more subtle changes in gene expression involving a variety of transcription factors associated with developmental processes. Even though ca. 30 % of all transcripts regulated by acclimation to HEP were already alternatively expressed in the stress response, these genes did not reflect the wide spread metabolic reprogramming observed in the stress response and hence I hypothesize that these two processes are strictly separate, even though they overlap temporally. Long term acclimation to HEP is more likely to function on a developmental as opposed to a metabolic level.

Through the redox state of the PETC the chloroplast functions as a complex sensor for environmental cues, such as light, temperature, salt stress and nutrient availability. It can communicate these cues to the nucleus via retrograde signaling, which in turn and via the induction of chloroplast remodeling (Figure 6.1), allows the plant to acclimate to the new conditions. Yet on top of that, this information can be used to reprogram virtually all compartments of the cell and via long distance transport through the vascular system it can reach remote regions within the plant, such as roots and meristems and hence affect plant growth, development and morphology (Gray et al, 1997). In 1982 Arnon introduced this concept as “the grand design of photosynthesis” which was re-visited by Anderson et al in 1995, who concludes: “*the grand design of photosynthesis with exquisite regulation ensures that the responses of both*

photoreceptors and Photosystems II and I, acting as their own light sensors, are inextricably linked with feedback metabolic responses from photosynthesis itself, which allow plants to respond to both sudden and sustained fluctuations in environmental cues."

Figure 6.1. A Model of Chloroplast Redox Sensing and its Effects on Both a Cellular and an Organismal Scale. Environmental cues such as high light (sun) and low temperature (snowflake) are sensed in the chloroplast through the alteration of the redox state of the photosynthetic apparatus. This information about a redox imbalance is exchanged between the chloroplast and the mitochondrion via the carbon metabolism and both organelles communicate with the nucleus through retrograde regulation, leading to remodeling of the components of photosynthetic apparatus in order to re-establish the energy balance. In vascular plants the information of photosynthetic redox imbalance can also be transported to distant sinks, such as storage organs or meristematic regions, thus affecting growth, morphology and development. The long distance signaling utilizes the vascular system for transport, both ways, this way the plant allows for a feedback regulation of photosynthetic energy balance. Thus photosynthesis can affect the phenotype of an entire plant similar to photomorphogenesis events, controlled by sensors of light quality. PS II: photosystem II; PS I: photosystem I; PQH₂: reduced plastoquinone; pmf: proton motive force; Fd: ferredoxin; Trx: thioredoxins; Prx: peroxiredoxins.



6.1 *SUMMARY*

In summary the main conclusions of this thesis are:

1. – The greening experiments showed for the first time that IM can act as a safety valve for electrons in the PETC since its function as a PQH₂ oxidase is necessary during early stages of chloroplast development (3 – 12 h) to assure the development of functional thylakoids when the plants are experiencing elevated levels of EP.
2. – EP controls the extent of leaf sectoring in all variegated mutants we tested and it is not light or temperature per se that regulates white sector formation, irrespective whether the mutant is impaired in compounds of the PETC, or the mutation causing the variegated phenotype originates elsewhere.
3. – HEP short-term stress signaling indeed regulates a large variety of cellular processes impairing the vast majority of all metabolic pathways extending, far beyond chloroplast remodeling. It consists of a complex interplay of different sensors in the PETC, each with distinct functions and while both, PS II and PQH₂ clearly each play a significant role as sensors, they can only account for a small part of the HEP-stress response.
4. – In *Arabidopsis*, acclimation to HEP is functionally a distinct process from the HEP stress response, but they do overlap temporally, as ca one third of the genes regulated by acclimation are already alternatively expressed during the first hour of the stress response. Unlike the short term stress response, long term acclimation to HEP does not affect photosynthesis related gene expression.

6.2 *Future Research*

Future studies on variegation should examine, whether all variegation mutants in *Arabidopsis*, but also other species are controlled by HEP. The tomato *ghost* mutant, for example is believed to be homologous to *im* in *Arabidopsis* (Barr et al, 2004) and apart from chlorotic leaf sectors, the mutation appears to affect the chromoplast of the fruit as well. The *Arabidopsis* variegated mutant *chm* (created by Rédei 1973) has been reported to display variegation due to defects in its mitochondria which secondarily result in defective plastids (Yu et al, 2007), but has never been described to display light or temperature dependency in regard to its variegation. Aluru and co-workers (2006) describe a whole array of distinct variegated mutants, which I propose should all be examined for their dependency on HEP.

HEP dependent retrograde signaling on the other hand is a growing field of research and while a lot of productive studies have examined the effects of the different components of the PETC on gene expression, the signal transduction pathways remain mostly unknown (Fernández & Strand, 2008). I propose that the identification of signal transport from the chloroplast to the nucleus will clarify how the various signals are integrated or kept separate in order to affect nuclear gene expression.

6.3 References:

- Aluru, M.R., Yu, F., Fu, A., and Rodermel, S.R. (2006) *Arabidopsis* variegation mutants: New insights into chloroplast biogenesis. *J. Exp. Bot.* 57: 1871–1881.
- Anderson, J.M., Chow, W.S. and Park, Y.-I. (1995). The grand design of photosynthesis: acclimation of the photosynthetic apparatus to environmental cues. *Photosyn. Res.* 46, 129-139
- Arnon, D.I. (1982). Sunlight, earth life: the grand design of photosynthesis. *The Sciences* 22, 22-27.
- Barr, J., White, W.S., Chen, L., Bae, H., and Rodermel, S.R. (2004) The GHOST terminal oxidase regulates developmental programming in tomato fruit. *Plant Cell Environ.* 27: 840–852
- Bräutigam, K., Dietzel, L., Kleine, T., Ströher, E., Wormuth, D., Dietz, K.J., Radke, D., Wirtz, M., Hell, R., Dörmann, P., Nunes-Nesi, A., Schauer, N., Fernie, A.R., Oliver, S.N., Geigenberger, P., Leister, D., and Pfannschmidt, T. (2009) Dynamic plastid redox signals integrate gene expression and metabolism to induce distinct metabolic states in photosynthetic acclimation in *Arabidopsis*. *Plant Cell.* 21: 2715–2732.
- Ensminger, I., Busch, F., and Hüner, N.P.A. (2006) Photostasis and cold acclimation: sensing low temperature through photosynthesis. *Physiol. Plant.* 126: 28-44.
- Escoubas, J.M., Lomas, M., LaRoche, J., and Falkowski, P.G. (1995) Light intensity regulation of cab gene transcription is signaled by the redox state of the plastoquinone pool. *Proc. Natl. Acad. Sci. USA* 92: 10237–10241.
- Gray, G.R., Chauvin, L.-P., Sarhan, F. and Hüner, N.P.A. (1997). Cold acclimation and freezing tolerance. A complex interaction of light and temperature. *Plant Physiol* 114, 467-474.
- Hüner, N.P.A., Öquist, G., and Sarhan, F. (1998) Energy balance and acclimation to light and cold. *Trends Plant Sci.* 3: 224–230.
- Josse, E.M., Alcaraz, J.P., Labouré, A.M., and Kuntz, M. (2003) In vitro characterization of a plastid terminal oxidase (IM). *Eur. J. Biochem.* 270: 3787–3794.
- Rosso, D., Ivanov, A.G., Fu, A., Geisler-Lee, J., Hendrickson, L., Geisler, M., Stewart, G., Król, M., Hurry, V., Rodermel, S.R., Maxwell, D.P., and Hüner, N.P.A. (2006) IMMUTANS does not act as a stress-induced safety valve in the protection of the photosynthetic apparatus of *Arabidopsis* during steady-state photosynthesis. *Plant Physiol.* 142: 1–12.
- Martínez-Zapater JM. (1993) Genetic analysis of variegated mutants in *Arabidopsis*. *Journal of Heredity* 84, 138–140.
- Maxwell, D.P., Laudenbach, D.E., and Hüner, N.P.A. (1995). Redox Regulation of Light-Harvesting Complex II and cab mRNA Abundance in *Dunaliella salina*. *Plant Physiol.* 109: 787-795.
- Miura, E., Kato, Y., Matsushima, R., Albrecht, V., Laalami, S., and Sakamoto, W. (2007) The balance between protein synthesis and degradation in chloroplasts determines leaf variegation in *Arabidopsis yellow variegated* mutants. *Plant Cell* 19: 1313–1328.
- Ndong, C., Danyluk, J., Hüner, N.P., and Sarhan, F. (2001) Survey of gene expression in winter rye during changes in growth temperature, irradiance or excitation pressure. *Plant Mol Biol.* 45(6): 691-703

- Niyogi, K.K. (2000). Safety valves for photosynthesis. *Curr Opin Plant Biol* 3: 455–460.
- Peltier, G., Cournac, L. (2002). Chlororespiration. *Annu Rev Plant Biol* 53: 523–550.
- Piippo, M., Allahverdiyeva, Y., Paakkarinen, V., Suoranta, U.M., Battchikova, N., Aro, E.M. (2006) Chloroplast-mediated regulation of nuclear genes in *Arabidopsis thaliana* in the absence of light stress. *Physiol Genomics* 25: 142–152.
- Schneider, J.C.; Hugly, S.; Somerville, CR (1994) Chilling sensitive mutants of *Arabidopsis*. *Weeds World* 1: 2-6.
- van der Graaff, E.; Hooykaas, P.; Lein, W.; Lerchl, J.; Kunze, G.; Sonnewald, U.; Boldt, R. (2004) Molecular analysis of "de novo" purine biosynthesis in solanaceous species and in *Arabidopsis thaliana*. *Front Biosci* 1;9:1803-16.
- Wilson, K.E., Krol, M., and Hüner, N.P.A. (2003) Temperature-induced greening of *Chlorella vulgaris*. The role of the cellular energy balance and zeaxanthin-dependent nonphotochemical quenching. *Planta* 217: 616–627.
- Wu, D., Wright, D.A., Wetzell, C.M., Voytas, D.F., and Rodermel, S.R. (1999) The IMMUTANS variegation locus of *Arabidopsis* defines a mitochondrial alternative oxidase homolog that functions during early chloroplast biogenesis. *Plant Cell* 11: 43–55.
- Yu, F.; Fu, A.; Aluru M.; Park, S.; Xu, Y.; Liu, H.; Liu, X.; Foudree, A.; Nambogga M.; Rodermel, S.R. (2007). Variegation mutants and mechanisms of chloroplast biogenesis. *Plant, Cell and Environment* 30: 350–365.

7 VITA

Name: Rainer Bode

Post-secondary Education and Degrees: Universität Göttingen
Göttingen, Germany
2000-2006 Diplom

University of Oulu
Oulu, Finland
2002-2003, ERASMUS Exchange Program

Western University Canada
London, Canada
2007-2012 Ph.D.

Honours and Awards: Outstanding Oral Presentation
American Society of Plant Biologists
Mid-West Section, Lincoln, Nebraska, USA
2012

Related Experience: Teaching Assistant
The University of Western Ontario
2007-2012

Publications:

Rosso, D.; Bode, R.; Li, W.; Król, M.; Saccon, D.; Wang, S.; Schillaci, L.A.; Rodermel, S.R.; Maxwell, D.P.; Hüner, N.P.A. (2009). Photosynthetic Redox Imbalance Governs Leaf Sectoring in the *Arabidopsis thaliana* Variegation Mutants *immutans*, *spotty*, *var1*, and *var2*. *Plant Cell*, Vol. 21: 3473–3492

McDonald, A.E.; Ivanov, A.G.; Bode, R.; Maxwell, D.P.; Rodermel, S.R.; Hüner, N.P.A. (2011). Flexibility in photosynthetic electron transport: The physiological role of plastoquinol terminal oxidase (PTOX). *Biochimica et Biophysica Acta* 1807 (2011) 954–967

Rosso, D.; Bode, R.; Li, W.; Król, M.; Rodermel, S.R.; Maxwell, D.P.; Hüner, N.P.A. (2012). Redox Control of Leaf Variegation and Chloroplast Biogenesis in *Arabidopsis thaliana*. In: Itoh, S.; Mohanty, P. and Guruprasad, K.N. *Photosynthesis: Overviews on Recent Progress & Future Perspective*. IK International Publishing House Pvt. Ltd, New Delhi

Hüner, N.P.A.; Bode, R.; Dahal, K.; Hollis, L.; Rosso, D. (2012) Chloroplast Redox Imbalance Governs Phenotypic Plasticity: the “Grand Design of Photosynthesis” Revisited. *Frontiers Plant Science*. *Accepted*

Hüner, N.P.A., Bode, R., Dahal, K., Busch, F., Possmayer, M., Szyszka, B., Rosso, D., Ensminger, I., Król, M., Ivanov, A.G., Maxwell, D.P.A. (2012) Shedding Some Light on Cold Acclimation, Cold Adaptation and Phenotypic Plasticity. *Botany*. *Submitted*